CRYSTALLOGRAPHIC STUDIES IN THE V-P-AS-O SYSTEM

CRYSTALLOGRAPHIC STUDIES IN THE V-P-AS-O SYSTEM

By

NORA E. MIDDLEMISS, B.Sc.

A Thesis

Submitted to the School of Graduate Studies

in Partial Fulfilment of the Requirements

for the Degree

Doctor of Philosophy

McMaster University

September 1978

DOCTOR OF PHILOSOPHY (1978)
(Chemistry)

McMASTER UNIVERSITY
Hamilton, Ontario.

TITLE: Crystallographic Studies in the V-P-As-O System

AUTHOR: Nora E. Middlemiss, B.Sc. (McGill University)

SUPERVISORS: Professors C. Calvo and I. D. Brown

NUMBER OF PAGES: x, 177

ABSTRACT:

The crystal structures of VOP_2SiO_8, $VO(PO_3)_2$, $V(PO_3)_3$, $(VO)_2P_2O_7$ and $VAsO_5$ have been determined with the help of x-rays, and are compared with the known structures in the V-P-As-O system. All the vanadium atoms in the mixed oxides are octahedrally coordinated and the $V^{+4}O_6$ and $V^{+5}O_6$ octahedra are all characterized by one short vanadyl bond. $V^{+3}O_6$ groups are nearly regular. The tetrahedral phosphorus is found in structural elements ranging from infinite metaphosphate chains ($V(PO3)_3$, $VO(PO_3)_2$), to pyrophosphate groups ($(VO)_2P_2O_7$) to isolated tetrahedra ($VAsO_5$ and VOP_2SiO_8). Both structural and substitutional disordering is evident in the V-P-As-O system, and is discussed together with a detailed model for stacking faults in $VAsO_5$.

Some of the phases in the V-P-As-O system are known to catalyze the oxidation of butene to maleic anhydride, and certain structural features of the compounds are related to this catalytic activity. α-VPO_5 can be related to $(VO)_2P_2O_7$ through the formation of shears in a manner similar to shear formation in V_2O_5, and such a mechanism is proposed as a means whereby an α-VPO_5 catalyst can change into $(VO)_2P_2O_7$, the known composition of the spent catalyst.

ACKNOWLEDGEMENTS

I would like to thank Dr. Crispin Calvo for suggesting this research, and for his patience, help and understanding during the course of my work. I would also like to thank the members of my supervisory committee, Drs. I. D. Brown, J. A. Morrison, and C. V. Stager, for their invaluable assistance in preparing this thesis.

The many worthwhile discussions with Dr. H. N. Ng, and the technical assistance of R. Faggiani have helped to produce a successful conclusion to this work. Thanks are due to Dr. F. C. Hawthorne for interesting discussions and data on the $V(PO_3)_3$ structure.

The financial support from the Government of Ontario through Ontario Graduate Scholarships, and from McMaster University are gratefully acknowledged.

Finally, I would like to thank my husband, Keith, for his moral support and understanding during this research, and for his assistance in preparing this manuscript.

TABLE OF CONTENTS

LIST OF FIGURES

LIST OF TABLES

CHAPTER 1

Introduction

§ 1.1 Scope and Perspective

Vanadium oxides and vanadium phosphorus oxides are known to act as heterogeneous catalysts in certain organic reactions such as the oxidation of butene to maleic anhydride[1]. Such catalysis must depend on the crystal structures of these oxides and a study of their crystallography is therefore essential in order to understand the mechanism of the catalytic processes.

The crystal structures of most vanadium oxides are known[2-10] and will be briefly reviewed. The crystal structures of three vanadium phosphorus oxides, $V^{+4}O(PO_3)_2$, $V^{+3}(PO_3)_3$ and $(V^{+4}O)_2P_2O_7$, will be presented and compared to the known crystal structures of the two forms of VPO_5[11,12]. Many oxide catalysts are supported on silica gel and the crystal structure of $V^{+4}OP_2SiO_8$, readily formed from $VO(PO_3)_2$ and SiO_2, will be described in order to determine the possible influence of a supporting medium. The question of possible substitution of arsenic for phosphorus in some of the phases of the V-P-O system will be raised, and the crystal structure of $V^{+5}AsO_5$ will be presented as well as evidence for a solid solution of the form $VP_xAs_{1-x}O_5$ over the range $0 \leq x \leq 1$. Certain features of these structures will be related to catalytic activity.

§ 1.2 The Vanadium Oxides

Systems containing vanadium and oxygen form a very diverse series of compounds. Not only can the vanadium exist in different oxidation

states, it is also found in a variety of coordinations. Pentavalent vanadium can be found tetrahedrally coordinated in isolated tetrahedra (i.e. the VO_4 tetrahedra are not connected to other VO_4 groups), but in vanadium oxides this coordination is usually found in infinite corner-sharing metavanadate chains, $(VO_3)_\infty$, (fig.1-1(a)) (e.g. $NaVO_3$[13]) and in pyrovanadate groups, $V_2O_7^{-4}$, (fig.1-1(b)) consisting of two corner-sharing tetrahedra (e.g. $Zn_2V_2O_7$[14]). Both V^{+5} and V^{+4} can exist in 5-fold and octahedral coordination. These groups usually have one V-O bond, often called the vanadyl bond, which is shorter than the other V-O bonds in the group, and which distorts the idealized polyhedral symmetry. The V-O bond <u>trans</u> to the vanadyl bond is generally very long (octahedral coordination, fig.1-1(c)), or missing (5-fold coordination, fig. 1-1(d)). This long bond is often formed to a vanadyl oxygen in another polyhedron. Trivalent vanadium also exists in octahedral coordination, but does not usually have the vanadyl geometry, the octahedra being nearly regular (fig. 1-1(e)). The 5 or 6-fold coordination polyhedra can be found isolated or condensed in 1,2, or 3 dimensions.

Dickens and Wiseman[15] have reviewed the crystallography of oxide bronzes and related mixed valence oxides, and the crystallography of the vanadium oxides can best be described using their terminology. VO_6 octahedra can be found in corner-sharing chains (fig.1-2(a)), edge-sharing chains (rutile chains, fig.1-2(c)), or double chains composed of two edge-sharing octahedra sharing corners with two adjacent sets of edge-sharing octahedra (fig.1-2(b)). Adjacent octahedra can also share edges in a zigzag pattern to form a single ribbon as shown viewed from three perpendicular directions in figure 1-3(a). Double ribbons can be

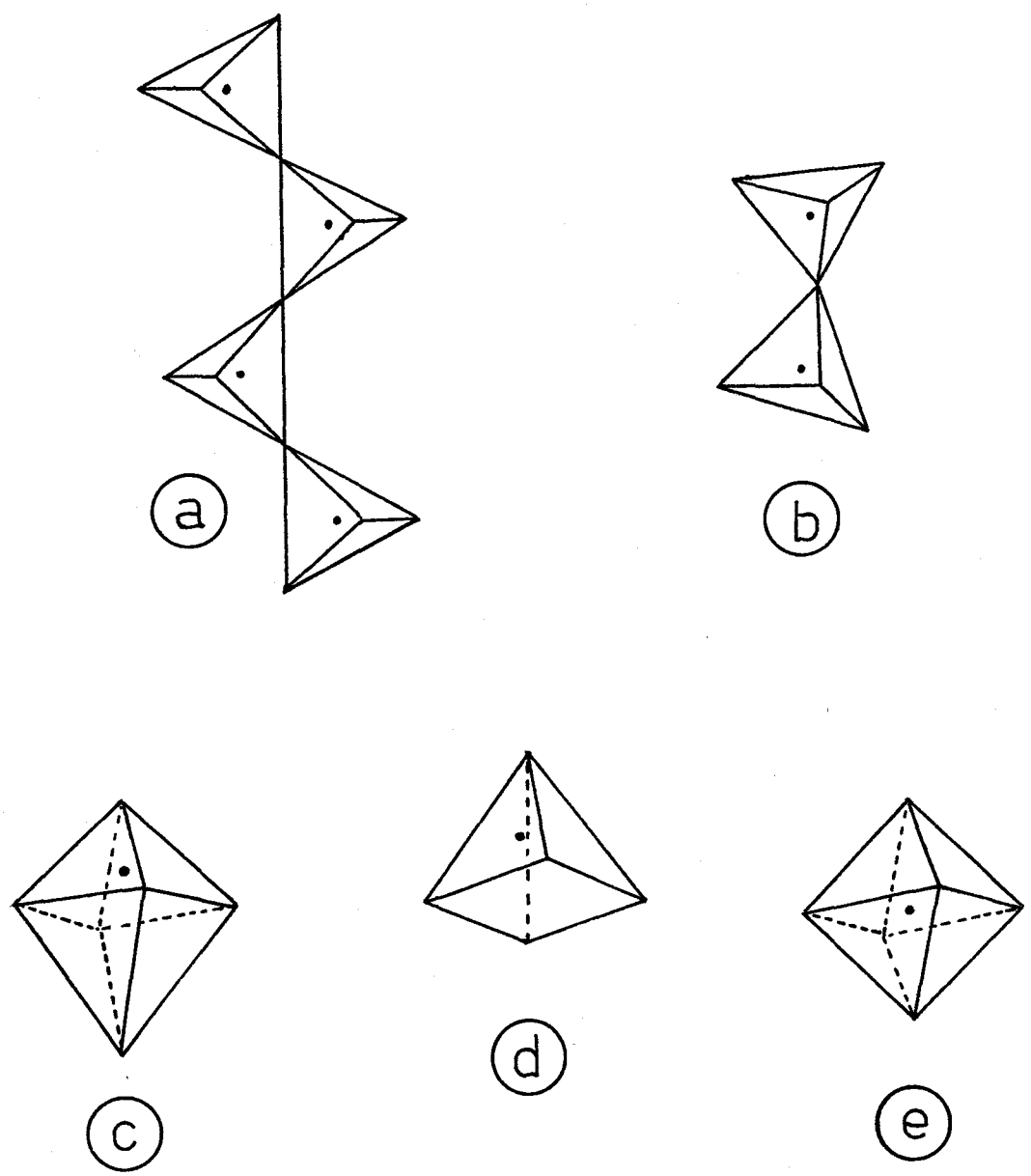

Figure 1-1. Structural elements found in vanadium oxides. The unconnected dot represents the position of the vanadium atom, and oxygen atoms are found at the apices of the polyhedra.
(a) metavanadate chain, (b) pyrovanadate group,
(c) octahedron with short vanadyl bond, (d) 5-fold coordinate group with vanadyl bond, (e) regular octahedron.

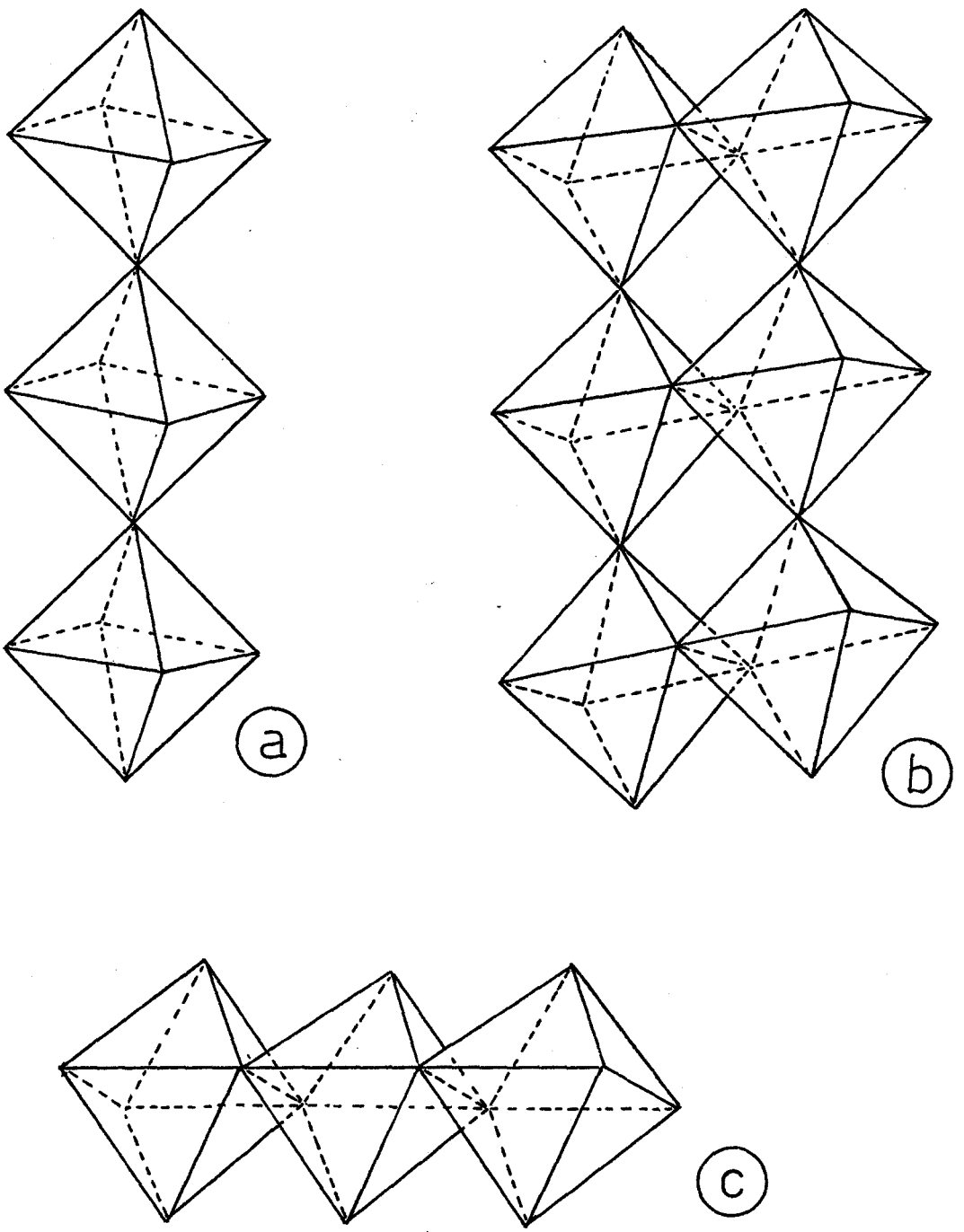

Figure 1-2. (a) Single corner-sharing octahedral chain
(b) Double corner-sharing octahedral chain
(c) Edge-sharing or rutile octahedral chain

formed by two such single ribbons sharing edges as shown in figure 1-3(b). If parallel adjacent single ribbons share corners they can form single sheets as shown head-on in figure 1-4(a). In a similar fashion double ribbons can share edges to form double sheets (figure 1-4(b)) or corners to form zig-zag sheets (fig. 1-4(c)).

Most vanadium oxides can be considered members of the series V_nO_{2n+1} or V_nO_{2n-1} with n=2,3,4,6 for the former and n=2-7 for the latter. VO_2 is one important vanadium oxide which does not fall in either of these series but bridges the two. Most of these oxides are mixed oxidation state compounds and, while it is often possible to assign integer oxidation numbers to individual vanadium atoms using the bond-valence parameters of Brown[16], some V atoms appear to have partial valences.

V_2O_5, the first member of the V_nO_{2n+1} series, is known to exist in two polymorphic forms. α-V_2O_5[2], stable under ordinary conditions, consists of single octahedral sheets (fig.1-4(a)) stacked so that the vanadyl oxygens within one sheet form the long axial V-O bonds of the octahedra in an adjacent sheet. β-V_2O_5[17], found at high pressures, consists of zig-zag sheets (fig.1-4(c)) which are not noticeably bonded together and thus readily slip to introduce stacking faults, giving rise to diffuse scattering in the diffraction pattern.

V_3O_7[3] contains alternating double (fig.1-2(b)) and single (fig.1-2(a)) corner-sharing chains which are linked to each other at the corners by single ribbons (fig.1-3(a)). The single ribbons are essentially 5-fold rather than octahedrally coordinated.

V_4O_9[4] contains single ribbons (fig.1-3(a)) which link to each other and to double ribbons (fig.1-3(b)). Like V_3O_7, the polyhedra of the single

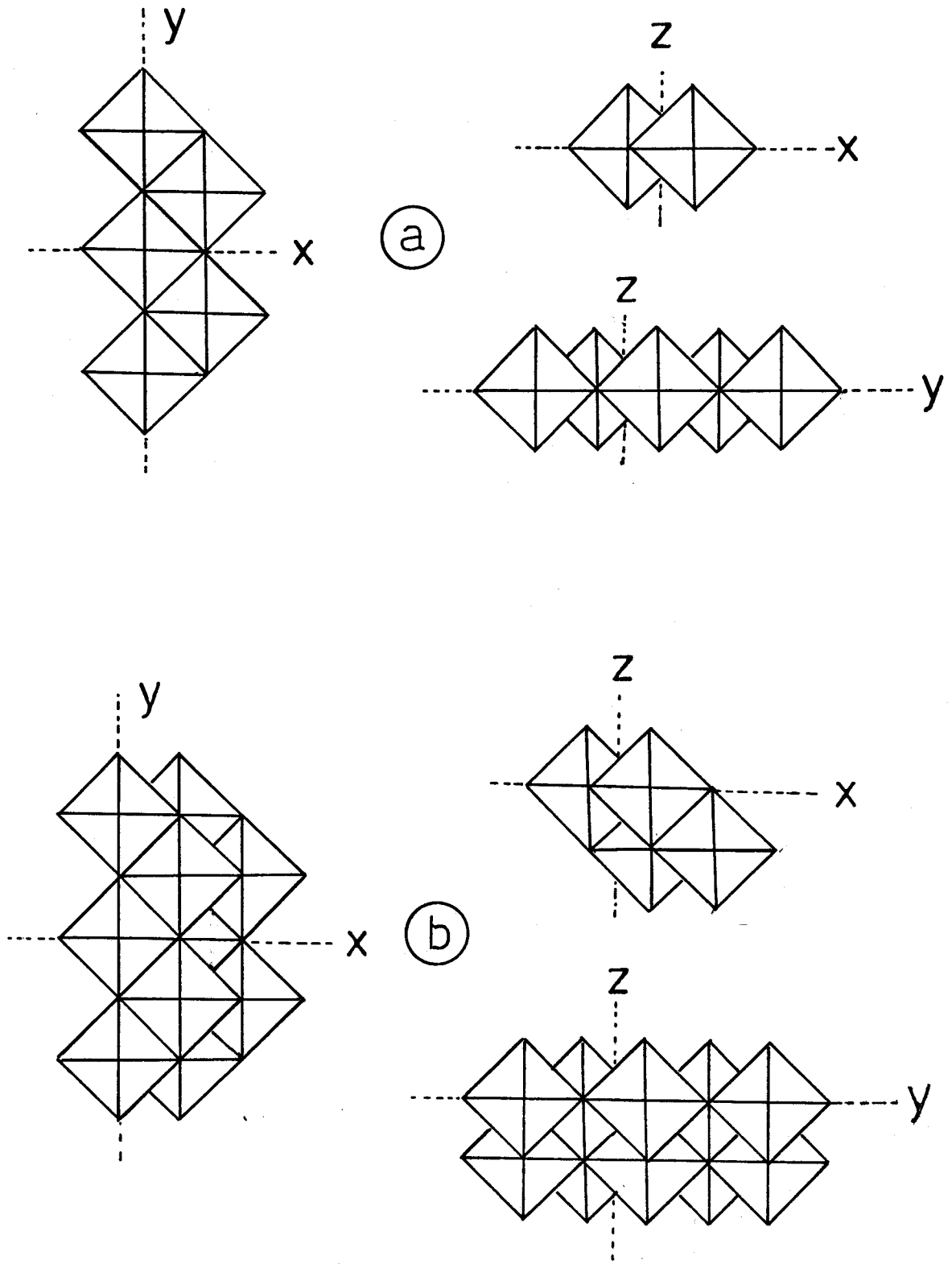

Figure 1-3. (a) Single octahedral ribbons and (b) Double octahedral ribbons as viewed from three perpendicular directions.

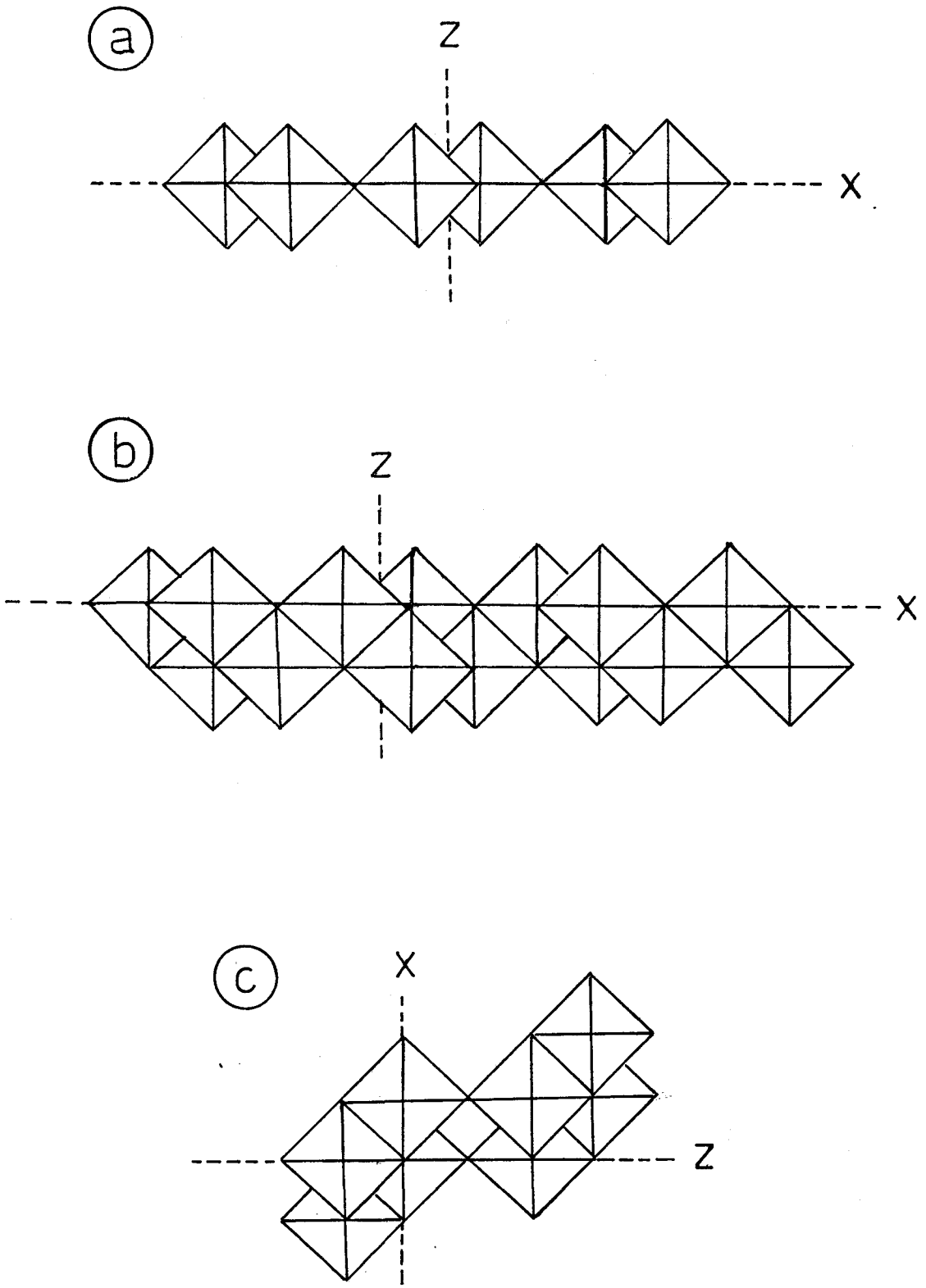

Figure 1-4. (a) Single octahedral sheet
(b) Double octahedral sheet
(c) Zig-zag octahedral sheet

ribbons are 5-fold coordinated. A second form of V_4O_9 has been reported[18] but its structure is unknown.

The last structure of the V_nO_{2n+1} series, V_6O_{13}[5], contains alternating single (fig.1-4(a)) and double sheets (fig.1-4(b)) sharing corners at the vanadyl oxygens of the double sheets.

Vanadium dioxide, VO_2, exists in at least two polymorphic forms. One structure consists of double sheets (fig.1-4(b)) sharing corners at the vanadyl oxygens of one sheet[6], and is thus related to the V_nO_{2n+1} series. The other form is a distorted rutile structure containing edge-sharing (fig.1-2(c)) octahedral chains connected by corner-sharing[7]. As will be seen, this form is related to the V_nO_{2n-1} series.

The V_nO_{2n-1}[8,9,10] structures contain two parts. A corundum type structure, containing two octahedra sharing a face and each sharing an edge with neighbouring octahedra, is joined to the next corundum part by rutile chains. The length of the chains depends on n. When n=2, these chains are not present[8], and they increase monotonically in length as n increases from 3[9,10]. VO_2[7] contains only rutile chains and may be regarded as a structure where $n\to\infty$.

Vanadium bronzes are compounds which in general have formulae $M_xV_yO_z$ where M is a metal, y and z are integers and x can be non-integral. The average oxidation state of the vanadium for particular y and z values changes over a range of x values without changing the basic structure. These bronzes have structural features similar to those of the vanadium oxides. γ-$Li_xV_2O_5$[19] has α-V_2O_5-like octahedral sheets, δ-$Ag_xV_2O_5$[20] has the double sheets seen in VO_2, and θ-$Al_xV_2O_5$[21] has alternating single and double sheets as in V_6O_{13}. β-$Na_xV_6O_{15}$[22] has double octahedral ribbons

sharing one corner each with two neighbouring double ribbons and being bridged to two more double ribbons by single ribbons. $Li_xV_3O_8$[23] has alternating single and double ribbons.

§ 1.3 The Phosphorus Oxides

Like vanadium, phosphorus exhibits multiple valences, but the P^{+5} form is the most stable form and does not reduce readily. Pentavalent phosphorus is only found tetrahedrally coordinated, but the tetrahedra can link to produce a variety of structural elements. As is the case for $V^{+5}O_4$ tetrahedra, $P^{+5}O_4$ groups can share corners to produce infinite metaphosphate chains (e.g. $NaPO_3$[24]) and pyrophosphate groups (e.g. $Zn_2P_2O_7$[25]). Rings of corner-sharing tetrahedra are also prevalent (e.g. $Na_3P_3O_9$[26] has rings of three phosphate groups, and $Na_4P_4O_{12}$[27] has rings of four phosphate groups). Substitution of vanadium for phosphorus (and vice versa) might be expected to occur in compounds where the coordination is tetrahedral. However, since the vanadium oxides have vanadium in 5-fold or octahedral coordination, the phosphorus oxides, or mixed phosphorus-vanadium oxides, are expected to have different structures from the corresponding vanadium oxides.

Phosphorus pentoxide exists in three crystalline forms. The H-Form[28] is the most common and contains four phosphate tetrahedra each of which shares a corner with each of the other three tetrahedra to form discrete P_4O_{10} groups of tetrahedral symmetry. The O-Form[29] contains rings of ten phosphate tetrahedra linked in a three-dimensional network. The O'-Form[30] contains sheets of linked six-membered rings.

§ 1.4 The Arsenic Oxides

Like phosphorus and vanadium, arsenic displays variable oxidation

states, but is most commonly found in the +5 state. Pentavalent arsenic is found tetrahedrally in structural elements similar to those of phosphorus. Meta-arsenate chains can be found in $NaAsO_3$[31], rings in $K_3As_3O_9$[32], and pyroarsenate groups in $Mg_2As_2O_7$[33]. As^{+5} is also found octahedrally coordinated, but, unlike vanadium, the octahedra are usually quite regular and contain no bond analogous to the vanadyl bond. The AsO_6 octahedra are not found as highly condensed as the VO_6 octahedra, corner-sharing being the prevalent mode of joining neighbouring AsO_6 groups.

Although the crystal structure of hydrated arsenic pentoxide has been known for some time[34], the structure of anhydrous As_2O_5 has only been determined very recently[35]. It consists of zig-zag chains of corner-sharing AsO_6 octahedra which are joined to neighbouring chains by AsO_4 tetrahedra in such a way that each tetrahedron shares corners with two octahedra in each of two chains. This intricate arrangement avoids edge-sharing polyhedra by having both tetrahedral and octahedral coordinations present. Both kinds of polyhedra are quite regular in shape.

§ 1.5 The V-P-As-O System

Pentavalent P, V and As can all be found tetrahedrally coordinated, and substitution of P^{+5} for V^{+5} in $NaVO_3$[36] and As^{+5} for P^{+5} in $NaPO_3$[37] has been found. However, substitution of one for any other does not often occur. This can be due to the preferred octahedral and 5-fold coordination of V^{+5}, thereby preventing P substitution, and the abundance of condensed octahedra and of vanadyl groups found for V and not for As. Mixed oxides can usually be expected to have different crystal structures from the single oxides of V,P and As, although to date very little is known about them.

In the early sixties, Nador[38] investigated the V_2O_5-P_2O_5 system and concluded that, on melting mixtures of these oxides, oxygen is liberated and some vanadium is reduced from V^{+5} to oxidation states of +4 and +3. A study of the electron spin resonances of samples with different stoichiometries allowed him to conclude that the V_2O_5-P_2O_5 system consisted of a single two-component system and two three-component systems with upper and lower boundaries as shown in figure 1-5. The boundaries established the existence of $(VO)_2P_2O_7$ and $V(PO_3)_3$, but no indication was given about the composition of other phases.

Ladwig[39] also noticed a reduction of all forms of $V^{+5}PO_5$ (formed from a 1:1 mixture of V_2O_5 and P_2O_5) at temperatures greater than 700°C, forming a V^{+4} compound. This observation was recently verified by Bordes and Courtine[40] and the reduction product was identified as $(VO)_2P_2O_7$. Bordes and Courtine[40] established the presence of $P_2O_7^{-4}$ and vanadyl groups in this compound from IR and UV spectra. The reduction of VPO_5 is contrary to the observations of Jordan and Calvo[11], who report no appreciable mass loss of α-VPO_5 up to 1140°C, well beyond its melting point.

VPO_5 itself is found in several forms and has been rather extensively studied. The structures and properties of α-VPO_5[11,39,41], β-VPO_5[12,39,41] and the hydrates of VPO_5[39,41] have all been reported. Since these compounds are fundamental to the V-P-As-O system, they will be briefly described.

The structure of α-VPO_5[11] consists of layers containing alternating corner-sharing VO_6 octahedra and PO_4 tetrahedra (fig.1-6). The VO_6 octahedra contain the typical vanadyl oxygens perpendicular to the plane of figure 1-6, which form long bonds to VO_6 groups in the next layer. This is the only connection between layers. The layers may be disordered by

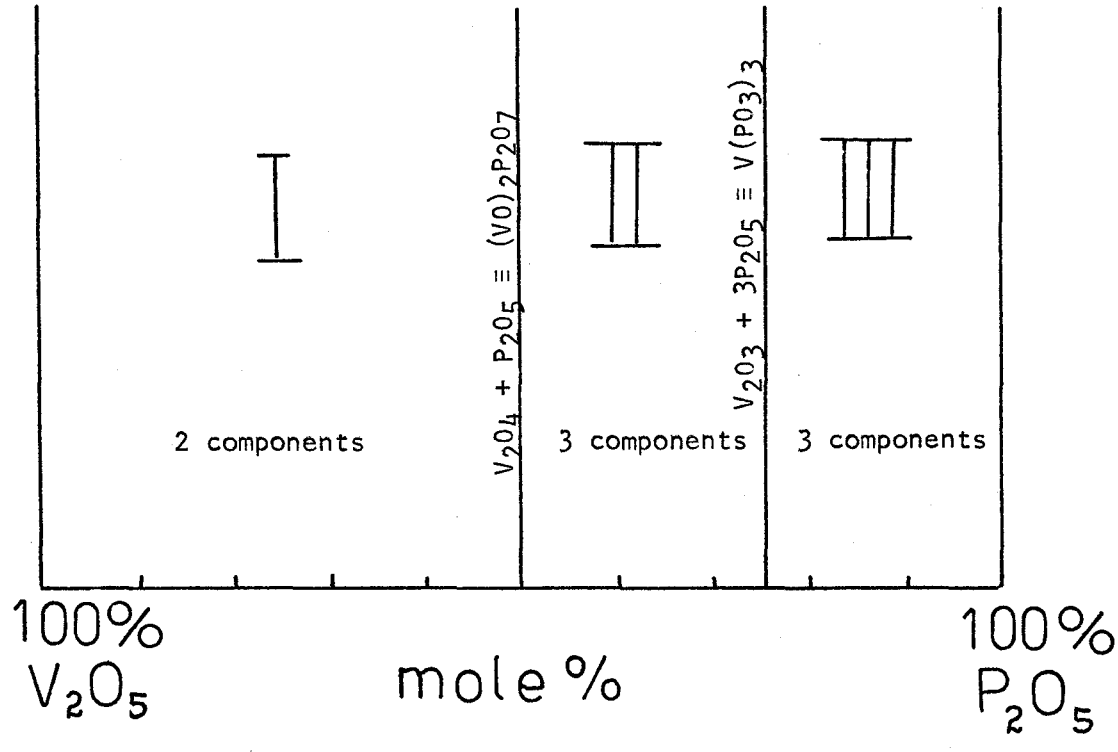

Figure 1-5. Regions in the vanadium phosphorus oxide system as proposed by Nador[38].

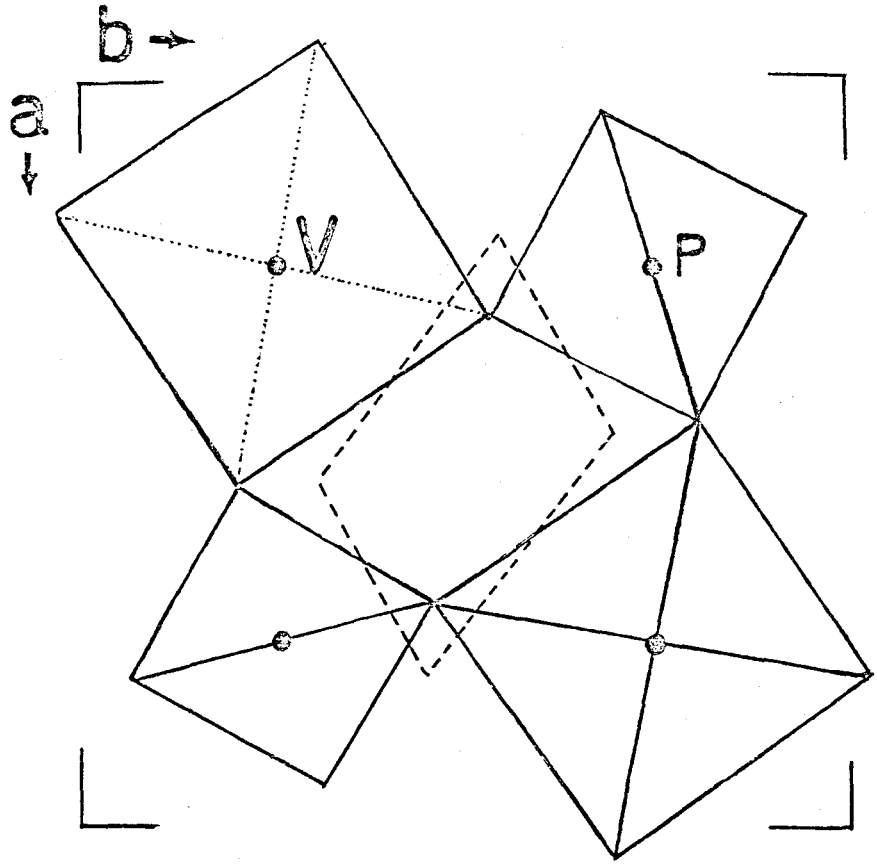

Figure 1- 6. The crystal structure of α-VPO_5 as projected down the c-axis. The disordered positions of the oxygens are at the apices of the dashed parallellogram.

a slight rotation about the direction of the vanadyl bonds as indicated in figure 1-6 by the dashed lines. Because of the layered structure, crystals of α-VPO_5 grow in mica-like sheets. Evidence for some vanadium substitution at the phosphorus site has been found[42].

β-VPO_5[12] (figure 1-7) contains chains of VO_6 octahedra parallel to a arranged with the vanadyl oxygen of one group forming the long axial V-O bond of the next group. The psuedo 4-fold axes of the VO_6 groups are alternately tilted by $+30^\circ$ and -30° with respect to the direction of the chain. This tilting makes it possible for a phosphate group to share an oxygen with each of two VO_6 octahedra in one chain. The other two phosphate oxygens are shared with a VO_6 group in each of two other chains.

Ladwig[39] has described the production of $VPO_5.2H_2O$ from a V_2O_5-phosphoric acid mixture and has shown that, on heating it slowly, $VPO_5.H_2O$ is formed at 60-80°C and at 150°C α-VPO_5 is formed. He also noticed an expansion of the c-axis of α-VPO_5 on hydration. This led him to conclude that the structure of the hydrates must be the layered structure of α-VPO_5 with water molecules interstitially between the layers. No hydrates are known to form from β-VPO_5, nor is there any evidence for an $\alpha \rightarrow \beta$ transition.

A preparation for $V^{+4}O(PO_3)_2$, its blue colour and its insolubility in most solvents were reported by Ladwig[43] in 1968. Preparations for this compound and $V(PO_3)_3$ have also been reported recently and separately by Lavrov, et al.[44] and Tofield, et al.[45]. From IR data, Lavrov concluded that $VO(PO_3)_2$ is a metaphosphate and Tofield interpreted the diffuse transmission spectrum to show the existence of vanadyl groups. Both conclude $V(PO_3)_3$

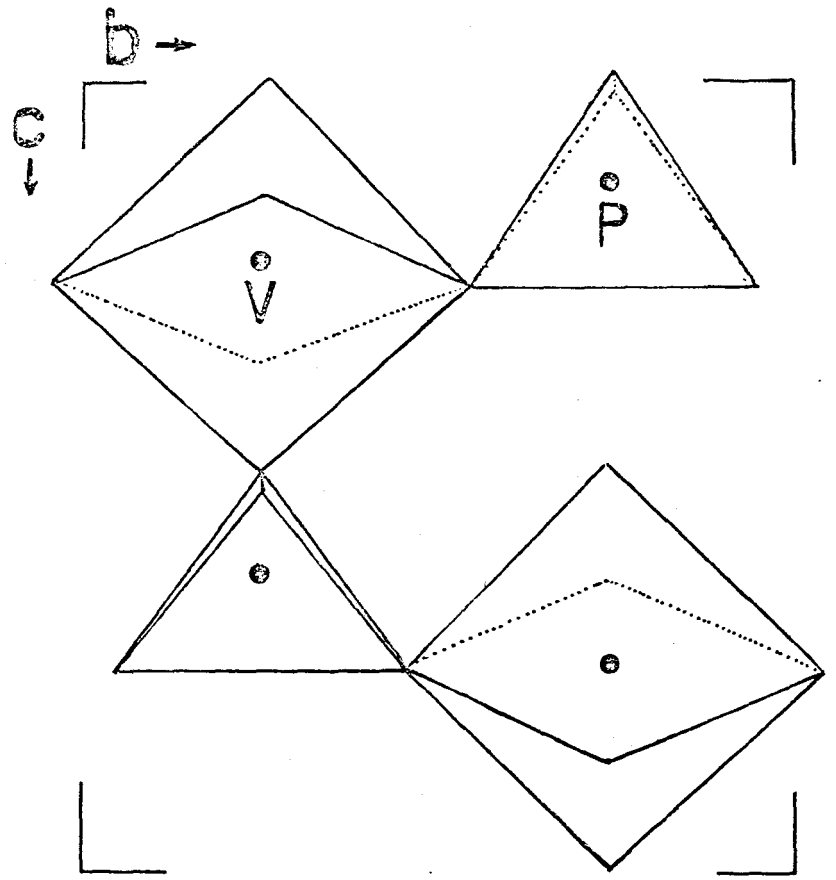

Figure 1-7. The crystal structure of β-VPO_5 projected down the a-axis. The second half of the cell can be generated from the one shown by a centre of symmetry at $(\frac{1}{2},\frac{1}{2},\frac{1}{2})$.

contain metaphosphate chains.

The crystal structure of VOP_2SiO_8 was solved independently by ourselves and Rice, et al[46] but their work appeared in print prior to ours[47].

Very little is known about the crystalline vanadium arsenic and phosphorus arsenic oxides. The existence of $VAsO_5$ and its hydrate has been reported[48,49], and a powder pattern of the anhydrous material appears to be the same as that of α-VPO_5. No other vanadium arsenic oxides are known. Crystals of the form $As_xP_{2-x}O_5$ have been studied[50] and were found to be isostructural with As_2O_5 for $1 \leq x \leq 2$ from powder data.

§ 1.6 Reduction of Vanadium Oxides

V_2O_5 consists of single octahedral sheets, V_6O_{13} consists of alternating single and double octahedral sheets, and VO_2 consists of double octahedral sheets. If one sheet in the V_2O_5 structure is cooperatively moved along a shear plane as in figure 1-8(a), then a double sheet will be formed. By this mechanism, geometrically at least, conversion of V_2O_5 into V_6O_{13}[51] (fig.1-8(b)) can be accomplished by moving every third sheet of V_2O_5 in such a fashion, and conversion into VO_2 can be accomplished by moving every second sheet along the shear plane. Studies have been done to determine if such a reduction mechanism does in fact occur. Electron microscope studies, whereby carbon is deposited on the surface of a crystal and is thus capable of aiding reduction by forming CO and CO_2, have failed to show VO_2 production from V_2O_5, but have confirmed the conversion of V_6O_{13} into VO_2[52] and a cooperative movement of octahedra as depicted in figure 1-9 has been suggested for the mechanism of this reduction. The reduction of V_2O_5 to V_6O_{13} under these conditions has been the subject of some controversy. Fiermans and Vennik[53] have noted

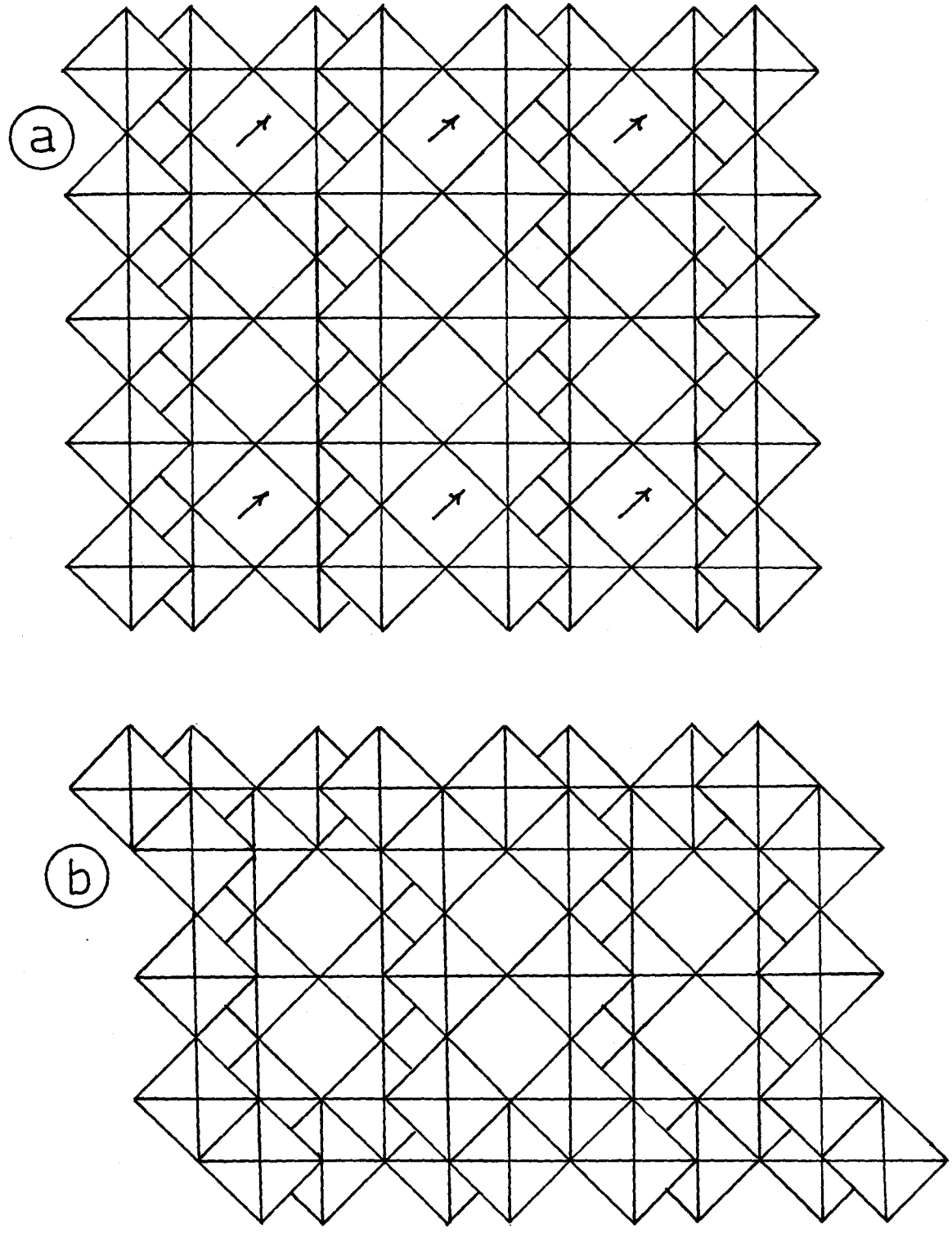

Figure 1-8. Schematic diagram of V_2O_5 (a) forming V_6O_{13} (b) by a shear in the direction indicated by the arrows.

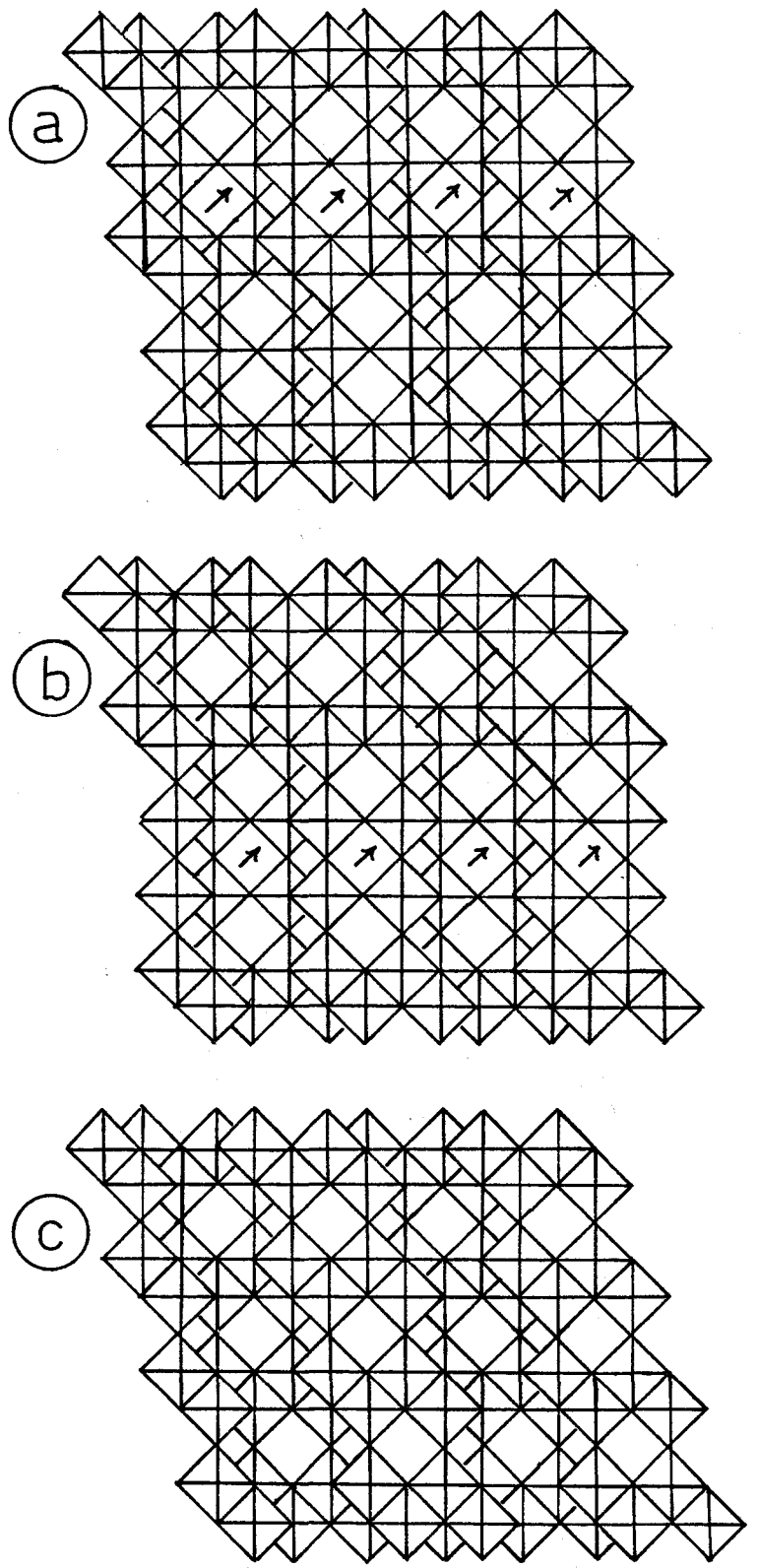

Figure 1-9. Formation of VO_2 (c) from V_6O_{13} (a) through the cooperative movement of octahedra ((a) and (b))

and studied this transition by low energy electron diffraction, but Tilley and Hyde[54] have found no evidence for such a shear using transmission electron microscopy. These authors did find a reduced vanadium oxide phase produced which was later identified as a new V_4O_9 phase by Grymonprez[18], et al.

The possibility of V_2O_5 and V_6O_{13} reducing through the formation of shear structures and/or vacancy formation appears likely but has not been conclusively established. In each of the cases studied, the vanadyl oxygen is the oxygen which is removed. This is exactly the mechanism which is suggested for the action of a V_2O_5 catalyst in the oxidation of hydrocarbons by Sachtler[55] to account for the production of V^{+4} in spent catalysts. He suggested that the vanadyl oxygens exposed on the surface of V_2O_5 were removed during the catalytic process. The vacancies so created can diffuse into the bulk of the V_2O_5 catalysts. This is an easy process since the $V^{+4}O_5$ groups so established can have many configurations. When the vacancies are at the appropriate oxygen sites for a shear to occur, the V_6O_{13} configuration is formed. Although no direct structural evidence is available, there is evidence that the vanadium is reduced in the catalytic process and that the vanadyl oxygen is released[56,57].

§ 1.7 Vanadium Phosphate Catalysts

A great number of patents in the US, Japan, and Germany exist for the use of vanadium phosphate catalysts in the commercial production of maleic anhydride from butene, butane and other hydrocarbons, but very little academic literature is available. The oxidation of butene (either 1-butene or 2-butene) over vanadium phosphates is thought to proceed by the following steps[58,59,60].

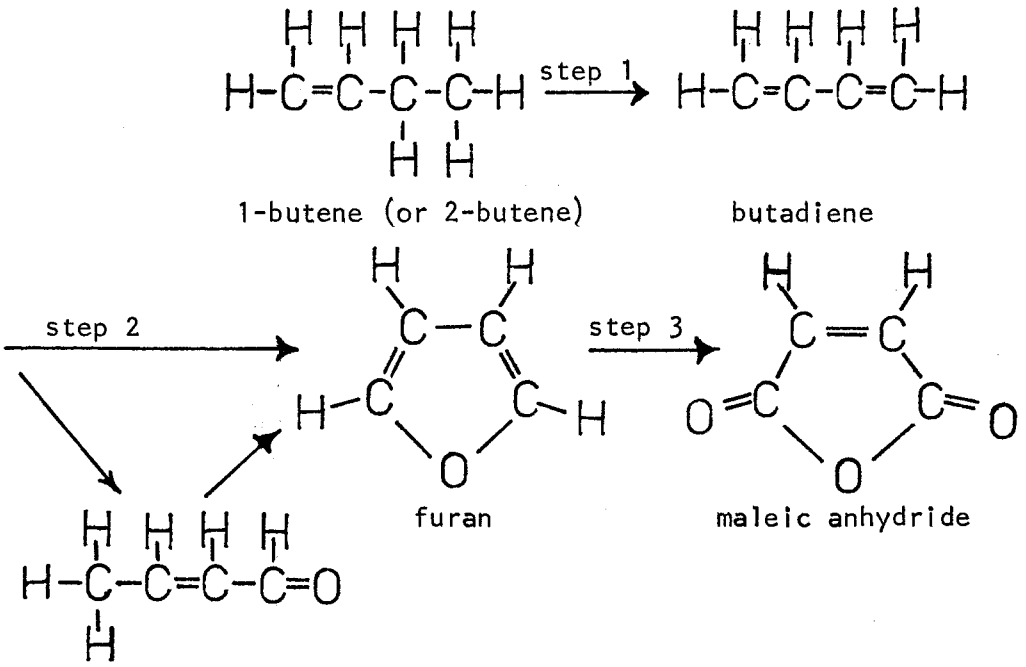

Seeboth et al.[59,60] found that crotonaldehyde was often an intermediate in step 2 as shown above.

Ai[58] found that, although the activity (i.e. the number of sites active in catalysis) decreased from pure vanadium oxide catalysts to vanadium phosphates, the selectivity of the butene → maleic anhydride reaction (or the preferred production of the desired product rather than side-products) increased with phosphorus content. This has also been observed by several other workers[40,56,59,61]. Ai considered each step in the reaction and found that phosphorus addition increased the selectivity in step 1 and step 2 and decreased it in step 3.

Ai and Suzuki[62] found that the affinity of V_2O_5 catalysts for basic (i.e. electron donating) olefins decreases with P_2O_5 content, and hence the acid strength of vanadium phosphate catalysts must be smaller that that of V_2O_5. They suggest that this lower acid strength enhances the probability of maleic acid production rather than side-products such

as acetic acid, acetaldehyde and carbon dioxide.

VPO_5, when used as a catalyst, reduces to $(V^{+4}O)_x(V^{+5}O)_{1-x}PO_{4-x/2}$[40,59,60] with the end-product being $VOPO_{3.5} \equiv (VO)_2P_2O_7$. Bordes and Courtine[40] found that on slow heating of VPO_5 to around 750°C, a metastable intermediate, $VPO_{4.75}$, was formed which reduced on further heating to $VPO_{4.5}$. In addition, both α and β-VPO_5 were found to reduce to $VPO_{4.5}$, but only α-VPO_5 was formed on re-oxidation.

Nakamura[61] found that the yield of a catalyzed reaction decreased rapidly as the average oxidation number of the vanadium became less than 4.0. He concluded that the redox cycle between V^{+5} and V^{+4} is mainly responsible for the catalysis, and that the vanadyl bond was important in the process. He suggested a mechanism whereby oxygen from the air would add to the vanadium at the side opposite the vanadyl bond, thereby forming a sixth oxygen bond which is available for oxidation of the butene (fig.1-10). One supposes that at the surface the long V-O bond is missing, a not unreasonable assumption since charge conservation would require something of this sort. This mechanism was suggested for the P:V = 2:1 catalyst since Nakamura found it to be the most selective. Bordes and Courtine[40] however, found that $VO(PO_3)_2$ was not catalytically active.

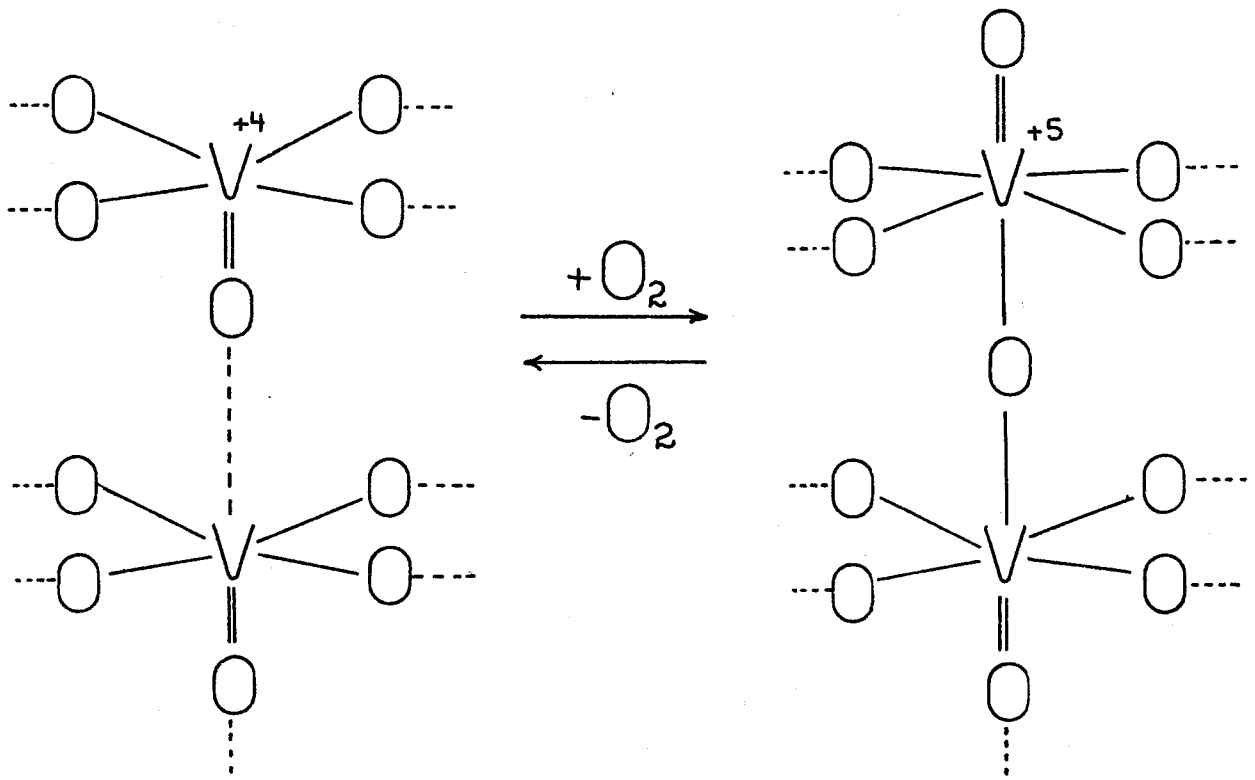

Figure 1-10. Redox mechanism occuring during catalysis using a vanadium phosphate catalyst as suggested by Nakamura[61]. The equatorial oxygen atoms are bonded to vanadium and phosphorus atoms. The axial atoms are only bonded to vanadium.

CHAPTER 2

The Theory of X-Ray Diffraction

§ 2.1 Scattering of X-Rays

X-rays fall in the short wavelength, high energy region of the electromagnetic spectrum, and, like all electromagnetic radiation, can be scattered from matter inelastically (Compton scattering) with a change in wavelength or elastically, without a change in wavelength. It is the elastic scattering that enables one to determine crystal structures.

Many good books have been written describing the theory of x-ray scattering*; only the main ideas and those particularly relevant to this thesis will be summarized here.

If we consider an incident x-ray wave of wave-vector $\underline{k}_o$ scattered elastically from an electron at an arbitrary origin and one at a distance $\underline{r}$ away, the amplitude of the resultant wave-vector $\underline{k}$ will be proportional to $\exp(i\Delta\underline{k}\cdot\underline{r})$ where $\Delta\underline{k} = \underline{k}_o - \underline{k}$. If instead the scattering occurs from an electron distribution with electron density $\rho(\underline{r})$, then the resulting amplitude will be

$$A(\Delta\underline{k}) = \int \rho(\underline{r}) \exp(i\Delta\underline{k}\cdot\underline{r})\, dV, \qquad (2\text{-}1)$$

where the integral is over the volume containing the charge density.

An ideal crystal has three-dimensional translational symmetry. If the repeating unit, i.e. the unit cell, is defined by the vectors $\underline{a}$, $\underline{b}$ and $\underline{c}$, then for an ideal crystal, the electron density at a point $\underline{r}$ is $\rho(\underline{r}) = \rho(\underline{r}+x\underline{a}+y\underline{b}+z\underline{c})$ for all integers x,y and z. Using this relationship,

*see for example books by Zachariasen[63], Cowley[64], James[65] or Warren[66].

the amplitude in equation 2-1 now becomes, for an ideal crystal,

$$A(\Delta\underline{k}) = \sum_{xyz} \exp(i\Delta\underline{k}\cdot\underline{R}) \int_{u.c.} \rho(\underline{r})\exp(i\Delta\underline{k}\cdot\underline{r})dV\,, \tag{2-2}$$

where $\underline{R} = x\underline{a}+y\underline{b}+z\underline{c}$, and the integration is carried out over the volume of the unit cell, and the sum is over the dimension of the crystal. For a crystal containing N_x, N_y and N_z unit cells in the x,y and z directions,

$$\sum_{xyz} \exp(i\Delta\underline{k}\cdot\underline{R}) = \sum_{x=1}^{N_x} \exp(i\Delta\underline{k}\cdot x\underline{a}) \sum_{y=1}^{N_y} \exp(i\Delta\underline{k}\cdot y\underline{b}) \sum_{z=1}^{N_z} \exp(i\Delta\underline{k}\cdot z\underline{c})$$

$$= \frac{(1-\exp(iN_x\Delta\underline{k}\cdot\underline{a}))}{(1-\exp(i\Delta\underline{k}\cdot\underline{a}))} \cdot \frac{(1-\exp(iN_y\Delta\underline{k}\cdot\underline{b}))}{(1-\exp(i\Delta\underline{k}\cdot\underline{b}))} \cdot \frac{(1-\exp(iN_z\Delta\underline{k}\cdot\underline{c}))}{(1-\exp(i\Delta\underline{k}\cdot\underline{c}))}\,. \tag{2-3}$$

The intensity of the scattered wave is

$$I = A(\Delta\underline{k})A^*(\Delta\underline{k})$$

$$= \sum_{xyz} \exp(i\Delta\underline{k}\cdot\underline{R}) \sum_{xyz} \exp(-i\Delta\underline{k}\cdot\underline{R}) \int_{u.c.} \rho(\underline{r})\exp(i\Delta\underline{k}\cdot\underline{r})dV \int_{u.c.} \rho(\underline{r})\exp(-i\Delta\underline{k}\cdot\underline{r})dV, \tag{2-4}$$

where the designation (*) implies the complex conjugate of the expression. Upon substitution of equation 2-3 into 2-4 and simplification of the sums,

$$I = \int_{u.c.} \rho(\underline{r})\exp(i\Delta\underline{k}\cdot\underline{r})dV \int_{u.c.} \rho(\underline{r})\exp(-i\Delta\underline{k}\cdot\underline{r})dV$$

$$\cdot \frac{\sin^2(\frac{1}{2}(\Delta\underline{k}\cdot N_x\underline{a}))}{\sin^2(\frac{1}{2}(\Delta\underline{k}\cdot\underline{a}))} \cdot \frac{\sin^2(\frac{1}{2}(\Delta\underline{k}\cdot N_y\underline{b}))}{\sin^2(\frac{1}{2}(\Delta\underline{k}\cdot\underline{b}))} \cdot \frac{\sin^2(\frac{1}{2}(\Delta\underline{k}\cdot N_z\underline{c}))}{\sin^2(\frac{1}{2}(\Delta\underline{k}\cdot\underline{c}))}\,. \tag{2-5}$$

Because N_x, N_y and N_z are very large numbers, this expression has sharp maxima at

$$\Delta\underline{k} = 2\pi\underline{H} = 2\pi(h\underline{a}^* + k\underline{b}^* + \ell\underline{c})\,, \tag{2-6}$$

where h, k and ℓ are integers and $\underline{a}^*$, $\underline{b}^*$ and $\underline{c}^*$ are called reciprocal lattice vectors and are defined as:

$$\underline{a}^* = \frac{\underline{b}\times\underline{c}}{\underline{a}\ \underline{b}\times\underline{c}} \qquad \underline{b}^* = \frac{\underline{c}\times\underline{a}}{\underline{a}\ \underline{b}\times\underline{c}} \qquad \underline{c}^* = \frac{\underline{a}\times\underline{b}}{\underline{a}\ \underline{b}\times\underline{c}}\,. \tag{2-7}$$

For very large N_x, N_y and N_z, the maxima are so sharp that the intensity is non-zero only for $\underline{k} = 2\pi\underline{H}$, and has a value N^2 where $N = N_x N_y N_z$. This is one formulation of Bragg's law, and shows that x-ray scattering from ideal crystals, rather than being a continuum, consists of a distinct number of "reflections" defined by condition 2-6.

Using Bragg's law, equation 2-2 now becomes

$$A(\Delta\underline{k}) = A(\underline{H}) = N \int_{u.c.} \rho(\underline{r}) \exp(2\pi i \underline{H}\cdot\underline{r}) dV$$

$$= NF, \qquad (2\text{-}8)$$

where N is the number of unit cells in the crystal and F, the structure factor, defined as equal to the integral in equation 2-8, is the Fourier transform of the electron density distribution $\rho(\underline{r})$.

In a crystal, the electron density can be considered as the sum of electron densities of individual atoms:

$$\text{i.e. } \rho(\underline{r}) = \sum_j \rho_j(\underline{r}'+\underline{r}_j), \qquad (2\text{-}9)$$

where $\underline{r}_j$ is the position vector of the centre of the $j^{\underline{th}}$ atom and $\underline{r}'$ is a vector within this atom. Consequently, the structure factor for a crystal considering the different atoms in the unit cell separately becomes,

$$F(\underline{H}) = \sum_j \int \rho_j(\underline{r}') \exp(2\pi i \underline{H}\cdot(\underline{r}'+\underline{r}_j)) dV$$

$$= \sum_j f_j \exp(2\pi i \underline{H}\cdot\underline{r}_j), \qquad (2\text{-}10)$$

where the integral is now over the volume of one atom. f_j, the atomic scattering factor, is the Fourier transform of the electron density of the $j^{\underline{th}}$ atom.

$$f_j = \int \rho_j(\underline{r}') \exp(2\pi i \underline{H}\cdot\underline{r}') dV. \qquad (2\text{-}11)$$

Atomic scattering factors have been calculated for theoretical free atoms using various types of wave-functions such as Hartree-Fock[67] and Slater[68] functions and are tabulated in the literature.

§ 2.2 Space Groups and Crystal Symmetry

Not only do crystals have three-dimensional translational symmetry with respect to the unit cell distances, the atoms within an individual unit cell can also be related by rotational and reflection symmetry. It can be shown[63] that all possible combinations of such symmetry operations can be classified in 230 space groups.

Some symmetry operations can restrict the values of h, k and ℓ for the vector $\underline{H}$ for which the intensity has a non-zero value. For example, a body-centred space group has an atom at $x+\frac{1}{2}$, $y+\frac{1}{2}$, $z+\frac{1}{2}$ for every atom at x, y, z. The structure factor for such a space group will be

$$\begin{aligned} F(\underline{H}) &= \sum_j f_j \exp(2\pi i \underline{H}\cdot\underline{r}_j) \\ &= \sum_m f_m \exp(2\pi i(hx+ky+\ell z)) + f_m \exp(2\pi i(hx+\tfrac{1}{2}h+ky+\tfrac{1}{2}k+\ell z+\tfrac{1}{2}\ell)) \\ &= \sum_m f_m \exp(2\pi i(hx+ky+\ell z))(1+\exp(2\pi i(\tfrac{1}{2}h+\tfrac{1}{2}k+\tfrac{1}{2}\ell)), \end{aligned} \qquad (2\text{-}12)$$

where the sum over m is over pairs of atoms related by body-centred symmetry. The last term in the expression will be zero if $h+k+\ell \neq 2n$ where n is an integer. Thus if all $h+k+\ell \neq 2n$ reflections for a particular crystal have zero intensity, that crystal has a body-centred space group.

Sets of reflections with zero-intensity (such as the $h+k+\ell \neq 2n$ ones for body-centred crystals) are called systematic extinctions. Systematic extinctions can be found for glide planes, screw axes and centering conditions. A careful examination of the systematic extinctions

for a particular crystal will often yield the space group for the crystal, or reduce the possible space groups to two or three that have the same extinctions.

§ 2.3 Deviations from Translational Periodicity

So far, it has been assumed that crystals have perfect translational symmetry in three dimensions. Real crystals in fact deviate from this periodicity in several ways. Atoms vibrate about an equilibrium position (thermal motion), and need not always be in phase with corresponding atoms in other unit cells; certain atoms may randomly occupy one of several possible positions in different unit cells (positional disorder), and sometimes different kinds of atoms may occupy the same position in different cells (substitutional disorder). In addition, unit cells may not be aligned exactly with respect to neighbouring cells. This misalignment can occur between blocks of perfectly aligned cells (mosaic spread), layers of cells (one-dimensional disorder or stacking faults), or chains of cells (two-dimensional disorder). Thermal motion occurs in all crystals. The other kinds of disorder may or may not occur to a significant extent depending on the crystal. Disorders considered in this thesis will be briefly discussed.

(a) Thermal motion

Atoms at any instant in time are located at $\underline{r}' = \underline{r}_j + \underline{\delta}_j$ where $\underline{r}_j$ is the position vector for the average position of atom j and $\underline{\delta}_j$ is the instantaneous displacement from this position. It is a function of time and of temperature, increasing as the latter increases. The structure factor thus becomes, formally,

$$F(\underline{H}) = \sum_j f_j \exp(2\pi i \underline{H}\cdot(\underline{r}_j + \underline{\delta}_j)), \qquad (2\text{-}13)$$

and the intensity is

$$I = N^2 \sum_{i,j} f_j f_i^* \exp(2\pi i \underline{H}\cdot(\underline{r}_j+\underline{\delta}_j)) \exp(-2\pi i \underline{H}\cdot(\underline{r}_i+\underline{\delta}_i))$$

$$= N^2 \sum_{i,j} f_j f_i^* \exp(2\pi i \underline{H}\cdot(\underline{r}_j-\underline{r}_i)) \exp(2\pi i \underline{H}\cdot(\underline{\delta}_j-\underline{\delta}_i)). \qquad (2\text{-}14)$$

This is the instantaneous intensity at any one time. Experimentally, the time average of this value is observed. This time average is indicated by $\langle \cdots \rangle$.

$$\langle I \rangle = N^2 \sum_{i,j} f_j f_i^* \exp(2\pi i \underline{H}\cdot(\underline{r}_j-\underline{r}_i)) \langle \exp(2\pi i \underline{H}\cdot(\underline{\delta}_j-\underline{\delta}_i)) \rangle . \qquad (2\text{-}15)$$

For small displacements,

$$\langle \exp 2\pi i \underline{H}\cdot(\underline{\delta}_j-\underline{\delta}_i) \rangle = 1 + i\langle 2\pi \underline{H}\cdot(\underline{\delta}_j-\underline{\delta}_i) \rangle - \tfrac{1}{2}\langle (2\pi \underline{H}\cdot(\underline{\delta}_j-\underline{\delta}_i))^2 \rangle - \cdots$$

$$\simeq 1 - \tfrac{1}{2}\langle (2\pi \underline{H}\cdot(\underline{\delta}_j-\underline{\delta}_i))^2 \rangle$$

$$= \exp(-\pi \langle (\underline{H}\cdot(\underline{\delta}_j-\underline{\delta}_i))^2 \rangle)$$

$$= \exp(-\pi \langle (\underline{H}\cdot(\underline{\delta}_j-\underline{\delta}_i))^2 \rangle) \exp(-\pi \langle (\underline{H}\cdot(\underline{\delta}_j-\underline{\delta}_i))^2 \rangle)$$

$$\cdot \exp(2\pi \langle (\underline{H}\cdot\underline{\delta}_j)(\underline{H}\cdot\underline{\delta}_i) \rangle), \qquad (2\text{-}16)$$

since odd powers average to zero and large powers in the Taylor series are negligible.

Thus the average intensity

$$I = N^2 \sum_{i,j} f_j \exp(2\pi i (\underline{H}\cdot\underline{r}_j)) \exp(\pi \langle (\underline{H}\cdot\underline{\delta}_j)^2 \rangle) f_i^* \exp(2\pi i (\underline{H}\cdot\underline{r}_i)) \exp(\pi \langle \underline{H}\cdot\underline{\delta}_i)^2 \rangle)$$

$$\cdot (1 + \exp(2\pi \langle (\underline{H}\cdot\underline{\delta}_j)(\underline{H}\cdot\underline{\delta}_i) \rangle) - 1)$$

$$= N^2 \left| \sum_j f_j \exp(2\pi i (\underline{H}\cdot\underline{r}_j)) \exp(-2M_j) \right|^2 + \text{second term containing } (\exp(2\pi \langle (\underline{H}\cdot\underline{\delta}_j)(\underline{H}\cdot\underline{\delta}_i) \rangle) - 1) . \qquad (2\text{-}17)$$

$2M_j$ is called the Debye-Waller factor and is equal to $\langle (\underline{H}\cdot\underline{\delta}_j)^2 \rangle \pi$.

The first term in expression 2-17 has a sharp maximum intensity at the Bragg reflection. The second term will give rise to a small diffuse background called thermal diffuse scattering which is negligible in intensity compared to the Bragg reflection.

Thus, when taking thermal motion into account, the structure factor must be modified to

$$F(\underline{H}) = \sum_j f_j \exp(2\pi i(\underline{H}\cdot\underline{r}_j))\exp(-2M_j) \cdot \qquad (2\text{-}18)$$

It is customary to write

$$2M_j = \beta^j_{11}h^2 + \beta^j_{22}k^2 + \beta^j_{33}\ell^2 + \beta^j_{12}hk + \beta^j_{13}h\ell + \beta^j_{23}k\ell \, , \qquad (2\text{-}19)$$

where the β are known as the anisotropic thermal coordinates and describe the ellipsoid of vibration of atom j at the temperature considered.

(b) Positional and Substitutional Disorder

Bragg's law will no longer be completely valid when disordering occurs, and equation 2-1 becomes

$$\begin{aligned} A(\Delta\underline{k}) &= \sum_{xyz} \exp(i\Delta\underline{k}\cdot\underline{R}) \int_{u.c.} \rho(\underline{r})\exp(i\Delta\underline{k}\cdot\underline{r})dV \\ &= \sum_{xyz} \exp(i\Delta\underline{k}\cdot\underline{R}) \sum_j f_j(\Delta\underline{k})\exp(i\Delta\underline{k}\cdot\underline{r}_j) \\ &= \sum_{xyz} \exp(i\Delta\underline{k}\cdot\underline{R})F'(\Delta\underline{k}) \, , \end{aligned} \qquad (2\text{-}20)$$

where $\underline{R}$, as before, is $x\underline{a}+y\underline{b}+z\underline{c}$, and where the F' may be different for each unit cell. They can differ in magnitude due to a difference in f_j values (substitutional disorder) or in phase due to a difference in $\underline{r}_j$ values (positional disorder) or both.

Equation 2-20 can be re-arranged as

$$A(\Delta\underline{k}) = \sum_{xyz} (F_p + F_{np})\exp(i\Delta\underline{k}\cdot\underline{R}) \, , \qquad (2\text{-}21)$$

where the F' have been divided into a periodic part (F_p) which represents the "average" structure factor for the cells, and stays the same for all the cells, and a non-periodic part (F_{np}) which varies from cell to cell and represents the deviations from the average cell. The intensity using equation 2-21 now becomes

$$I = \left| \sum_{xyz} \exp(i\Delta\underline{k}\cdot\underline{R})F_p \right|^2 + \left| \sum_{xyz} \exp(i\Delta\underline{k}\cdot\underline{R})F_{np} \right|^2$$
$$+ \sum_{xyz} \exp(i\Delta\underline{k}\cdot\underline{R})F_p \sum_{xyz} \exp(-i\Delta\underline{k}\cdot\underline{R})F^*_{np}$$
$$+ \sum_{xyz} \exp(-i\Delta\underline{k}\cdot\underline{R})F^*_p \sum_{xyz} \exp(i\Delta\underline{k}\cdot\underline{R})F_{np} \quad . \qquad (2\text{-}22)$$

$\sum_{xyz} \exp(i\Delta\underline{k}\cdot\underline{R})F_p$ occurs in the first and last two terms of equation 2-22, and has a non-zero value only at the Bragg points defined by $\Delta\underline{k} = 2\pi\underline{H}$. The intensity arising due to the first term is thus the Bragg intensity associated with the average cell. The sum of the non-periodic parts normally cancels out in the last two terms if the average cell has been properly chosen. The second term can be non-zero for any value of $\Delta\underline{k}$, its magnitude depending on the kind and extent of disorder. In general, this term represents a diffuse background for the Bragg reflection.

(c) Stacking Faults

When a crystal consists of a layered structure in such a way that one layer may be displaced from or be different in contents from the other layers, a one-dimensional disorder in the direction perpendicular to the layers is present. This disorder can be recognized in the diffraction pattern by the existence of streaks through the Bragg peaks in the $\underline{c}^*$ direction for disorder in the $\underline{c}$ direction. The diffraction intensities have been calculated generally for such disorders by Jagodzinski[69],

Kakinoki and Komura[70] and Cowley[71]. The resulting expressions and their derivations will not be reproduced here, but may readily be found in the literature. The intensity expressions usually do not yield to convenient calculations except for special cases where simplifications can be made. One such case will be discussed in chapter 8, and the intensity expression for it will be derived at that time. In general, the intensity can be broken up into terms of intensity produced due to layers stacked without faults, with one fault, with two faults, etc., and the total intensity is the sum of all these terms.

(d) Mosaic Spread

Crystals normally consist of many small "mosaic" blocks which contain cells in perfect alignment, but which are slightly misaligned with respect to each other. The amount of misalignment is called the mosaic spread of the crystal. The mosaic blocks are larger in dimension than the coherence length of x-rays, thus each block produces a diffracted beam independent of the others, and the total intensity of the diffracted beams is equal to the sum of the individual beams from each block. Since the mosaic spread is usually small compared to the reciprocal cell dimensions, the effect of the blocks is a slight broadening of the Bragg peak in the diffraction pattern.

When an x-ray beam is scattered from a reflecting plane, energy is transferred to the diffracted wave, thus reducing the incident beam intensity. When this effect occurs within one mosaic block, the integrated intensity of that block is lessened. This is known as primary extinction. Secondary extinction occurs when the incident beam is attenuated between the blocks before it reaches a particular block. The mosaic blocks are

normally small enough, or can be made small enough, so that the effect of primary extinction is negligible, but secondary extinction often has an appreciable effect on the intensities and is most noticeable with strong reflections. Zachariasen[72] has worked out the value of the secondary extinction correction and Larson[73] has suggested it may be used to relate the observed and calculated intensities by means of the formula

$$F^2_{obs} = F^2_{calc}(1 - g\beta F^2_{calc.})^{-\frac{1}{2}}, \qquad (2\text{-}23)$$

where F_{obs} and F_{calc} are the observed and calculated structure factors respectively, β is an effective absorption coefficient as derived by Zachariasen[72] and g is a measure of the amount of secondary extinction. It is normally an experimentally determined parameter.

§ 2.4 Effect of Domain Size on Intensities

When disorder is present in a crystal, it becomes important to consider the distance between each kind of unit cell. If each kind of unit cell is grouped in a domain which has dimensions small compared to the coherence length of the x-rays, then the total scattering amplitude will be the sum of the amplitudes of each of the cell kinds. If the domain dimensions are much greater than the x-ray coherence length, the total intensity will be the sum of the intensities of each of the cell kinds. Thus,

$$F_{total} = F_a + F_b, \qquad (2\text{-}24)$$

or

$$I_{total} = |F_a + F_b|^2 \qquad (2\text{-}25)$$

for a domain consisting of cells of type "a" and one consisting of type "b" cells, when the domain size is much smaller than the coherence length,

and,

$$I_{total} = |F_a|^2 + |F_b|^2 , \qquad (2\text{-}26)$$

when the domain size is much greater than the coherence length. Equations 2-25 and 2-26 may be combined to give

$$I_{total} = |F_a|^2 + |F_b|^2 + \alpha\{F_a F_b^* + F_a^* F_b\} , \qquad (2\text{-}27)$$

where $0 \leq \alpha \leq 1$.

Coherence lengths of x-rays are of the order of one micron[64]. Thus $\alpha=1$ when the domain dimensions are much less than a micron and $\alpha=0$ when the domain dimensions are much greater than a micron. It follows that, for domains about the length of a micron, α must have a value intermediate between 0 and 1.

§ 2.5 Intensity Corrections

Intensities will show the effects of absorption of some intensity by the crystal, polarization of the reflected x-rays, extinction, and in addition will be affected by the geometry of the apparatus used to diffract the x-rays from a crystal.

(a) Absorption

A certain amount of energy can be absorbed from the x-ray beam to produce electronic excitations and to remove electrons from atoms. Such absorption decreases the intensity of the scattered beam.

$$I/I_o = \exp(-\mu_\lambda t) , \qquad (2\text{-}28)$$

where I is the transmitted intensity, I_o is the incident intensity, t the path length, and μ_λ the linear absorption coefficient of the material for radiation of wave-length λ. This absorption coefficient can be expressed as

$$\mu_\lambda = d \sum_n x_n \mu_n , \qquad (2\text{-}29)$$

where d is the density of the material, x_n is the fraction of atoms of type n in the unit cell, and μ_n is the mass absorption coefficient of atom n. It is listed in the International Tables for X-Ray Crystallography, Volume II[74] for all atoms. The atomic absorption coefficient increases with wavelength, atomic masses of the atoms, and density. Corrections for absorption become increasingly important as these effects increase in size. In practice, it is often useful to grind crystals into spheres or cylinders of known radii, since for such simple geometries it is easy to calculate the path length for various scattering angles.

(b) Polarization

An x-ray beam has an associated electric field which can be resolved into a component parallel ($E_{\parallel}$) and a component perpendicular ($E_{\perp}$) to the reflection plane. The intensity of the beam is equal to the square of the electric field. I.e. $I = E^2 = E_{\parallel}^2 + E_{\perp}^2$. The parallel component of the electric field reflects with 100% efficiency, but the perpendicular component reflects with an efficiency of cos2θ:

$$(E_{\parallel})_{\text{reflected}} = (E_{\parallel})_{\text{incident}},$$

$$(E_{\perp})_{\text{reflected}} = (E_{\perp})_{\text{incident}}\cos 2\theta. \qquad (2\text{-}30)$$

If the initial beam was unpolarized, then $E_{\parallel}^2$ and $E_{\perp}^2$ are each equal to $\frac{1}{2}E^2$. and the intensity of the reflected beam is

$$\begin{aligned} I = E^2_{\text{reflected}} &= (E_{\parallel})^2_{\text{reflected}} + (E_{\perp})^2_{\text{reflected}} \\ &= (E_{\parallel})^2_{\text{incident}} + (E_{\perp})^2_{\text{incident}}\cos 2\theta \\ &= I_{\text{incident}}(\tfrac{1}{2} + \tfrac{1}{2}\cos 2\theta). \end{aligned} \qquad (2\text{-}31)$$

If the initial beam was crystal monochromatized, then $E_{\parallel}^2 : E_{\perp}^2 = 1 : \cos^2 2\theta_c$

where θ_c is the Bragg angle for the monochromating crystal. Thus,

$$E_{\parallel}^2 = E(1 + \cos^2 2\theta_c) \quad \text{and}$$

$$E_{\perp}^2 = E\cos^2 2\theta_c(1 + \cos^2 2\theta_c) . \tag{2-32}$$

This gives a reflected intensity of

$$I = I_{\text{incident}}\left(\frac{1 + \cos^2 2\theta_c \cos^2 2\theta}{1 + \cos^2 2\theta_c}\right) . \tag{2-33}$$

(c) Lorentz effect

Since mosaic spread introduces a finite breadth to the Bragg peak, and since an x-ray beam is never perfectly collimated, intensities are usually integrated over a volume large enough to include deviations from the point at which the Bragg peak occurs. To do this integration, the crystal is usually rotated about an axis parallel to the reflecting plane and normal to the incident x-ray beam so that the total intensity from the whole range of possible contributions can be measured. This total intensity is

$$I_{\text{integrated}} = \iint R^2 I dt dA , \tag{2-34}$$

where dA is the element of area of the surface receiving the reflected beam at a distance R from the crystal. This surface will be normal to the reflected beam. dt is the time during which the crystal is in a reflecting position while it is being rotated through distance dl. dl must be perpendicular to the incident beam and in the plane of both the incident and reflected beams.

If the angular velocity is ω, then $dt=\omega dl$. dl makes an angle of $\pi/2-2\theta$ with the reflected beam, and thus $dl = (\cos(\pi/2-2\theta))^{-1}dx = (\sin 2\theta)^{-1}dx$ where dx is an element of length along the reflected beam. We thus have

$$dtdA = \omega dl dA = \omega(\sin 2\theta)^{-1} dx dA = \omega(\sin 2\theta)^{-1} dV, \qquad (2\text{-}35)$$

where the element of volume dV is now independent of the Bragg angle. The integrated intensity now is

$$I_{integrated} = \int\int R^2 I \omega(\sin 2\theta)^{-1} dV = I_{measured}(\sin 2\theta)^{-1}. \qquad (2\text{-}36)$$

Thus the total intensity depends upon $(\sin 2\theta)^{-1}$ for this kind of crystal rotation. The factor $(\sin 2\theta)^{-1}$ is known as the Lorentz factor. For different kinds of crystal rotations, the Lorentz factor will vary.

§ 2.6 The Phase Problem

Structure factors can be written in the form $F_H = |F_H| \exp(\alpha_H)$ where α_H is called the phase angle and $|F_H|$ is the amplitude of the structure factor. Since $\sqrt{I_H} = |F_H|$, only the amplitude can be determined from intensity measurements. The structure factor is the Fourier transform of the electron density. Therefore the electron density is

$$\rho(\underline{r}) = V^{-1} \sum_{\underline{H}} F_H \exp(-2\pi i \underline{H} \cdot \underline{r}). \qquad (2\text{-}37)$$

This expression cannot be evaluated, and hence ρ cannot be calculated unless α_H is known. This is known as the "phase problem" of crystallography. Likely phases can be calculated by proposing models for the possible structure of the unit cell and comparing the moduli of the structure factors of such models with those measured experimentally.

§ 2.7 Methods of Solving the Phase Problem

(a) Isostructural Crystals

If the reflections of a particular crystal are similar in intensity to those of another crystal which has the same unit cell dimensions and a similar chemical formula (e.g. $NaVO_3$ and $LiVO_3$), then the crystals are likely isostructural, and the coordinates for one crystal represent a good model for the other crystal.

(b) The Patterson Function

The general Patterson function $P(\underline{u})$, is defined as the convolution of the electron density with itself.

$$P(\underline{u}) = \rho(\underline{u}) * \rho(-\underline{u})$$

$$= \int_{-\infty}^{\infty} \rho(\underline{R})\,\rho(\underline{R}+\underline{u})\,d\underline{R}\,, \qquad (2\text{-}38)$$

where the convolution (*) is defined as shown.

For a crystal with translational symmetry, this becomes

$$P(\underline{u}) = N \int_{u.c.} \rho(\underline{R})\,\rho(\underline{R}+\underline{u})\,d\underline{R} \qquad (2\text{-}39)$$

$$= N \int_{u.c.} \sum_{\underline{H}'} \sum_{\underline{H}} \frac{F_{H'}}{V} \exp(-2\pi i \underline{H}' \cdot \underline{u}) F_H \exp(-2\pi i H \cdot (\underline{R}+\underline{u})\,d\underline{R}$$

$$= \frac{N}{V^2} \sum_{\underline{H}'} \sum_{\underline{H}} F_{H'} F_H \exp(-2\pi i \underline{H} \cdot \underline{u}) \int_{u.c.} \exp 2\pi i (\underline{H}'+\underline{H}) \cdot \underline{R}\; d\underline{R}\,. \qquad (2\text{-}39)$$

The integral is zero unless H' = -H when it has a value equal to the volume of the unit cell. The volume of the unit cell multiplied by the number of unit cells is equal to the volume of the crystal. The Patterson simplifies to

$$P(\underline{u}) = V^{-1} \sum_{H} F_H F_{-H} \exp(-2\pi i \underline{H} \cdot \underline{u})$$

$$= V^{-1} \sum_{H} |F_H|^2 \exp(2\pi i \underline{H} \cdot \underline{u}). \text{ (since } F_{-H} = F_H^*) \qquad (2\text{-}40)$$

The variable $\underline{u}$ represents the distance between two points, and when this distance is the distance between two atoms in the unit cell, the value for $P(\underline{u})$ will be large. Thus, by examining a map of a Patterson function distances between atoms may be determined, and these distances in turn may suggest possible structural models.

(c) Other Methods

Models may also be determined by direct methods, which involve the statistical evaluation of phases, or through the use of anomalous dispersion,

which introduces a shift in the peaks of the Patterson function for different radiations. This shift is related to the absorption of x-rays by the individual atoms and thus varies with the kind of atom. These methods were not used in this work and will not be discussed further.

§ 2.8 Crystal Structure Refinement

(a) Electron Density and Difference Maps.

An initial model of a crystal structure often includes only some of the atoms, or includes atoms in approximate positions. From such a model, however, structure factors may be calculated and hence phases may be proposed for the experimental structure factors. An electron density distribution can now be calculated, and, if the proposed phases are close to the correct ones, this distribution will have peaks at the atomic positions of all the atoms. These positions may now be used to calculate new structure factors which should be closer to the experimental ones. This procedure can be repeated until no further improvement in the agreement is found.

Instead of an electron density map, a difference map is often used. This is a plot of the function $\sum_{H} \Delta F \exp(i\alpha) \exp(-2\pi i \underline{H} \cdot \underline{r})$ where ΔF is the difference between the amplitude of the observed and calculated structure factors, and α is the phase determined from the model. This function is an electron density function which has the electron density of the model subtracted from the total electron density, and should show peaks which reflect positions of new atoms, or a combination of a positive and negative peak to reflect a corrected and incorrect position of an atom respectively.

(b) Least Squares Refinement

Improvement of a crystal structure model by repeated evaluation of electron density maps, or difference maps, is tedious and will not as a rule give thermal coordinates or small variations of atomic positions. A more convenient method of improving models is through the least squares refinement of the fit of the experimental structure factors to the calculated ones.

If a model for a crystal structure is described by the variables p_i, i=1,...no. of variables (n), which may be positional, temperature or scale parameters, then a better structure factor (i.e. one which is closer to the experimental one) can be expanded in terms of a Taylor series about the structure factors with parameters p_i:

$$kF_c = kF_c(p_i) + \sum_i \left(\frac{\partial kF_c}{\partial p_i}\right)_{p_i} \Delta p_i + \ldots , \qquad (2\text{-}41)$$

where k is a scale factor which brings the structure factor on the same scale as the intensity.

This expansion is substituted into the function

$$D = \sum_H w(|F_o| - k|F_c|)^2 , \qquad (2\text{-}42)$$

where w is a weighting function which will be discussed in the next section. If the model is reasonably close to the "true" structure, then second and subsequent terms in the Taylor expansion of kF_c are very small and may be neglected. Thus,

$$D = \sum_H w(|F_o| - k|F_c(p_i)| + \sum \left(\frac{\partial kF_c}{\partial p_i}\right)_{p_i} \Delta p_i)^2 . \qquad (2\text{-}43)$$

D is now minimized with respect to all the variables.

$$\frac{\partial D}{\partial p_i} = 0 \qquad i=1,\ldots n \ . \qquad (2\text{-}44)$$

This produces upon simplification a set of n equations in the shifts p_i of the form

$$a_{i1}\Delta p_1 + a_{i2}\Delta p_2 + \ldots + a_{in}\Delta p_n = v_i \ , \tag{2-45}$$

where $a_{ij} = \sum_H w \frac{\partial |kF_c|}{\partial p_i} \cdot \frac{\partial |kF_c|}{\partial p_j}$, $v_i = \sum_H w(|F_o| - k|F_c|)\frac{\partial |kF_c|}{\partial p_i}$.

The set of these equations can be written in matrix form:

$$A\underline{\Delta P} = \underline{V} \ , \tag{2-46}$$

where the a_{ij} are the elements of matrix A, the p_i elements of vector $\underline{P}$, and the v_i elements of vector $\underline{V}$.

Equation 2-46 can be solved:

$$\underline{\Delta P} = A^{-1}\underline{V} \ , \tag{2-47}$$

where A^{-1} is the inverse matrix of A. The values of Δp_i so found can be used as a correction to the model and the above procedure can be repeated with the corrected variables until further corrections are negligible.

If the elements of the inverse matrix A^{-1} are denoted by b_{ij}, the standard deviation for any parameter p_i is

$$\sigma_{p_i} = (b_{ii}(\sum_H w(|F_o| - |F_c|)^2(m-n)^{-1})^{\frac{1}{2}}, \tag{2-48}$$

where m is the number of reflections.

The correlation between variables is measured by the correlation coefficient

$$\delta_{ij} = b_{ij}/b_{ii}^{\frac{1}{2}}b_{jj}^{\frac{1}{2}} \ , \tag{2-49}$$

which can vary between -1 and +1. For values close to +1 or -1, serious problems in refinement can result. These may be circumvented to a certain extent by treating one correlated variable as a constant during one cycle of refinement and the other variable as a constant during the next cycle

of refinement. Scheringer[75] discusses some of the correlation problems in detail.

The goodness of fit of the calculated structure factors compared to the observed structure factors is measured by the residual

$$R = \frac{\Sigma||F_o| - |F_c||}{|F_o|}, \tag{2-50}$$

or the weighted residual

$$R_w = \left(\frac{\Sigma|w|F_o| - |F_c||^2}{|F_o|^2}\right)^{\frac{1}{2}}. \tag{2-51}$$

§ 2.9 Weighting Schemes

All reflections are not measured with the same accuracy and they should be weighed in a structure refinement. These weights cannot be determined *a priori* since the errors in measurement are not well defined and, as a consequence, they present a rather controversial topic for crystallographers. One train of thought suggests that reflections should be weighted by the standard deviation of the photon count for the reflection. This scheme does not take into account machine errors, and is likely to give too large a weight to the very intense reflections. Cruickshank[76] suggests that a scheme of the form $(a+b|F_o|+c|F_o|^2)^{-1}$ be used. He argues that the variation of the difference between the observed and calculated structure factors is usually quadratic with respect to the observed structure factor, and hence, the weighting scheme should reflect this form. Too large a weight is usually given to the very weak reflections by these kind of schemes. In this work, weights of the form $(a+b|F_o|+c|F_o|^2+d(\sigma/|F_o|)^2)^{-1}$ have been used, incorporating both of the above ideas.

CHAPTER 3

The Preparation and X-Ray Intensities Collection for the Crystals

§ 3.1 Crystal Preparation

VPO_5 in either the α, β, or hydrated form can be used as a precursor for the growth of $VO(PO_3)_2$, $V(PO_3)_3$, VOP_2SiO_8 and $(VO)_2P_2O_7$ crystals. The first two can be prepared from any form of VPO_5 by varying the temperature and the amount of phosphoric acid required as illustrated in figure 3-1. $(VO)_2P_2O_7$ is a direct reduction product of VPO_5 heated to about 800°C in an inert atmosphere. The VOP_2SiO_8 crystals can be prepared from VPO_5, H_3PO_4 and quartz, although they are more easily prepared by vapour phase transport in iodine from $VO(PO_3)_2$ and SiO_2[77]. Also, this material is very often found as a byproduct when V_2O_5 and P_2O_5 are mixed and heated in an evacuated quartz tube. The vanadium invariably appears to reduce under these conditions. $VAsO_5$ has no direct preparative relationship to the other compounds, but its study was undertaken to see the similarities and/or differences between the vanadium phosphate and vanadium arsenate compounds. Its preparation is similar to the preparation of VPO_5 from the melt. Although most of the crystals can be grown readily, preparations often produce glasses as by-products and in fact crystals of both VOP_2SiO_8 and $VO(PO_3)_2$ have been found which show some vitreous character on precession photographs.

(a) Preparation of VOP_2SiO_8, $VO(PO_3)_2$ and $V(PO_3)_3$

A 1:1 V_2O_5:P_2O_5 mix was heated in a sealed, evacuated quartz tube to about 900°C. The sample was then cooled at a rate of 3°/hr. to

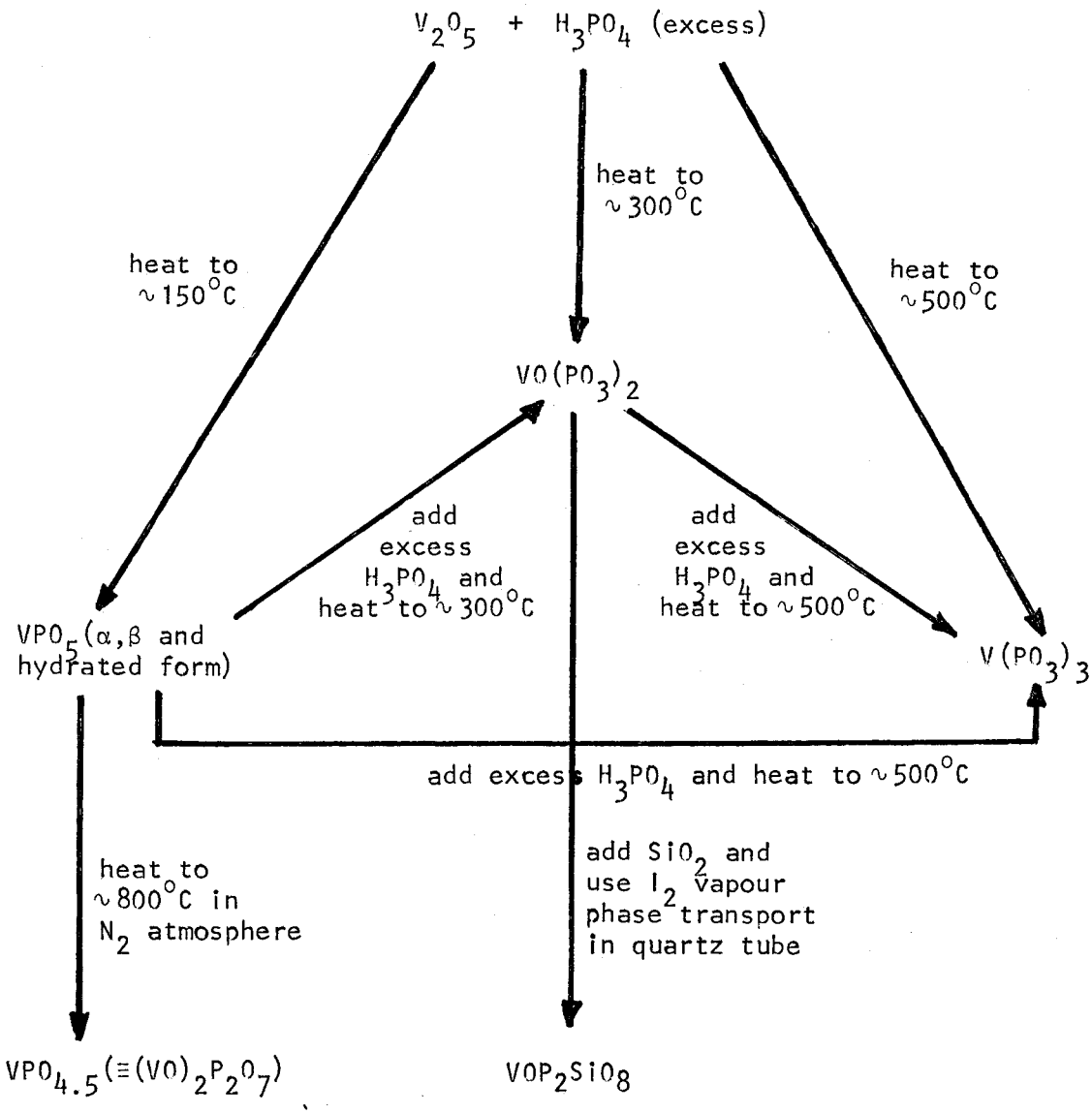

Figure 3-1. Relationship between the preparations of the various vanadium phosphorus oxides.

500°C. The furnace was turned off at this point and the sample was allowed to cool to ambient temperature. The resulting crystalline mixture contained crystals identified as being VOP_2SiO_8, $VO(PO_3)_2$ and $V(PO_3)_3$, by comparison of their crystal parameters obtained from single crystal precession photographs to those of Tofield, et al.[45,77]. At least one and possibly more than one unidentified crystalline phase was also present as indicated by the presence of lines not belonging to any of the identified crystals in a powder pattern taken of a bulk sample of the mixture. These crystals probably have a V:P ratio greater than one since the identified crystals are all phosphorus rich and the mixture was originally made with V:P being 1:1. Unfortunately, none of these unidentified crystals was suitable for x-ray structure analysis. It is likely that they contain reduced vanadium since no VPO_5 was found in the mixture and the colours of the crystals were all blue or green, which are the colours usually associated with V^{+4} and V^{+3}. A yellow colour is usually noted for V^{+5}. Crystals of VOP_2SiO_8 and $V(PO_3)_3$ from this mixture were found to be the best available crystals of their kind and were ground to spheres and used for structure determination.

The same preparation as described above was repeated with a cooling rate of 15°/hr. The resulting product consisted mostly of a glass and small crystals of VOP_2SiO_8 embedded on the surface away from the quartz container wall. Small crystals of $VO(PO_3)_2$ were found in the bottom of the tube. No other crystals were found. It was thought that the crystals of VOP_2SiO_8 and $VO(PO_3)_2$ could be vanadium rich with vanadium either replacing some of the silicon with V^{+4} or replacing some of the phosphorus with V^{+5}, since the lattice parameters for both these

crystals were slightly larger than found in other crystals of their kind. An analysis of the crystals and the glass was attempted by electron microprobe. Results (which will be discussed later) were inconclusive in showing non-stoichiometry in the crystals, and showed the glass to have a V:P ratio of 1:1 with at most 1% silicon.

Crystals of $V(PO_3)_3$ were also prepared using the method of Lavrov, et al.[44] and Tofield, et al.[45], by heating a 10:1 phosphoric acid: V_2O_5 mixture to 500°C overnight. The crystals which precipitated were of unequal dimensions and could not be ground easily into good spheres. They were not used to collect intensity measurements for solving the structure, but were used for all other experiments.

Crystals of $VO(PO_3)_2$ were prepared following the method of Tofield, et al.[45] using a 10:1 phosphoric acid:V_2O_5 mixture heated overnight to 300°C. The resulting crystals were very often twinned or compacted. Better crystals were obtained by heating VSO_5 in the stoichiometric amount of phosphoric acid required to give V:P = 1:2. These crystals were ground to spheres and used for intensity measurements. A powder pattern of $VO(PO_3)_2$ reported by Lavrov, et al.[44] could not be indexed for the cell parameters of the crystals produced above.

Details of the crystal appearance, crystal data and intensity measurements for these crystals are listed in table 3-1.

(b) Preparation of $(VO)_2P_2O_7$

Bordes and Courtine[40] report that $(VO)_2P_2O_7$ can be prepared by the reduction of VPO_5 (all forms) under nitrogen atmosphere at 800°C. VPO_5 was prepared by grinding together thoroughly a 1:1, V:P mixture of V_2O_5 and $NH_4H_2PO_4$, and heating it in a platinum crucible at a rate of

Table 3-1. Crystal Data

Crystal	$V^{+4}OP_2SiO_8$	$V^{+4}O(PO_3)_2$	$V^{+3}(PO_3)_3$	$(V^{+4}O)_2P_2O_7$	$V^{+5}AsO_5$
Appearance	blue rectangular plates - max 3mm long, 0.3mm thick	blue rods with diameters up to 0.2mm, lengths up to 1.5mm	green rods with diameters up to 0.5mm, lengths up to 3mm	green, rhombic roughly equi-dimensional up to 1 mm in length	yellow, mica-like layers of indefinite length, max. thickness 0.05 mm
Crystal used for Intensity Measurements	ground sphere radius 0.125 mm	ground sphere radius 0.1 mm	ground sphere radius 0.1 mm	ground sphere radius 0.15 mm	rod length 0.12 mm width 0.05 mm
Crystal System	tetragonal	tetragonal	monoclinic	orthorhombic	monoclinic
Lattice Parameters					
a(Å)	8.723(1)	10.960(1)	10.615(2)	9.571(4)	6.35(3)
b(Å)			19.095(4)	7.728(5)	6.32(3)
c(Å)	8.151(1)	4.2529(4)	9.432(1)	16.568(6)	8.256(5)
β(or γ)(°)			β=97.94(1)		γ≃90(1)
Z	4	4	12	8	4
Systematic Extinctions	hk0, h+k≠2n 0kℓ, ℓ≠2n hhℓ, ℓ≠2n	0kℓ, k+ℓ≠2n h0ℓ, h+ℓ≠2n 00ℓ, ℓ≠4n h+k+ℓ≠2n	0kℓ, k≠2n h0ℓ, ℓ≠2n h+k+ℓ≠2n	0kℓ, k≠2n h0ℓ, ℓ≠2n	hk0, h+k≠2n 00ℓ, ℓ≠2n
Possible Space Groups	P4/ncc	$I\bar{4}2d$ or $I4_1md$	Ic or I2/c	Pbcm or $Pbc2_1$	$P2_1/n$ (c unique)

table 3-1. cont.

Crystal	VOP_2SiO_8	$VO(PO_3)_2$	$V(PO_3)_3$	$(VO)_2P_2O_7$	$VAsO_5$
Diffractometer used	Syntex $P\bar{1}$	Syntex $P2_1$	Syntex $P2_1$	Syntex $P\bar{1}$	Syntex $P\bar{1}$
Scan rate	variable scan rate between 2 and 24°/min depending on the peak intensity. The fastest rate is used for the strongest peaks, and the slowest for the weakest peaks				
Maximum 2θ (Mo K_α radiation)	65	70	60	65	65
No. of symmetry independent non-zero reflections	571	336	2467	1900	1118
μ (cm^{-1})	24	26	12	38	134
Density (g/cc)					
calculated	3.05	2.92	3.03	3.34	4.1
measured	insufficient material	2.9±0.1	3.0±0.1	insufficient material	4.0±0.1

50°C/hr. to about 500°C. After two hours, the product was removed from the furnace, allowed to cool and ground to a fine powder. This mixture was placed in a platinum dish and heated to 800°C overnight in a nitrogen atmosphere. The temperature was then raised to 1000°C (i.e. above the melting point of $(VO)_2P_2O_7$), kept there for about an hour and then lowered at a rate of 6°/hr. to 600°C. The furnace was shut off at this point and the crystals allowed to cool to room temperature at which time the nitrogen atmosphere was removed. The resulting product consisted of a mixture of glass and $(VO)_2P_2O_7$ crystals. A roughly equidimensional crystal was ground to a sphere and used for x-ray intensity measurements.

(c) Preparation of $VAsO_5$ (and $VAs_xP_{1-x}O_5$)

Equimolar amounts of V_2O_5 and As_2O_5 were weighed and ground together. This sample was heated to about 300°C for several hours and then allowed to cool. The ground mixture was heated in a platinum crucible to 900°C and then allowed to cool through the melting point of $VAsO_5$, estimated by comparison with VPO_5 to be about 800°C, at a rate of 5°/hr. There was no sample in the crucible when cooled, and investigation showed that the material volatilized before melting. A sample was prepared the same way as before but sealed under air in a quartz tube before heating to 900°C. Air was kept in the tube in an effort to prevent possible reduction of the vanadium, as occurs for vanadium-phosphorus oxide mixes in vacuo. The sample was cooled at a rate of 5°/hr. to 300°C after which the furnace was switched off and the sample allowed to cool by itself to room temperature. The resulting crystals existed in thin, mica-like sheets. It was not possible to grind a crystal to a sphere since the sheets were too thin, so a rod was used for x-ray intensity measurements.

Crystals of $VAs_xP_{1-x}O_5$ were grown in a quartz tube under air as above using samples prepared from the appropriate amounts of V_2O_5, As_2O_5 and $NH_4H_2PO_4$. No crystals suitable for single-crystal work were prepared but powder patterns were taken of these samples and showed the structures to be similar to, if not the same as, that of α-VPO_5.

§ 3.2 Measurement of X-Ray Diffraction Intensities

For each crystal, preliminary photographs (precession or Weissenberg) were taken to determine the lattice parameters and possible space groups (through the use of the International Tables, Vol. I[78]) from the diffraction symmetry. The crystal was then centred on an automatic diffractometer and accurate lattice parameters were determined by least squares fitting to 15 reflections accurately centred at both positive and negative 2θ values, with the average taken to be the diffraction angle.

The uncorrected intensity measurements were corrected for background, Lorentz, polarization and absorption effects. Only intensities with values greater than the background were considered. Spherical absorption corrections (International Tables, Vol. II[74]) were applied to all intensity measurements except those for $VAsO_5$. The latter had cylindrical[74] absorption corrections applied. Standard deviations were estimated automatically by the computer based on the counting statistics of the intensity measurements. The intensities of three standard reflections were measured every fifty reflections in order to make sure that the crystal was still in its proper position and that the intensity of the x-ray source was constant. After all corrections were applied, equivalent reflections were averaged, and the square roots of the intensities were taken in order to give the absolute value of the structure factors.

§ 3.3 Solution of Crystal Structures

Refinement of atomic and thermal coordinates was carried out using full-matrix least-squares methods for all crystals. A secondary extinction parameter, as suggested by Zachariasen[72] and Larson[73] was refined for each crystal. Atomic scattering factors for free atoms were obtained from Cromer and Mann[67]. Unless otherwise indicated, substitutional and positional disorder was treated by refining the parameters (co-ordinates and occupation) for an average cell. I.e. only the first term in equation 2-22 is considered significant.

CHAPTER 4

The Crystal Structure and Substitutional Disorder of VOP_2SiO_8

§ 4.1 Solution of the Crystal Structure

Two isostructural crystals of VOP_2SiO_8 were studied. The first had lattice parameters a=8.723(1) Å, c=8.151(1) Å and was found together with other crystalline phases grown from a V_2O_5-P_2O_5 melt in an evacuated silica tube. The second crystal, found at the surface of a V-P oxide glass prepared in an evacuated silica tube, had lattice parameters of a=8.733(2) Å and c=8.185(2) Å. The structure was solved for crystal I, and the final atomic and thermal co-ordinates obtained were used as starting parameters in the least-squares refinement for crystal II.

From the systematic extinctions, (hk0, h+k≠2n; 0kℓ, ℓ≠2n; hhℓ, ℓ≠2n) the space group was uniquely determined to be P4/ncc. Since general positions in this space group are sixteen-fold, and there are only 4,8 and 4 atoms of V, P, and Si respectively in a unit cell, these atoms must lie on special positions of 4, 8 and 4-fold symmetry respectively. From the Patterson function, a peak at (0.36,0.36,0) was assigned to the distance between two phosphorus atoms at positions x,x,¼ and -x,-x,¼ with x=0.18. A peak at (0.32,-0.18,0.10), determined to be the P-V vector, placed V at ½,0,0.35, and thus Si had to be at the origin as verified by the Patterson map. The remaining oxygen atoms were found from a difference Fourier map. All coordinates were refined using full-matrix least-squares methods. Anisotropic thermal coordinates were refined after the positional coordinates stopped changing significantly.

The refined coordinates for crystal II were not much different from those for crystal I, but the Si-O distance was found to be slightly larger. This suggested vanadium was substituting at the silicon site, and the occupation number of silicon was varied in the least-squares refinement of both crystals to allow for some substitution of vanadium. No substitution was indicated for crystal I, but the refinement for crystal II showed 5% substitution of V for Si. The substituted vanadium is most likely to be V^{+4} (although this oxidation state is not normally found tetrahedrally coordinated) or V^{+5}. The latter would require charge compensation at the other sites, probably V^{+3} substituted at the V^{+4} site or Si^{+4} substituted at the P^{+5} site. None of the above substitutions could be substantiated by refinement of the occupation of V and P, since the scattering factors for Si and P and for V^{+4} and V^{+3} are not sufficiently different to distinguish such small amounts of substitution.

Weighting schemes for both crystal refinements were chosen so that $\langle w\Delta F^2 \rangle$ was essentially independent of $\langle F_o \rangle$. The final R-factors were R = 0.032 and R_w = 0.026 ($w = (0.62-0.0175|F|+0.000315|F|^2+775(\sigma/F)^2)^{-1}$) for crystal I and R = 0.048 and R_w = 0.038 ($w = (1.26-0.034|F|+0.0007|F|^2+800(\sigma/F)^2)^{-1}$) for crystal II. Final coordinates are listed in table 4-1 (crystal I) and table 4-2 (crystal II).

§ 4.2 Description of the Structure

Like α-VPO_5[11] and the isostructural α-VSO_5[79], the structure consists of chains of VO_6 octahedra along four-fold axes which are bridged to neighbouring chains by corner-sharing PO_4 tetrahedra (fig. 4-1 and 4-2). The vanadium atom is displaced 0.37 Å from the equatorial plane of the $V^{+4}O_6$ octahedron, thereby forming a short axial (vanadyl) and a long axial

Table 4-1. Positional and thermal coordinates of VOP_2SiO_8 (crystal I). Values for the thermal coordinates are multiplied by 10^4. Standard deviations are given within parentheses.

Atom	x	y	z	† $U_{11}(Å^2)$	$U_{22}(Å^2)$	$U_{33}(Å^2)$	$U_{12}(Å^2)$	$U_{13}(Å^2)$	$U_{23}(Å^2)$
V	½	0	0.35298(7)	60(3)	U_{11}	92(2)	0	0	0
P	0.17901(9)	x	¼	61(3)	U_{11}	85(2)	4(2)	0(3)	0(3)
Si	0	0	0	80(4)	U_{11}	68(3)	0	0	0
O(1)	½	0	0.5480(3)	134(12)	U_{11}	113(9)	0	0	0
O(2)	0.6523(2)	0.1620(2)	0.3077(2)	89(6)	74(5)	174(5)	-23(4)	-8(5)	46(5)
O(3)	0.6390(2)	0.4392(2)	0.3889(2)	105(5)	126(5)	113(5)	3(4)	27(5)	-33(5)

† The U_{ij} and β_{ij} are related by $\beta_{ij} = 2\pi^2 b_i b_j U_{ij}$ where the b_i are the magnitudes of the corresponding reciprocal lattice vectors.

Table 4-2. Positional and thermal coordinates of VOP_2SiO_8 (crystal II). Values for the thermal coordinates are multiplied by 10^4. Standard deviations are given within parentheses.

Atom	x	y	z	$U_{11}(Å^2)$	$U_{22}(Å^2)$	$U_{33}(Å^2)$	$U_{12}(Å^2)$	$U_{13}(Å^2)$	$U_{23}(Å^2)$
V	½	0	0.3527(1)	65(5)	U_{11}	110(4)	0	0	0
P	0.1795(1)	x	¼	62(5)	U_{11}	87(4)	1(3)	0(3)	0(3)
Si	0	0	0	79(9)	U_{11}	62(6)	0	0	0
O(1)	½	0	0.5464(5)	127(18)	U_{11}	117(14)	0	0	0
O(2)	0.6529(2)	0.1614(2)	0.3068(2)	102(10)	77(9)	178(8)	-27(6)	-10(7)	41(7)
O(3)	0.6395(2)	0.4386(2)	0.3886(2)	107(8)	133(9)	113(7)	3(7)	26(7)	-35(7)

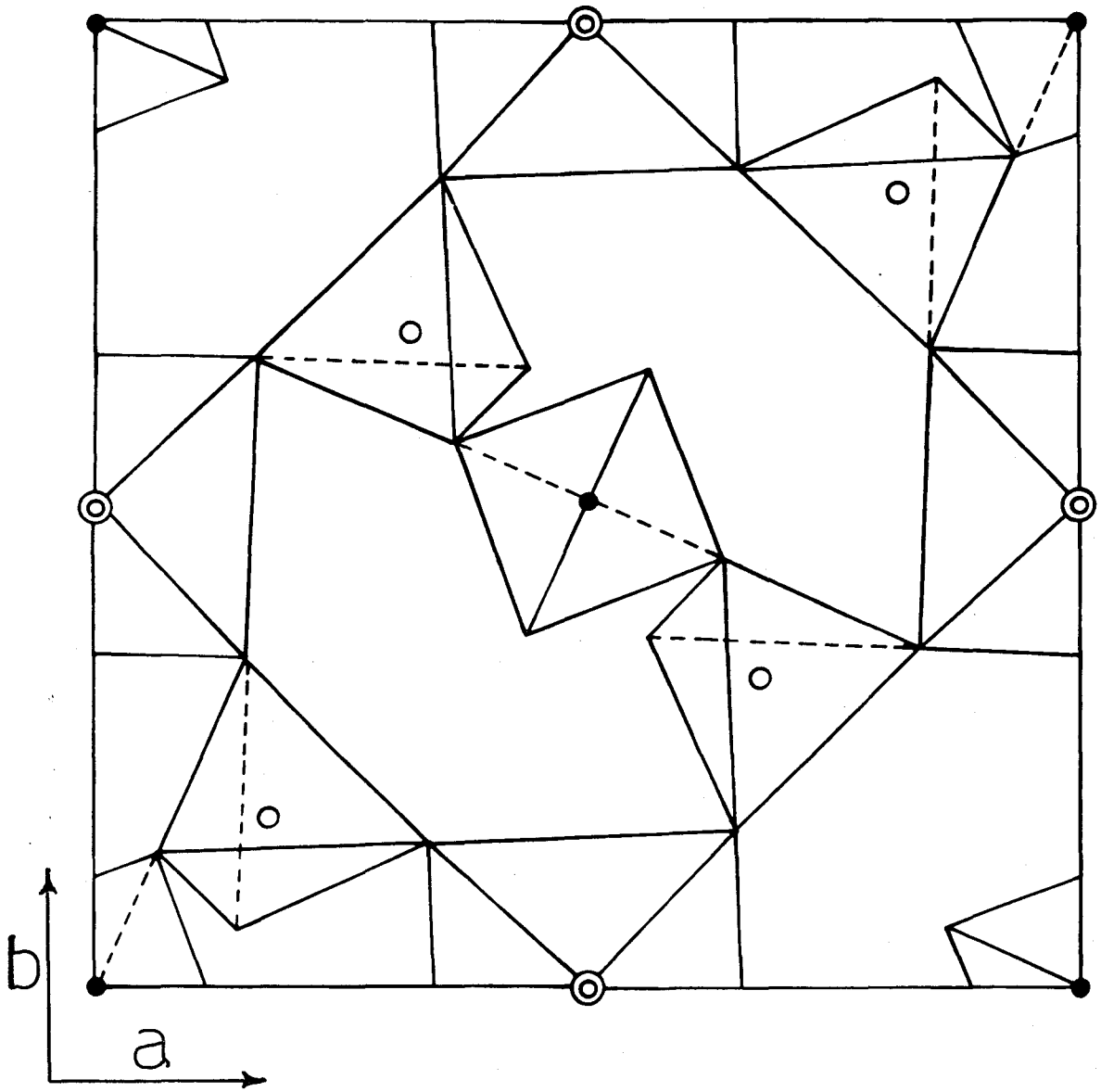

Figure 4-1. A half-cell projection of the structure of VOP_2SiO_8. The remainder of the cell can be generated by a $\underline{c}$ glide plane parallel to the face diagonal.

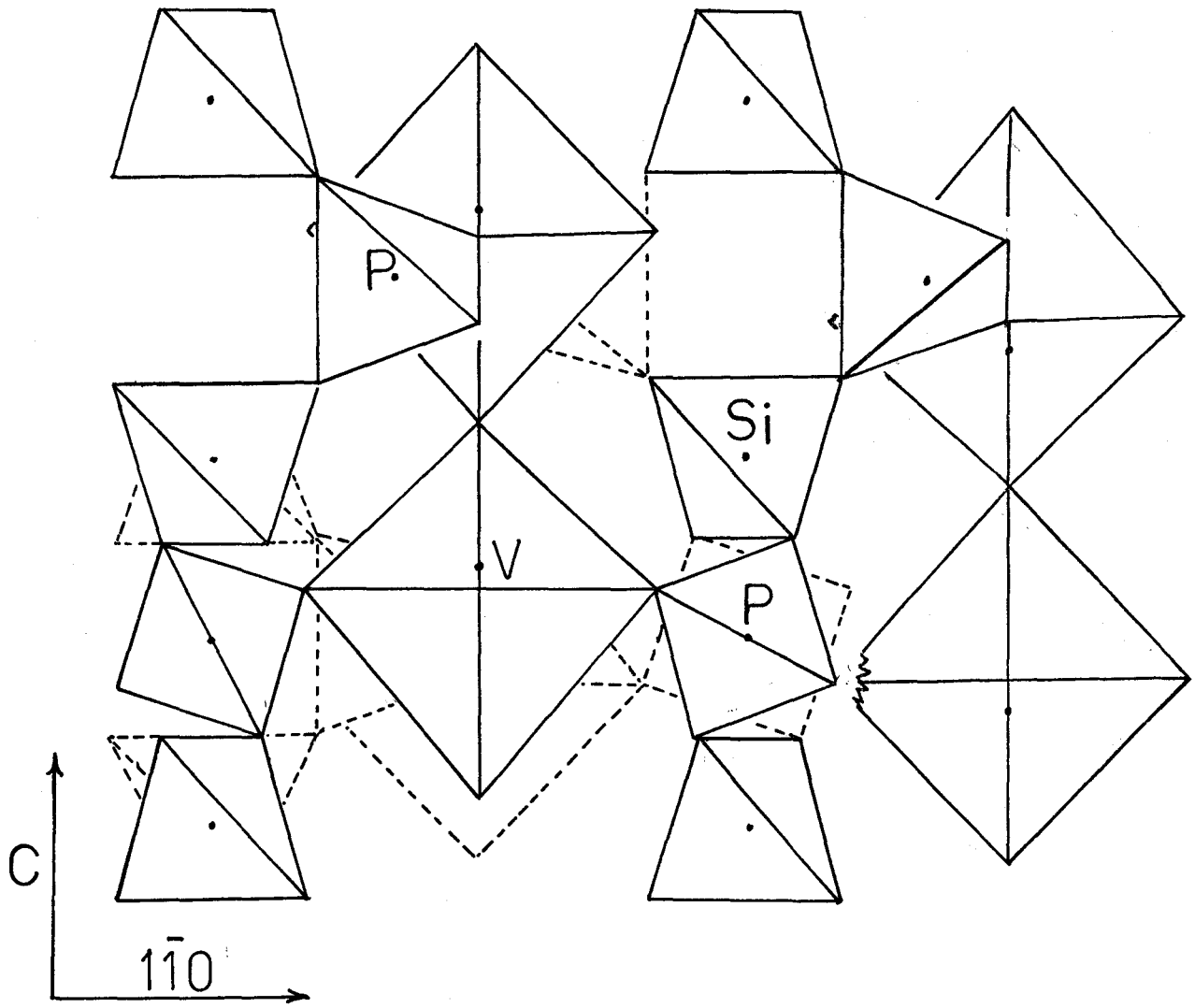

Figure 4-2. The structure of VOP_2SiO_8 as projected on the 1$\bar{1}$0 plane.

V-O bond. The oxygens around V^{+4} form an almost regular octahedron with O-O distances of 2.743. 2.757 and 2.871 Å (equatorial-equatorial, short axial-equatorial, long axial-equatorial distances respectively)

Linked PO_4 and VO_6 groups lie in planes perpendicular to c. These planes are joined by the axial vanadyl bonds as well as SiO_4 tetrahedra which join adjacent planes by corner-sharing with two phosphate groups in each plane (fig.4-2). This is in contrast to α-VPO_5 where distinct layers exist, held together only by the long and short axial bonds.

The phosphate group has C_2 symmetry with the longer bonds involving the P-O-Si bridge and the shorter ones the P-O-V bridge. Baur's[94] bond order distance relationships and Brown's[16] bond-valences predict this trend but predict differences of 0.036 and 0.146 Å respectively compared with the actual value of 0.088 Å.

The SiO_4 group forms an almost perfect tetrahedron with an Si-O bond-length in the range normally reported for silicon containing minerals[80]. Compounds of this type of structure with phosphorus in the silicon position are not expected to occur since phosphate groups are not known to link four other phosphate groups in this fashion.

Rice, et al.[46] independently reported essentially the same structure for VOP_2SiO_8. Their bond lengths and angles and those of crystal I and crystal II do not differ significantly (table 4-3).

§ 4.3 Substitutional Disorder

Substitutional disorder is one possible explanation for the discrepancy in the lattice parameters shown in table 4-4. The two crystals in this work were compared with respect to composition (from electron

Table 4-3. Bond angles (°) and distances (Å) for $VOP_2Si_xV_{1-x}O_8$. Estimated standard deviations are indicated in parentheses.

	crystal I x = 1.00(1)	crystal II x = 0.95(1)	Rice, et al.[46]
VO_6 group			
bond			
$V-O(1)^{i}$	1.590(3)	1.585(4)	1.591(2)
$V-O(1)^{ii}$	2.486(3)	2.508(4)	2.492(1)
$V-O(2)^{i}$ x4	1.974(2)	1.978(2)	1.977(1)
angle			
$O(1)^{i}-V-O(2)^{i}$	100.77(7)	100.97(7)	100.81(3)
$O(2)^{i}-V-O(2)^{iii}$	88.00(8)	87.93(8)	87.98(2)
$O(2)^{i}-V-O(2)^{iv}$	158.45(7)	158.07(9)	158.37(7)
SiO_4 group			
bond			
$Si-O(3)^{v}$ x4	1.604(2)	1.614(2)	1.610(1)
angle			
$O(3)^{v}-Si-O(3)^{vii}$	111.23(9)	111.17(11)	111.58(7)
$O(3)^{v}-Si-O(3)^{vi}$	108.60(9)	108.63(11)	108.43(4)
PO_4 group			
bond			
$P-O(2)^{v}$ x2	1.483(2)	1.483(2)	1.492(1)
$P-O(3)^{v}$ x2	1.571(2)	1.572(2)	1.572(1)
angle			
$O(2)^{iii}-P-O(2)^{v}$	113.23(9)	113.07(12)	113.04(8)
$O(2)^{iii}-P-O(3)^{iii}$	110.52(9)	110.69(10)	110.48(5)
$O(2)^{iii}-P-O(3)^{v}$	109.47(9)	109.35(12)	109.44(5)
$O(3)^{iii}-P-O(3)^{v}$	103.17(9)	103.25(11)	103.56(8)

Table 4-3 cont.

angles at bridging oxygens

angle	Crystal I	Crystal II	Rice, et al.
V-O(2)-P	146.56(8)	146.40(10)	146.36(6)
P-O(3)-Si	142.36(8)	142.50(10)	142.21(6)

Symmetry code

i)	x	y	z	iv)	-x	-y	z
ii)	-x	y	$\frac{1}{2}$+z	v)	$\frac{1}{2}$+x	$\frac{1}{2}$-y	$\frac{1}{2}$-z
iii)	$\frac{1}{2}$-y	$\frac{1}{2}$+x	z	vi)	$\frac{1}{2}$-y	$\frac{1}{2}$-x	$\frac{1}{2}$+z
				vii)	$\frac{1}{2}$-x	$\frac{1}{2}$+y	$\frac{1}{2}$-z

Table 4-4. Lattice parameters for $VOP_2Si_xV_{1-x}O_8$

a	c	Reference
8.723(1)	8.151(1)	This work, crystal I for x = 1.00(1)
8.733(2)	8.185(3)	This work, crystal II for x = 0.95(1)
8.697(8)	8.119(8)	Tofield, et al.[77] from powder pattern
8.747(2)	8.167(2)	Rice, et al.[46] from single crystal

microprobe analysis), lattice parameters and bond lengths. The electron microprobe analysis gave molar ratios of V:Si:P = 1.0(1):1.0(1):2.0 for crystal I and ratios of V:Si:P = 1.05(10):0.95(9):2.0 for crystal II. The lattice parameters for the second crystal are larger as are the Si-O bond-lengths (table 4-3). This evidence, together with the least-squares refinement of the occupation number of the silicon for crystal II, suggests vanadium substitution at the silicon site. The electron microprobe data alone are inconclusive, but the additional information available leads one to suggest that the errors in these data may perhaps be smaller than estimated and the differences may be significant.

Crystals of the form $VOP_xSi_yV_zO_8$ can probably be prepared with various values of x, y and z. However, the solid solution behaviour of this system remains to be investigated; the presently available data merely suggest that substitution and/or vacancy formation is possible.

CHAPTER 5

Crystal Structure and Disorder in $VO(PO_3)_2$

§ 5.1 Solution of Structure

The structure was determined for two isostructural tetragonal crystals. Crystal I was prepared from VSO_5 and H_3PO_4 (p.45) and has cell parameters a=10.960(1) Å, c=4.253(1) Å. Crystal II, grown in a vanadium rich atmosphere (p.44) has cell parameters a=10.975(3) Å, c=4.253(1) Å. The structure was first solved for crystal I, and the coordinates obtained were used as starting coordinates in the least-squares refinement for crystal II.

The space group was established as either $I4_1md$ or $I\bar{4}2d$ from the systematic extinctions ($0k\ell$, $k+\ell\neq 2n$; $h0\ell$, $h+\ell\neq 2n$; 00ℓ, $\ell\neq 4n$; $h+k+\ell\neq 2n$). Since there are only four vanadium atoms per unit cell, they must necessarily lie on the 4_1 or $\bar{4}$ axes for the respective space groups. From the Patterson function, the phosphorus atom can be placed ($\frac{1}{4}$,0.16,0) from V, and an oxygen atom (denoted O(V)), bonded axially to V, at a point (0,0,0.38) away. This gives the following trial models:

A: for $I4_1md$, V at 0,0,0
P at 0.25,0.16,0.0
O(V) at 0,0,0.38 or 0,0,-0.38

The phosphorus position is sixteen-fold and, since there are only eight phosphorus atoms, these atoms will have to be disordered, each position having half occupancy.

B: for $I\bar{4}2d$, V at 0,0,0

P at $\frac{1}{4}$,0.16,0

O(V) at 0,0,0.38

Again the phosphorus has to be disordered as for model A, and so does the O(V) atom.

C: for $I\bar{4}2d$, an alternative model is

V at 0,0,0.12

P at $\frac{1}{4}$,0.16,-1/8

O(V) at 0,0,0.5

This alternative will require the V and O(V) atoms to be disordered, occupying with half-occupancy positions at 0,0,±z. The phosphorus atom here will not be disordered since it sits on an 8-fold special position.

All the foregoing models were tried. The remaining oxygen atoms were found from difference maps, and were disordered for each model where the phosphorus positions were disordered. The completely refined (by full-matrix least-squares) models gave R-factors of 0.23, 0.21 and 0.097 for models A, B and C respectively. Model C was therefore assumed to be the correct one. Since the two disordered positions for O(V) were $\frac{1}{4}\mathring{A}$ or less apart, only the isotropic thermal coordinate was refined for this atom, and the position was determined by successively placing the atom at z = 0.47, 0.475, 0.48, 0.485, 0.49 and 0.495, and picking the position which yielded the lowest R-factor. Since the R-factor for model C was still high, refinement of this model was tried in each of the sub-groups of $I\bar{4}2d$ ($I\bar{4}$, Fdd2, and $I2_12_12_1$). The first sub-group would require the glide-plane extinctions to be accidental, while the last two sub-groups, which are orthorhombic, would require the equivalence

of a and b to be accidental. None of these lower symmetry sub-groups improved the agreement significantly.

A final difference map gave residual peaks at 0.16,¼,-1/8 and its symmetry related points. This, together with the quite high R-factors, suggests further disordering. Possible models for this disordering will be discussed later but, when they were refined, no significant improvement was noted in the agreement. Final coordinates for crystal I are in table 5-1, and for crystal II in table 5-2.

Since the second crystal has a larger value for a, and the P-O(2) bond length is 0.02 Å larger than that for the first crystal (table 5-3), the possibility of vanadium substitution at the phosphorus site was investigated. The occupation for the phosphorus atom in both crystals was varied in the least-squares refinement to allow for vanadium substitution. The refinement showed no significant change for crystal I, and 6% substitution of V for P in crystal II. This amount is suggestive, but far from conclusive, of substitution of V for P in crystal II. The occupational refinement is probably not very accurate since the phosphate chain may be disordered, thereby making the occupation of any individual phosphorus position less than one.

The 0,2,2 reflection had a large difference between F_o and F_c and, since it was by far the strongest reflection, it was assumed to be greatly affected by extinction and was given zero weight in the refinement for both crystals. A weighting scheme $((19.9-0.906|F|+0.0154|F|^2+1000(\sigma/F)^2)^{-1})$ was used with crystal I to give final R=0.097 and R_w=0.114. The R-values for crystal II are R=0.12 and R_w=0.14 ($w=(15.5-0.15|F|+0.0162|F|^2+1000(\sigma/F)^2)^{-1}$).

Table 5-1. Positional and thermal coordinates for $VO(PO_3)_2$ (crystal I). Values for the thermal coordinates are multiplied by 10^4. Estimated standard deviations are in parentheses.

Atom	x	y	z	$U_{11}(Å^2)$	$U_{22}(Å^2)$	$U_{33}(Å^2)$	$U_{12}(Å^2)$	$U_{13}(Å^2)$	$U_{23}(Å^2)$
V	0	0	0.0960(20)	130(20)	110(20)	130(20)	20(20)	0	0
P	1/4	0.1614(3)	-1/8	100(20)	70(20)	120(20)	0	40(20)	0
O(1)	0.1901(9)	1/4	5/8	110(40)	150(40)	160(40)	0	0	10(40)
O(2)	0.1486(7)	0.0934(7)	0.0300(20)	170(30)	170(30)	250(40)	-80(30)	-60(30)	10(30)
O(V)	0	0	0.4750(50)	140(30)†					

† Isotropic thermal coordinate

Table 5-2. Positional and thermal coordinates for $VO(PO_3)_2$ (crystal II). Values for the thermal coordinates are multiplied by 10^3. Estimated standard deviations are in parentheses.

Atom	x	y	z	$U_{11}(Å^2)$	$U_{22}(Å^2)$	$U_{33}(Å^2)$	$U_{12}(Å^2)$	$U_{13}(Å^2)$	$U_{23}(Å^2)$
V	0	0	0.089(2)	17(3)	11(3)	12(2)	7(2)	0	0
P	1/4	0.161(1)	-1/8	11(2)	9(2)	13(2)	0	7(2)	0
O(1)	0.190(1)	1/4	5/8	11(6)	20(5)	30(7)	0	0	16(7)
O(2)	0.149(1)	0.093(1)	0.039(3)	22(5)	20(5)	22(5)	-4(4)	-7(4)	6(4)
O(V)	0	0	0.475(5)	18(5)†					

† Isotropic thermal coordinate

Table 5-3. Bond angles (°) and distances (Å) for the two crystals of $VO(PO_3)_2$. Estimated standard deviations are indicated in parentheses.

VO_6 group

bond	crystal I	crystal II	angle	crystal I	crystal II
V-O(V)	1.62(1)	1.64(1)	O(V)-V-O(V)^{i}	180	180
V-O(V)^{i}	2.63(1)	2.61(1)	O(V)-V-O(2)	98.3(3)	96.4(4)
V-O(2) x2	1.944(8)	1.94(1)	O(V)-V-O(2)^{i}	105.6(3)	105.7(4)
V-O(2)^{i} x2	1.997(8)	2.00(1)	O(2)-V-O(2)^{i}	87.8(3)	88.3(5)
			O(2)-V-O(2)^{ii}	163.5(5)	167.2(7)
			O(2)^{i}-V-O(2)^{iii}	148.8(5)	148.5(6)

PO_4 group

bond	crystal I	crystal II	angle	crystal I	crystal II
P-O(1) x2	1.582(5)	1.584(6)	O(1)-P-O(2) x2	107.1(5)	107.5(6)
P-O(2) x2	1.492(9)	1.510(12)	O(1)-P-O(2)^{iv} x2	108.6(4)	108.0(7)
			O(1)-P-O(1)^{v}	104.4(3)	104.2(4)
			O(2)-P-O(2)^{iv}	120.0(5)	120.5(7)

bridging angles

angle	crystal I	crystal II
V-O(2)-P	162.0(4)	158.9(6)
V-O(2)^{vi}-P^{vi}	138.2(4)	136.8(6)
P-O(1)-P	131.0(4)	130.9(5)

Symmetry operations

i) x -y -z

ii) -x -y z

iii) -x y -z

iv) $\frac{1}{2}$-x y 3/4-z

v) $\frac{1}{2}$-x $\frac{1}{2}$-y $\frac{1}{2}$+z

vi) -y x -z

§ 5.2 Description of the Structure

Like VOP_2SiO_8 and α-VPO_5, the vanadium atom has one long and one short axial bond directed along a $\bar{4}$-fold axis. These bonds join adjacent VO_6 groups to form chains in the c direction. The V^{+4} atom is displaced by about 0.4 Å along the $\bar{4}$ axis from the centre of the VO_6 octahedron. Unlike VOP_2SiO_8 and α-VPO_5, the equatorial oxygen atoms do not lie in a plane. $\bar{4}$ symmetry places two diagonally opposite oxygen atoms about 1/8 Å above the z=0 plane, and the other two about 1/8 Å below this plane. Neighbouring VO_6 chains are parallel, but corresponding octahedra are displaced by $+\frac{1}{4}\underline{c}$ or $-\frac{1}{4}\underline{c}$ from neighbouring groups.

The VO_6 chains are corner-shared with phosphate tetrahedra which are linked together to make up infinite $(PO_3)_\infty$ metaphosphate chains. Each of the metaphosphate chains links four VO_6 chains (figs. 5-1 and 5-2). The phosphate groups within a chain are related by a 2_1 axis in the (001) direction at $(\frac{1}{4},\frac{1}{4},z)$. The chains are related to their four neighbouring chains by a $\bar{4}$ axis at the origin parallel to c. The two distinct P-O(-V) and P-O(-P) bond lengths of 1.492(9) and 1.582(5) have a difference of 0.090 Å falling between the values predicted by Brown[16] (0.146 Å) and Baur[94] (0.065 Å). A complete table of bond-lengths and angles is given in table 5-3.

This structure is different from that of any of the three known polymorphs of SiP_2O_7[81,82,83] even though stoichiometrically the two structures are similar ($VO(PO_3)_2$ could be written as VP_2O_7). All the polymorphs of SiP_2O_7 consist of P_2O_7 groups joined by SiO_6 octahedra. Each octahedron shares corners with six P_2O_7 groups. Structures of the form MP_2O_7 (isostructural to a cubic polymorph of SiP_2O_7 according to powder

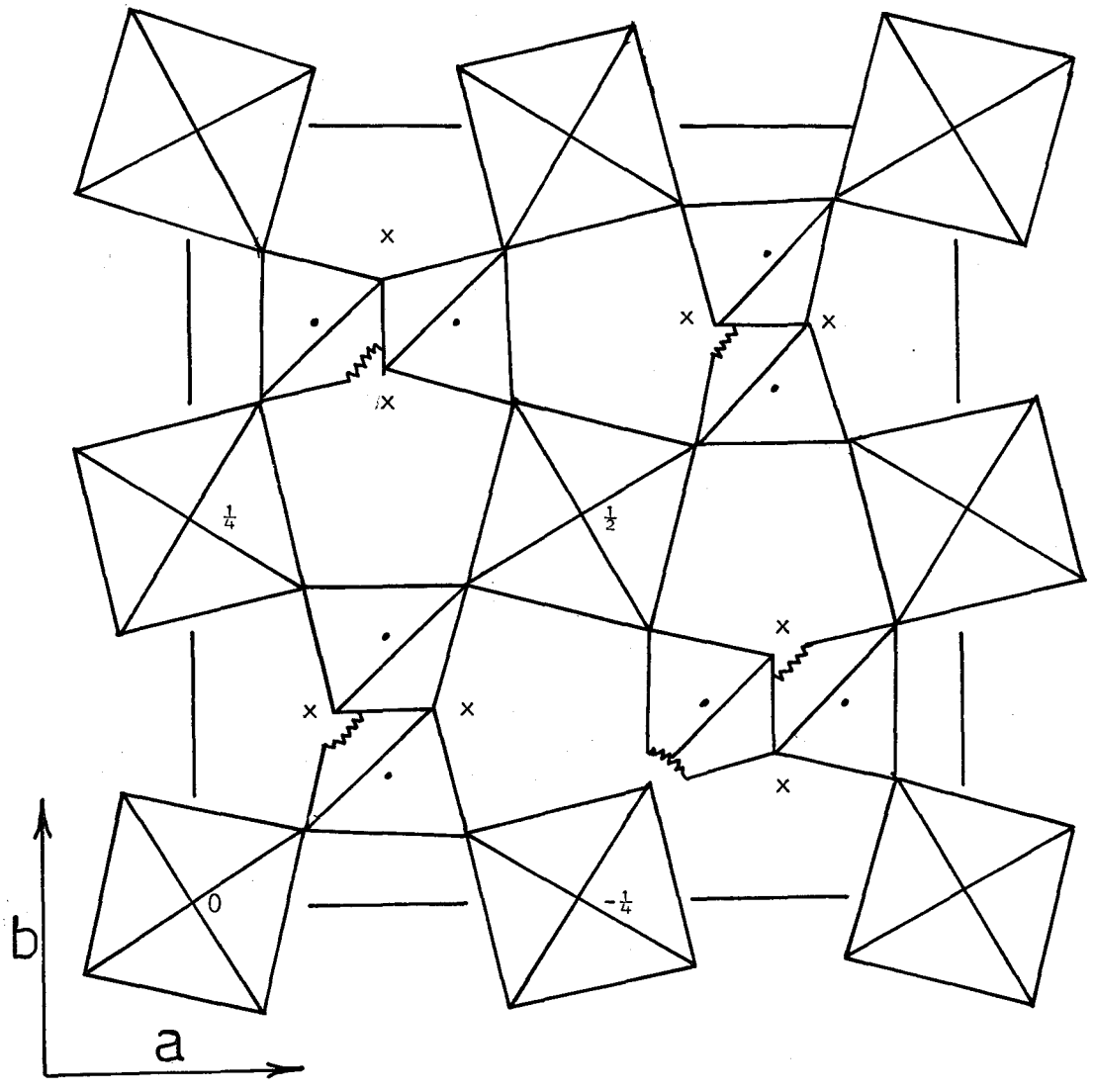

Figure 5-1. The crystal structure of $VO(PO_3)_2$ projected down the c axis. The vanadium atoms are disordered being located approximately ±0.096 above and below the z-values indicated on the diagram. The positions of residual density are indicated by (x).

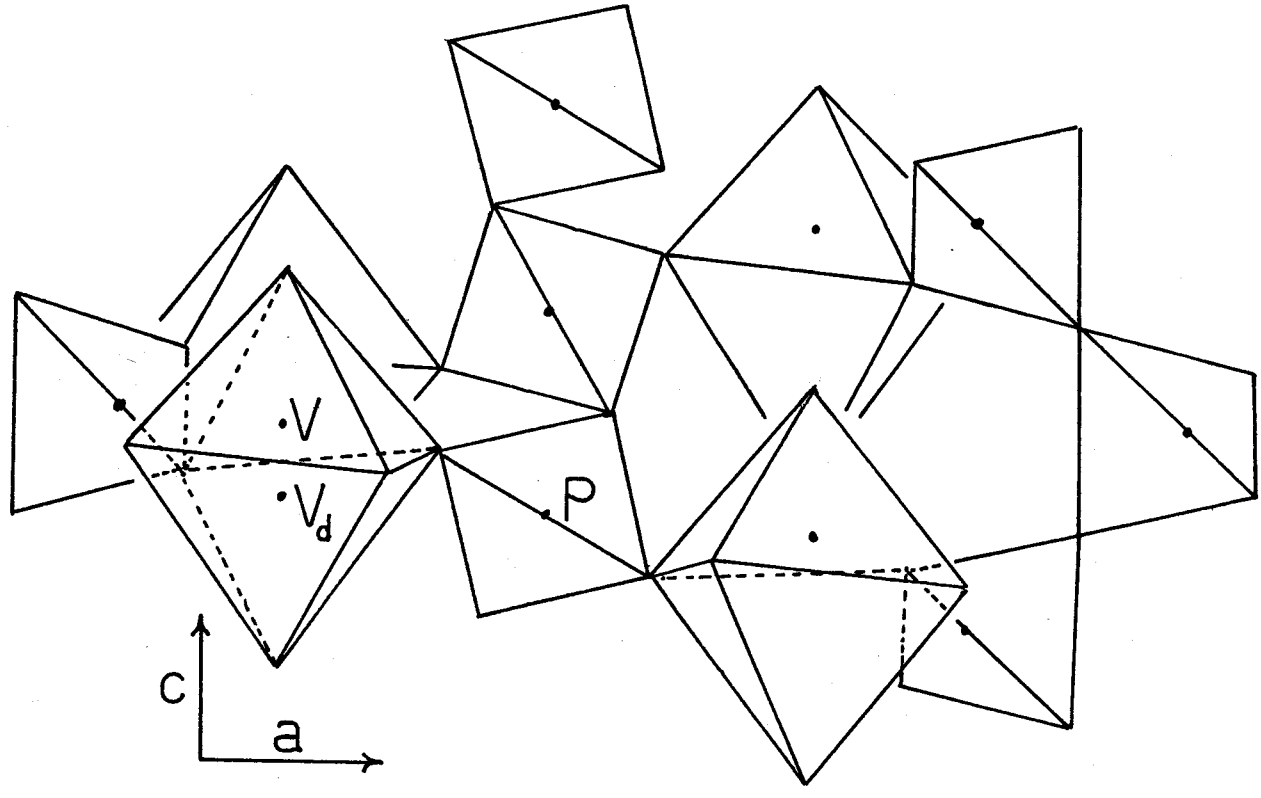

Figure 5-2. The crystal structure of $VO(PO_3)_2$ projected along the b-axis The two possible positions of the vanadium atom are indicated as V and V_d within one of the octahedra.

patterns) also exist for M = Si[81], Ge[84], Sn[85], Zr[86], Pb, Ti, Hf, Ce and U[87,88]. It is likely that the difference in structures arises from the characteristic vanadyl and long axial V-O bonds which occur in all known structures containing V^{+4}, but are unknown for most of the other cations. The short V-O bond has a bond valence of 1.6, and it would be difficult for a PO_4 group to share such an oxygen atom.

§ 5.3 Substitutional Disorder

Bordes and Courtine[40] have reported the preparation of powders all having the same powder pattern and having the composition $VO(P_xV_{1-x}O_3)_2$ over the range $1 \leq x \leq 0.9$. It is reasonable to assume that such crystals are substitutionally disordered with V^{+5} at the phosphorus site. The crystals studied in this thesis fall within the range found by Bordes and Courtine according to the least-squares refinement of occupations. Other evidence for either crystal being substitutionally disordered is not very good. Electron microprobe analysis gave a value of x=1.0(1) for crystal I and x=0.9(1) for crystal II. The differences in bond lengths, as shown in table 5-3, are also within the standard error. It is possible that the errors in both structures are over-estimated, but no real conclusion can be drawn as to the extent of substitutional disordering.

§ 5.4 Positional Disorder

The vanadium atoms with their corresponding vanadyl oxygens can exist in one of two positions as determined from the refinement. The VO_6 chains can consequently have the vanadyl bonds pointing either along $\underline{c}$ or $-\underline{c}$. Such disordering would produce diffuse lines through the Bragg reflections parallel to $\underline{a}^*$ and $\underline{b}^*$. Two-week-long exposures of

the h0ℓ and 0kℓ photographs showed such diffuse lines as illustrated schematically in figure 5-3. They are very weak since only a change in the vanadium atom position contributes significantly to the disordering; the change of position for O(V) being of negligible magnitude. The diffuse streaks appear to be of uniform intensity indicating the disorder is perfectly random. Thus, any one VO_6 chain can have the vanadyl bonds point in the +c or -c direction, and its neighbouring chains all have an equal probability of being oriented in either direction.

The residual peaks found in the final difference map suggest that additional disorder may be present. Three possible models for such disordering were considered.

A. The structure is reflected in the $1\bar{1}0$ plane. This would introduce additional disordered vanadium atoms at the points $0,\frac{1}{2},3/4\pm0.096$ and $\frac{1}{2},0,\frac{1}{4}\pm0.096$.

B. The structure is rotated about $(\pm\frac{1}{4},\pm\frac{1}{4},z)$. This would introduce vanadium atoms displaced by $-\frac{1}{4}$ in z from the original positions.

C. The metaphosphate chains undergo a 4_1 rotation at $(\pm\frac{1}{4},\pm\frac{1}{4},z)$. This would require no further disordering of the vanadium positions.

All three of these models were tested as follows. The atoms were assumed to partially occupy the positions in the basic structure and partially the positions in the disordered structure in such a way that the total occupation is equal to the number of atoms in the chemical formula. A least-squares refinement of the occupations (keeping the total occupation constant) using observed and calculated structure factors was then carried out. All such refinements invariably increased the R-factor. It was then felt that perhaps the domain size was large enough to make

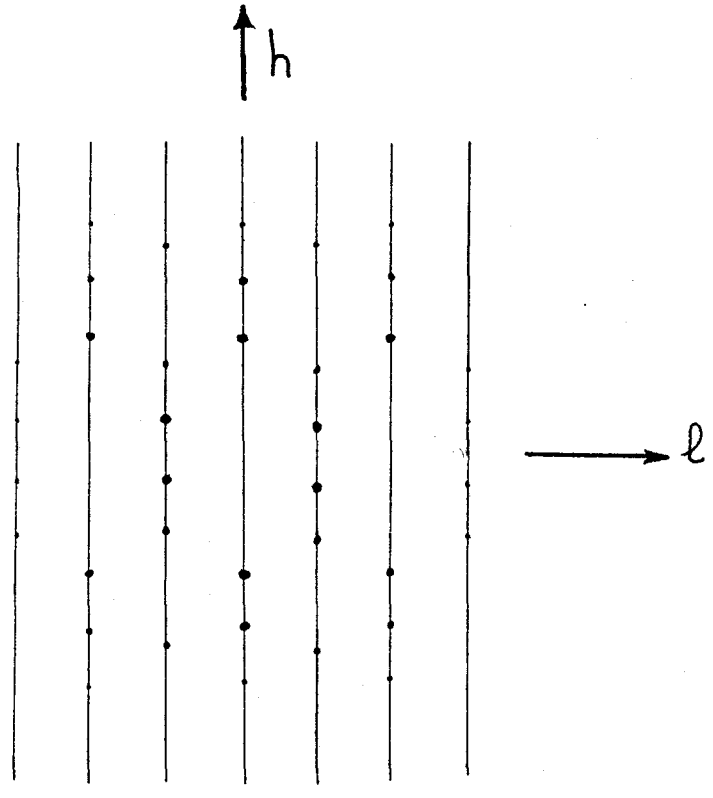

Figure 5-3. A schematic representation of the hOℓ projection of $VO(PO_3)_2$ showing the diffuse streaks going through the Bragg diffraction spots. The intensity of the streaks has been greatly exaggerated.

the structure factors of the basic and disordered structures no longer additive. A least-squares refinement was then carried out on the parameter α and the occupation, x, in $I_{obs} = |F_1|^2 + |xF_2|^2 + \alpha(xF_1F_2^* + xF_1^*F_2)$ where F_1 is the structure factor for the basic structure, F_2 is the structure factor for the disordered positions, F_i^* is the complex conjugate of F_i, and I_{obs} is the observed intensity. The absolute values of F_1 and F_2 are nearly the same, but their phases differ. No convergence was found for $0 \leq \alpha \leq 1$ which is the range possible for α(see p.32). The domain size, therefore, does not seem to be a factor preventing a suitable solution of the disordering.

One of the problems with the foregoing models is that a reorientation of the VO_6 groups is required, which is large enough to introduce considerable strain. Such strain could be avoided if the disorder represents a cooperative reorientation within a complete plane perpendicular to $\underline{c}$. Such a model would produce streaks along $\underline{c}^*$ which were not observed. Another means of minimizing such a strain is the introduction of an average VO_6 orientation at the boundaries between two structural positions. E.g. if for one structure the bridging V-O-P oxygen is located at (0.15,0.09,0.03) and for the disordered structure it is located at (0.09,0.15,0.03) as in model C, then the boundary bridging oxygens could be located at (0.12,0.12,0.03) and the corresponding points determined by the $\bar{4}$ operation. This would keep the geometry of the VO_6 group reasonable and would introduce some strain in the metaphosphate chain which can be easily compensated for by a slight rotation. If the domains are small enough, boundary effects can be considerable, and the models tested will not work unless all these effects have been considered.

An attempt was made to see if the disordering would disappear at

lower temperatures. hkℓ reflections were compared at room temperature and at -150°C. No significant changes in intensities were observed.

CHAPTER 6

The Crystal Structure and Thermal Behaviour of $V(PO_3)_3$

§ 6.1 Solution of the Crystal Structure

The structure determination was begun by Dr. F.C. Hawthorne with a unit cell of a=10.615Å, b=6.365Å, c=9.432Å, β=97.9° and space group is Ic or I2/c. He solved the structure in I2/c and refined it to an R-factor of about 20% from the Patterson function. Some of the bond-lengths and angles in his solution were unsatisfactory.

Subsequently, I took a week-long-exposure precession photograph of $V(PO_3)_3$ which showed that the b-axis is triple that of Hawthorne, but the possible space groups remain the same. Only k=3n reflections have strong intensities. The structure must consist of three of Hawthorne's cells, with small structural variations from one to the next. This is only possible in the non-centrosymmetric space group Ic. Tofield, et al.[45] also selected Ic as the space group on the basis of second harmonic generation, and found the lattice parameters of the tripled cell.

A difference map from the k=3n reflections based on the atomic positions in the large cell (supercell) that correspond to those of Hawthorne's cell (subcell) failed to yield any structural variations from the substructure. The heavy atoms were displaced from the substructure positions by 0.01 in different directions, one at a time, and a least-squares refinement was carried out varying only the coordinates in the third of the cell containing the atom for which the initial displacement was made. If the R-factor decreased, this displacement was allowed: if

it increased, another displacement was tried. This process was continued in conjunction with a lowering R-factor until all the positions were simultaneously varied, at which point the isotropic thermal coordinates were also included in the least squares refinement. Computer limitations prevented anisotropic thermal coordinates from being refined. Final coordinates are listed in table 6-1. Since there was no a priori reason for assuming any direction for the shifts from the average cell, the possibility of a false minimum in the least squares fit exists.. A β^{89} synthesis, which is a Fourier sum of terms of the form $(|F_o|^2/|F_c|)\exp(i\phi_c)$, where F_o is the observed structure factor, F_c the calculated structure factor, and ϕ_c the calculated phase angle, was calculated based on the vanadium and phosphorus atom positions. This synthesis is an electron density map which applies the weight F_o/F_c to the structure factors. If $F_c>>F_o$, at least some of the atomic co-ordinates which contribute significantly to the value for F_c must be wrong. The weight, F_o/F_c, will be small, and hence peaks which would result from incorrectly placed atoms will be depressed. If $F_c<<F_o$, unknown atomic positions must contribute significantly to F_c. The weight for such a structure factor will be large and peaks indicating unknown atom positions will therefore be enhanced. No solutions different from the one refined were found from the β map. Recently, the structure of $Al(PO_3)_3$ has been determined[90] . It is isostructural with the model of $V(PO_3)_3$ proposed here, suggesting that this structure is correct.

The final R and R_w were 0.091 and 0.065 respectively ($w=(46-0.53|F|+0.0023|F|^2+1000(\sigma/F)^2)^{-1}$). The agreement for only the $k\neq 3n$ reflections was R=0.134 and R_w=0.094. The larger values are not unreasonable since

Table 6-1. Positional and thermal coordinates for $V(PO_3)_3$. Estimated standard deviations are indicated in parentheses.

Atom	x	y	z	U(Å^2)
V(a)	¼	0.0798(2)	¼	0.0057(5)
V(b)	0.2529(5)	0.4115(2)	0.2479(6)	0.0049(5)
V(c)	0.2308(3)	0.7549(2)	0.2631(4)	0.0056(6)
P(1)	0.9756(6)	0.1442(3)	0.7657(7)	0.0059(8)
P(2)	0.0156(5)	0.4803(2)	0.7409(6)	0.0063(8)
P(3)	0.0027(5)	0.8142(2)	0.7476(6)	0.0043(7)
P(4)	0.1026(5)	0.3018(2)	0.4404(6)	0.0051(8)
P(5)	0.0967(5)	0.6370(2)	0.4420(6)	0.0050(8)
P(6)	0.1168(6)	0.9681(3)	0.4363(7)	0.0073(9)
P(7)	0.8791(6)	0.6965(2)	0.5748(7)	0.0056(9)
P(8)	0.8809(6)	0.3629(2)	0.5710(6)	0.0036(8)
P(9)	0.8961(5)	0.0267(3)	0.5561(6)	0.0056(8)
O(a,2)	0.9033(10)	0.5190(6)	0.7784(13)	0.0106(21)
O(a,3)	0.0884(10)	0.1321(5)	0.2112(12)	0.0062(19)
O(a,6)	0.1501(12)	0.9981(6)	0.2994(14)	0.0068(22)
O(a',6')	0.2262(13)	0.0544(7)	0.0417(16)	0.0120(26)
O(a,7)	0.8502(11)	0.6635(6)	0.7091(13)	0.0092(20)
O(a,8)	0.7808(10)	0.6097(6)	0.9585(13)	0.0051(20)
O(b,2)	0.1211(11)	0.4803(7)	0.1862(13)	0.0114(22)
O(b,3)	0.8865(12)	0.8371(7)	0.8006(15)	0.0145(24)
O(b,4)	0.1266(12)	0.3577(6)	0.3473(15)	0.0159(24)

table 6-1 cont.

Atom	x	y	z	U(Å^2)
O(b,5)	0.2044(11)	0.3651(6)	0.0631(13)	0.0085(20)
O(b,9)	0.8769(11)	0.9686(6)	0.6562(13)	0.0049(19)
O(b',9')	0.8011(11)	0.9652(6)	0.9295(13)	0.0045(20)
O(c,1)	0.0930(13)	0.8251(7)	0.2191(15)	0.0112(24)
O(c',1')	0.8775(11)	0.1913(6)	0.8121(13)	0.0057(21)
O(c,4)	0.2022(12)	0.7099(7)	0.0734(15)	0.0130(24)
O(c,5)	0.1070(10)	0.6876(5)	0.3255(12)	0.0086(19)
O(c,7)	0.7683(11)	0.2840(6)	0.9689(14)	0.0083(21)
O(c,8)	0.8414(10)	0.3298(6)	0.6975(13)	0.0106(21)
O(4,3)	0.0835(10)	0.2294(6)	0.3723(12)	0.0068(19)
O(4,8)	0.9695(10)	0.6892(6)	0.0056(13)	0.0091(20)
O(5,2)	0.0776(10)	0.5603(5)	0.3814(11)	0.0058(18)
O(5,7)	0.9679(11)	0.3545(6)	0.0103(14)	0.0136(22)
O(6,1)	0.0125(13)	0.9079(7)	0.3906(16)	0.0091(25)
O(6,9)	0.0360(11)	0.9765(6)	0.0181(13)	0.0062(21)
O(7,3)	0.9673(11)	0.7633(6)	0.6137(13)	0.0095(21)
O(8,2)	0.9770(12)	0.4235(7)	0.6178(15)	0.0139(24)
O(9,1)	0.9072(12)	0.0973(7)	0.6453(15)	0.0115(25)

these are the weaker reflections and have a smaller relative accuracy.

§ 6.2 Description of the Structure

The structure of the average cell is shown in figure 6-1. It consists of tetrahedral $(PO_3)_\infty$ chains which zig-zag in the c direction. VO_6 octahedral are found between these chains and are bridged to neighbouring VO_6 groups in the a direction by a phosphate tetrahedron in each of two chains, and in the c direction by two phosphate groups in each of two chains. The structure differs from VPO_5, and $VO(PO_3)_2$ in the lack of vanadyl bonds, and VO_6 chains.

As can be seen from figure 6-2, the major differences between each third of the cell along b lie in the orientations of the polyhedra. There do not appear to be large differences between the corresponding bond lengths and angles for the polyhedra in the three parts of the cell (table 6-2).

The different types of bonds and angles are summarized in table 6-3. The P-O(-P) bond lengths are consistently larger than the P-O(-V) bond lengths, the average difference of 0.10 Å falling between the values predicted by Baur[94](0.08Å) and Brown[16](0.15Å). The (V-)-O-P-O(-P) angle is consistently the largest angle in all the PO_4 tetrahedra, and the angle (P-)O-P-O(-P) is consistently the smallest, although the (P-)O-P-O(-V) angle of one phosphate group is sometimes smaller than the (P-)O-P-O(-P) angle in another. The VO_6 octahedra are close to being regular since the maximum difference between V-O bonds in any one group is 0.07(2) Å, and the axial and equatorial angles at the vanadium atoms are close to 180° and 90° respectively.

Table 6-4 gives the distances between corresponding atoms in

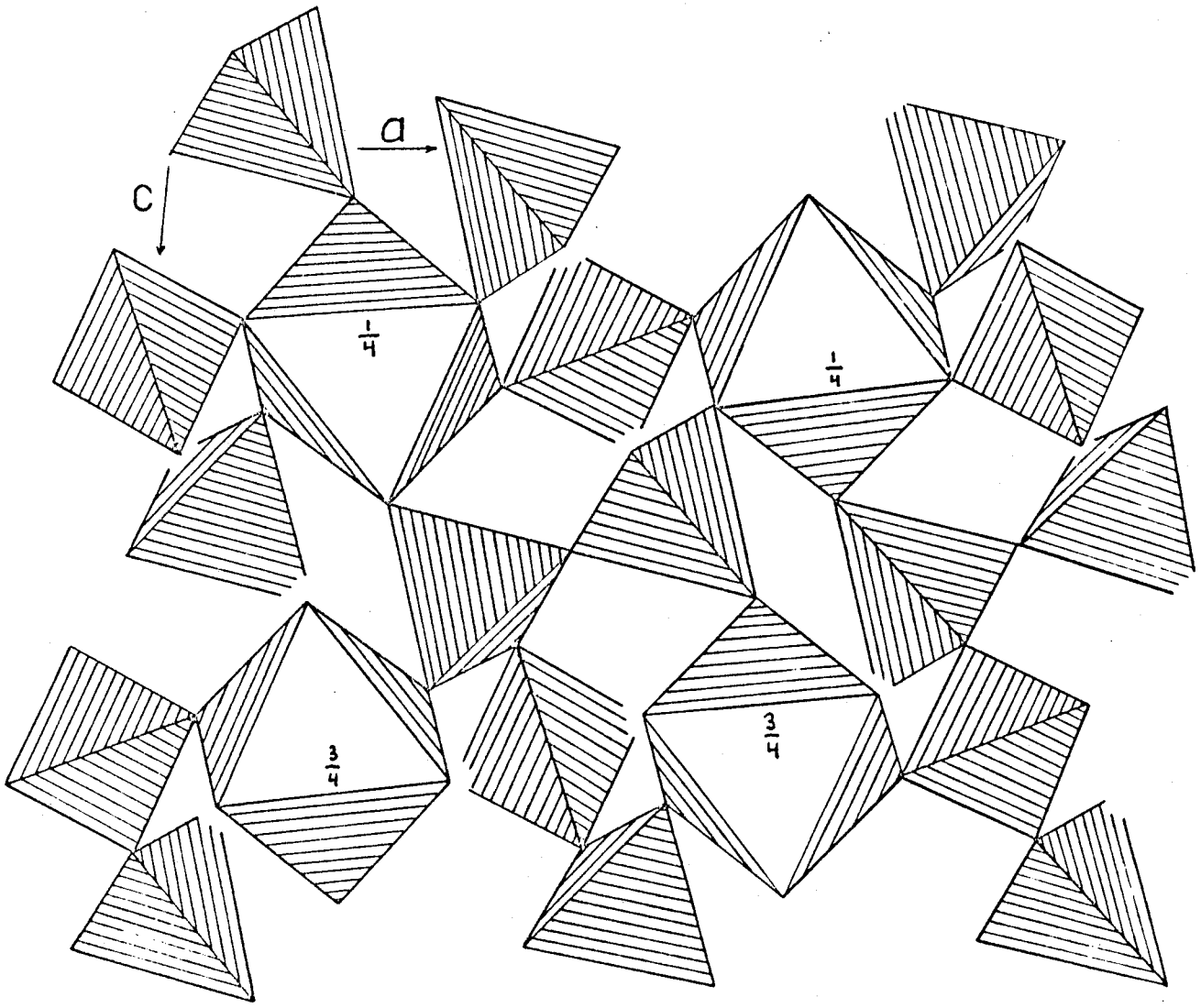

Figure 6-1. The average structure of $V(PO_3)_3$ projected down the b axis. The approximate y coordinates of the V^{+3} atoms are shown with respect to the small cell. Phosphorus atoms lie within the tetrahedra.

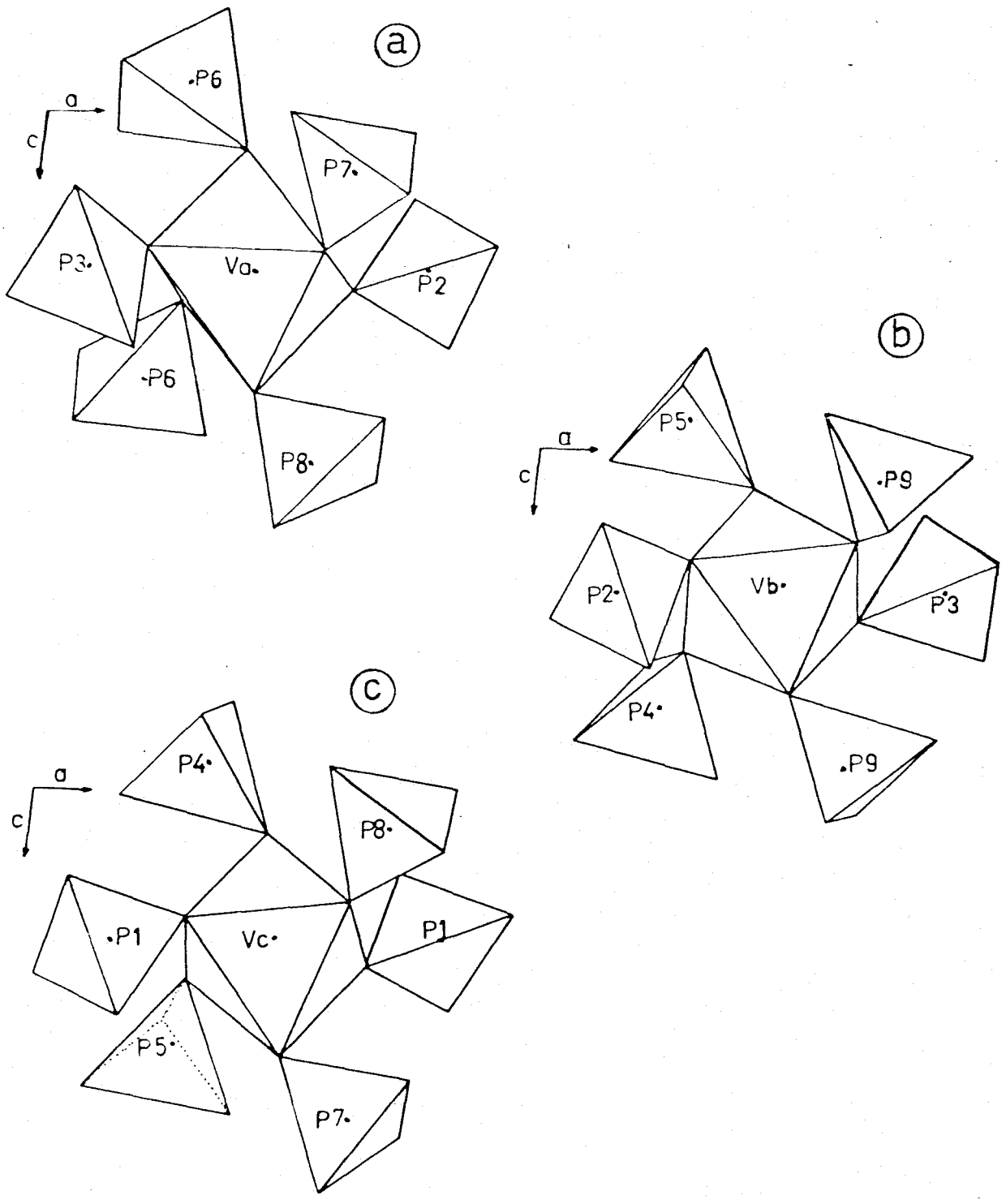

Figure 6-2. The environments about the vanadium atoms near x,z = $\frac{1}{4},\frac{1}{4}$ for the three ranges (a) $0 \leq y \leq 1/3$, (b) $1/3 \leq y \leq 2/3$ (c) $2/3 \leq y \leq 1$.

Table 6-2. Bond Geometry in $V(PO_3)_3$. The oxygen atoms are listed sequentially counterclockwise as they appear in diagram 5-2. They are labelled according to the atoms they bridge. Estimated standard deviations are in parentheses.

VO_6 groups - bonds are of the type V(x)-O(x,y)

distances (Å) for $V(a)O_6$			distances (Å) for $V(b)O_6$			distances (Å) for $V(c)O_6$		
x	y	distance	x	y	distance	x	y	distance
a	2	1.99(1)	b	3	2.02(1)	c'	1'	1.98(1)
a	7	1.99(1)	b'	9'	2.00(1)	c	8	2.00(1)
a'	6'	2.01(2)	b	5	1.96(2)	c	4	1.97(2)
a	3	1.98(1)	b	2	1.95(1)	c	1	1.98(1)
a	6	1.98(1)	b	4	2.02(1)	c	5	1.99(1)
a	8	2.03(2)	b	9	2.00(2)	c	7	2.01(2)

angles are of the type O(x,y)-V(x)-O(x,z)

angles (°) for $V(a)O_6$				angles (°) for $V(b)O_6$				angles (°) for $V(c)O_6$			
x	y	z	angle	x	y	z	angle	x	y	z	angle
a	2	7	92.6(5)	b	3	9'	90.5(5)	c	1'	8	92.0(5)
a	2	6'	88.9(6)	b	3	5	89.4(7)	c	1'	4	87.8(6)
a	2	3	172.6(6)	b	3	2	176.5(9)	c	1'	1	175.4(6)
a	2	6	87.9(5)	b	3	4	90.9(5)	c	1'	5	93.7(5)
a	2	8	90.8(6)	b	3	9	93.6(7)	c	1'	7	84.2(6)
a	7	6'	90.1(6)	b	9'	5	88.3(6)	c	8	4	93.1(6)
a	7	3	91.1(5)	b	9'	2	89.5(5)	c	8	1	84.3(5)
a	7	6	177.5(6)	b	9'	4	177.2(6)	c	8	5	174.3(5)
a	7	8	86.8(6)	b	9'	9	89.1(5)	c	8	7	93.2(6)
a	6'	3	84.6(6)	b	5	2	87.1(7)	c	4	1	95.1(7)
a	6'	6	92.3(6)	b	5	4	94.2(6)	c	4	5	87.8(6)
a	6'	8	176.9(5)	b	5	9	176.0(6)	c	4	7	170.0(6)

table 6-2 cont.

angles (°) for $V(a)O_6$

x	y	z	angle
a	3	6	88.7(5)
a	3	8	95.8(5)
a	6	8	90.8(6)

angles (°) for $V(b)O_6$

x	y	z	angle
b	2	4	89.3(5)
b	2	9	89.9(6)
b	4	9	88.4(6)

angles (°) for $V(c)O_6$

x	y	z	angle
c	1	5	90.0(5)
c	1	7	93.3(7)
c	5	7	86.8(6)

PO_4 groups - bonds are of the type P(x)-O(y,x)

distances (Å) for $P(2)O_4$

x	y	distance
2	a	1.49(1)
2	5	1.60(2)
2	b	1.49(1)
2	8	1.60(2)

distances (Å) for $P(3)O_4$

x	y	distance
3	b	1.46(1)
3	4	1.59(2)
3	a	1.48(1)
3	7	1.60(2)

distances (Å) for $P(1)O_4$

x	y	distance
1	c'	1.49(1)
1	6	1.55(2)
1	c	1.50(1)
1	9	1.55(2)

angles are of the type O(x,y)-P(y)-O(z,y)

angles (°) for $P(2)O_4$

x	y	z	angle
a	2	5	107.2(8)
a	2	b	119.6(7)
a	2	8	112.1(9)
5	2	b	106.7(8)
5	2	8	108.0(8)
b	2	8	102.6(8)

angles (°) for $P(3)O_4$

x	y	z	angle
b	3	4	107.3(9)
b	3	a	118.5(7)
b	3	7	109.6(9)
4	3	a	106.9(8)
4	3	7	108.1(7)
a	3	7	106.0(8)

angles (°) for $P(1)O_4$

x	y	z	angle
c'	1	6	106.1(9)
c'	1	c	119.6(7)
c'	1	9	106.8(9)
6	1	c	110.0(9)
6	1	9	103.3(9)
c	1	9	109.7(9)

distances (Å) for $P(6)O_4$

x	y	distance
6	a'	1.48(2)
6	a	1.50(2)

distances (Å) for $P(5)O_4$

x	y	distance
5	b	1.50(2)
5	c	1.48(1)

distances (Å) for $P(4)O_4$

x	y	distance
4	c	1.48(2)
4	b	1.48(2)

table 6-2 cont.

distances(Å) for $P(6)O_4$

x	y	distance
6	1	1.61(2)
6	9	1.62(1)

angles (°) for $P(6)O_4$

x	y	z	angle
a'	6	a	115.6(8)
a'	6	1	114.7(9)
a'	6	9	106.6(10)
a	6	1	106.1(10)
a	6	9	111.3(7)
1	6	9	101.8(6)

distances (Å) for $P(8)O_4$

x	y	distance
8	a	1.49(2)
8	c	1.46(2)
8	2	1.57(2)
8	4	1.55(1)

angles (°) for $P(8)O_4$

x	y	z	angle
a	8	c	118.4(7)
a	8	2	108.3(8)
a	8	4	110.7(9)
c	8	2	109.8(10)
c	8	4	107.7(7)
2	8	4	100.3(6)

distances (Å) for $P(5)O_4$

x	y	distance
5	2	1.58(1)
5	7	1.60(1)

angles (°) for $P(5)O_4$

x	y	z	angle
b	5	c	117.2(7)
b	5	2	107.4(9)
b	5	7	107.3(7)
c	5	2	110.9(9)
c	5	7	113.0(7)
2	5	7	99.6(6)

distances (Å) for $P(9)O_4$

x	y	distance
9	b'	1.46(2)
9	b	1.49(1)
9	1	1.59(2)
9	6	1.58(1)

angles (°) for $P(9)O_4$

x	y	z	angle
b'	9	b	117.2(8)
b'	9	1	109.7(8)
b'	9	6	112.6(9)
b	9	1	107.7(9)
b	9	6	109.3(7)
1	9	6	98.7(7)

distances (Å) for $P(4)O_4$

x	y	distance
4	3	1.56(1)
4	8	1.59(1)

angles (°) for $P(4)O_4$

x	y	z	angle
c	4	b	117.9(9)
c	4	3	109.0(9)
c	4	8	105.4(8)
b	4	3	110.9(9)
b	4	8	112.4(7)
3	4	8	100.8(6)

distances (Å) for $P(7)O_4$

x	y	distance
7	c	1.48(2)
7	a	1.49(2)
7	3	1.60(1)
7	5	1.54(1)

angles (°) for $P(7)O_4$

x	y	z	angle
c	7	a	116.3(7)
c	7	3	109.9(8)
c	7	5	111.4(10)
a	7	3	109.1(10)
a	7	5	106.1(8)
3	7	5	103.1(6)

Table 6-3. Average bond geometry in $V(PO_3)_3$

	Length(Å)		
Bond	Maximum	Minimum	Average
V - O	2.03(1)	1.95(1)	1.99
P - O(-P)	1.62(1)	1.54(1)	1.58
P - O(-V)	1.50(1)	1.46(1)	1.48

	Angle(°)		
Angle	Maximum	Minimum	Average
O-V-O(axial)	177.5(5)	170.0(5)	175.2
O-V-O	95.8(5)	84.2(5)	90.0
(P-)O-P-O(-P)	108.1(6)	98.7(7)	102.6
(P-)O-P-O(-V)	114.7(8)	102.6(8)	108.8
(V-)O-P-O(-V)	119.6(7)	115.6(8)	117.7

Table 6-4. Distances between corresponding atoms in figure 6-2 when those in 6-2(b) are translated by $-\underline{b}/3$ and those in 6-2(c) are translated by $-2\underline{b}/3$. Oxygen atoms for each polyhedron are listed sequentially starting at the oxygen bridging the P and V atoms and going counterclockwise. Values are in Å.

Atom a from diag. 6-2(a)	Atom b from diag. 6-2(b)	Atom c from diag. 6-2(c)	distance between a and b	distance between a and c	distance between b and c
V(a)	V(b)	V(c)	0.05	0.30	0.35
P(2)	P(3)	P(1)	0.16	0.52	0.36
O(a,2)	O(b,3)	O(c¦1')	0.41	0.46	0.43
O(5,2)	O(4,3)	O(6,1)	0.12	0.76	0.83
O(b,2)	O(a,3)	O(c,1)	0.49	0.51	0.53
O(8,2)	O(7,3)	O(9,1)	0.16	0.83	0.74
P(6)	P(5)	P(4)	0.23	0.21	0.10
O(a¦6')	O(b,5)	O(c,4)	0.54	0.47	0.24
O(a,6)	O(c,5)	O(b,4)	0.70	0.74	0.28
O(6,1)	O(5,2)	O(4,3)	0.76	0.83	0.12
O(6,9)	O(5,7)	O(4,8)	1.12	1.12	0.06
P(8)	P(9)	P(7)	0.23	0.04	0.28
O(a,8)	O(b¦9')	O(c,7)	0.62	0.20	0.61
O(c,8)	O(b,9)	O(a,7)	0.79	0.13	0.81
O(8,2)	O(9,1)	O(7,3)	0.83	0.16	0.74
O(4,8)	O(6,9)	O(5,7)	1.12	0.06	1.12

figure 6-2 when those in 6-2(b) and 6-2(c) are translated by -$\underline{b}$/3 and -2$\underline{b}$/3 respectively. As can be seen, two of the vanadium atoms nearly superimpose, and the third, V_c, is displaced only by about 1/3 Å. The phosphorus atoms, similarly, are quite close to superposition, the biggest difference being about ½ Å between P(1) and P(3). The largest displacement of the oxygen atoms from superposition is 1.2 Å, the average is 0.6 Å. This is quite a substantial difference when we consider that a P-O bond has an average value of 1.53 Å. The angles subtended at the oxygen atoms by the cations to which they bond range from 135° to 151° (9 values) when both cations are phosphorus and from 133° to 158° (18 values) otherwise. No strong correlation exists between these angles and the distortions of the polyhedra.

It is conceivable that some V^{+5} could substitute for P^{+5} in the phosphate groups, and this could be the source of some of the polyhedral distortions. The occupations for V^{+5} at the tetrahedral site were not significantly different from zero when varied in the least-squares analysis.

§ 6.3 Thermal Behaviour of $V(PO_3)_3$

In an effort to determine if the differences between the sub and super cells increase or decrease with temperature, the intensities of five strong k=3n reflections and the 25 strongest k≠3n reflections were measured at room temperature, 300°C and 500°C. These intensities were normalized to the room temperature ones. The results, shown in figure 6-3, indicate that, although the errors are large, the k≠3n reflection intensities become substantially weaker with increasing temperature while those for k=3n only weaken slightly. Error bars represent the standard deviations of the intensity ratios.

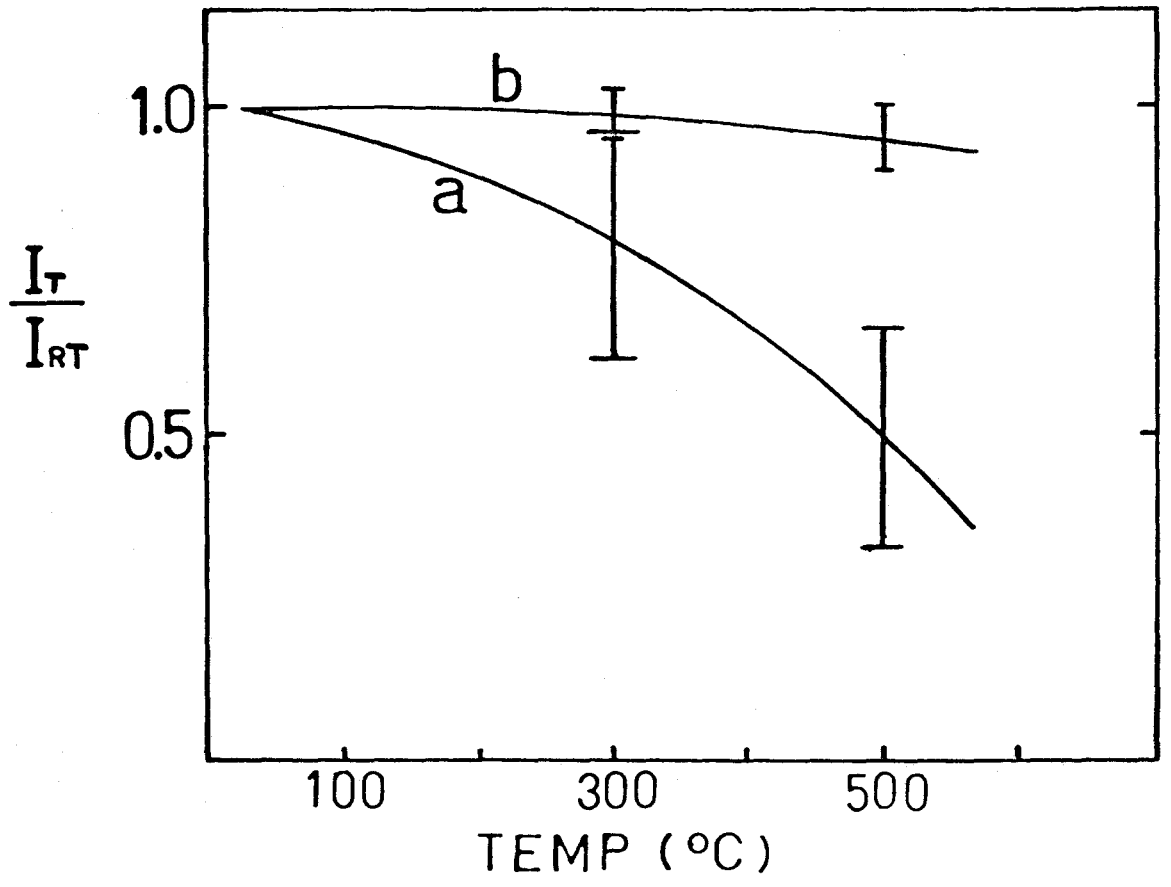

Figure 6-3. The ratio of the intensity at various temperatures compared to room temperature for (a) 25 strongest reflections with $k \neq 3n$ and (b) 5 strong reflections with $k = 3n$.

The relative decrease in intensity of the $k \neq 3n$ reflections indicates a breakdown of the superstructure. Each third of the cell will more closely resemble the other two thirds as the temperature increases. In fact, one might predict that, at about 650°C (by extrapolating the graph in figure 6-3), each third of the supercell will have the same structure, which is likely to be different from the room temperature substructure since the latter has some unlikely bond lengths and angles.

A second order phase transition to the subcell structure is predicted to occur around 650°C. Lavrov, et al.[44] found no evidence for a phase transition between room temperature and 1000°C by DTA; a result which was confirmed by us. However, second order phase transitions will not show up in DTA experiments.

$Cr(PO_3)_3$ is known to exist in six polymorphic forms[91,92], one of which has a powder pattern like $V(PO_3)_3$. No evidence has been found that $V(PO_3)_3$ can exist in or change to any other polymorphic form. Trimetaphosphates for the trivalent metal ions of Al, Ti, Fe and Mo[92,93,95,96] have also been reported to be structurally the same (from powder patterns) as $V(PO_3)_3$. None of these show the extensive polymorphism of $Cr(PO_3)_3$.

The crystal structure and thermal behaviour of $V(PO_3)_3$ has been published in the Canadian Journal of Chemistry[97].

CHAPTER 7

Crystal Structure of $(VO)_2P_2O_7$

§ 7.1 Solution of the Structure

From the systematic extinctions ($h0\ell$, $\ell \neq 2n$ and $0k\ell$, $k \neq 2n$), the space group was determined to be centrosymmetric Pbcm, or non-centrosymmetric $Pbc2_1$. The latter is an unconventional setting of $Pca2_1$ chosen to make conversion from the centrosymmetric space group easier. Precession photographs showed reflections with $(h+\frac{1}{2}\ell) \neq 2n$ and with $k \neq 2n$ to be weak, indicating a pseudo-translational symmetry of $\frac{1}{2}\underline{a}+\frac{1}{4}\underline{c}$ and a similarity of structure at $y=\frac{1}{2}$ and $y=0$ respectively. Examination of the Patterson function corroborated these conclusions, and suggested the vanadium positions of (0.5,0.0,0.1) and (0.0,0.0,0.35) for the centrosymmetric space group, as well as the phosphorus positions of (0.2,0.05,0.0) (or (0.2,-0.05,0.0)) and (0.3,0.05,0.25) (or (0.3,-0.05,0.0)). A Patterson peak at $0.4\underline{b}$ indicated that the phosphorus atoms are contained in P_2O_7 groups with the P-P vectors parallel to $\underline{b}$.. This placed two more phosphorus atoms at a distance of about $0.4\underline{b}$ from the previous phosphorus positions. Each of the two distinct P_2O_7 groups can be either above or below the plane at y=0. All of the four possible combinations of these placements were tried as models and the one with the lowest R-factor was chosen. In the centrosymmetric space group, these models refined to give P-P distances of about 3.6 Å, and R-factors ranging from 0.52 to 0.48. Refining the same partial models in $Pbc2_1$ eliminated the problem of the long P-P distances as well as giving substantially better R-factors

(0.35 for the best model). All further refinements were carried out in the non-centrosymmetric space group. The vanadyl oxygen positions were readily identified from a difference Fourier map based on the phosphorus and vanadium positions, but three oxygen atoms for each phosphate tetrahedron were indicated on this map at positions in the y=0 plane which gave P-O distances that were too short. In addition, residual peaks were found at positions related by a mirror plane at y=0 to the phosphorus positions. Placing the phosphate oxygen atoms in their most probable positions failed to give acceptable geometries on refinement.

Bordes and Courtine[40] found antiphase boundaries prevalent in $(VO)_2P_2O_7$ electron micrographs. Such boundaries could explain the phosphorus mirror peaks and would give an average of two possible positions for each phosphate oxygen atom related by the symmetry of the antiphase boundary, if these positions are close to each other and the antiphase boundaries are plentiful. Possible antiphase boundaries will be discussed later.

In addition to the psuedo-symmetry already mentioned, the pyrophosphate, P_2O_7, groups have two pseudo-mirror planes: one in the P-O-P plane and one perpendicular to this through the bridging oxygen. The large amount of pseudo-symmetry makes the correlation coefficients between positional coordinates large (values as high as 0.9 were found) and tends to prevent least-squares convergence to the actual atomic coordinates. In an effort to obtain the most accurate starting positions for the refinement of the oxygen coordinates, the P_2O_7 group positions were refined by rigid group least-squares refinement. The P-O bond lengths in the phosphate tetrahedra were predicted using Baur's[94] and Brown's[16] models (table 7-1). Since the actual bond lengths for the phosphate groups

Table 7-1. Predicted bond lengths in the phosphate tetrahedra of $(VO)_2P_2O_7$. O_b is the oxygen atom bridging the two tetrahedra in the P_2O_7 group, O_1 is the oxygen atom which is bonded to the two vanadium atoms, and O_2 and O_3 are the oxygen atoms bonded to one vanadium atom each.

Bond	Predicted value based on Brown's[16] model (Å)	Predicted value based on Baur's[94] model (Å)	Average predicted value (Å)
$P-O_b$	1.62	1.595	1.61
P-01	1.55	1.60	1.575
P-02	1.50	1.53	1.515
P-03	1.50	1.53	1.515

considered in the previous chapters were mid-way between the predicted values based on Brown's and Baur's models, the averages of these predicted values for the $(VO)_2P_2O_7$ structure were the ones used in the rigid group refinement. In addition, it was assumed that the four oxygen atoms were at the corners of a regular tetrahedron with the phosphorus atom placed to give the calculated bond lengths. The position and orientation of each of the tetrahedra were refined until shifts per error ceased to be significant. The R-factor was 0.26 at this point. The resulting coordinates, when used as initial parameters in the least-squares refinement of the individual atomic positions, still failed to converge to values which yielded satisfactory geometries.

Two models for antiphase boundaries were then tried as follows:
Model I - For each pyrophosphate group, a second group, related by a mirror plane at y=0 to the first, was added to the model, and the occupation of the groups was refined so that the total occupancy remained 1.0. Convergence was obtained at an occupancy of 0.5 for each group. The positional and isotropic thermal coordinates were then refined.
Model II - For each P_2O_7 group, a second group related by a mirror plane at x=0 to the first, was added to the model, and the occupation of the groups and the coordinates were then refined as for model I.
Both Model I and Model II gave the same structure (within the standard errors), but the estimated standard deviations of the coordinates were very large. Positional and thermal coordinates are given in table 7-2 and bond geometries in table 7-3. The standard deviations of the intensities were used as weights since the models were not accurate enough to determine a weighting scheme based on Cruickshank coefficients. The

Table 7-2. Positional and Isotropic Thermal coordinates for $(VO)_2P_2O_7$ Estimated standard deviations are in parentheses.

Atom	x	y	z	U(A^2)
V1	0.5150(9)	0.035(1)	0.963	0.013(1)
V2	0.4991(8)	-0.044(1)	-0.0938(8)	0.006(1)
V3	0.0043(9)	0.042(1)	0.3457(8)	0.009(1)
V4	-0.0006(8)	0.0501(8)	-0.3437(7)	0.005(1)
P1	0.205(2)	0.030(3)	0.002(2)	0.005(3)
P2	0.203(2)	0.422(3)	0.003(2)	0.007(3)
P3	0.287(2)	-0.031(3)	0.262(2)	0.004(3)
P4	0.295(2)	0.576(3)	0.254(2)	0.006(3)
01	0.375(6)	0.008(10)	-0.005(5)	0.008(10)
02	0.150(7)	-0.060(9)	-0.078(4)	0.011(10)
03	0.151(7)	-0.068(9)	0.079(5)	0.014(10)
04	0.166(6)	0.230(8)	-0.006(4)	0.008(11)
05	0.350(8)	0.461(9)	0.014(5)	0.012(11)
06	0.139(6)	0.484(10)	0.078(4)	0.007(11)
07	0.145(7)	0.499(10)	-0.072(4)	0.006(12)
08	0.141(6)	0.004(10)	0.253(4)	0.004(11)
09	0.356(7)	-0.002(10)	0.177(4)	0.004(11)
010	0.360(7)	0.078(9)	0.322(4)	0.010(10)
011	0.290(6)	-0.221(8)	0.291(4)	0.009(10)
012	0.129(7)	0.544(8)	0.252(5)	0.006(10)

Table 7-2 cont.

Atom	x	y	z	U(A^2)
O13	0.366(7)	0.495(10)	0.323(4)	0.006(11)
O14	0.361(8)	0.589(10)	0.185(5)	0.017(12)
OV1	0.517(4)	0.248(7)	0.093(3)	0.024(8)
OV2	0.536(3)	-0.228(4)	-0.090(2)	0.005(7)
OV3	0.009(6)	0.263(7)	0.341(3)	0.020(9)
OV4	0.021(3)	0.250(5)	-0.339(2)	0.005(7)

Table 7-3. Bond Geometries for $(VO)_2P_2O_7$. Estimated standard deviations are indicated in parentheses, and all values are in angstroms, or degrees.

Bond Lengths

Bond	Length	Bond	Length	Bond	Length	Bond	Length
V1-01	2.15(8)	V2-01	1.94(7)	V3-08	2.04(7)	V4-08	2.14(7)
V1-05	1.96(8)	V2-05	2.30(8)	V3-012	2.02(7)	V4-012	2.14(7)
V1-09	2.05(7)	V2-010	1.96(7)	V3-02	1.95(7)	V4-03	1.93(8)
V1-014	1.94(8)	V2-013	1.92(7)	V3-07	1.94(7)	V4-06	1.88(7)
V1-0V1	1.64(5)	V2-0V2	1.47(5)	V3-0V3	1.71(6)	V4-0V4	1.56(4)
V1-0V1	2.24(5)	V2-0V2	2.47(5)	V3-0V3	2.16(6)	V4-0V4	2.33(4)
P1-01	1.64(7)	P2-05	1.46(8)	P3-08	1.43(7)	P4-012	1.61(7)
P1-02	1.59(8)	P2-06	1.47(8)	P3-09	1.57(7)	P4-013	1.47(8)
P1-03	1.56(8)	P2-07	1.48(8)	P3-010	1.48(7)	P4-014	1.34(8)
P1-04	1.60(7)	P2-04	1.53(7)	P3-011	1.58(7)	P4-011	1.56(7)
P1-P2	3.02(3)			P3-P4	3.05(3)		

Bond Angles

Bonds	Angles	Bonds	Angles
0V1-V1-01	95(3)	0V2-V2-01	108(3)
0V1-V1-05	105(3)	0V2-V2-05	81(3)
0V1-V1-09	100(3)	0V2-V2-010	75(3)
0V1-V1-014	79(3)	0V2-V2-013	113(3)
01-V1-05	81(3)	01-V2-05	78(3)
01-V1-09	92(3)	01-V2-010	174(3)
01-V1-014	173(3)	01-V2-013	96(3)
05-V1-09	154(3)	05-V2-010	97(3)

Table 7-3 cont.

Bonds	Angles	Bonds	Angles
05-V1-014	101(3)	05-V2-013	167(3)
09-V1-014	89(3)	010-V2-013	89(3)
0V3-V3-08	95(3)	0V4-V4-08	104(3)
0V3-V3-012	89(3)	0V4-V4-012	103(3)
0V3-V3-02	89(3)	0V4-V4-03	94(3)
0V3-V3-07	100(3)	0V4-V4-06	95(3)
08-V3-012	80(3)	08-V4-012	75(3)
08-V3-02	170(3)	08-V4-03	93(3)
08-V3-07	93(3)	08-V4-06	160(3)
012-V3-02	91(3)	012-V4-03	161(3)
012-V3-07	170(3)	012-V4-06	93(3)
02-V3-07	95(3)	03-V4-06	95(3)
01-P1-02	103(4)	05-P2-06	103(4)
01-P1-03	109(4)	05-P2-07	113(4)
01-P1-04	109(4)	05-P2-04	116(4)
02-P1-03	110(4)	06-P2-07	115(4)
02-P1-04	106(4)	06-P2-04	108(4)
03-P1-04	118(4)	07-P2-04	103(5)
08-P3-09	107(4)	012-P4-013	115(4)
08-P3-010	115(5)	012-P4-014	118(5)
08-P3-011	103(4)	012-P4-011	98(4)
09-P3-010	109(4)	013-P4-014	119(5)
09-P3-011	108(4)	013-P4-011	102(4)
010-P3-011	114(4)	014-P4-011	101(4)

final R and R_w were both 0.18.

§ 7.2 Description of the Structure (figure 7-1)

$(VO)_2P_2O_7$ contains chains parallel to b consisting of two edge-sharing VO_6 octahedra, corner-sharing axial oxygens to two more octahedra above and below. The axial oxygens form the typical vanadyl bond to one vanadium and long bond to the other vanadium. The two edge-sharing octahedra have vanadyl bonds which point in opposite directions along the b axis. Pyrophosphate groups are found parallel to these chains with each half of these groups sharing an edge-shared oxygen of one double chain and an unshared equatorial oxygen of each of two other double chains.

Both pyrophosphate groups are in eclipsed configuration with equal P-O-P angles of 150°. These angles are larger than the normal bridging angle range of 127-138° for eclipsed configurations[98]. This could be due to the lack of any additional long range bonding to the bridging oxygen atom which is often found for the eclipsed configuration, or due to the O-O spacing in the double VO_6 chains. The P_2O_7 groups are very symmetric, containing two pseudo-mirror planes, one perpendicular to c through the two phosphorus atoms, and one perpendicular to b through the bridging oxygen.

The standard deviations for the bond lengths and angles are too large to allow meaningful comparisons. However, the average P-O bonds for the bridging, two-coordinate and three-coordinate oxygens respectively are 1.57(4), 1.50(3) and 1.54(4) they equal within the errors the predicted values in table 7-1. The average equatorial V-O bond lengths for the two and three-coordinated oxygens are 1.95(3) and 2.09(3)

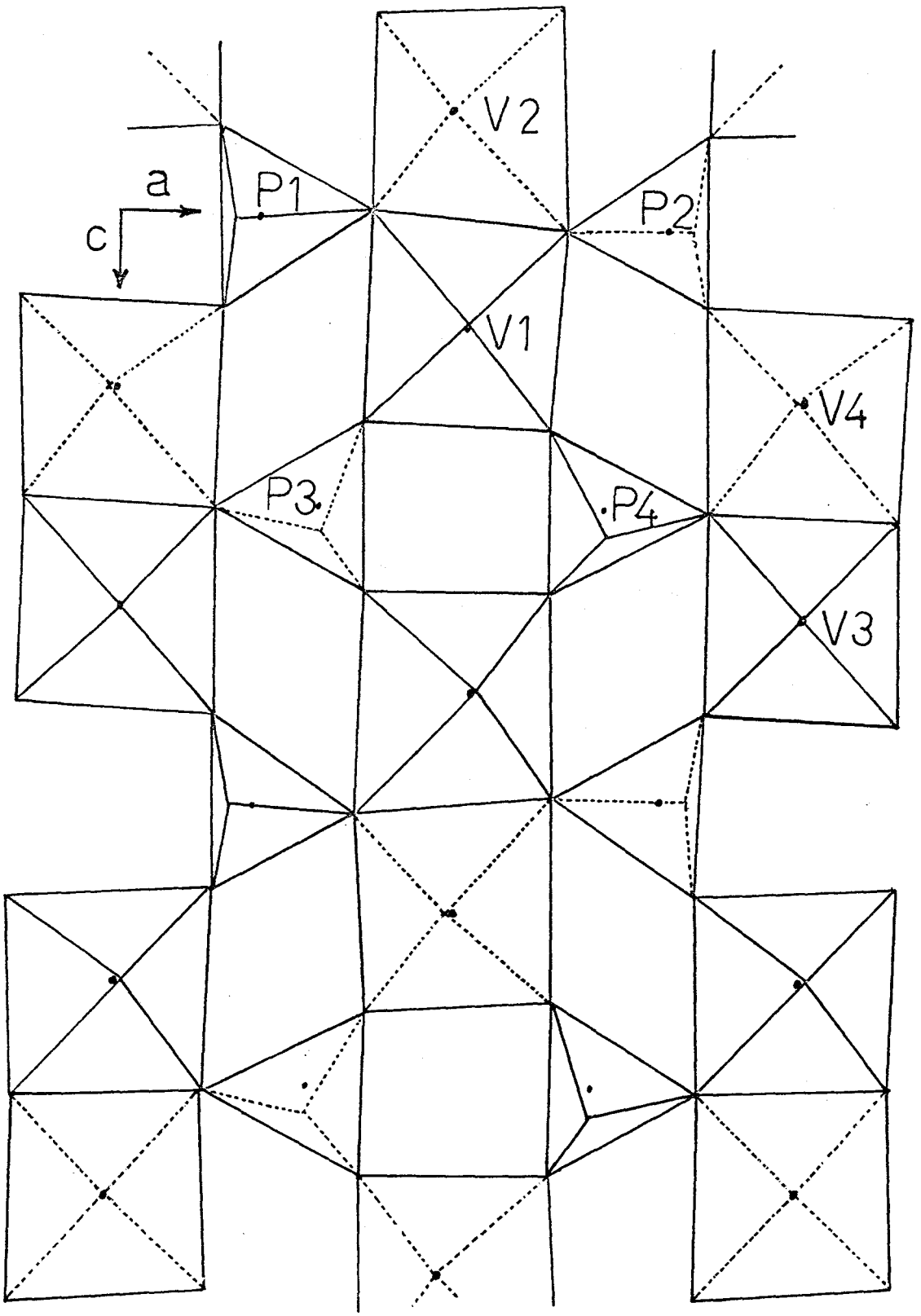

Figure 7-1. The crystal structure of $(VO)_2P_2O_7$ as projected down the b-axis. Only half the structure is shown. The remaining part of the cell may be generated by a b-glide.

They compare favourably with the predicted values based on Brown's[16] (1.95 and 2.11) and Baur's[94] model (1.94 and 2.08). The average vanadyl bond length of 1.60(3) is also in the range of those found for $V^{+4}O_6$ octahedra. The O-V-O angles between the vanadyl oxygen and the equatorial oxygen atoms should all be greater than 90° since the vanadyl bond is by far the strongest bond in the octahedron. The fact that some of these bond angles are substantially smaller than 90° probably reflects inaccuracies in the structure determination.

§ 7-3 Validity of the Structure

Since the R-factors and standard deviations of the positional coordinates are very large, some of these coordinates may be wrong. The general topology of the crystal structure contains no undesirable features, and, as will be seen in chapter 9, accounts for the conversion of VPO_5 to $(VO)_2P_2O_7$. In addition, Bordes and Courtine[40] have confirmed the presence of P_2O_7 groups. Thus, it is unlikely that the topology is in error. It is possible that one of the P_2O_7 groups is actually reflected in a mirror plane perpendicular to b, but such a reversal would likely introduce more angles less than 90° in the VO_6 octahedra. Antiphase boundaries possibly exist perpendicular to b, but they introduce the necessity of three joined PO_4 tetrahedra at the boundaries. Antiphase boundaries perpendicular to a are more likely since they do not require such a feature.

CHAPTER 8

Crystal Structure and Disorder for $VAsO_5$

§ 8.1 Solution of the Structure

The unit cell for $VAsO_5$ has a = 6.35(3)Å, b=6.32(3)Å, c=8.256(5)Å, $\gamma \simeq 90(1)^\circ$, Z = 4, space group $P2_1/n$ (c-axis unique). The unconventional setting of the space group was chosen to enable direct comparison with α-VPO_5.

The diffraction pattern of $VAsO_5$ shows streaks through the Bragg spots parallel to $\underline{c}^*$, and, in addition, shows some diffraction spots slightly displaced along $\underline{c}^*$ from the Bragg positions (figure 8-1). These features introduce errors in the measured intensities. Thus the structure refinement was not expected to give a low R-factor although the intensities were accurate enough to provide the basic structure. Intensities for displaced reflections were assigned to the nearest Bragg point in the structure determination.

The positions of the arsenic and vanadium atoms were readily determined from the Patterson function. A difference map, based on the least squares refined positions of these two atoms, showed peaks with maxima up to $\frac{1}{2}$ Å in diameter for the oxygen positions. More exact positions for the oxygen atoms within the volume from the difference map were calculated assuming approximate V-O-(As) and As-O bond lengths of 1.90 and 1.68 Å respectively. The vanadyl oxygen bond was assumed to be 1.6 Å. Atomic positions so derived and isotropic temperature factors refined readily to an R-factor of 0.23. Anisotropic temperature coordinates refinement was

attempted but was unsuccessful.

A difference map at this point showed some residual peaks. Since the diffraction pattern indicated one dimensional disorder and the structure is layered, it was assumed that these peaks were due to stacking faults. A model for such faults will be described in section 8-4. Introduction of these faults into the least squares refinement, by placing atoms in positions defined by the displacement vectors of the faults relative to their "normal" positions, was attempted. The occupation number of these atoms was refined in such a way that the total occupation of any atom in the cell remained at 1. The refinement indicated that each of two stacking faults occurred 10(1) % of the time. The R-factor at this point was R =0.192, and R_w = 0.198. Unit weights were used since it was felt that the systematic errors due to the stacking faults were much larger than the random errors and thus nothing would be gained by any other weighting scheme.

Final co-ordinates are given in table 8-1.

§ 8.2 The Basic Structure of $VAsO_5$

Crystalline $VAsO_5$ contains layers like those of α-VPO_5 containing VO_6 octahedra sharing equatorial oxygens with four different AsO_4 tetrahedra, all of which share corners with four VO_6 groups (figure 8-2). The structure differs substantially from that of α-VPO_5 in the stacking of such layers (figure 8-3). In α-VPO_5, the layers are only displaced from each other along the c-axis, being connected at the vanadyl oxygens. In $VAsO_5$, the layers are displaced horizontally as well as along c, thereby forming double layers in which two VO_6 groups share an edge in such a way that an equatorial and a long-bonded axial oxygen of one group form a

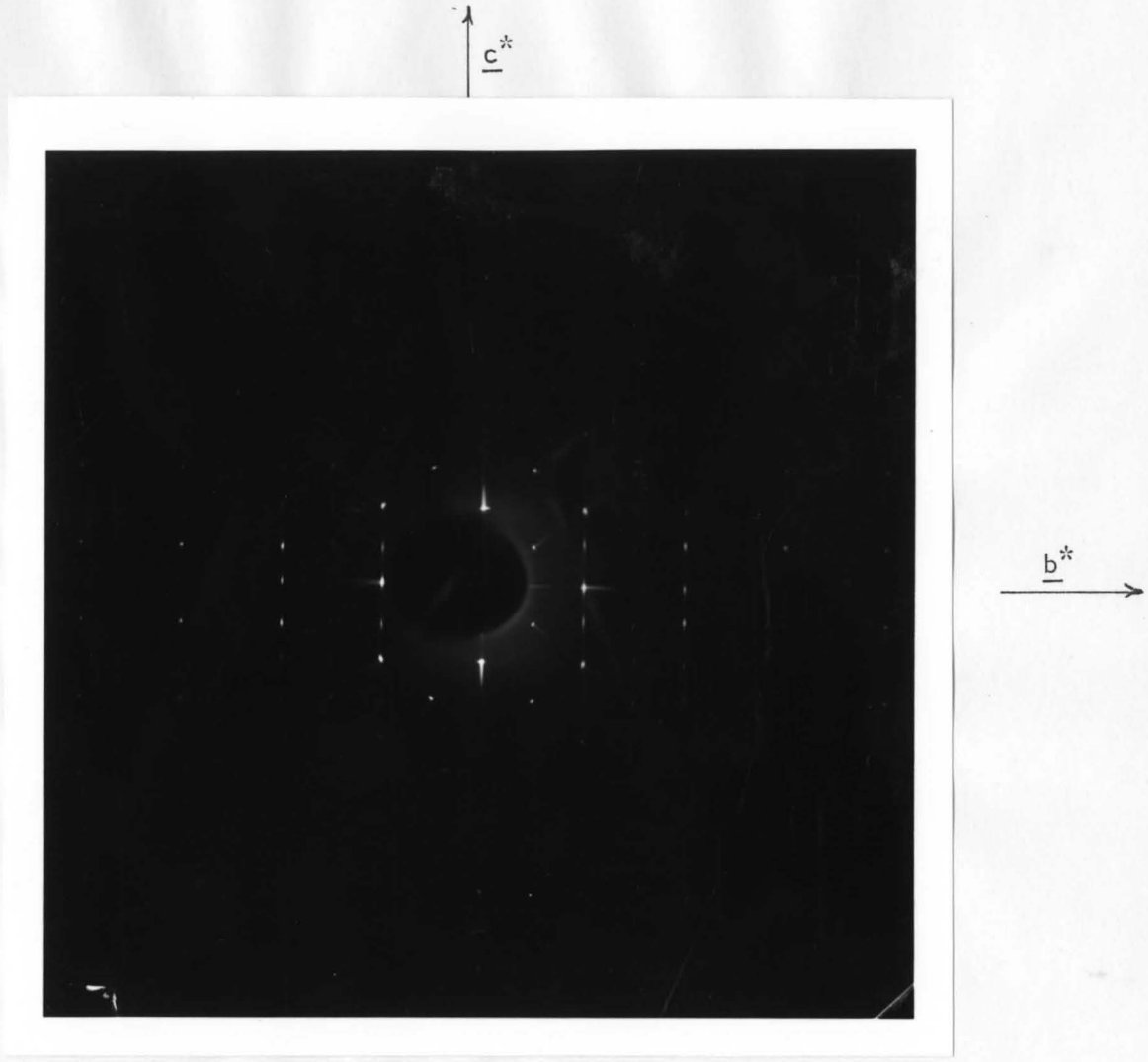

Figure 8-1. The 0kℓ diffraction pattern of $VAsO_5$, showing the diffuse streaks due to stacking faults along the $\underline{c}^*$ direction and displacement of some spots from the Bragg points (e.g. the 021 and $02\bar{1}$ spots)

Table 8-1. Positional and Thermal coordinates for $VAsO_5$. Estimated standard deviations are indicated in parentheses.

Atom	x	y	z	U($Å^2$)
As	0.1582(3)	0.4619(3)	0.2480(3)	0.0028(5)
V	0.1575(6)	0.9646(6)	0.3288(4)	0.0030(7)
O(1)	0.218(3)	0.259(3)	0.364(2)	0.004(3)
O(2)	0.109(3)	0.671(3)	0.369(2)	0.010(3)
O(3)	0.863(3)	0.008(3)	0.378(2)	0.002(3)
O(4)	0.446(3)	0.899(3)	0.364(2)	0.004(3)
O(V)	0.141(3)	0.949(3)	0.137(3)	0.014(4)

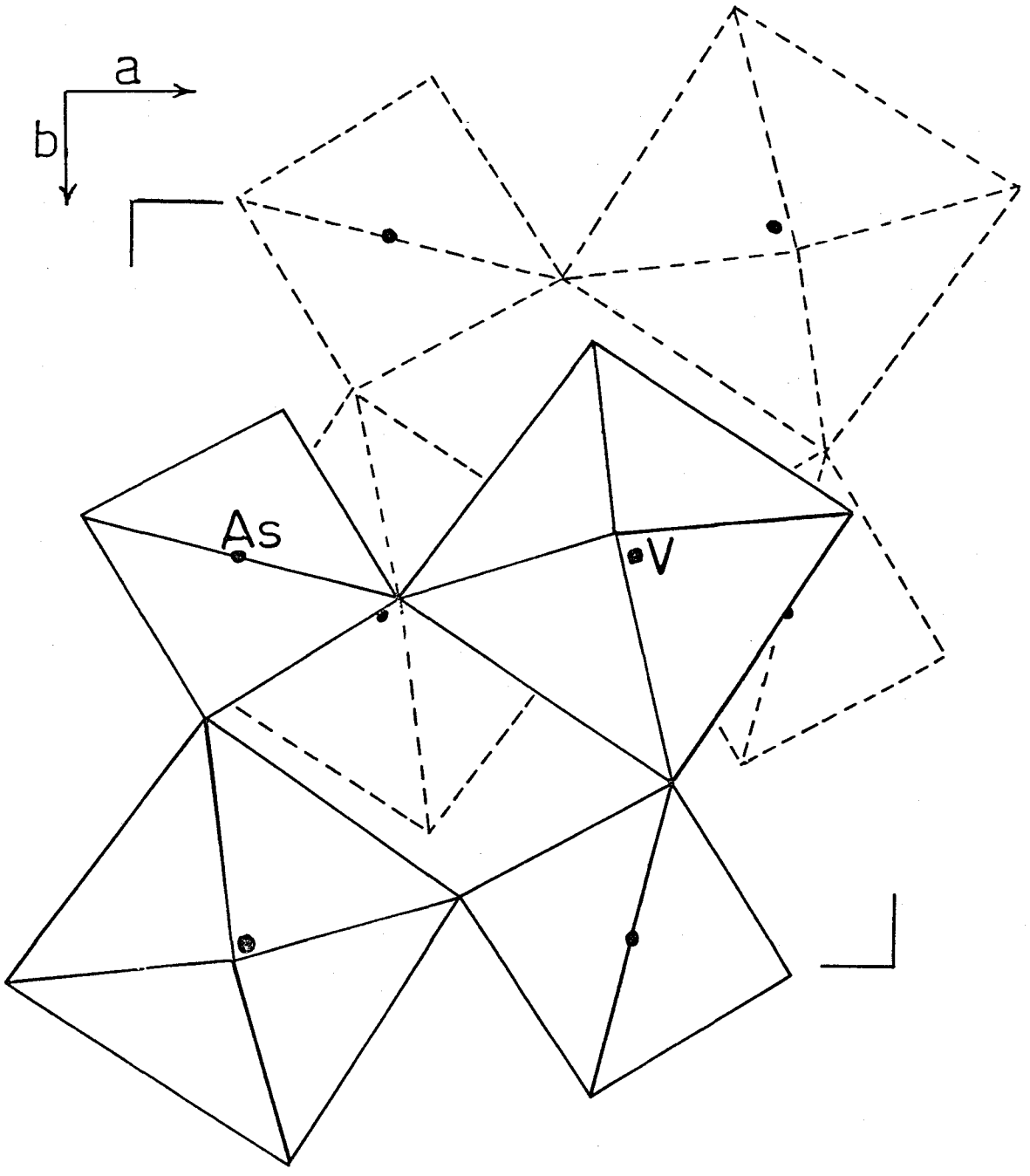

Figure 8-2. The structure of $VAsO_5$ as projected along the $\underline{c}$ axis, The dotted polyhedra are related to the others by a centre of inversion at the origin.

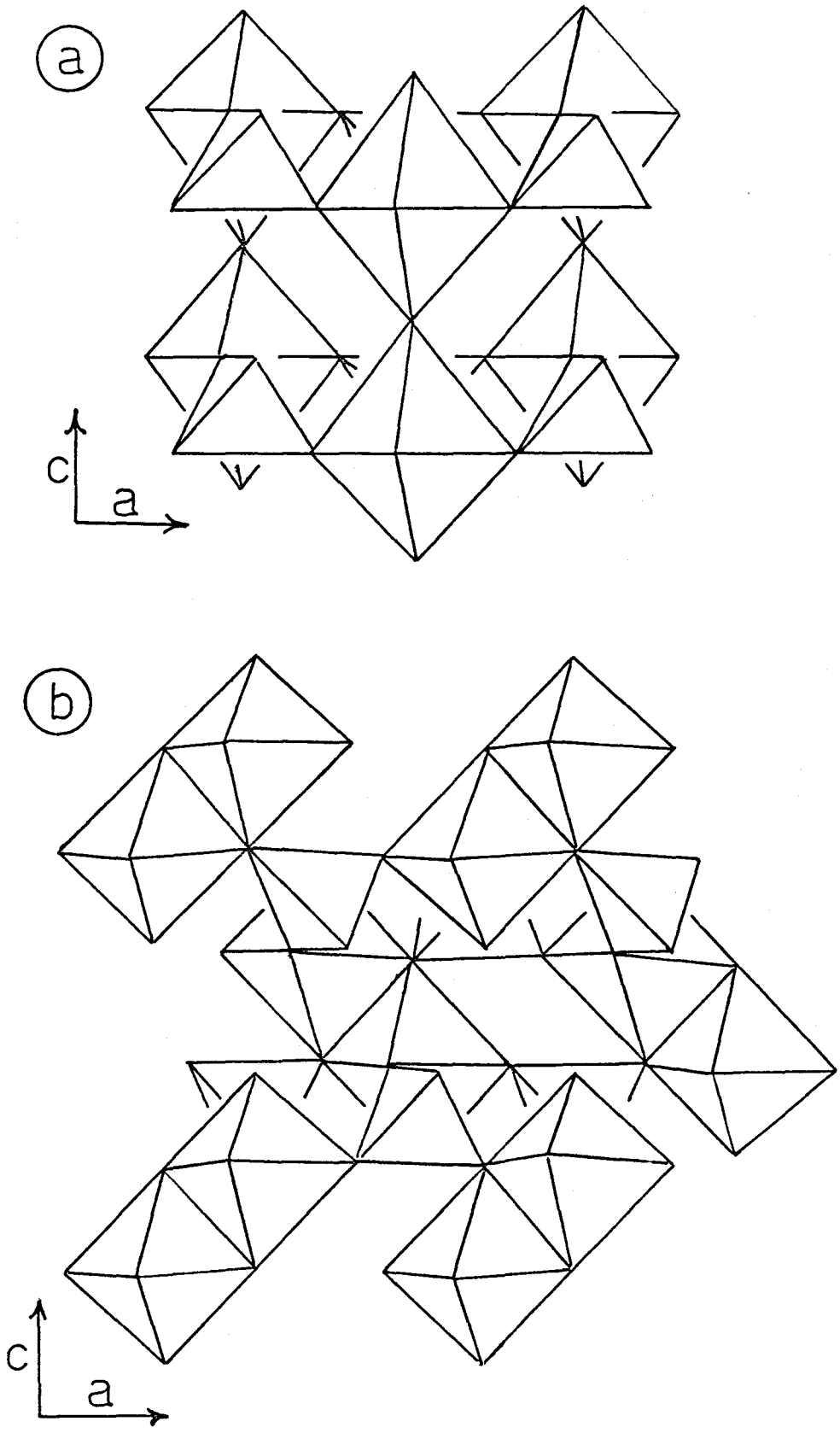

Figure 8-3. The structures of α-VPO_5 (a) and $VAsO_5$ (b) as projected on the ac plane, showing the difference in the stacking of the layers. The $VAsO_5$ layers can be produced from the α-VPO_5 layers by a translation of a layer perpendicular to and slightly down along c.

long-bonded axial and equatorial oxygen respectively of the other group. The vanadyl bonds of these two edge-sharing groups point in opposite directions, and the vanadyl oxygens are uni-coordinated. Within one layer, the VO_6 groups alternately share edges with groups in the layer above and below. The formation of these edge-shared groups accounts for the $VAsO_5$ c-axis being slightly less than twice the α-VPO_5 c-axis (8.256 Å c.f. 8.868 Å).

As can be seen from table 8-2, the bond distances for the equatorial V-O bonds are slightly larger than the corresponding ones for α-VPO_5. This is compensated for by a shorter "long" V-O bond. O-V-O and O-As-O angles do not differ greatly from the corresponding ones in α-VPO_5, the greatest difference of 6° existing for axial-equatorial angles in VO_6. These differences are undoubtedly due to the different stacking of the layers. It is surprising that the As-O(3) bond is no longer than the other As-O bonds as would be predicted by bond valence calculations. However, the total As valence using Brown's[16] bond-valence parameters is 4.94 and that for Vanadium is 4.99; both in good agreement with the expected value.

§ 8.3 Theory of Diffraction from Stacking Faults

Although several authors have treated the topic of diffraction from stacking faults [69,70], the treatment given by Cowley [71] lends itself most readily to computations. It will be briefly reviewed here for the case of two possible stacking faults with equal probability, which, as will be seen in section 8-4, applies to $VAsO_5$.

For convenience, and to prevent confusion later on, a layer of unit cells perpendicular to c will be called a sheet, to differentiate it

Table 8-2. Bond lengths and angles in $VAsO_5$ with standard deviations in parentheses. The corresponding bond lengths for α-VPO_5 have been listed for comparison.

Bond	Distance (Å)	corresponding α-VPO_5 distance	Bond	Distance (Å)	corresponding α-VPO_5 distance
V-O(1)	1.874(17)	1.858(7)	As-O(1)	1.690(16)	1.541(8)
V-O(2)	1.905(19)	1.858(7)	As-O(2)	1.690(19)	1.541(8)
V-O(3)	1.929(16)	1.858(7)	As-O(3)	1.685(15)	1.541(8)
V-O(4)	1.896(16)	1.858(7)	As-O(4)	1.680(17)	1.541(8)
V-O(V)	1.592(21)	1.580(11)			
V-O(3)x*	2.431(16)	2.853(11)			

*O(3)x refers to O(3) when it forms a long V-O bond

Bonds	Angle(°)	corresponding α-VPO_5 angle	Bonds	Angle(°)	corresponding α-VPO_5 angle
O(1)-V-O(2)	160.7(8)	156.7(4)	O(1)-As-O(2)	109.9(9)	109.1(4)
O(1)-V-O(3)	91.6(7)	87.7(4)	O(1)-As-O(3)	108.4(8)	109.7(4)
O(1)-V-O(4)	89.4(7)	87.7(4)	O(1)-As-O(4)	107.9(8)	109.7(4)
O(2)-V-O(3)	87.1(7)	87.7(4)	O(2)-As-O(3)	111.5(8)	109.7(4)
O(2)-V-O(4)	84.9(8)	87.7(4)	O(2)-As-O(4)	111.7(9)	109.7(4)
O(3)-V-O(4)	158.5(7)	156.7(4)	O(3)-As-O(4)	108.2(8)	109.7(4)
O(3)x-V-O(1)	77.6(6)	78.4(2)	O(V)-V-O(1)	103.3(9)	101.6(2)
O(3)x-V-O(2)	83.5(7)	78.4(2)	O(V)-V-O(2)	95.9(9)	101.6(2)
O(3)x-V-O(3)	74.4(6)	78.4(2)	O(V)-V-O(3)	99.0(9)	101.6(2)
O(3)x-V-O(4)	84.9(6)	78.4(2)	O(V)-V-O(4)	101.7(9)	101.6(2)
O(3)x-V-O(V)	173.3(9)	180(exact)			

from the structural layer as described in section 8-2. Thus, for $VAsO_5$, two layers make up a sheet, and the sheet is the repeating unit in the $\underline{c}$ direction.

When no faults occur, sheets stack along $\underline{c}$ with corresponding points in adjacent sheets related by the vector $\underline{c}$. If a fault of type 1 occurs, these points in the layer immediately before and immediately after the fault will be related by $\underline{c}+\underline{S}_1$, or by $\underline{c}+\underline{S}_2$ for a fault of type 2, where $\underline{S}_1$ and $\underline{S}_2$ are the displacement vectors of the faults. The electron density distribution of the two kinds of faults will be denoted by Δ_1 and Δ_2 and will have Fourier transforms denoted by G_1 and G_2. The electron density of the sheet and its Fourier transform will be ρ and F respectively. When a fault of type 1 or 2 occurs, the crystal will have the environment shown in figure 8-4. If the probability of either type of fault occurring is α (i.e. both faults have equal probability, α), then the probability of no fault occurring after any layer is $1-2\alpha$ (=A).

Following the general calculations by Cowley[71] for this specific case, the zero$^{\underline{th}}$ component of the generalized Patterson function involves only the intra-sheet vectors and is,

$$P_o(\underline{u}) = N \{ A\rho(\underline{u})*\rho(-\underline{u}) + \alpha(\rho(\underline{u}) + \Delta_1(\underline{u}))*(\rho(-\underline{u}) + \Delta_1(-\underline{u})) + \alpha(\rho(\underline{u}) + \Delta_2(\underline{u}))*((\rho(-\underline{u}) + \Delta_2(-\underline{u})) \}, \qquad (8\text{-}1)$$

where N is the number of sheets and $\underline{u}$ is a real space vector.
The Fourier transform of this expression gives the zero$^{\underline{th}}$ intensity component:

$$I_o = N \{A|F|^2 + \alpha|F+G_1|^2 + \alpha|F+G_2|^2 \}. \qquad (8\text{-}2)$$

The first component of the Patterson function involves vectors between nearest neighbour sheets. Since the first sheet can be faulted by $\underline{S}_1$ or $\underline{S}_2$ or unfaulted, and its neighbour can also be faulted by $\underline{S}_1$ or $\underline{S}_2$ or unfaulted, the possible

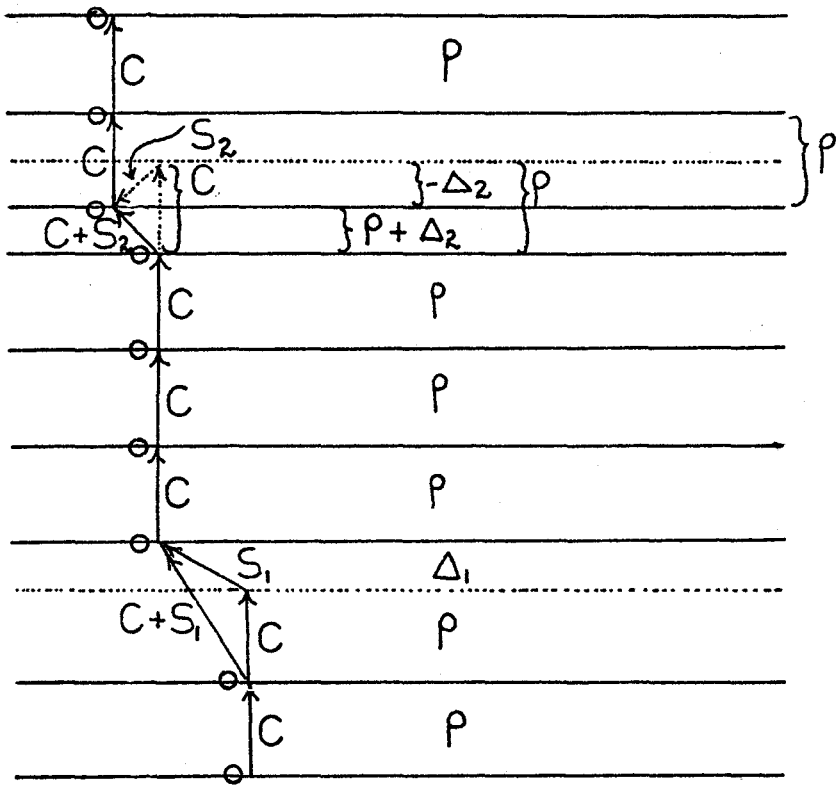

Figure 8-4. The arrangement of layers with two different kinds of stacking faults. The stacking fault with displacement vector $\underline{S}_1$ adds electron density to the normal sheet, and the one with displacement vector $\underline{S}_2$ subtracts electron density from the normal sheet.

combinations of two sheets is unfaulted-unfaulted, unfaulted-faulted(1), unfaulted-faulted(2), faulted(1)-unfaulted, faulted(1)-faulted(1), faulted(1)-faulted(2), faulted(2)-unfaulted, faulted(2)-faulted(1), and faulted(2)-faulted(2), where the number in brackets indicates the kind of fault. If the probability of finding a faulted layer is α and an unfaulted one is A, then the probability of finding a faulted one followed by a faulted one is α^2, two unfaulted ones is A^2, and a faulted one with an unfaulted one is $A\alpha$. The first component of the Patterson function thus becomes

$$\begin{aligned} P_1(\underline{u}) = N \{ & \delta(\underline{u}-\underline{c})A^2\rho(\underline{u})*\rho(-\underline{u}) + \delta(\underline{u}-\underline{c})A\alpha\rho(\underline{u})*(\rho(-\underline{u})+\Delta_1(-\underline{u})) \\ & + \delta(\underline{u}-\underline{c})A\alpha\rho(\underline{u})*(\rho(-\underline{u})+\Delta_2(-\underline{u})) + \delta(\underline{u}-(\underline{c}+\underline{S}_1))\alpha A(\rho(\underline{u})+\Delta_1(\underline{u}))*\rho(-\underline{u}) \\ & + \delta(\underline{u}-(\underline{c}+\underline{S}_1))\alpha^2(\rho(\underline{u})+\Delta_1(\underline{u}))*(\rho(-\underline{u})+\Delta_1(-\underline{u})) \\ & + \delta(\underline{u}-(\underline{c}+\underline{S}_1))\alpha^2(\rho(\underline{u})+\Delta_1(\underline{u}))*(\rho(-\underline{u})+\Delta_2(-\underline{u})) \\ & + \delta(\underline{u}-(\underline{c}+\underline{S}_2))\alpha A(\rho(\underline{u})+\Delta_2(\underline{u}))*(\rho(-\underline{u})) \\ & + \delta(\underline{u}-(\underline{c}+\underline{S}_2))\alpha^2(\rho(\underline{u})+\Delta_2(\underline{u}))*(\rho(-\underline{u})+\Delta_1(-\underline{u})) \\ & + \delta(\underline{u}-(\underline{c}+\underline{S}_2))\alpha^2(\rho(\underline{u})+\Delta_2(\underline{u}))*(\rho(-\underline{u})+\Delta_2(-\underline{u})) \} \end{aligned} \tag{8-3}$$

which Fourier transforms to give

$$\begin{aligned} I_1 = N \{ & \exp(2\pi i\underline{h}\cdot\underline{c})\{A^2|F|^2 + \alpha AF^*(F+G_1) + \alpha AF^*(F+G_2)\} \\ & + \exp(2\pi i\underline{h}\cdot(\underline{c}+\underline{S}_1))\{\alpha A(F+G_1)^*F + \alpha^2|F+G_1|^2 + \alpha^2(F+G_1)^*(F+G_2)\} \\ & + \exp(2\pi i\underline{h}\cdot(\underline{c}+\underline{S}_2))\{\alpha A(F+G_2)^*F + \alpha^2(F+G_2)^*(F+G_1) + \alpha^2|F+G_2|^2\} \}, \end{aligned} \tag{8-4}$$

where $\underline{h}$ is a reciprocal space vector which need not be integral.

In general, the interaction of sheets, n sheets apart, will give rise to the $n^{\underline{th}}$ Patterson component which Fourier transforms to give the $n^{\underline{th}}$ intensity component. When considering sheets, n sheets apart, there are a total of n+1 sheets, and the probability of various faulted and unfaulted arrangements must be calculated. Since the interaction is only

between the first and last sheet, there are several arrangements which will give rise to the same term in the intensity. For instance, the arrangement UF_1UU and UUF_1U where U stands for unfaulted and F_1 stands for a faulted sheet of type 1 will give rise to identical terms in the intensity expression. The different kinds of terms have been summarized in table 8-3. The probability part contains not only the probability of finding the particular type of layers but also takes into account the number of arrangements possible giving the same term as described above. The full $n^{\underline{th}}$ component of the intensity can thus be found by multiplying the exponential, probability and structure factor parts for each term and then summing the terms.

The total intensity is the sum of all the intensities for both positive and negative n. In practice n runs from $-\infty$ to $+\infty$ since crystals are usually large enough to neglect termination effects of the series. The $-n^{\underline{th}}$ component of the intensity is mainly the complex conjugate of the $n^{\underline{th}}$ component, and can thus readily be evaluated.

Upon summing all the components of intensity, factoring the sums and performing subsequent simplifications, the final intensity becomes

$$I = \sum_{n=-\infty}^{\infty} I_n$$

$$= T/D + X \tag{8-5}$$

where

$$D = 1 + A^2 + 2\alpha^2 - 2A\cos(2\pi\underline{h}\cdot\underline{c}) - 2\alpha\cos(2\pi\underline{h}\cdot(\underline{c}+\underline{S}_1))$$
$$- 2\alpha\cos(2\pi h\cdot(c+S_2)) + 2\alpha A\cos(2\pi\underline{h}\cdot\underline{S}_1) + 2\alpha A\cos(2\pi\underline{h}\cdot\underline{S}_2)$$
$$+ 2\alpha^2\cos(2\pi\underline{h}\cdot(\underline{S}_1-\underline{S}_2)) \tag{8-6}$$

Table 8-3. Terms in the generalized expression for the $n^{\underline{th}}$ intensity component when considering two kinds of stacking faults.

exponential	probability	structure factor	explanation
$\exp(2\pi i \underline{h}\cdot n\underline{c})$	A^n	$\lvert F\rvert^2$	no faults in any sheets
"	αA^{n-1}	$F^*(F+G_1)$	faults of type 1 in the last (i.e. $(n+1)^{\underline{th}}$) sheet
"	αA^{n-1}	$F^*(F+G_2)$	faults of type 2 in the last sheet
$\exp(2\pi i \underline{h}\cdot(n\underline{c}+x\underline{S}_1))$ $x<n$	$\frac{(n-1)!\alpha^x A^{n-x}}{(n-x-1)!x!}$	$\lvert F\rvert^2$	x faults of type 1 in the inner (i.e. $2^{\underline{nd}}$ to $n^{\underline{th}}$) sheets
"	$\frac{(n-1)!\alpha^{x+1} A^{n-x-1}}{(n-x-1)!x!}$	$F^*(F+G_1)$	x faults of type 1 in the inner sheets and one in the last sheet
"	$\frac{(n-1)!\alpha^{x+1} A^{n-x-1}}{(n-x-1)!x!}$	$F^*(F+G_2)$	x faults of type 1 in the inner sheets and one of type 2 in the last sheet
"	$\frac{(n-1)!\alpha^x A^{n-x}}{(n-x)!(x-1)!}$	$(F+G_1)^*F$	(x-1) faults of type 1 in the inner sheets and one in the first sheet
"	$\frac{(n-x)!\alpha^{x+1} A^{n-x-1}}{(n-x)!(x-1)!}$	$\lvert F+G_1\rvert^2$	(x-1) faults of type 1 in the inner sheets and one each in the first and last sheets
"	$\frac{(n-x)!\alpha^{x+1} A^{n-x+1}}{(n-x)!(x-1)!}$	$(F+G_1)^*(F+G_2)$	(x-1) faults of type 1 in the inner sheets, one of type 1 in the first sheet and one of type 2 in the last sheet

Table 8-3 cont.

exponential	probability	structure factor	explanation
$\exp(2\pi i \underline{h}\cdot(n(\underline{c}+\underline{S}_1))$	$\alpha^n A$	$(F+G_1)^*F$	a fault of type 1 in each layer except the last one
"	α^{n+1}	$\lvert F+G_1\rvert^2$	a fault of type 1 in all layers
"	α^{n+1}	$(F+G_1)^*(F+G_2)$	a fault of type 2 in the last layer and of type 1 in all the others
$\exp(2\pi i \underline{h}\cdot(n\underline{c}+x\underline{S}_1+y\underline{S}_2)$ $(x+y)<n$	$\frac{(n-1)!\alpha^{x+y}A^{n-x-y}}{(n-x-y-1)!x!y!}$	$\lvert F\rvert^2$	x faults of type 1 and y faults of type 2 in the inner layers
"	$\frac{(n-1)!\alpha^{x+y+1}A^{n-x-y-1}}{(n-x-y-1)!x!y!}$	$F^*(F+G_1)$	a fault of type 1 in the last layer and x of type 1 y of type 2 in the inner layers
"	$\frac{(n-1)!\alpha^{x+y+1}A^{n-x-y-1}}{(n-x-y-1)!x!y!}$	$F^*(F+G_2)$	a fault of type 2 in the last layer and x of type 1 y of type 2 in the inner layers
"	$\frac{(n-1)!\alpha^{x+y}A^{n-x-y}}{(n-x-y)!(x-1)!y!}$	$(F+G_1)^*F$	a fault of type 1 in the first layer and x-1 of type 1 y of type 2 in the inner layers
"	$\frac{(n-1)!\alpha^{x+y+1}A^{n-x-y-1}}{(n-x-y)!(x-1)!y!}$	$\lvert F+G_1\rvert^2$	faults of type 1 in the first and last layers and x-1 of type 1 y of type 2 in the inner layers

Table 8-3 cont.

exponential	probability	structure factor	explanation
$\exp(2\pi i \underline{h}\cdot(n\underline{c}+x\underline{S}_1+y\underline{S}_2))$ $(x+y)<n$	$\frac{(n-1)!\alpha^{x+y+1}A^{n-x-y-1}}{(n-x-y)!(x-1)!y!}$	$(F+G_1)^*(F+G_2)$	faults of type 1 in the first and type 2 in the last layers. x-1 fault of type 1 and y of type 2 in the inner layers
"	$\frac{(n-1)!\alpha^{x+y}A^{n-x-y}}{(n-x-y)!(y-1)!x!}$	$(F+G_2)^*F$	a fault of type 2 in the first layer and x of type 1 y-1 of type 2 in the inner layers
"	$\frac{(n-1)!\alpha^{x+y+1}A^{n-x-y-1}}{(n-x-y)!(y-1)!x!}$	$(F+G_2)^*(F+G_1)$	a fault of type 2 in the first and type 1 in the last layers. x faults of type 1 and y-1 of type 2 in the inner layers
"	$\frac{(n-1)!\alpha^{x+y+1}A^{n-x-y-1}}{(n-x-y)!(y-1)!x!}$	$\lvert F+G_2\rvert^2$	faults of type 2 in the first and last layers and x of type 1 y-1 of type 2 in the inner layers
$\exp(2\pi i \underline{h}\cdot(n\underline{c}+x\underline{S}_1+(n-x)\underline{S}_2))$	$\frac{(n-1)!\alpha^{n}A}{(n-x-1)!x!}$	$(F+G_2)^*F$	fault of type 2 in the first layer and x of type 1 and n-x-1 of type 2 in the inner layers
"	$\frac{(n-1)!\alpha^{n}A}{(n-x)!(x-1)!}$	$(F+G_1)^*F$	fault of type 1 in the first layer and x-1 of type 1 and n-x of type 2 in the inner layers
"	$\frac{(n-1)!\alpha^{n+1}}{(n-x)!(x-1)!}$	$\lvert F+G_1\rvert^2$	faults of type 1 in the first and last layers and x-1 of type 1, n-x of type 2 in the inner layers

Table 8-3 cont.

exponential	probability	structure factor	explanation
$\exp(2\pi i\underline{h}\cdot(n\underline{c}+x\underline{S}_1+(n-x)\underline{S}_2))$	$\frac{(n-1)!\alpha^{n+1}}{(n-x)!(x-1)!}$	$(F+G_1)^*(F+G_2)$	x-1 faults of type 1 and n-x of type 2 in the inner layers, and a fault of type 1 in the first and type 2 in the last layers
"	$\frac{(n-1)!\alpha^{n+1}}{(n-x-1)!x!}$	$(F+G_2)^*(F+G_1)$	x faults of type 1 and n-x-1 of type 2 in the inner layers, and a fault of type 2 in the first and type 1 in the last layers
"	$\frac{(n-1)\alpha^{n+1}}{(n-x-1)!x!}$	$\lvert F+G_2\rvert^2$	faults of type 2 in the first and last layers and x of type 1 n-x-1 of type 2 in the inner layers
$\exp(2\pi i\underline{h}\cdot(n\underline{c}+y\underline{S}_2))$ $y<n$	same as for $\exp(2\pi i\underline{h}\cdot(n\underline{c}+x\underline{S}_1))$ but with subscripts 1 and 2 reversed and y instead of x		
$\exp(2\pi i\underline{h}\cdot(n(\underline{c}+\underline{S}_2))$	same as for $\exp(2\pi i\underline{h}\cdot(n(\underline{c}+\underline{S}_1))$ but with subscripts 1 and 2 reversed		

$$T = 2\mathrm{Re}\{\exp(2\pi i\underline{h}\cdot\underline{c})\{1-A\exp(-2\pi i\underline{h}\cdot\underline{c})-\alpha\exp(-2\pi i\underline{h}\cdot(\underline{c}+\underline{S}_1))-\alpha\exp(2\pi i\underline{h}\cdot(\underline{c}+\underline{S}_2))\}$$
$$\cdot\{F+\alpha G_1+\alpha G_2\}\{AF^*+\alpha(F^*+G_1^*)\exp(2\pi i\underline{h}\cdot\underline{S}_1)+\alpha(F^*+G_2^*)\exp(2\pi i\underline{h}\cdot\underline{S}_2)\}\} \quad (8\text{-}7)$$

and $$X = |F|^2 + 2\alpha\mathrm{Re}F^*G_1 + 2\alpha\mathrm{Re}F^*G_2 + \alpha|G_1|^2 + \alpha|G_2|^2 \quad (8\text{-}8)$$

§ 8.4 Stacking Faults of $VAsO_5$

Two possible models for stacking faults were considered. Since expression VIII-5 has the greatest value at points where D is a minimum, D was calculated for both models to see if the minima for D fell at points where the intensity was a maximum in the diffraction pattern.

Model I:

$VAsO_5$ and α-VPO_5 appear to form solid solutions over the full composition range (see section 8-5) and hence it would seem possible that, once in a while, a stacking arrangement as in α-VPO_5 can be found rather than the edge-sharing arrangement. There are four possible arrangements of such faults (figure 8-5). Figure 8-5(a) and (c) and also (b) and (d) are mirror images of each other, and these faults would thus be expected to occur with the same probability. The denominator for an expression like equation 8-5 was found for the case of four faults with two each of equal probability, and this denominator was evaluated for $0k\ell$ points. The minima of the denominator did not fall at k and ℓ values for which the intensity was a maximum, and hence this model was discarded.

Model II:

The VO_6 octahedra in $VAsO_5$ alternately share one of two edges. The difference map in the final stages of refinement showed residual electron density in places which suggest that, once in a while, a "mistake" is made and octahedra in two subsequent layers share edges in the same

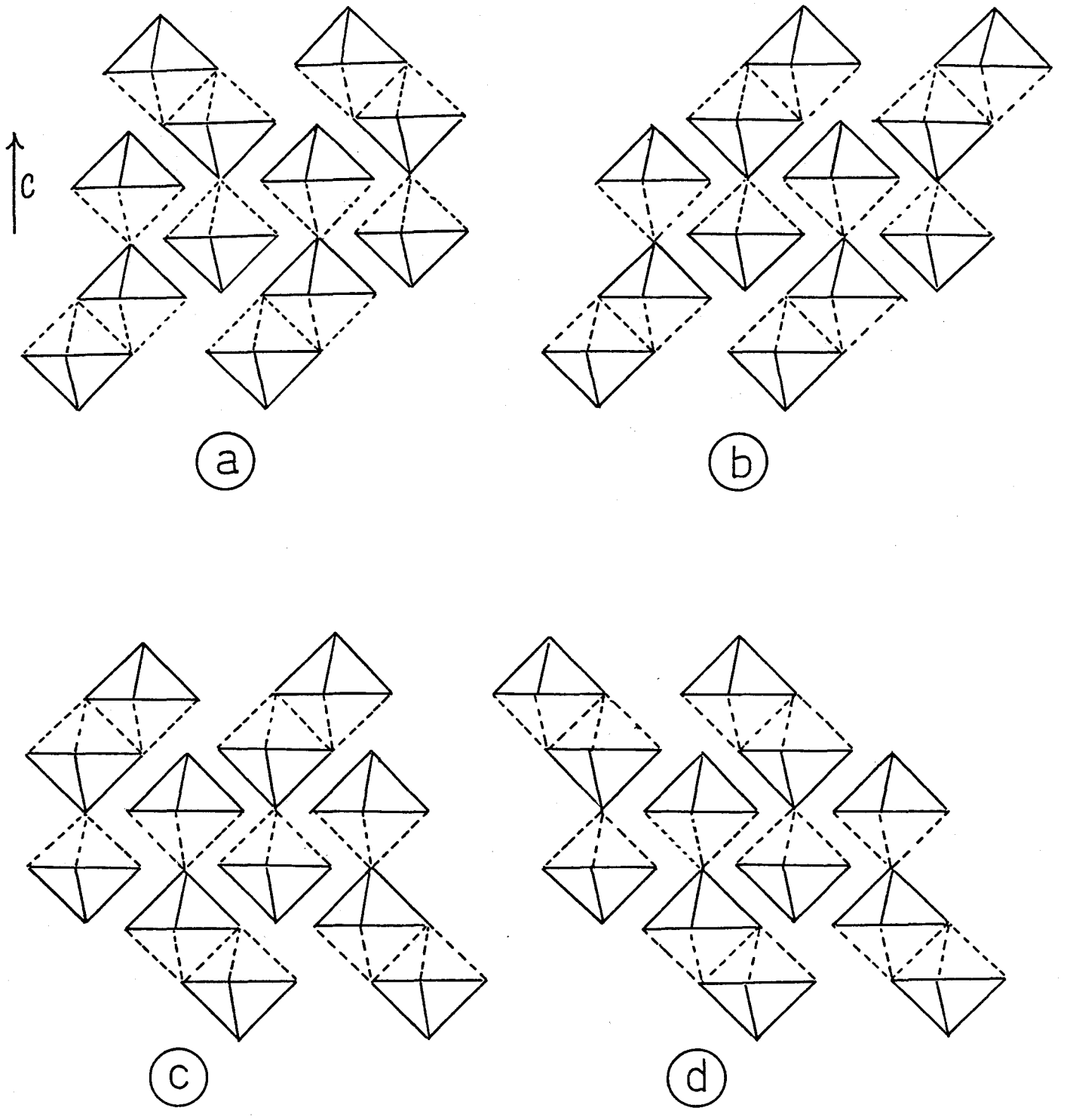

Figure 8-5. Four possible stacking faults for $VAsO_5$, Model I. The VO_6 octahedra are idealized with the long oxygen bonds shown by the dotted lines. For clarity, the phosphate tetrahedra have been omitted.

direction. Two possible faults can be formed as shown in figure 8-6. These faults can be formed geometrically by the removal of an A layer (figure 8-6(b)) or a B layer (figure 8-6(c)) and a shift of the following layers which will give the fault structures indicated. Since the two possible faults are mirror images of each other, and since there is no *a priori* reason to assume one more probable than the other, each fault is considered to have equal probability. The expressions in the preceding section consider $\underline{S}_1$ and $\underline{S}_2$ to have the same origin with respect to the unit cell, and hence it is more convenient to consider the fault in fig.8-6(b) to be formed by the addition of a B layer (rather than removal of an A layer). The net result is the same, and vectors $\underline{S}_1$ and $\underline{S}_2$ now have a common origin with $\underline{c}$ components of $+\frac{1}{2}$ and $-\frac{1}{2}$ and $\underline{b}$ components of about -0.45 and + 0.45 respectively. This model gave shifted positions from the Bragg peaks of about the right size and in the right direction for 0kℓ points. The best fit appeared to fall at about α=0.23. Smaller values of α gave too small a deviation from the Bragg position and much larger values gave deviations that were too large. Small changes in the coordinates of the fault vectors changed the size of the minima in the denominator and the value of the intensities. The full intensity was calculated for 02ℓ points over the range $-4.1 \leq \ell \leq 4.1$ for α=0.23 and various $\underline{b}$ and $\underline{c}$ components of the fault vectors ranging in absolute value from 0.42-0.48 and 0.48-0.52 respectively. The best fit for the intensity for the 02ℓ points was found at the $\underline{b}$ and $\underline{c}$ components for $\underline{S}_1$ of (-0.43,0.5) and (0.43,-0.5) for $\underline{S}_2$. Experimental and calculated values are shown in figure 8-7. The experimental intensities were obtained from a 02 precession photograph (fig.8-1) using an optical microdensitometer and were corrected for Lorentz and

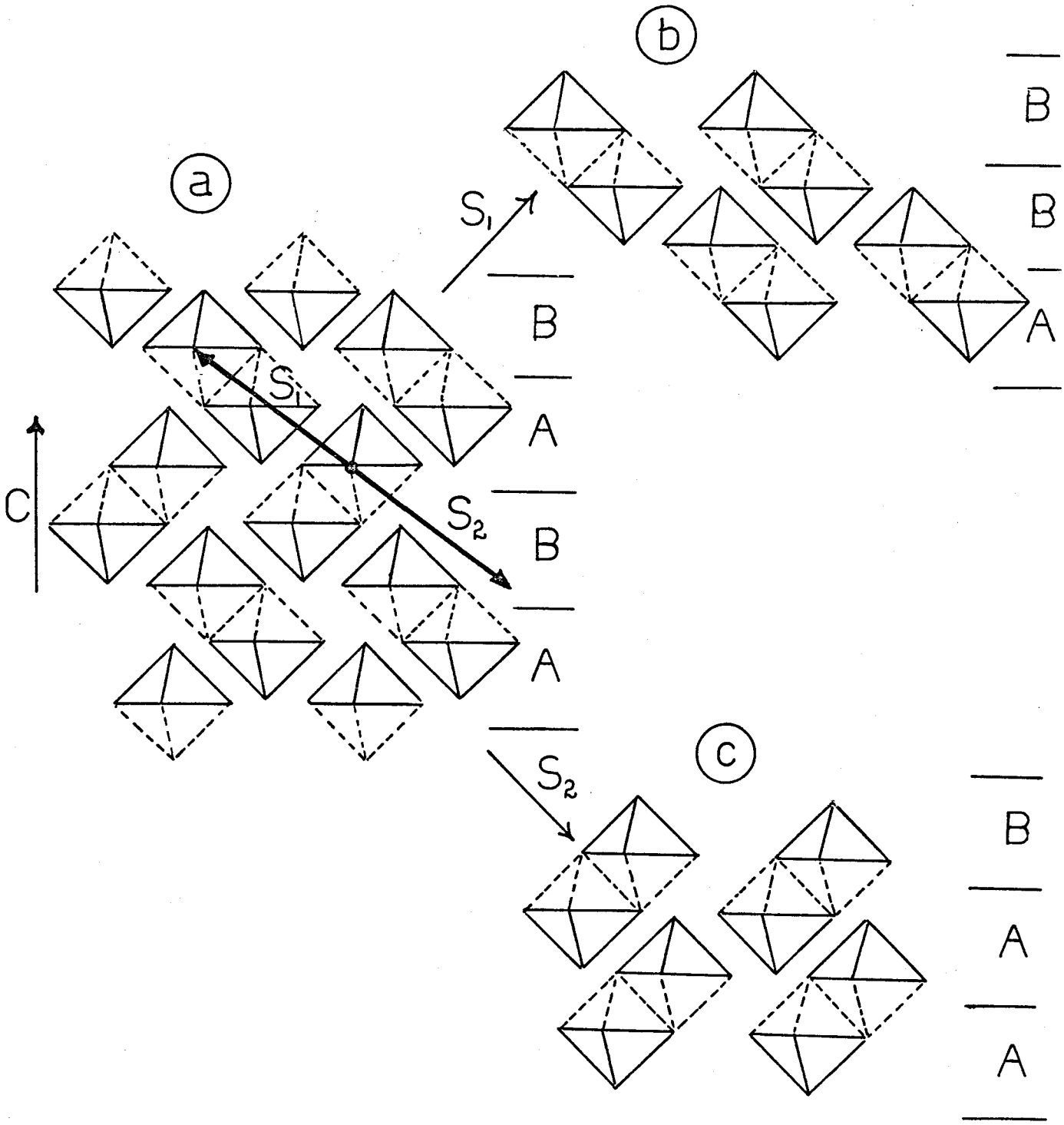

Figure 8-6. Model II stacking faults for $VAsO_5$. (a) shows the two possible fault vectors, and (b) and (c) show the appearance of each of the faults.

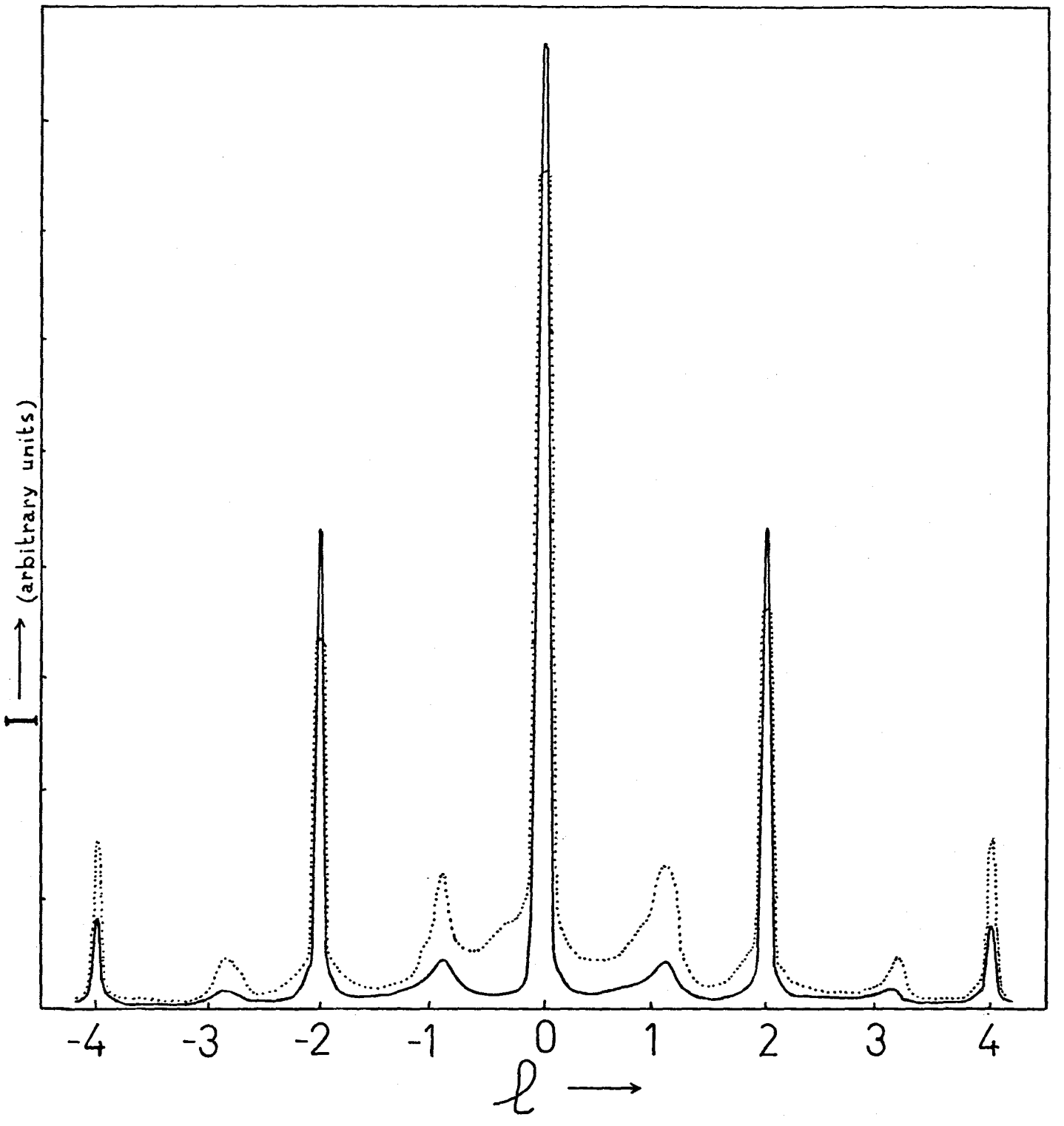

Figure 8-7. Observed (.....) and calculated (——) intensities for the 02ℓ line. Observed intensities have been corrected for Lorentz and polarization effects.

polarization effects. The background was estimated from optical density measurements immediately adjacent to the 02ℓ line and this background was subtracted from the measured intensities. The fit, though far from perfect, seems good enough to indicate that this model must represent the major stacking faults that occur. When the intensities were calculated using formula 8-5 with G_1 and G_2 both equal to zero (i.e. making no correction for the density modification at the faults) the intensity profile differed by at most and usually considerably less than 10% from that for the model containing the G-values. This shows that the modification of the electron density at the faults does not significantly affect the intensity profile, and hence a least-squares refinement of α when fitting $F+\alpha G_1+\alpha G_2$ to the observed structure factor is likely to underestimate its value. This is in agreement with the results (α=0.1 from least-squares and 0.23 from the intensity profile calculation). Cowley[99] observed this effect as well for stacking faults in magnesium fluorogermanate. The probability of a stacking fault occurring is very high (there is only a 54% probability of no fault occurring) and it is surprising that the refinement of the basic structure yielded an R-value as low as 0.2.

§ 8.5 The Solid Solution $V(As,P)O_5$

Bordes and Courtine[40] have found that α-VPO_5 and $VAsO_5$ form a solid solution of the form $VAs_{1-x}P_xO_5$ over the whole range of $0 \leq x \leq 1$. This result has been confirmed by us. Samples of composition x=0.1, 0.5 and 0.75 were prepared by the procedure outlined in chapter 3. All of the crystals were yellow, mica-like sheets similar to those of the end members of the solution range. Single crystals suitable for x-ray analysis were not found, but a and c parameters were determined from powder diffraction

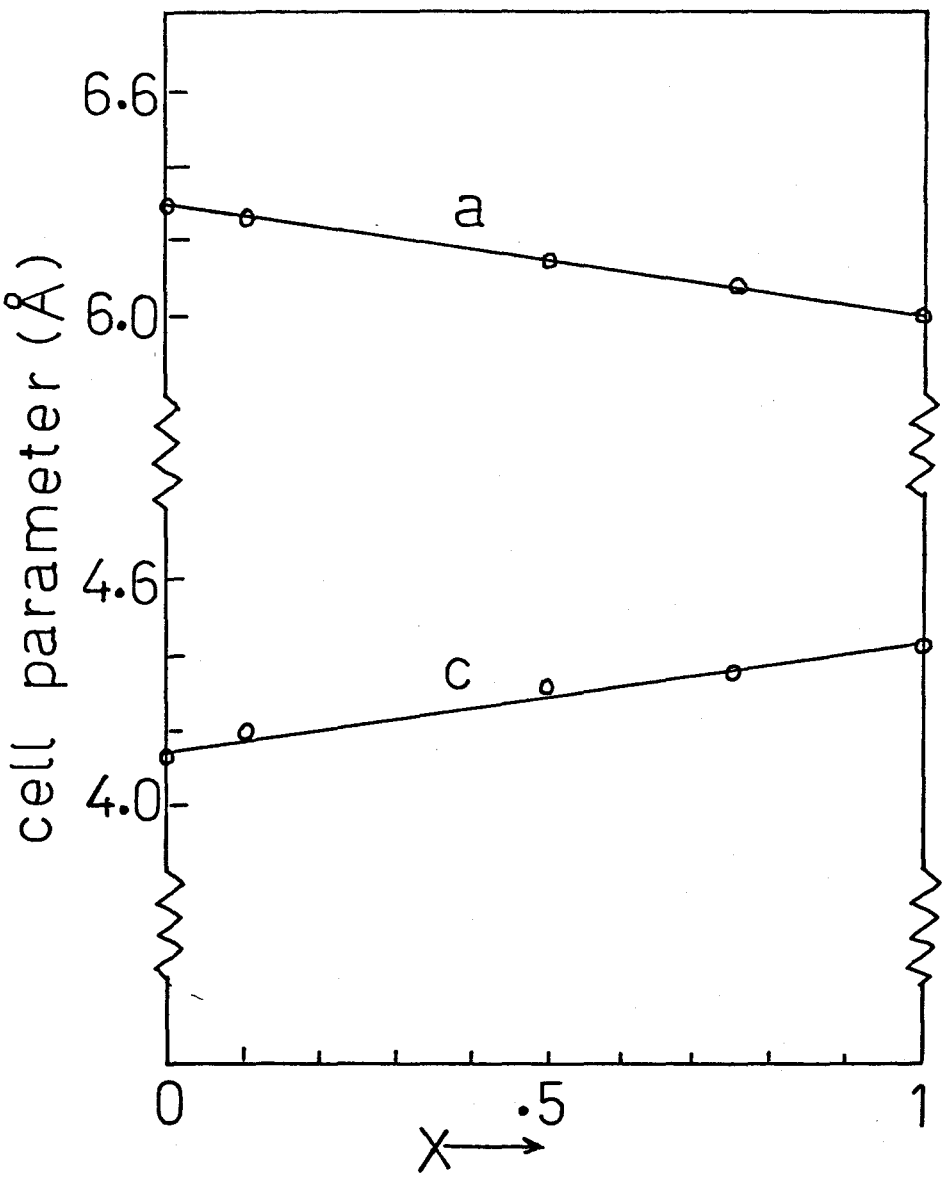

Figure 8-8. Cell parameters for $VAs_xP_{1-x}O_5$

data. The results are shown in figure 8-8. The parameters for α-VPO_5 were obtained from Jordan, et al.[11] and the $VAsO_5$ parameters are those determined from single crystal diffraction, with the c-axis divided by two to correspond to the layer length rather than the actual axis length in order to make comparisons with α-VPO_5 possible. The a parameters fall nicely on a straight line reflecting the change in size of the tetrahedral cation. The c parameters do not fit as well on a straight line, although the trend is suggestive of a gradual change from $VAsO_5$-like stacking to α-VPO_5-like stacking as x increases. Perhaps this could be accomplished by stacking faults as in model I section 4, of increasing frequency as x increases. Single crystal intensities will have to be considered in order to determine the actual change in structure over the whole range of x.

§ 8.6 Thermal Behaviour of $VAsO_5$

A DTA analysis of $VAsO_5$ shows a strong endotherm at about 560°C on heating, following which the speciman gradually volatilizes until all is gone before the melting point estimated at about 800°C. When single crystals of $VAsO_5$ are gradually heated, the diffraction pattern does not change significantly until about 560°C, when the crystal invariably crumbles. The nature of the structure of $VAsO_5$ remains to be determined above 560°C, although it seems evident that a structural phase transition takes place at this temperature. Materials such as the H-form of P_2O_5[28] which volatilize readily often contain discrete molecular units in the crystalline phase. The molecular units are held together by forces which are weaker than those in extended bonded networks. The energy required to remove molecules from molecular crystals is therefore smaller than

that required for network crystals. The molecular crystals can, therefore, be expected to volatilize more readily. Since $VAsO_5$ in the high temperature form does readily volatilize, it might contain molecular units rather than consisting of a network of bonds like the low temperature form.

CHAPTER 9

Discussion and Conclusion

§ 9.1 The V-P-As-O System

The crystals in this study are all of the type M_nO_{2n+1} with n=2,3, or 4, and M a combination of any of V, P, As or Si.

The n=2 compound, $VAsO_5$, with M_2=VAs, is structurally related to other M_2O_5 compounds in the V-P-As-O system. Vanadium is always found octahedrally coordinated with one long V-O bond trans to a short vanadyl bond. The vanadyl oxygen is sometimes uni-coordinated ($VAsO_5$ and β-V_2O_5[17]) and sometimes forms a long V-O bond to another VO_6 group (α-V_2O_5[2], α and β-VPO_5[11,12]). Some of the compounds form layers (α-VPO_5[11], $VAsO_5$, α and β-V_2O_5[2,17]), which, except for β-V_2O_5, (see p.5) are held together by long V-O bonds. These layers form stacking faults easily, and evidence for such disorder has been found for all except α-V_2O_5. α-VPO_5 and $VAsO_5$ vary only in the stacking arrangement of the layers. A solid solution of the form $VAs_xP_{1-x}O_5$ exists over the full range $0 \leq x \leq 1$, and crystals throughout this range have the same layer structure as the end members but, presumably, the stacking arrangement changes with composition.

The H form of P_2O_5[28] is composed of molecular groups and the other forms of P_2O_5[29,30] and As_2O_5[35] are network crystals which readily rearrange to yield molecular units when volatilizing at increased temperatures. The high temperature form of $VAsO_5$, as well as the above phosphorus and arsenic oxides, readily volatilizes. Thus the high temperature $VAsO_5$ is probably more closely related in structure to these oxides than to the layered oxides.

All the M_2O_5 compounds with M a combination of any of V, As and P should have M in the +5 oxidation state. Valences, calculated from Brown's[16] bond-valence parameters and experimental bond-lengths, and corresponding coordinations are given in table 9-1. The errors on these experimental valences are large since the valence is $(\underline{r}/\underline{R})^{-N}$, where N and $\underline{R}$ are tabulated parameters and $\underline{r}$ is the experimental bond length, and $(d\underline{r}/d\underline{R})$ is large.

$VO(PO_3)_2$ is an n=3 compound with M_3=VP_2. Like $V_3O_7^3$, it contains single chains of corner-sharing $V^{+4}O_6$ octahedra. These octahedra each have the vanadyl oxygen forming a long V-O bond to the next octahedron in the chain. $VO(PO_3)_2$ shows disorder in the position of the vanadium atom and the corresponding direction of the vanadyl bond, but no such disorder is known for V_3O_7.

The 5 coordinate groups in the single ribbons in $V_3O_7^3$ are similar to the metaphosphate chains in $VO(PO_3)_2$. If the 5 coordinate groups are changed to tetrahedra in such a way that the removed bond is one which was formed to an edge-sharing oxygen, a metavanadate chain results (fig.9-1). The oxidation state of P in the metaphosphate chain and V in the single ribbon is +5.

Only the double octahedral $V^{+4}O_6$ chains in V_3O_7 do not have a counterpart in $VO(PO_3)_2$.

Table 9-2 lists the structural features and oxidation states of vanadium and phosphorus in the two M_3O_7 compounds. The agreement of the valences with the expected integral values is as good as for the M_2O_5 groups, and hence there is no reason to expect that any structural elements are likely to have non-integral valences.

Table 9-1. Coordinations and Experimental Valences for M_2O_5 compounds in the V-P-As-O System. Valences were calculated using the bond-valence parameters of Brown[16]..

Compound	M	Coordination of M	Valence of M
α-V_2O_5	V	octahedral	5.11
β-V_2O_5	V	octahedral	accurate bond lengths not available
α-VPO_5	V	octahedral	5.34
α-VPO_5	P	tetrahedral	4.98
β-VPO_5	V	octahedral	5.26
β-VPO_5	P	tetrahedral	5.16
$VAsO_5$	V	octahedral	4.99
$VAsO_5$	As	tetrahedral	4.94
As_2O_5	As	octahedral	4.78
As_2O_5	As	tetrahedral	5.02
H-P_2O_5	P	tetrahedral	4.89
O-P_2O_5	P	tetrahedral	5.20
O-P_2O_5	P	tetrahedral	5.24

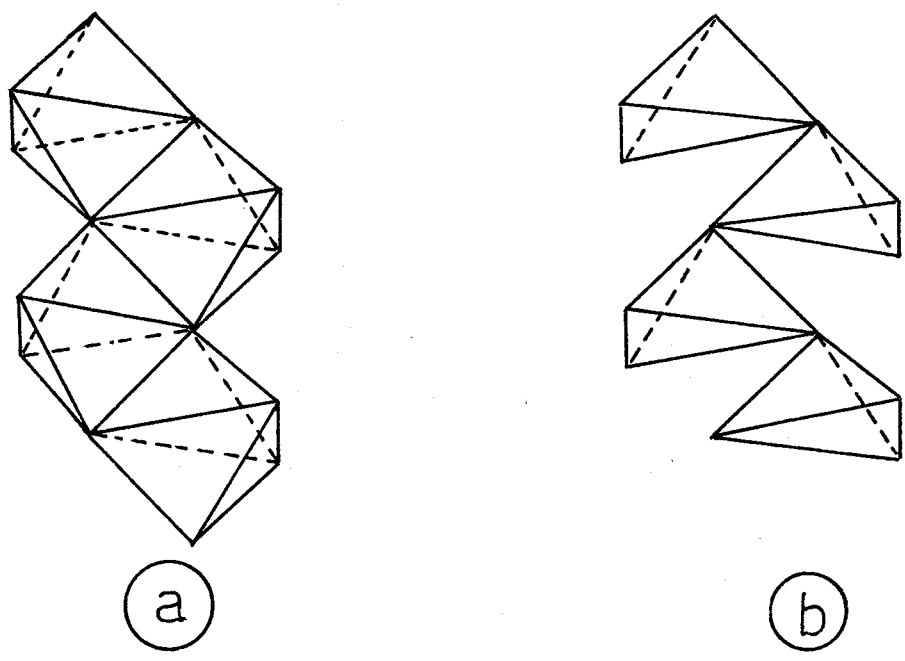

Figure 9-1. Relationship between a 5 coordinate ribbon (a) and a meta- chain (b)

Table 9-2. Structural Elements and Valences for M_3O_7 compounds in the V-P-O System. Valences were calculated using the bond valence parameters of Brown[16].

Compound	M	Structural element	Valence of M
V_3O_7	V	single octahedral chain	4.17
$VO(PO_3)_2$	V	single octahedral chain	3.99
V_3O_7	V	single 5-fold coord. ribbon	4.96
"	"	"	5.17
"	"	"	5.16
$VO(PO_3)_2$	P	meta-phosphate chain	5.08
V_3O_7	V	double octahedral chain	4.24

The compounds VOP_2SiO_8, $(VO)_2P_2O_7$ and $V(PO_3)_3$ all are of the type M_4O_9 with M_4=VP_2Si, V_2P_2 and VP_3 respectively. Although they are all three-dimensional network crystals, they are not as closely structurally related to each other and $V_4O_9^4$ as are the groups with n=2 and 3. VOP_2SiO_8 contains $V^{+4}O_6$ corner-sharing chains, $(VO)_2P_2O_7$ contains $V^{+4}O_6$ double chains, and V_4O_9 contains double octahedral ribbons in which one of the two distinct vanadium atoms has an approximate valence of +5 and the other an average valence of +4.5. In addition, V_4O_9 contains single 5 coordinate ribbons in which two distinct atoms also have average valences of +5 and +4.5 respectively. These valences were estimated through the use of figure 9-2. Bond valences were calculated for each group based on Brown's[16] bond-valence parameters for V^{+4} and also for V^{+5}. These values, when applied to the graph in figure 9-2, gave the approximate percentage of V^{+5} and V^{+4}, thereby making the evaluation of an average valence possible. Since the valences calculated for n=2 and n=3 compounds were only accurate to within about 0.2 valence units, values that deviated from +4 or +5 by less than this amount were considered to be essentially integral, as were values for P and Si. The structural elements above all contain vanadium with the typical vanadyl bond. This bond is not present in the regular isolated $V^{+3}O_6$ octahedra of $V(PO_3)_3$.

$P^{+5}O_4$ tetrahedra are isolated in VOP_2SiO_8 (each connecting to two VO_6 and two SiO_4 groups), exist as pyrophosphate groups in $(VO)_2P_2O_7$ and as metaphosphate chains in $V(PO_3)_3$. VOP_2SiO_8 also contains isolated SiO_4 tetrahedra. The single ribbons of V_4O_9 are similar to the metaphosphate chains in $V(PO_3)_3$, but do not have much resemblance to the

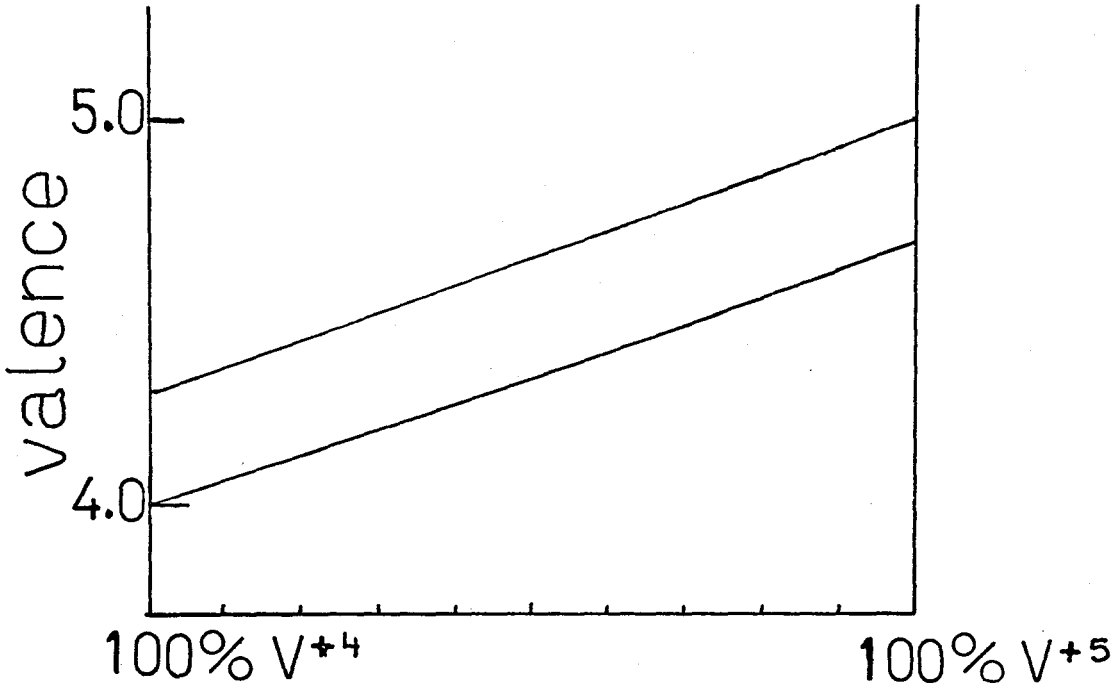

Figure 9-2. Valence for mixtures of V^{+4} and V^{+5} when calculated using bond-valence parameters for V^{+5} (a) and V^{+4} (b). The values were calculated assuming octahedral coordination.

other tetrahedral groups in M_4O_9 compounds. Valences and structural elements for these compounds are summarized in table 9-3. Bond lengths for $(VO)_2P_2O_7$ and $V(PO_3)_3$ are numerous and not very accurate, and the valences for the same structural elements in each of these compounds were averaged before inclusion in the table.

V_6O_{13}[5] is the only n=6 compound known in the V-P-As-O system. It contains single ribbons with V^{+4} and double ribbons with the two distinct vanadium atoms having average valences of +5 and +4.5. The valences and structural elements are summarized in table 9-4.

§ 9.2 Reduction of VPO_5

Like the $V_2O_5 \rightarrow V_6O_{13} \rightarrow VO_2$ transition described in chapter 1, the reduction of VPO_5 (both α and β forms) to $(VO)_2P_2O_7$ can readily be accomplished by the formation of shear planes. These shear planes can form in every second, every third, ... or every $n^{\underline{th}}$ layer, thereby producing a variety of structures intermediate in composition between VPO_5 and $VPO_{4.5}$.

Figure 9-3 shows how α-VPO_5 can form shear planes leading eventually to the $(VO)_2P_2O_7$ structure by a cooperative movement of VO_6 octahedra along the $1\bar{1}0$ direction. During this shift, the phosphate tetrahedra rotate in such a way that the corner, previously shared with one of the octahedra which are to be joined together, points up or down to share an oxygen with a PO_4 group in the layer above or below. This requires that the corresponding phosphate tetrahedra in adjacent α-VPO_5 layers must rotate in opposite directions in order to be able to form P_2O_7 groups. Since the VPO_5 layers are all identical, there is no <u>a priori</u> reason why one phosphate should rotate differently from any

Table 9-3. Valences and structural elements of M_4O_9 compounds in the V-P-Si-O system. Valences were calculated using Brown's[16] valence-bond parameters and average valences were estimated from calculated ones using figure 9-2.

Compound	M	Structural Element	Valence based on V^{+4} parameters	Valence based on V^{+5} parameters	Average valence
VOP_2SiO_8	V	octahedral chains	4.20		
$(VO)_2P_2O_7$	V	double octahedral chains	4.0*		4.0*
V_4O_9	V	double octahedral ribbons	4.37	4.66	4.5
"	"	"		4.86	
"	"	single 5 coord. ribbon	4.43	4.70	4.5
"	"	"	4.02		
VOP_2SiO_8	P	isolated tetrahedra			5.24
"	Si	isolated tetrahedra			4.20
$(VO)_2P_2O_7$	P	pyrophosphate groups			5.20*
$V(PO_3)_3$	P	metaphosphate chains			5.20*
"	V	isolated regular octahedra			3.18*

*value based on the average for structural units of the same kind.

Table 9-4. Valences and structural elements of V_6O_{13}.

Structural Element	Valence based on V^{+4} parameters	Valence based on V^{+5} parameters	Average valence
single octahedral ribbons	4.06		
double octahedral ribbons		4.82	
double octahedral ribbons	4.30	4.56	4.5

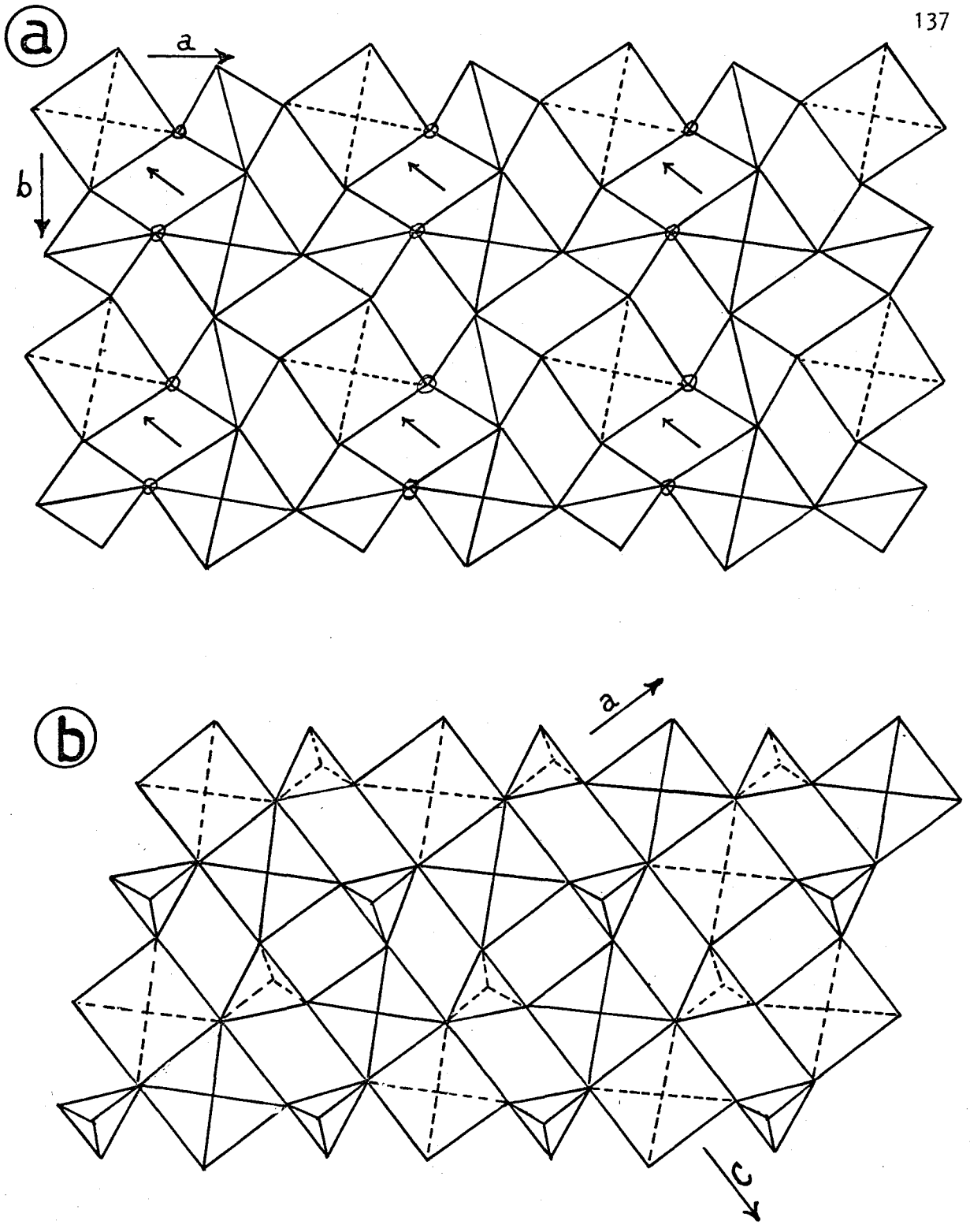

Figure 9-3. Reduction of α-VPO_5 (a) to $(VO)_2P_2O_7$ (b) through the cooperative movement of octahedra along the direction indicated by the arrows. Phosphate tetrahedra twist to form pyrophosphate groups in the directions shown in (b). (o) indicate possible vacancy sites. Only ½ of these need be formed for the layer to shift.

other, and, hence, it is reasonable to expect that the P_2O_7 groups can be found either above or below the ac plane of $(VO)_2P_2O_7$. Such disorder has, in fact, been found (chapter 7). The direction of the vanadyl bond in every second row of double octahedra is reversed from that in α-VPO_5. This is likely a result of the rotation of the phosphate groups which now have three corners essentially in the ac plane of $(VO)_2P_2O_7$.

The proposed transition of β-VPO_5 to $(VO)_2P_2O_7$ is shown in figure 9-4. As for the case above, a cooperative movement of octahedra is required, this time in the $\bar{1}\bar{1}\bar{1}$ direction. The shift involves the joining of two octahedra that are not connected by phosphate groups, one being at an a coordinate near 0 and the other at an a coordinate near $\frac{1}{2}$. The phosphate groups rotate to form pyrophosphate groups with phosphate groups above (or below). In β-VPO_5 the phosphate groups share two corners with two octahedra in one chain, and it is one of these corners that most likely shifts to form the P_2O_7 group. The polyhedra in β-VPO_5 are all linked in a plane perpendicular to a, but because of the likely shift explained above (and shown in diagram 9-4), the shear will form at a 45° angle to this plane.

The production of $(VO)_2P_2O_7$ can occur in stages starting with the formation of vacancies, and following with the gradual collapse or shearing of planes. The intermediate compositions VPO_x, $4.5 \leq x \leq 5$, will have partially a VPO_5 structure and partially a $(VO)_2P_2O_7$ structure. The cell dimensions of the two end members of the composition range are sufficiently commensurate that these kinds of domains can readily be formed. Titanium, niobium and tungsten oxides are known to form similar

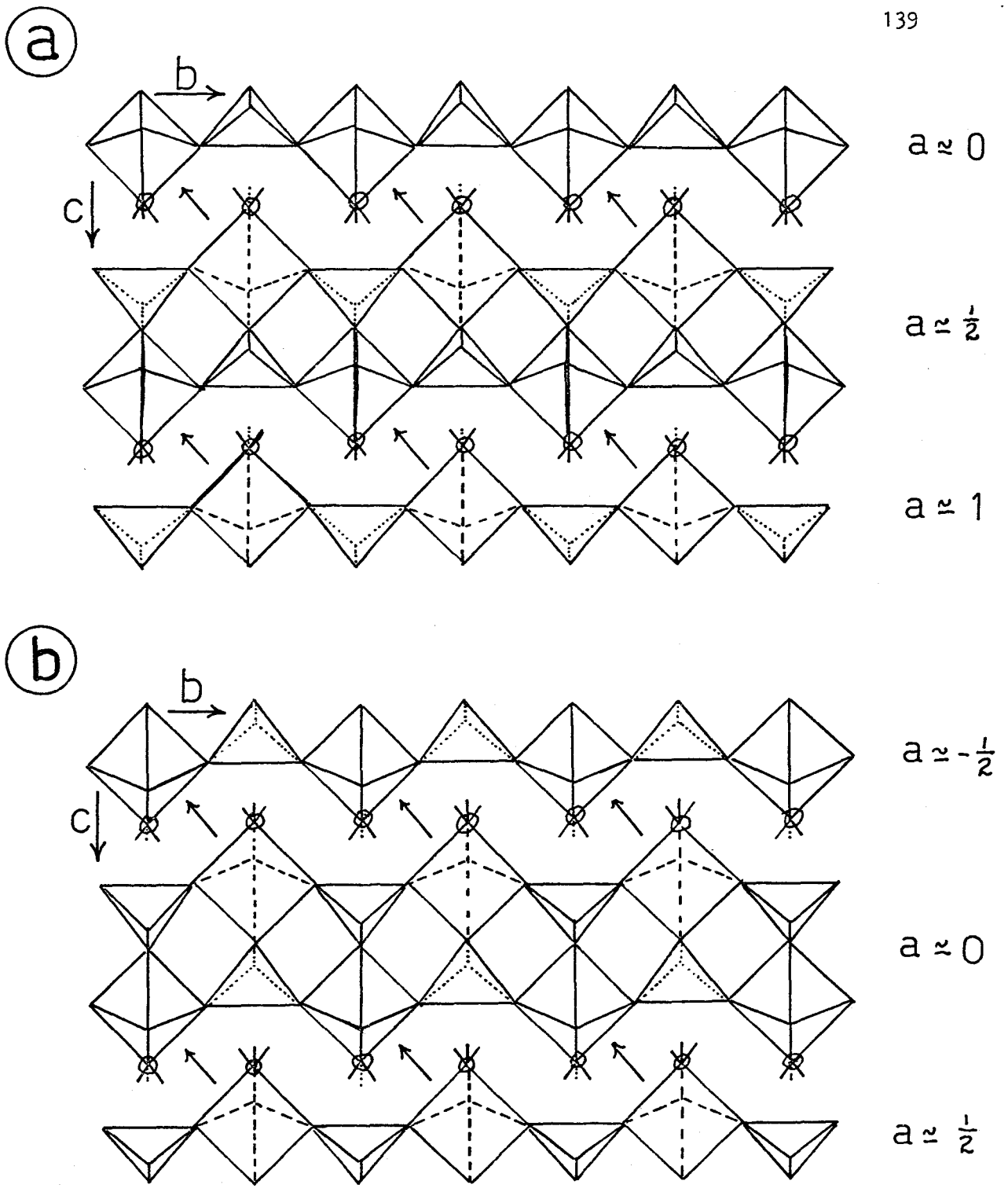

Figure 9-4. Reduction of β-VPO_5 to $(VO)_2P_2O_7$. (a) and (b) show the cooperative movements of octahedra required in two halves of the unit cells. The end product is as in figure 9-3(b). (o) indicates possible vacancy formation during catalysis. Only ½ of these vacancies must be formed for the layers to shift. Although all polyhedra are connected in the bc plane, part of layers at different levels along a have been shown to facilitate illustrating the octahedral shifts.

shear structures, and models for these structures have been proposed by comparing the electron microscope images to theoretically calculated ones[100,101,102]. This technique is still in its infancy, but could be useful in determining the exact defect structure of $(VO)_2P_2O_7$. The structure of the intermediate $VPO_{4.75}$ found by Bordes and Courtine[40] at high temperature (about 750-800°C) during the incomplete reduction of both forms of VPO_5, can readily be predicted by joining every other two rows of octahedra in either form of VPO_5. The structures produced from α and β-VPO_5 respectively are shown in figures 9-5 and 9-6. Note that of necessity, this model requires polymorphism of $VPO_{4.75}$.

§ 9.3 Vanadium Phosphate Catalysts

When VPO_5 is used as a catalyst in the oxidation of butene to maleic anhydride, $(VO)_2P_2O_7$ is known to be produced[40,59,60]. The catalyst reduction could produce vacancies at the surface which can then migrate into the bulk of the material, and, when they become sufficiently concentrated and are situated at the appropriate places (such as those marked on diagrams 9-3 and 9-4), the movement of octahedra can occur to produce $(VO)_2P_2O_7$. One scheme for the diffusion of vacancies through the double octahedral vanadate chains is shown in figure 9-7. A vanadyl oxygen is removed during catalysis, and this is replaced by an equatorial oxygen which is replaced by a vanadyl oxygen and so on, until sufficient vacancies are created at the equatorial oxygens for collapse of the structure. This mechanism can produce intermediate stoichiometries as well.

Other structures in this study, with the exception of $VAsO_5$, cannot readily undergo a similar rearrangement. $V(PO_3)_3$ has vanadium in the +3 oxidation state and reduction is thus not likely. In addition,

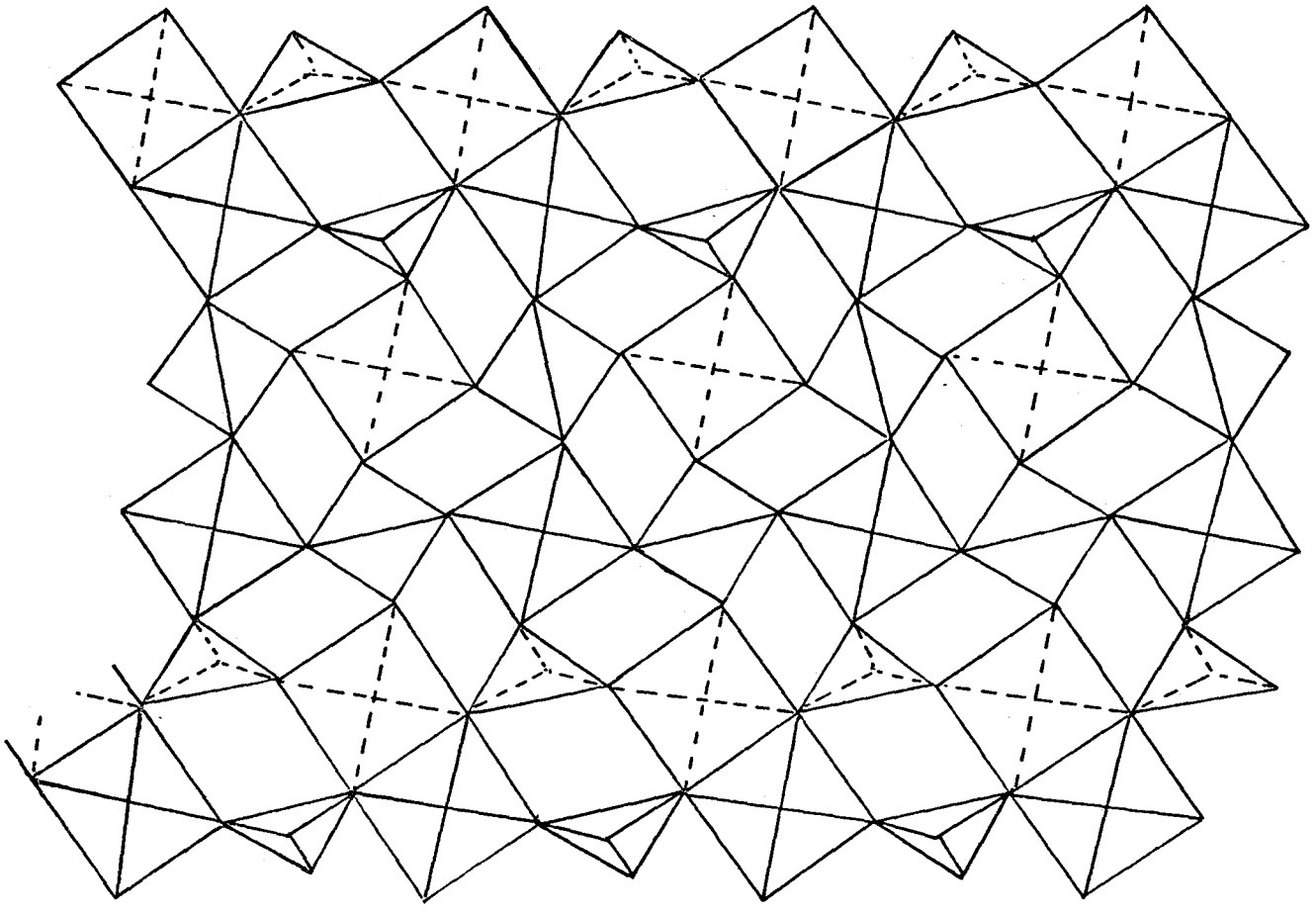

Figure 9-5. Proposed structure of $VPO_{4.75}$ derived from the incomplete reduction of α-VPO_5. The second layer is the same as this one with the direction of the phosphate groups forming P_2O_7 groups reversed.

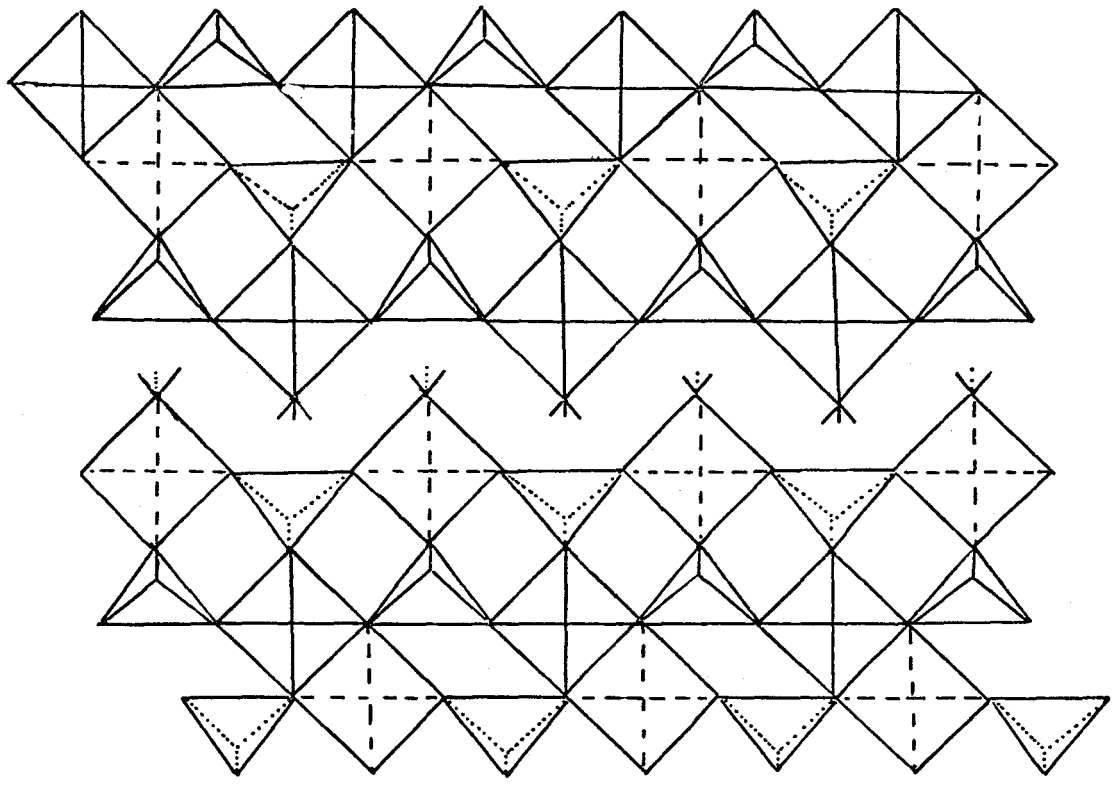

Figure 9-6. Proposed structure of $VPO_{4.75}$ derived from the incomplete reduction of β-VPO_5. The second layer consists of the second layer of β-VPO_5 joining rows of essentially $(VO)_2P_2O_7$-like groups.

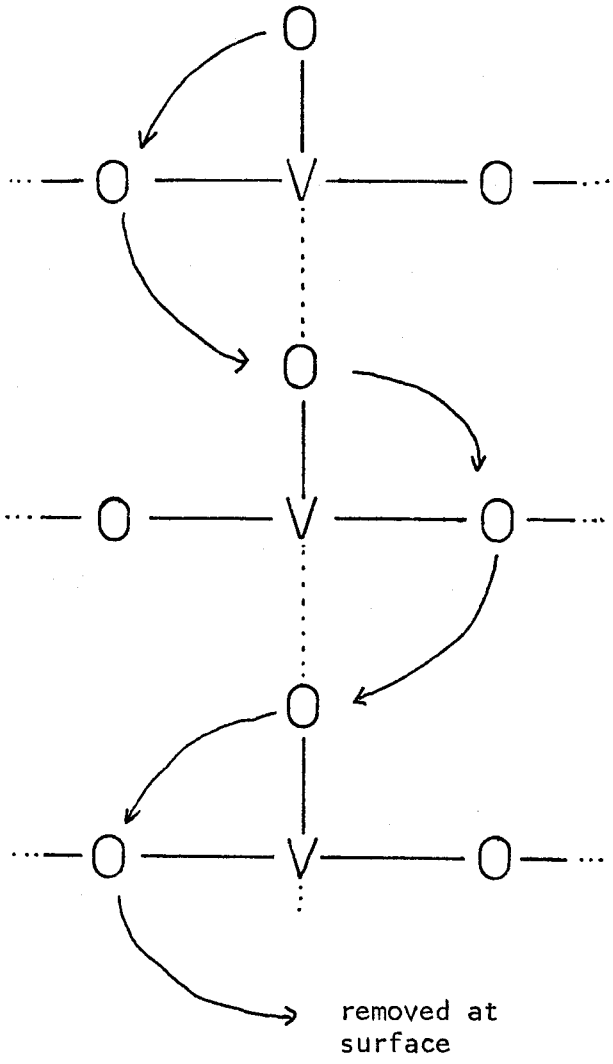

Figure 9-7. Suggested mechanism for the diffusion of oxygen vacancies during catalysis. Only the vanadate chain is shown, and only two oxygen atoms in the equatorial positions are shown. The mechanism only involves the two equatorial oxygen atoms as indicated on figure 9-3.

the vanadate octahedra are too far apart to make their condensation and the diffusion of vacancies possible. Both VOP_2SiO_8 and $VO(PO_3)_2$ contain octahedral VO_6 chains connected by PO_4-SiO_4-PO_4-... tetrahedral chains in the former and meta-phosphate chains in the latter. Neither of these connective chains can readily condense to allow the edge-sharing of VO_6 groups, since neighbouring connective chains are too far away, and edge-sharing of tetrahedra is unlikely. Bordes and Courtine[40] report that $VO(PO_3)_2$ is catalytically inactive and it seems likely (although not confirmed) that VOP_2SiO_8 is also inactive. If this is in fact the case, care must be taken when supporting vanadium phosphate catalysts on silica, that no reaction occurs between the silica and the catalyst to produce VOP_2SiO_8. $VAsO_5$ can undergo a reduction with a mechanism like that of α-VPO_5 in principle, although a shifting of layers is required. It is not known if $VAsO_5$ is catalytically active.

Nakamura[61] found that a V:P=1:2 catalyst was most selective and proposed the mechanism shown in figure 1-8. If his catalyst was in fact $VO(PO_3)_2$ (in contradiction to the results of Bordes and Courtine[40]) his mechanism seems plausible in view of the structure for $VO(PO_3)_2$. The VO_6 chains are disordered in the vanadium and vanadyl bond positions and oxygen can thus be readily added to (or removed from) one of these chains at the surface, thereby reversing the vanadyl bond direction. This would of necessity be a surface reaction only, since migration into the bulk is unlikely.

The increase in selectivity with phosphorus concentration suggests a catalytic mechanism involving equatorial oxygens in the VO_6 groups which are bonded to phosphate groups rather than a mechanism which

involves shears at the vanadyl oxygens since the latter do not change significantly in environment from V_2O_5 to VPO_5. Since the V-O bonds are longer than P-O bonds, one might logically expect the P-O bond energy to be greater, and more energy is involved in the removal of an oxygen atom bonded to one V and one P atom than an oxygen bonded to two vanadium atoms. If the activation energy of the main reaction in the catalytic process is smaller than that of the side reactions, it follows that the vanadium phosphate catalysts will catalyze fewer side reactions. The decrease in activity of the vanadium phosphate catalysts compared to the vanadium oxide catalysts could be due to the migration of vacancies being "easier" (i.e. energetically more favourable) in the vanadium oxides.

§ 9.4 Conclusions

The structures in the V-P-As-O system are difficult to determine since vanadium can exist in a variety of condensations, coordinations and oxidation states, and can readily change from one of these to any other. It is therefore not surprising that most of the crystalline phases of this system exhibit structural disorders and many exhibit polymorphism. Also, the ready formation of glasses (an extreme structural disorder of the crystal) is to be expected.

APPENDIX

Observed (FO) and calculated (FC) structure factor amplitudes.

A.1 VOP_2SiO_8 Crystal I
All values are multiplied by 10.

L=0

H	K	|FO|	|FC|
1	1	111	93
2	0	784	775
2	2	1741	1742
3	1	618	644
3	3	772	743
4	0	86	137
4	2	1180	1168
4	4	1212	1216
5	1	430	408
5	3	660	670
5	5	132	129
6	0	1908	1900
6	2	470	481
6	4	548	534
6	6	1210	1225
7	1	386	382
7	3	268	278
7	5	297	296
7	7	542	547
8	0	189	183
8	4	856	873
8	6	78	86
8	8	596	590
9	1	316	301
9	3	7	23
9	5	354	348
9	7	102	100
9	9	92	93
10	0	253	245
10	2	516	508
10	4	692	687
10	6	359	365
10	8	369	365
11	1	138	124
11	3	537	531
11	5	173	172
11	7	131	126
12	0	723	715
12	2	226	224
12	4	273	272
13	1	259	259

L=1

H	K	|FO|	|FC|
2	1	993	990
3	1	154	148
3	2	148	127
4	1	447	461
4	2	368	350
4	3	251	235
5	1	270	260
5	2	257	256
5	3	253	247
5	4	123	123
6	1	211	218
6	2	213	210
6	3	113	119
6	4	120	114
6	5	259	263
7	1	83	83
7	2	531	529
7	3	65	62
7	4	556	557
7	5	49	54
7	6	125	118
8	1	236	229
8	2	47	50
8	3	20	6
8	4	89	86
8	5	60	66
8	6	36	36
8	7	221	216
9	1	89	89
9	2	235	240
9	3	106	107
9	4	399	401
9	5	36	39
9	6	46	44
9	7	37	46
9	8	115	125
10	1	331	325
10	2	66	68
10	3	126	128
10	4	42	49
10	5	235	238
10	6	37	7
10	7	280	273
10	8	32	10
11	1	42	47
11	2	130	130
11	3	22	24
11	4	46	65
11	5	79	74
11	6	38	35
11	7	50	22
12	1	141	136
12	2	32	39
12	3	133	131
12	4	103	96
12	5	99	101
13	1	25	1
13	2	170	174

L=2

H	K	|FO|	|FC|
0	0	1140	1136
1	0	817	820
1	1	593	587
2	0	1274	1277
2	1	693	693
2	2	73	64
3	0	622	551
3	1	301	334
3	2	466	480
3	3	159	138
4	0	796	774
4	1	613	607
4	2	43	40
4	3	761	788
4	4	45	54
5	0	517	517
5	1	148	144
5	2	299	310
5	3	722	719
5	4	240	247
5	5	43	44
6	0	639	623
6	1	333	342
6	2	709	703
6	3	182	180
6	4	514	524
6	5	425	427
6	6	424	422
7	1	435	433
7	2	361	359
7	0	903	911
7	3	109	90
7	4	81	80
7	5	313	302
7	6	381	385
7	7	293	291
8	0	632	646
8	1	95	89
8	2	92	73
8	3	376	383
8	4	99	87
8	5	353	357
8	6	451	453
8	7	196	192
8	8	173	182
9	0	251	248
9	1	281	272
9	2	314	311
9	3	89	82
9	4	263	255
9	5	432	429
9	6	177	175
9	7	59	57
9	8	264	273
9	9	94	71
10	0	172	175
10	1	214	209
10	2	131	131
10	3	490	461
10	4	58	56
10	5	200	195
10	6	160	164
10	7	41	23
10	8	149	148
11	0	175	167
11	1	30	9
11	2	171	163
11	3	538	535
11	4	178	174
11	5	99	94
11	6	263	266
11	7	170	159
12	0	205	198
12	1	302	300
12	2	241	247
12	3	148	151
12	4	196	199
12	5	209	202
13	0	313	313
13	1	281	281

L=3

H	K	|FO|	|FC|
2	1	216	237
3	1	45	35
3	2	518	494
4	1	752	736
4	2	233	221
4	3	115	117
5	1	165	156
5	2	342	340
5	3	116	114
5	4	538	539
6	1	163	165
6	2	73	82
6	3	18	13
6	4	111	105
6	5	87	88
7	1	76	89
7	2	368	375
7	3	57	62
7	4	445	437
7	5	68	67
7	6	228	229
8	1	148	140
8	2	39	23
8	3	132	128
8	4	69	64
8	5	171	165
8	7	147	138
9	1	68	85
9	2	265	274
9	3	57	62
9	4	153	157
9	5	20	2
9	6	193	195
9	7	60	59
9	8	73	82
10	1	302	300
10	2	29	2
10	3	63	66
10	4	65	60
10	5	91	88
10	6	52	31
10	7	318	316
10	8	33	25
11	1	26	33
11	2	34	22
11	3	33	30
11	4	53	53
11	5	61	49
11	6	56	52
12	1	298	292
12	2	48	55
12	3	37	37
12	4	76	84

L=4

H	K	|FO|	|FC|
0	0	33	22
1	0	916	900
1	1	461	491
2	0	726	734
2	1	231	241
2	2	272	252
3	0	70	26
3	1	625	630
3	2	656	661
3	3	1321	1351
4	0	46	46
4	1	109	119
4	2	196	181
4	3	608	614
5	0	442	429
5	1	906	921
5	2	316	317
5	3	127	138
5	4	246	247
5	5	781	790
6	0	491	489
6	1	549	559
6	2	442	448
6	3	45	58
6	4	255	272
6	5	284	276
6	6	403	403
7	0	414	417
7	1	433	432
7	2	141	130
7	3	362	367
7	4	138	136
7	5	425	430
7	6	387	397
7	7	532	538
8	0	432	436
8	1	291	285
8	2	123	109
8	3	200	206
8	4	86	87
8	5	191	198
8	6	254	253
8	7	173	170
8	8	343	342
9	0	35	26
9	1	365	365
9	2	295	295
9	3	592	592
9	4	365	359
9	5	125	121
9	6	41	13
9	7	425	427
9	8	120	132
10	0	165	167
10	1	79	75
10	2	65	62
10	3	341	329
10	4	108	111
10	5	135	132
10	6	34	26
10	7	84	88
11	0	175	173
11	1	598	598
11	2	206	210
11	4	168	172
11	5	497	503

H	k	|Fo|	|Fc|
12	0	175	182
12	1	225	220
12	2	145	152
12	3	27	39

L=5

2	1	354	349
3	1	149	152
3	2	190	185
4	1	563	560
4	2	204	205
4	3	99	87
5	1	180	180
5	2	268	277
5	3	235	240
5	4	369	372
6	1	212	209
6	2	246	244
6	3	55	32
6	4	28	41
6	5	57	61
7	1	39	16
7	2	315	316
7	3	43	24
7	4	380	388
7	5	41	9
7	6	214	216
8	1	140	138
8	2	45	43
8	3	49	53
8	4	56	58
8	5	104	108
8	6	81	79
8	7	117	113
9	1	46	25
9	2	190	191
9	3	100	108
9	4	177	171
9	5	99	95
9	6	129	125
9	7	33	3
9	8	69	64
10	1	332	326
10	2	141	145
10	3	62	53
10	4	36	6
10	5	173	172
10	6	28	32
11	1	41	41
11	2	40	25
11	3	46	4
11	4	55	53
11	5	59	62
12	1	243	248

L=6

0	0	32	26
1	0	156	163
1	1	330	332
2	0	786	776
2	1	578	585
2	2	392	400
3	0	466	462
3	1	382	383
3	2	162	160
3	3	624	635
4	0	571	588
4	1	599	607
4	2	546	546
4	3	191	196
4	4	505	502
5	0	256	265
5	1	168	170
5	2	289	289
5	3	374	367
5	4	288	288
5	5	290	303
6	0	194	195
6	1	77	71
6	2	601	595
6	3	504	513
6	4	352	357
6	5	251	260
6	6	207	212
7	0	318	312
7	1	86	93
7	2	395	396
7	3	18	14
7	4	270	276
7	5	39	37
7	6	96	79
7	7	51	14
8	0	737	745
8	1	111	115
8	2	112	113
8	3	289	283
8	4	245	250
8	5	254	260
8	6	613	623
8	7	183	187
8	8	72	83
9	0	443	455
9	1	195	187
9	2	160	161
9	3	401	412
9	4	28	45
9	5	176	167
9	6	325	333
9	7	56	53
10	0	218	220
10	1	301	298
10	2	411	416
10	3	138	149
10	4	326	327
10	5	223	225
11	0	173	182
11	1	120	119
11	2	126	120
11	3	237	229

L=7

2	1	494	500
3	1	33	18
3	2	126	134
4	1	339	337
4	2	39	19
4	3	106	104
5	1	24	23
5	2	180	176
5	3	23	37
5	4	110	115
6	1	238	237
6	2	61	45
6	3	97	94
6	4	34	7
7	1	16	7
7	5	285	290
7	2	300	298
7	3	27	14
7	4	366	370
7	5	31	7
7	6	141	130
8	1	164	161
8	2	8	13
8	3	52	46
8	4	42	5
8	5	59	36
8	6	30	23
8	7	119	115
9	1	24	8
9	2	90	88
9	3	47	12
9	4	255	253
9	5	42	29
9	6	19	4
10	1	315	319
10	2	16	26
10	3	82	72
10	4	20	8

L=8

0	0	757	755
1	0	248	241
1	1	419	433
2	0	195	193
2	1	202	198
2	2	418	418
3	0	412	412
3	1	250	250
3	2	270	263
3	3	651	653
4	0	278	269
4	1	186	186
4	2	209	205
4	3	153	151
4	4	172	180
5	0	207	206
5	1	214	222
5	2	242	237
5	3	245	236
5	4	236	233
5	5	317	324
6	0	407	405
6	1	258	255
6	2	156	152
6	3	221	214
6	4	336	336
6	6	294	289
7	0	21	30
7	1	185	188
7	2	172	177
7	3	49	35
7	4	269	273
7	5	106	101
7	6	155	154
7	7	39	36
8	1	247	258
8	2	455	456
8	3	154	154
8	4	320	314
8	5	144	145
8	6	78	87
9	0	165	168
9	1	151	149
9	2	191	183
9	3	439	446
9	4	183	193
10	0	284	286
10	1	176	174

L=9

2	1	270	270
3	1	72	69
3	2	71	54
4	1	340	341
4	2	129	124
4	3	79	77
5	1	107	108
5	2	166	162
5	3	149	141
5	4	221	220
6	1	167	165
6	2	141	144
6	3	50	31
6	4	49	41
6	5	108	111
7	1	36	26
7	2	222	218
7	3	36	26
7	4	280	283
7	5	40	8
8	0	74	77
8	1	114	112
8	2	30	32
8	3	38	16
8	4	57	47

L=10

0	0	180	169
1	0	25	23
1	1	469	458
2	0	74	71
2	1	116	102
2	2	279	269
3	0	52	32
3	1	649	637
3	2	18	30
3	3	27	66
4	0	240	234
4	1	127	125
4	2	185	179
4	3	37	13
4	4	78	73
5	0	48	5
5	1	268	260
5	2	40	25
5	3	688	678
5	4	45	39
5	5	222	220
6	0	279	280
6	1	44	42
6	2	33	32
6	3	116	111
6	4	118	114
7	0	90	85
7	1	344	346
7	2	91	88
7	3	538	533
8	2	1070	1082

L=11

2	1	130	134
3	1	39	1
3	2	158	156
4	1	308	309
4	2	29	36
4	3	59	43
5	1	38	23
5	2	157	151
5	3	46	6

L=12

0	0	256	254
1	0	144	145
1	1	164	158
2	0	70	69
2	1	171	169
2	2	209	210
3	0	379	380

A.2 VOP_2SiO_8 Crystal II
All values are multiplied by 10.

L=0

H	k	|Fo|	|Fc|
1	1	86	83
2	0	736	746
2	2	1571	1531
3	1	609	620
3	3	778	714
4	0	105	153
4	2	1141	1130
4	4	1208	1186
5	1	431	393
5	3	649	650
5	5	140	146
6	0	1740	1762
6	2	488	489
6	4	550	544
6	6	1181	1190
7	1	392	378
7	3	283	296
7	5	303	298
7	7	528	539
8	0	186	180
8	2	1063	1069
8	4	850	860
8	6	80	87
8	8	603	600
9	1	301	288
9	3	52	19
9	5	334	338
9	7	84	80
9	9	75	89
10	0	272	263
10	2	516	501
10	4	668	680
10	6	388	379
10	8	379	361
11	1	143	111
11	3	523	522
11	5	165	182
11	7	108	119
12	0	739	711
12	2	253	232
12	4	280	275
13	1	261	249

L=1

H	k	|Fo|	|Fc|
2	1	915	935
3	1	162	152
3	2	152	130
4	1	453	463
4	2	368	346
4	3	246	232
5	1	264	256
5	2	252	253
5	3	255	247
5	4	115	121
6	1	224	234
6	2	207	208
6	3	128	124
6	4	111	108
6	5	264	269
7	1	75	76
7	2	512	516
7	3	55	55
7	4	548	550
7	5	41	50
7	6	138	133
8	1	221	213
8	2	75	56
8	3	14	3
8	4	76	83
8	5	47	51
8	6	52	34
8	7	193	201
9	1	75	87
9	2	233	240
9	3	97	108
9	4	393	402
9	5	53	37
9	6	81	49
9	7	58	41
9	8	113	122
10	1	324	328
10	2	87	70
10	3	135	127
10	4	48	44
10	5	231	236
10	6	30	2
10	7	275	273
10	8	52	11
11	1	48	48
11	2	136	125
11	3	48	21
11	4	59	57
11	5	78	76
11	6	40	33
11	7	50	19
12	1	153	150
12	2	44	33
12	3	111	133
12	4	102	92
12	5	105	110
13	1	55	0
13	2	151	164

L=2

H	k	|Fo|	|Fc|
0	0	1014	1044
1	0	739	786
1	1	624	589
2	0	1206	1201
2	1	682	686
2	2	76	54
3	0	637	535
3	1	328	338
3	2	458	475
3	3	196	158
4	0	782	768
4	1	591	596
4	2	50	56
4	3	766	772
4	4	50	69
5	0	509	519
5	1	169	152
5	2	300	310
5	3	739	722
5	4	229	244
5	5	59	45
6	0	617	606
6	1	321	333
6	2	691	706
6	3	192	183
6	4	497	525
6	5	426	423
6	6	421	407
7	0	885	894
7	1	452	443
7	2	346	354
7	3	105	82
7	4	65	74
7	5	321	312
7	6	374	379
7	7	309	297
8	0	635	656
8	1	84	90
8	2	95	70
8	3	366	380
8	4	76	96
8	5	345	351
8	6	461	460
8	7	185	186
8	8	179	177
9	0	243	240
9	1	288	270
9	2	298	303
9	3	103	96
9	4	260	253
9	5	429	429
9	6	169	173
9	7	74	53
9	8	262	266
9	9	87	85
10	0	159	173
10	1	206	209
10	2	132	145
10	3	475	470
10	4	64	65
10	5	185	168
10	6	140	163
10	8	169	162
11	0	166	159
11	1	32	14
11	2	158	159
11	3	542	535
11	4	178	175
11	5	90	94
11	6	249	259
11	7	183	169
12	0	193	181
12	1	292	294
12	2	245	250
12	3	146	141
12	4	178	202
12	5	196	195
13	0	313	305
13	1	299	289

L=3

H	k	|Fo|	|Fc|
2	1	220	231
3	1	45	43
3	2	523	492
4	1	746	726
4	2	232	218
4	3	124	124
5	1	160	153
5	2	333	328
5	3	124	119
5	4	531	532
6	1	175	179
6	2	91	89
6	3	28	11
6	4	98	98
6	5	86	76
7	1	74	82
7	2	371	373
7	3	74	57
7	4	446	439
7	5	68	62
7	6	248	231
8	1	127	131
8	2	16	29
8	3	124	126
8	4	68	60
8	5	166	159
8	6	38	3
8	7	121	128
9	1	70	78
9	2	272	273
9	3	60	63
9	4	156	162
9	5	51	3
9	6	192	199
9	8	45	75
10	1	306	296
10	2	21	4
10	3	47	70
10	4	70	55
10	5	105	84
10	7	313	310
10	8	33	19
11	1	61	36
11	2	44	32
11	3	27	27
11	4	82	46
11	5	51	52
11	6	50	49
12	1	298	299
12	2	35	45
12	3	22	33
12	4	53	77

L=4

H	k	|Fo|	|Fc|
0	0	58	58
1	0	899	875
1	1	440	482
2	0	686	706
2	1	235	241
2	2	332	282
3	0	52	29
3	1	620	636
3	2	567	650
3	3	1291	1283
4	0	23	25
4	1	119	121
4	2	222	198
4	3	613	607
4	4	59	28
5	0	433	424
5	1	876	904
5	2	308	315
5	3	113	131
5	4	240	246
5	5	790	786
6	0	519	507
6	1	539	554
6	2	422	435
6	3	74	59
6	4	230	253
6	5	275	274
6	6	432	418
7	0	415	416
7	1	410	423
7	2	131	131
7	3	364	378
7	4	132	135
7	5	419	422
7	6	377	393
7	7	524	534
8	0	404	424
8	1	274	281
8	2	140	129
8	3	195	205
8	4	61	71
8	5	184	197
8	6	219	239
8	7	163	168
8	8	360	355
9	0	32	24
9	1	358	371
9	2	299	293
9	3	568	577
9	4	352	354
9	5	140	124
9	7	417	429
9	8	125	131
10	0	173	186
10	1	75	73
10	2	29	52
10	3	344	328
10	4	100	96
10	5	132	132
10	6	20	13
10	7	82	84
11	0	165	173
11	1	586	599
11	2	213	206
11	3	37	15
11	4	166	167
11	5	502	504

H	K	|FO|	|FC|
11	6	119	103
12	0	183	183
12	1	234	218
12	2	144	136
12	3	68	38

L=5

2	1	351	344
3	1	147	149
3	2	203	194
4	1	550	558
4	2	209	209
4	3	107	94
5	1	177	182
5	2	268	269
5	3	227	236
5	4	364	367
6	1	212	212
6	2	235	233
6	3	34	33
6	4	42	44
6	5	59	60
7	1	17	14
7	2	311	315
7	3	25	21
7	4	392	388
7	6	216	218
8	1	116	130
8	2	54	46
8	3	19	55
8	4	49	61
8	5	93	101
8	6	71	72
8	7	115	106
9	1	41	33
9	2	206	199
9	3	110	109
9	4	186	180
9	5	84	85
9	6	147	131
9	7	32	1
9	8	49	64
10	1	334	320
10	2	139	141
10	3	57	56
10	5	161	163
10	6	46	33
11	1	25	37
11	2	32	13
11	3	20	2
11	4	50	42
11	5	73	62
12	1	255	250

L=6

1	0	141	151
1	1	308	317
2	0	766	789
2	1	568	579
2	2	402	407
3	0	457	460
3	1	393	381
3	2	155	150
3	3	597	615
4	0	570	594
4	1	594	598
4	2	542	552
4	3	180	188
4	4	500	507
5	0	257	261
5	1	150	162
5	2	280	284
5	3	389	371
5	4	284	282
5	5	292	300
6	0	187	200
6	1	67	58
6	2	592	603
6	3	497	512
6	4	354	362
6	5	245	254
6	6	201	219
7	0	306	307
7	1	69	78
7	2	379	390
7	3	35	13
7	4	263	268
7	5	91	20
7	6	61	72
7	7	25	18
8	0	730	751
8	1	127	111
8	2	114	117
8	3	280	278
8	4	247	259
8	5	247	254
8	6	608	625
8	7	180	182
8	8	68	80
9	0	437	448
9	1	186	187
9	2	152	152
9	3	387	388
9	4	49	39
9	5	166	171
9	6	324	330
9	7	49	50
10	0	206	215
10	1	306	295
10	2	419	423
10	3	121	141
10	4	327	333
10	5	204	217
11	0	167	172
11	1	108	112
11	2	115	115
11	3	235	238

L=7

2	1	503	500
3	1	60	18
3	2	119	129
4	1	336	336
4	2	35	22
4	3	101	108
5	1	41	26
5	2	171	173
5	3	64	38
5	4	114	106
6	1	234	236
6	2	38	46
6	3	106	97
6	4	30	8
6	5	281	283
7	1	53	8
7	2	289	297
7	3	42	14
7	4	367	368
7	5	41	5
7	6	146	136
8	1	160	154
8	3	66	43
8	4	29	7
8	5	54	26
8	6	37	23
8	7	118	111
9	1	43	5
9	2	111	100
9	3	49	13
9	4	264	264
9	5	17	28
9	6	16	7
10	1	315	315
10	2	48	26
10	3	62	73

L=8

0	0	725	761
1	0	229	223
1	1	420	444
2	0	205	195
2	1	198	190
2	2	435	423
3	0	407	407
3	1	237	236
3	2	256	245
3	3	644	655
4	0	289	273
4	1	182	180
4	2	219	207
4	3	144	135
4	4	200	184
5	0	189	188
5	1	228	233
5	2	230	227
5	3	232	223
5	4	236	226
5	5	338	340
6	0	412	406
6	1	242	240
6	2	158	157
6	3	212	210
6	4	359	343
6	5	133	147
6	6	305	285
7	0	38	21
7	1	187	195
7	2	168	170
7	3	54	56
7	4	267	265
7	5	106	105
7	6	141	140
7	7	37	42
8	0	66	77
8	1	248	246
8	2	461	460
8	3	136	141
8	4	333	313
8	5	133	134
8	6	87	86
9	0	167	167
9	1	127	134
9	2	165	171
9	3	438	448
9	4	179	176
10	0	303	292
10	1	166	164

L=9

2	1	274	271
3	1	72	69
3	2	68	55
4	1	341	339
4	2	127	127
4	3	82	81
5	1	113	109
5	2	153	155
5	3	143	139
5	4	220	211
6	1	165	167
6	2	137	140
6	3	57	33
6	4	55	42
6	5	122	113
7	1	87	25
7	2	217	219
7	3	38	23
7	4	268	283
7	5	36	9
8	1	106	108
8	2	33	35
8	3	50	15
8	4	57	48
9	1	50	34

L=10

0	0	159	145
1	0	32	29
1	1	462	452
2	0	70	89
2	1	111	90
2	2	265	248
3	0	47	10
3	1	638	630
3	2	31	37
3	3	106	66
4	0	226	219
4	1	102	112
4	2	162	154
4	3	55	8
4	4	78	48
5	0	57	3
5	1	265	255
5	2	73	14
5	3	676	676
5	4	36	26
5	5	229	213
6	0	269	254
6	1	38	50
6	2	48	48
6	3	99	95
6	4	70	100
6	5	47	28
7	0	91	84
7	1	350	343
7	2	96	77
7	3	526	521

L=11

2	1	118	130
3	1	55	0
3	2	158	158
4	1	303	309
4	2	60	32
4	3	48	46
5	1	27	19
5	2	149	145
5	3	48	5
6	1	108	94

L=12

0	0	228	251
1	0	126	137
1	1	172	165
2	0	83	57
2	1	172	158
2	2	220	220
3	0	359	363
3	1	67	30

A.3 $VO(PO_3)_2$ Crystal I

H	K	|Fo|	|Fc|
	L = 0		
0	2	10	9
0	4	51	55
0	6	51	57
0	8	71	75
0	10	3	2
0	12	79	81
0	14	9	7
0	16	19	20
1	3	53	52
1	5	12	16
1	9	17	17
1	11	4	7
1	13	3	10
1	15	17	19
1	17	22	25
2	4	60	61
2	6	62	63
2	8	46	53
2	10	53	58
2	12	6	2
2	14	42	44
2	16	22	22
3	5	46	47
3	7	14	16
3	9	39	40
3	11	38	41
3	13	7	7
3	15	14	14
3	17	12	13
4	4	66	65
4	6	107	96
4	8	10	11
4	10	36	40
4	12	28	31
4	14	27	29
4	16	12	15
5	7	6	2
5	9	40	44
5	11	35	40
5	13	9	15
5	15	8	7
5	17	4	2
6	6	43	44
6	8	74	75
6	10	38	40
6	12	37	37
6	14	6	5
6	16	39	40
7	9	16	17
7	11	20	24
7	13	15	18
7	15	5	4
8	8	15	16
8	10	35	36
8	12	30	31
8	14	22	25
9	11	10	13
9	13	4	4
9	15	21	21
10	10	28	29
10	14	34	36
11	13	8	5
12	10	9	1
12	12	44	46
	L = 1		
0	1	87	65
0	3	38	35
0	5	15	4
0	7	50	53
0	9	14	11
0	11	14	9
0	13	39	37
0	15	9	11
0	17	6	3
1	2	53	51
1	4	28	27
1	6	17	12
1	8	30	31
1	10	23	24
1	12	25	25
1	14	15	16
1	16	15	10
2	3	72	66
2	5	36	35
2	7	18	15
2	9	53	55
2	11	30	30
2	13	15	15
2	15	28	27
2	17	17	15
3	4	66	61
3	6	49	51
3	8	40	41
3	10	27	28
3	12	14	15
3	14	27	25
3	16	8	3
4	5	51	51
4	7	42	43
4	9	26	29
4	11	20	21
4	13	28	27
4	15	20	21
4	17	18	16
5	6	15	13
5	8	30	32
5	10	23	22
5	12	13	11
5	14	9	8
5	16	14	11
6	7	24	26
6	9	39	39
6	11	24	21
6	13	11	16
6	15	21	18
7	8	33	34
7	10	17	18
7	12	27	25
7	14	10	10
7	16	18	15
8	9	20	21
8	11	17	14
8	13	25	24
8	15	18	18
9	10	25	24
9	12	9	9
9	14	25	24
10	11	13	13
10	13	11	12
11	12	7	5
	L = 2		
0	2	17	16
0	4	60	61
0	6	76	77
0	8	41	45
0	10	10	8
0	12	6	10
0	14	18	18
0	16	22	22
1	1	73	62
1	3	28	27
1	5	28	28
1	7	34	32
1	9	35	33
1	11	37	37
1	13	27	26
1	15	13	9
2	4	44	45
2	6	48	52
2	8	38	41
2	10	9	6
2	12	14	14
2	14	6	6
2	16	16	13
3	3	48	46
3	5	58	57
3	7	34	32
3	9	23	18
3	11	24	22
3	13	15	11
3	15	21	21
4	6	11	13
4	8	15	17
4	10	25	27
4	12	14	16
4	14	6	3
5	5	47	47
5	7	29	26
5	9	26	24
5	11	20	21
5	13	13	7
5	15	23	22
6	8	17	18
6	10	30	32
6	12	32	35
6	14	15	16
7	7	23	21
7	9	26	24
7	11	25	25
7	13	13	9
7	15	16	15
8	8	6	3
8	10	19	20
8	12	18	19
8	14	12	12
9	9	25	26
9	11	28	28
9	13	17	15
11	11	28	28
	L = 3		
0	1	23	6
0	3	20	4
0	5	30	27
0	7	33	34
0	9	16	13
0	11	12	3
0	13	20	19
0	15	12	3
1	2	28	22
1	4	54	53
1	6	19	8
1	8	35	34
1	10	18	15
1	12	14	13
1	14	11	7
2	3	44	45
2	5	45	42
2	7	34	32
2	9	29	30
2	11	19	17
2	13	23	21
2	15	23	24
3	4	29	25
3	6	26	26
3	8	20	14
3	10	26	26
3	12	10	4
3	14	20	19
4	5	21	18
4	7	34	32
4	9	25	25
4	11	26	24
4	13	27	27
4	15	16	13
5	6	22	19
5	8	20	17
5	10	21	19
5	12	14	8
5	14	20	17
6	7	10	2
6	9	22	19
6	11	10	3
6	13	11	9
7	8	29	29
7	10	20	18
7	12	18	18
7	14	11	12
8	9	24	21
8	11	19	18
8	13	24	21
9	10	25	25
9	12	10	6
10	11	18	14
	L = 4		
0	0	55	58
0	2	27	27
0	4	45	44
0	6	14	14
0	8	24	25
0	10	12	15
0	12	34	33
0	14	10	9
1	3	8	13
1	5	34	34
1	7	24	25
1	9	10	7
1	11	9	13
1	13	9	4
2	2	49	51
2	4	20	16
2	6	11	5
2	8	12	11
2	10	33	32
2	12	8	9
2	14	20	17
3	5	8	8
3	7	6	4
3	9	6	8
3	11	14	15
3	13	11	11
4	4	20	16
4	6	43	45
4	8	10	9
4	10	15	12
4	12	19	16
5	7	11	12
5	9	16	18
5	11	25	26
5	13	18	19
6	6	15	18
6	8	42	39
6	10	10	6
6	12	13	11
7	9	16	16
7	11	21	22
8	8	12	9
8	10	13	9
8	12	15	14
9	11	7	4
10	10	30	25
	L = 5		
0	1	20	23
0	3	15	13
0	5	17	18
0	7	20	22
0	9	6	6
0	11	12	16
1	2	21	26
1	4	32	32
1	6	14	14

H	K	|FO|	|FC|
1	8	25	27
1	10	12	11
1	12	14	14
2	3	32	34
2	5	23	24
2	7	20	20
2	9	28	29
2	11	19	18
3	4	13	15
3	6	20	21
3	8	6	9
3	10	27	28
4	5	23	25
4	7	33	35
4	9	10	9
4	11	16	15
5	6	13	14
5	8	20	21
5	10	15	16
6	7	10	9
6	9	21	20
7	8	26	25
8	9	6	6

L = 6

H	K	|FO|	|FC|
0	2	10	11
0	4	22	21
0	6	18	20
0	8	18	20
1	1	22	23
1	3	14	17
1	5	16	15
1	7	13	12
2	4	16	17
2	6	18	20
2	8	9	12
3	3	14	14
3	5	14	15
3	7	14	14
4	6	11	11
5	5	23	23
5	7	22	21

A.4 $VO(PO_3)_2$ Crystal II

H	K	|FO|	|FC|
	L = 0		
0	2	6	10
0	4	47	49
0	6	48	51
0	8	65	66
0	10	2	2
0	12	73	72
0	14	7	5
0	16	18	19
1	3	47	46
1	5	11	17
1	7	3	5
1	9	13	17
1	11	5	8
1	13	5	8
1	15	16	20
1	17	20	24
2	4	54	54
2	6	55	56
2	8	42	49
2	10	48	54
2	12	4	1
2	14	37	40
2	16	18	20
3	5	39	44
3	7	12	16
3	9	33	38
3	11	32	38
3	13	5	7
3	15	13	13
3	17	10	13
4	4	59	57
4	6	95	80
4	8	11	10
4	10	33	37
4	12	24	29
4	14	25	27
4	16	14	12
5	7	3	1
5	9	35	42
5	11	32	38
5	13	11	15
5	15	7	7
5	17	2	3
6	6	35	42
6	8	63	67
6	10	34	37
6	12	31	34
6	14	4	4
6	16	36	36
7	9	14	18
7	11	18	24
7	13	14	17
7	15	4	3
8	8	13	14
8	10	30	33
8	12	27	29
8	14	23	23
9	11	11	13
9	13	3	4
9	15	18	19
10	10	25	29
10	14	31	32
11	13	4	5
12	12	40	41
	L = 1		
0	1	70	52
0	3	36	32
0	5	19	3
0	7	46	52
0	9	15	12
0	11	14	11
0	13	33	35
0	15	9	8
0	17	6	2

H	k	|FO|	|FC|
1	2	51	43
1	4	28	30
1	6	20	10
1	8	29	32
1	10	22	25
1	12	24	25
1	14	15	14
1	16	13	12
2	3	64	59
2	5	35	35
2	7	20	16
2	9	46	51
2	11	27	30
2	13	14	12
2	15	25	27
2	17	16	14
3	4	59	55
3	6	46	51
3	8	35	39
3	10	26	28
3	12	15	12
3	14	24	26
3	16	9	5
4	5	46	49
4	7	39	41
4	9	24	28
4	11	20	21
4	13	25	28
4	15	19	19
4	17	17	15
5	6	18	12
5	8	29	30
5	10	21	22
5	12	13	12
5	14	11	9
5	16	15	13
6	7	23	23
6	9	35	38
6	11	22	23
6	13	13	14
6	15	19	21
7	8	30	33
7	10	18	18
7	12	24	27
7	14	10	9
7	16	18	16
8	9	19	21
8	11	15	14
8	13	24	26
8	15	16	16
9	10	22	25
9	12	11	8
9	14	24	25
10	11	14	12
10	13	12	10
11	12	10	8
	L = 2		
0	2	14	14
0	4	51	56
0	6	66	70
0	8	36	43
0	10	8	5
0	12	8	11
0	14	16	17
0	16	19	21
1	1	65	58
1	3	33	24
1	5	33	21
1	7	35	32
1	9	35	33
1	11	34	37
1	13	27	25
1	15	15	9
2	4	39	43
2	6	52	49
2	8	34	33

H	K	|FO|	|FC|
2	10	6	5
2	12	11	10
2	14	6	8
2	16	12	11
3	3	48	46
3	5	56	55
3	7	36	33
3	9	25	19
3	11	26	23
3	13	18	12
3	15	22	18
4	6	11	9
4	8	3	3
4	10	14	16
4	12	21	26
4	14	13	18
4	16	4	3
5	5	45	45
5	7	31	27
5	9	28	25
5	11	24	19
5	13	17	7
5	15	24	24
6	8	15	17
6	10	26	31
6	12	29	34
6	14	15	14
7	7	25	20
7	9	27	23
7	11	25	25
7	13	17	9
7	15	18	12
8	10	16	20
8	12	16	18
8	14	9	11
9	9	27	29
9	11	27	24
9	13	19	16
10	12	4	3
11	11	29	31
	L = 3		
0	1	26	5
0	3	26	6
0	5	31	26
0	7	33	28
0	9	19	13
0	11	15	10
0	13	21	19
0	15	11	9
1	2	31	18
1	4	49	47
1	6	22	11
1	8	44	32
1	10	19	14
1	12	17	11
1	14	14	9
2	3	41	42
2	5	43	41
2	7	31	29
2	9	29	25
2	11	21	15
2	13	23	23
2	15	22	21
3	4	31	27
3	6	28	23
3	8	26	15
3	10	27	23
3	12	14	7
4	11	20	18
4	5	23	16
4	7	33	29
4	9	24	24
4	11	25	23
4	13	26	20
5	15	15	16
5	6	23	16

H	k	|FO|	|FC|
5	8	21	14
5	10	20	15
5	12	15	8
5	14	18	18
6	7	16	8
6	9	22	19
6	11	14	4
6	13	14	9
7	8	28	25
7	10	21	21
7	12	18	15
7	14	13	8
8	9	23	27
8	11	20	16
8	13	22	17
9	10	24	20
9	12	12	5
10	11	18	14
	L = 4		
0	0	47	53
0	2	23	27
0	4	41	35
0	6	17	11
0	8	24	24
0	10	13	16
0	12	31	31
0	14	9	9
1	3	10	14
1	5	28	33
1	7	21	26
1	9	9	5
1	11	10	11
1	13	6	3
2	2	44	44
2	4	18	14
2	6	12	7
2	8	14	10
2	10	31	29
2	12	10	11
2	14	18	16
3	5	5	10
3	7	4	5
3	9	5	8
3	11	12	15
3	13	11	9
4	4	17	16
4	6	39	41
4	8	10	10
4	10	16	10
4	12	18	15
5	7	10	10
5	9	15	18
5	11	23	26
5	13	16	18
6	6	14	20
6	8	38	34
6	10	10	5
6	12	14	11
7	9	14	14
7	11	20	21
8	8	11	14
8	10	12	7
8	12	15	11
9	11	3	4
10	10	27	23
	L = 5		
0	1	17	24
0	3	13	12
0	5	15	14
0	7	19	24
0	9	7	3
0	11	14	19
1	2	21	24
1	4	29	30

H	K	|FO|	|FC|
1	6	13	14
1	8	22	25
1	10	10	11
1	12	14	13
2	3	29	33
2	5	20	21
2	7	19	19
2	9	25	29
2	11	17	17
3	4	11	12
3	6	18	23
3	8	8	11
3	10	25	26
4	5	20	27
4	7	30	31
4	9	10	10
4	11	13	13
5	6	13	10
5	8	18	21
5	10	15	16
6	7	10	10
6	9	17	18
7	8	24	24
8	9	6	5

L = 6

H	K	|FO|	|FC|
0	2	10	10
0	4	19	20
0	6	17	18
0	8	18	17
1	1	22	25
1	3	18	17
1	5	17	16
1	7	14	15
2	4	15	15
2	6	17	18
2	8	11	10
3	3	15	16
3	5	15	17
3	7	14	16
4	6	10	10
5	5	22	26
5	7	21	20

A.5 $V(PO_3)_3$

K=0

H	L	|FO|	|FC|
-8	10	142	141
-8	12	13	34
-6	8	58	61
-6	10	42	49
-6	12	115	115
-4	6	120	127
-4	8	283	289
-4	10	33	29
-4	12	132	139
-2	4	269	279
-2	6	77	70
-2	10	141	150
-2	12	58	57
0	2	184	191
0	4	279	286
0	6	284	293
0	10	199	197
0	12	80	75
2	0	38	36
2	2	289	303
2	4	178	176
2	4	49	52
2	6	98	105
2	8	39	47
2	10	17	14
2	12	123	122
4	0	27	22
4	2	33	46
4	4	295	313
4	4	408	424
4	6	65	70
4	6	163	164
4	8	364	373
4	10	113	116
4	12	70	81
6	0	220	216
6	2	130	128
6	2	197	194
6	4	244	240
6	4	133	130
6	6	49	43
6	6	231	233
6	8	27	13
6	10	179	171
8	0	347	338
8	2	163	163
8	2	121	122
8	4	71	76
8	4	225	230
8	6	188	194
8	6	156	158
8	8	23	21
8	8	50	50
8	10	110	113
10	0	111	109
10	2	171	169
10	2	71	75
10	4	139	137
10	6	19	33
10	8	130	135
10	8	104	111
12	-10	17	31
12	0	24	22
12	2	97	94
12	2	213	212
12	4	221	214
12	4	79	86
12	6	56	56
12	6	38	33
12	8	63	66
12	8	46	53
14	0	129	129
14	2	21	22
14	4	56	42
14	6	95	115

K=1

H	L	|FO|	|FC|
-10	11	45	46
-8	9	55	57
-8	11	78	76
-7	8	32	40
-7	10	44	35
-7	12	41	48
-6	9	22	14
-6	11	11	13
-5	6	78	87
-5	8	12	27
-5	10	44	52
-5	12	37	55
-4	5	66	64
-4	7	56	54
-4	9	65	80
-4	11	108	115
-4	13	40	36
-3	4	21	10
-3	6	78	78
-3	8	27	29
-3	11	115	122
-3	12	20	19
-2	5	81	85
-2	7	33	35
-2	11	40	33
-2	13	33	22
-1	2	16	18
-1	4	66	66
-1	6	15	10
-1	8	79	78
-1	10	18	26
0	1	27	20
0	3	25	34
0	5	38	38
0	7	61	63
0	9	57	55
0	11	8	16
0	13	26	34
1	0	23	7
1	2	25	9
1	4	78	77
1	6	32	28
1	8	72	71
1	10	37	36
1	12	19	25
2	-1	22	20
2	3	43	43
2	7	31	35
2	9	27	35
2	11	33	26
3	0	61	64
3	2	24	22
3	-2	15	14
3	4	22	31
3	6	19	14
3	8	36	21
3	12	35	39
4	-1	18	9
4	-1	83	86
4	3	21	30
4	3	63	57
4	5	19	14
4	9	19	20
4	11	39	47
5	2	40	41
5	-2	151	152
5	4	26	10
5	-4	17	14
5	6	59	64
5	8	34	26
6	1	33	25
6	-1	17	29
6	5	15	20
6	-5	27	29
6	7	19	6
6	9	13	21

H	L	|FO|	|FC|
6	11	17	26
7	0	28	24
7	2	31	33
7	-2	120	127
7	4	42	42
7	-4	36	39
7	6	35	30
7	-6	150	156
7	8	23	23
7	10	5	20
8	1	50	45
8	-1	96	97
8	3	64	61
8	-3	114	126
8	5	39	37
8	-5	87	90
8	7	37	17
8	-7	104	105
9	0	54	60
9	2	103	104
9	-2	110	112
9	4	47	45
9	-4	33	23
9	5	19	13
9	-6	34	37
9	8	10	5
9	-8	87	91
10	1	8	23
10	-1	36	48
10	7	12	20
10	-7	51	46
11	0	37	40
11	2	94	97
11	-2	30	33
11	4	26	27
11	-4	58	55
11	6	48	33
11	-6	42	35
11	-8	40	31
11	-10	41	48
12	1	67	62
12	-1	51	57
12	3	84	83
12	-3	73	74
12	5	52	48
12	-5	73	78
12	-7	78	76
12	-9	76	74
13	0	39	42
13	2	17	22
13	-2	45	42
13	4	22	9
13	-4	66	68
13	-6	26	27
13	-8	50	38
14	-1	25	14
14	-3	47	43

K=2

H	L	|FO|	|FC|
-9	11	18	31
-8	10	73	73
-8	12	43	25
-7	9	35	38
-7	11	41	54
-6	8	69	78
-6	10	40	52
-6	12	67	60
-5	7	27	31
-5	9	69	69
-5	11	55	68
-4	6	99	105
-4	8	128	132
-4	10	40	36
-4	12	92	89
-3	5	19	14
-3	7	45	46
-3	9	62	61

H	L	|FO|	|FC|
-3	11	27	31
-2	6	18	12
-2	8	44	41
-2	10	110	104
-2	12	35	25
-1	3	26	35
-1	5	18	9
-1	7	5	29
-1	9	32	40
0	0	25	3
0	2	35	21
0	4	66	67
0	6	42	52
0	8	65	76
0	10	65	71
1	3	31	34
1	5	21	8
1	7	35	29
1	11	32	29
2	-2	25	29
2	4	23	26
2	6	15	11
2	10	40	32
2	12	25	25
3	1	44	47
3	-1	59	66
3	-3	60	62
3	9	31	38
4	0	15	28
4	-2	52	39
4	4	30	32
4	-4	9	13
4	8	14	32
4	10	47	41
5	-1	90	94
5	3	34	40
5	-3	57	56
5	5	27	25
5	-5	26	26
5	7	14	15
6	0	30	17
6	2	17	15
6	-2	129	124
6	-4	48	41
6	-6	128	131
6	8	34	32
6	10	26	21
7	1	39	39
7	-1	66	64
7	3	23	32
7	-3	99	97
7	5	62	62
7	-5	38	33
7	7	26	19
7	-7	38	31
7	9	26	20
8	0	177	175
8	2	29	29
8	-2	88	86
8	-4	35	35
8	-4	126	130
8	-6	76	85
8	8	27	26
8	-8	38	30
8	10	19	18
9	1	27	36
9	-1	27	20
9	3	69	72
9	-3	77	78
9	7	13	19
9	-7	35	36
9	5	25	40
9	-5	47	51
9	9	13	6
9	-9	32	28
10	0	52	59
10	2	70	72
10	-2	47	50

H	L	|FO|	|FC|
10	-4	15	24
10	-2	32	32
10	0	21	9
10	2	23	35
10	4	77	80
10	6	49	47
11	1	60	51
11	-1	24	36
11	3	43	55
11	-3	54	50
11	5	24	9
11	-5	45	50
11	7	19	17
11	-9	54	53
12	0	22	15
12	2	48	44
12	-2	89	89
12	4	99	96
12	-4	24	32
12	6	34	35
12	-6	51	56
12	-8	94	93
13	1	55	50
13	-1	45	37
13	3	21	28
13	-3	63	55
13	-7	12	25
14	0	52	51
14	2	21	26
14	-2	38	45
14	-4	49	57
14	-6	80	87

K=3

H	L	|FO|	|FC|
-9	10	67	64
-8	9	54	40
-8	11	44	48
-7	10	12	47
-7	12	71	59
-6	7	61	70
-6	9	113	112
-6	11	39	29
-5	6	205	213
-5	8	52	54
-5	10	86	93
-5	12	41	43
-4	5	276	280
-4	7	33	45
-4	9	56	65
-4	11	103	103
-3	4	100	107
-3	6	62	58
-3	8	71	79
-3	10	158	155
-3	12	62	66
-2	3	63	67
-2	5	168	169
-2	7	240	243
-2	9	73	80
-2	11	117	120
-2	13	47	57
-1	2	210	213
-1	4	28	19
-1	6	56	59
-1	8	124	128
-1	10	31	44
0	1	138	136
0	3	287	299
0	5	129	129
0	7	29	40
0	9	87	82
0	11	40	36
0	13	96	94
1	0	103	101
1	2	404	403
1	4	145	138
1	6	149	147
1	8	178	179
1	10	56	60
1	12	48	47
2	1	152	154
2	-1	458	430
2	3	81	89
2	5	280	288
2	7	58	67
2	9	192	196
2	11	52	50

H	L	|FO|	|FC|
3	0	287	272
3	2	297	291
3	-2	191	176
3	4	46	45
3	6	327	328
3	8	17	26
3	10	37	33
3	12	100	102
4	1	153	162
4	-1	124	124
4	3	98	93
4	-3	88	76
4	5	190	192
4	7	50	45
4	9	70	75
4	11	142	133
5	0	103	108
5	2	142	136
5	-2	112	109
5	4	27	36
5	-4	27	19
5	6	37	30
5	8	25	21
5	10	151	154
6	1	184	198
6	-1	161	156
6	3	185	187
6	-3	242	242
6	5	147	147
6	-5	102	107
6	7	176	183
6	9	83	81
6	11	55	59
7	0	37	34
7	2	138	136
7	-2	148	147
7	4	163	163
7	-4	62	57
7	6	35	34
7	-6	149	154
7	8	43	47
7	10	128	130
8	1	23	18
8	-1	186	192
8	3	190	193
8	-3	124	125
8	5	21	12
8	-5	22	24
8	7	37	32
8	-7	105	103
8	9	140	133
9	0	53	55
9	2	213	211
9	-2	139	144
9	4	82	86
9	-4	47	56
9	6	27	29
9	-6	51	49
9	8	136	127
9	-8	94	95
10	1	70	72
10	-1	165	169
10	3	89	84
10	-3	23	23
10	5	149	150
10	-5	71	73
10	7	41	47
10	-7	108	113
10	-9	42	33
11	0	47	54
11	2	123	123
11	-2	24	30
11	4	56	82
11	-4	68	59
11	6	70	80
11	-6	54	52
11	-10	20	10
12	1	96	97
12	-1	71	68
12	3	59	53
12	-3	51	50
12	5	119	119
12	-5	25	11
12	-7	31	36
12	-9	90	91
13	0	26	25
13	-2	84	85
13	4	6	27

H	L	|FO|	|FC|
13	-4	38	36
14	1	42	36
14	-1	47	49
14	-3	115	116
14	-5	26	32

K=4

H	L	|FO|	|FC|
-7	9	61	65
-7	11	36	18
-6	8	120	126
-6	10	107	114
-6	12	68	69
-5	7	56	55
-5	9	39	29
-5	11	55	42
-4	6	23	34
-4	8	80	82
-4	12	29	22
-3	5	52	54
-3	7	19	31
-3	11	18	27
-3	13	62	63
-2	4	42	38
-2	6	68	74
-2	8	72	78
-2	10	45	56
-2	12	61	60
-1	3	74	77
-1	5	13	17
-1	9	66	66
-1	11	39	38
-1	4	38	36
0	6	41	34
0	8	50	50
0	10	23	4
0	12	18	19
1	1	30	21
1	-1	18	13
1	3	25	23
1	5	66	66
1	7	32	38
1	9	44	49
1	11	24	20
2	0	72	70
2	-2	95	96
2	6	42	44
2	8	45	42
2	10	57	60
2	12	31	31
3	1	17	19
3	-1	34	37
3	3	33	32
3	-3	42	37
3	5	27	27
3	9	21	19
4	0	31	34
4	2	78	75
4	-2	36	24
4	4	15	25
4	-4	28	27
4	6	25	27
4	12	27	26
5	1	35	27
5	-1	62	55
5	-3	42	44
5	5	37	38
5	-5	9	15
5	7	23	27
5	9	17	14
5	11	36	17
6	0	61	61
6	2	47	40
6	-2	95	97
6	4	43	40
6	-4	154	157
6	6	12	27
6	-6	29	18
6	8	35	40
6	10	21	11
7	1	53	52
7	-1	10	17
7	-3	27	27
7	5	15	17
7	-5	115	120
7	7	26	20
7	-7	26	39
7	9	32	39

H	L	|FO|	|FC|
8	0	46	56
8	2	19	17
8	-2	33	23
8	4	23	24
8	-4	96	97
8	6	50	53
8	-6	36	34
8	8	62	63
9	1	53	66
9	-1	32	13
9	3	15	24
9	-3	28	16
9	5	12	6
9	7	10	9
9	-9	21	22
10	0	112	113
10	2	45	50
10	-2	65	68
10	4	101	102
10	-4	113	113
10	6	36	42
10	-6	125	135
10	8	13	11
10	-8	57	49
10	-10	65	67
11	1	41	37
11	-1	78	90
11	3	27	23
11	-3	45	50
11	-5	30	27
11	-7	50	51
11	-9	60	57
12	0	47	45
12	2	24	10
12	-2	27	31
12	4	55	53
12	-4	85	77
12	6	24	28
12	-6	14	19
12	-8	36	31
13	1	24	8
13	-1	31	39
13	3	17	12
13	-3	40	41
13	-5	47	47
14	0	34	40
14	2	93	95
14	-2	89	86
14	-4	66	63

K=5

H	L	|FO|	|FC|
-9	10	34	32
-8	9	51	56
-8	11	40	21
-7	8	67	64
-7	10	17	16
-7	12	34	20
-6	7	81	87
-6	9	101	101
-6	11	57	52
-5	6	91	101
-5	8	54	46
-5	10	21	16
-5	12	30	19
-4	5	35	35
-4	7	36	20
-4	9	5	8
-4	11	50	55
-3	4	15	24
-3	6	21	31
-3	8	63	62
-3	10	30	31
-3	12	34	32
-2	5	37	32
-2	7	105	105
-2	9	60	72
-2	11	93	55
-2	13	63	99
-1	2	33	59
-1	4	25	36
-1	10	33	28
-1	12	20	24
0	3	67	8
0	7	17	19
0	9	24	14
0	11	19	29

H	L	|FO|	|FC|
1	0	20	18
1	2	59	62
1	4	71	74
1	6	56	57
1	8	8	8
1	10	8	8
2	-1	118	116
2	1	13	18
2	3	10	7
2	5	80	81
2	9	40	46
2	11	10	29
3	0	8	6
3	-2	131	127
3	-2	60	58
3	6	17	11
3	10	23	9
3	12	23	27
4	1	43	45
4	-1	14	16
4	-3	64	67
4	9	20	19
4	11	15	7
5	-2	37	39
5	-2	38	37
5	-4	58	54
5	6	18	24
6	1	81	79
6	-1	86	85
6	3	73	70
6	-3	97	97
6	-5	23	40
6	5	99	114
6	7	25	30
6	9	27	26
7	2	31	32
7	-2	37	41
7	4	38	48
7	-4	20	38
7	-6	27	17
7	6	113	123
7	8	32	31
7	10	21	19
8	1	72	73
8	-1	44	49
8	3	17	22
8	-3	31	29
8	-5	37	31
8	7	64	53
9	0	17	19
9	2	44	44
9	-2	33	40
9	4	27	34
9	-4	58	52
9	6	22	21
9	8	20	17
9	-8	47	52
10	1	56	51
10	-1	127	130
10	3	40	37
10	-3	52	52
10	5	71	71
10	-5	91	90
10	7	19	21
10	-7	106	113
10	9	35	43
11	0	56	54
11	2	36	43
11	4	31	11
11	-4	32	28
11	6	45	45
11	-6	47	49
11	8	28	39
12	1	24	32
12	-1	27	29
12	3	36	14
12	-3	28	16
12	5	31	21
12	-5	46	33
12	7	16	23
13	0	25	14
13	2	21	23
13	-2	27	19
13	4	26	25
13	-4	42	37
13	6	71	69
14	-1	52	57
14	1	132	136
14	-3	37	41

K=6

H	L	|FO|	|FC|
-9	11	83	84
-8	10	30	11
-7	9	59	45
-7	11	34	27
-6	8	122	124
-6	10	82	90
-6	12	35	32
-5	7	33	37
-5	9	54	55
-5	11	59	63
-4	6	108	112
-4	8	34	20
-4	10	97	98
-4	12	19	17
-3	5	201	198
-3	7	60	57
-3	9	101	92
-3	11	14	35
-2	4	256	248
-2	6	221	230
-2	8	111	107
-2	10	77	76
-2	12	127	133
-1	3	287	289
-1	7	40	36
-1	9	186	187
-1	11	83	78
0	0	133	124
0	2	58	63
0	4	42	36
0	6	87	90
0	8	191	186
0	10	50	55
0	12	26	30
1	-1	239	230
1	1	147	145
1	3	63	61
1	5	167	169
1	7	235	240
1	9	25	13
1	11	10	21
2	0	267	272
2	2	191	184
2	-2	232	236
2	4	370	375
2	6	106	104
2	8	150	153
2	10	190	193
2	12	88	80
3	1	86	97
3	-1	130	119
3	3	65	63
3	-3	159	153
3	5	27	28
3	7	154	161
3	9	77	77
3	11	65	73
4	0	325	316
4	2	81	82
4	-2	222	205
4	4	22	20
4	-4	149	148
4	6	118	118
4	8	58	55
5	1	107	106
5	-1	210	199
5	3	66	71
5	-3	167	170
5	5	273	278
5	-5	214	208
5	7	47	41
5	11	115	110
6	0	180	177
6	2	276	273
6	-2	125	126
6	4	119	121
6	-4	217	222
6	6	127	126
6	-6	79	92
6	8	159	171
6	10	72	76
7	1	139	105
7	-1	177	171
7	3	237	242
7	-3	17	18

H	L	|FC|	|FC|
7	5	61	60
7	-5	73	63
7	7	32	20
7	-7	130	125
7	9	111	111
8	0	21	10
8	2	53	53
8	-2	83	79
8	4	153	151
8	-4	45	40
8	6	44	48
8	-6	59	62
8	8	107	109
8	-8	84	82
9	1	54	57
9	-1	20	24
9	3	129	131
9	-3	51	54
9	5	62	60
9	-5	82	82
9	7	49	49
9	-7	19	19
9	-9	27	32
10	0	146	144
10	2	68	72
10	-2	98	95
10	4	154	157
10	-4	65	73
10	6	125	128
10	-6	129	126
10	8	71	78
10	-10	55	66
11	1	104	104
11	-1	78	77
11	-3	89	91
11	5	68	66
11	-5	37	40
11	7	152	149
11	-7	52	54
11	-9	80	84
12	0	89	90
12	-2	39	47
12	4	31	24
12	-4	85	83
12	-6	31	30
12	-8	66	65
13	1	42	37
13	3	69	71
13	-3	63	67
13	-5	61	58
13	-7	61	64
14	-2	72	67
14	-4	41	42

K=7

H	L	|FO|	|FC|
-9	10	52	50
-8	9	97	99
-8	11	75	73
-7	8	62	58
-7	10	27	11
-7	12	8	28
-6	7	113	112
-6	9	23	25
-6	11	77	80
-5	6	107	113
-5	8	21	22
-5	10	54	50
-5	12	22	31
-4	7	32	25
-4	9	60	62
-4	11	19	38
-3	4	40	37
-3	8	26	16
-3	10	14	30
-3	12	33	49
-2	3	87	83
-2	5	22	19
-2	7	25	17
-2	9	47	46
-1	2	41	43
-1	4	62	51
-1	6	51	55
-1	8	52	51
-1	10	66	69
-1	12	38	42
0	1	25	15
0	3	61	55

H	L	|FO|	|FC|
0	5	55	58
0	7	48	57
0	9	62	66
0	11	59	49
1	0	36	37
1	2	25	19
1	4	13	22
1	6	34	20
1	8	12	2
2	1	24	28
2	-1	149	137
2	3	42	40
2	5	46	35
2	7	43	50
2	11	31	31
3	0	73	66
3	2	36	40
3	-2	16	21
3	4	49	53
3	6	8	20
3	12	15	19
4	-1	154	142
4	3	17	5
4	-3	153	146
4	5	15	10
4	7	17	14
4	11	20	10
5	1	85	83
5	2	46	42
5	-2	73	66
5	4	49	51
5	-4	93	82
5	8	6	4
5	10	22	12
6	1	98	91
6	-1	59	64
6	3	21	25
6	5	16	18
6	-5	83	85
6	7	21	24
6	9	12	10
7	0	11	10
7	2	39	39
7	-2	57	51
7	4	33	20
7	-4	37	42
7	6	20	28
7	-6	77	81
7	10	8	16
8	1	51	52
8	-1	41	39
8	3	28	24
8	-3	8	23
8	5	69	69
8	-5	114	114
8	7	25	15
8	-7	28	29
8	9	22	5
9	0	62	59
9	2	80	80
9	-2	64	66
9	4	46	45
9	-4	23	15
9	6	28	19
9	-6	61	62
9	9	56	60
9	-8	41	41
10	1	51	55
10	-1	58	51
10	3	31	26
10	-3	86	82
10	5	23	24
10	-5	29	31
10	7	40	61
10	-7	54	55
10	-9	81	84
11	0	31	39
11	2	65	65
11	-2	33	29
11	-4	28	31
11	6	46	44
11	-6	41	28
12	1	8	28
12	-1	82	88
12	3	40	45
12	-3	71	70
12	5	14	24
12	-5	30	39

H	L	|FO|	|FC|
12	-7	93	93
13	9	65	447
13	2	25	23
13	-4	45	45
13	-6	61	50
14	1	40	41
14	-1	81	75
14	-3	57	56

K=8

H	L	|FO|	|FC|
-8	10	70	64
-7	9	45	43
-7	11	39	30
-6	8	46	39
-6	10	39	45
-6	12	40	45
-5	7	54	51
-5	9	23	14
-5	11	68	70
-4	6	74	81
-4	8	37	40
-4	10	58	57
-4	12	26	24
-3	5	103	98
-3	7	50	50
-3	11	42	33
-2	4	32	22
-2	6	30	19
-2	12	26	23
-1	3	154	145
-1	5	45	44
-1	7	35	31
-1	9	64	52
0	4	24	19
0	6	16	15
0	8	38	51
0	10	47	46
0	12	46	50
1	1	43	34
1	-1	103	95
1	3	20	16
1	5	59	53
1	7	12	12
1	9	40	42
1	11	51	46
2	2	52	52
2	4	24	20
2	-2	96	93
2	8	20	9
2	6	50	46
2	8	19	24
2	10	52	51
3	1	9	5
3	-1	92	88
3	3	22	26
3	-3	10	34
3	5	25	18
3	7	60	57
3	9	23	10
3	11	33	38
4	0	62	51
4	2	45	38
4	-2	100	97
4	-4	41	45
4	6	13	11
4	8	15	15
4	10	4	8
5	1	161	156
5	-1	39	41
5	3	20	42
5	-3	16	20
5	-5	120	126
5	11	15	12
6	0	20	5
6	2	22	19
6	-2	31	27
6	4	53	54
6	6	6	19
6	-6	33	30
7	1	24	28
7	-1	91	96
7	3	47	39
7	-3	15	7
7	5	22	28
7	-5	52	58
7	7	24	17
7	-7	107	113

H	L	|FO|	|FC|
7	9	15	21
8	0	26	44
8	2	39	40
8	-2	53	54
8	4	29	33
8	-4	47	46
8	6	57	58
8	-6	22	11
8	8	64	65
9	1	45	47
9	-1	57	52
9	3	46	45
9	-3	48	52
9	5	5	6
9	-5	78	72
9	7	51	60
9	-7	43	51
10	0	36	31
10	-2	19	23
10	2	62	54
10	-4	23	42
10	6	35	19
10	-6	39	46
10	8	29	36
11	-1	25	20
11	1	51	44
11	-1	37	36
11	3	29	19
11	-3	70	71
11	5	25	24
11	-5	41	36
11	7	93	97
12	0	60	59
12	2	54	46
12	-2	75	79
12	4	20	31
12	-4	75	74
12	6	91	83
12	-6	66	65
13	1	60	52
13	-1	76	70
13	5	108	98
14	0	21	20
14	2	20	11
14	-4	37	28

K=9

H	L	|FO|	|FC|
-9	10	27	4
-8	9	55	67
-8	11	95	98
-7	8	45	39
-7	10	60	54
-6	7	123	126
-6	9	29	16
-6	11	92	88
-5	6	38	50
-5	8	47	45
-5	10	24	8
-5	12	31	43
-4	7	15	20
-4	9	95	101
-4	11	50	44
-3	4	66	52
-3	6	61	62
-3	8	14	15
-3	10	14	16
-2	3	194	193
-2	5	42	36
-2	7	111	118
-2	9	168	167
-2	11	40	37
-1	2	75	70
-1	4	58	64
-1	6	14	9
-1	8	26	26
-1	10	27	20
0	1	159	170
0	3	119	117
0	5	384	380
0	7	131	134
0	9	115	112
1	0	202	204
1	2	14	12
1	-2	141	134
1	4	111	106
1	6	124	125

H	L	|FO|	|FC|
1	8	32	16
1	10	70	71
1	12	15	26
2	1	267	255
2	-1	69	72
2	3	33	29
2	5	64	61
2	7	271	276
2	9	68	69
2	11	32	35
3	0	33	20
3	2	163	154
3	-2	100	98
3	4	134	135
3	6	40	41
3	8	50	52
3	10	31	26
4	1	257	249
4	-1	222	212
4	3	397	394
4	-3	395	392
4	5	32	23
4	7	112	112
4	9	217	216
4	11	20	27
5	0	28	30
5	2	25	25
5	-2	42	38
5	4	58	57
5	-4	65	62
5	6	7	11
5	8	8	15
5	10	61	58
6	1	79	77
6	-1	209	207
6	3	21	16
6	-3	117	112
6	5	136	134
6	-5	123	121
6	7	68	67
6	9	54	49
7	0	25	21
7	2	49	51
7	-2	37	43
7	4	36	28
7	-4	41	32
7	6	35	33
7	-6	33	28
8	1	294	293
8	-1	5	22
8	3	18	20
8	-3	87	81
8	5	241	240
8	-5	223	228
8	7	200	200
8	-7	23	24
8	9	52	50
9	0	89	85
9	2	33	20
9	-2	25	20
9	4	46	53
9	-4	44	42
9	6	22	17
9	-6	31	16
9	8	56	62
10	1	86	85
10	-1	20	12
10	3	90	95
10	-3	148	147
10	5	66	65
10	-5	22	8
10	7	127	127
10	-7	120	119
11	0	20	11
11	2	54	50
11	-2	46	49
11	4	31	37
11	-4	42	45
11	6	27	25
11	-6	31	31
12	1	11	17
12	-1	129	133
12	3	142	143
12	-3	68	63
12	5	81	79
12	-7	114	117
13	0	44	40

H	L	|FO|	|FC|
13	2	23	17
13	-2	26	40
13	-4	15	19
14	-1	96	94
14	-3	41	36

K=10

H	L	|FO|	|FC|
-8	10	41	51
-7	9	23	27
-7	11	54	56
-6	10	28	43
-5	7	18	27
-5	9	58	52
-5	11	50	53
-4	6	102	101
-4	8	74	81
-4	10	76	80
-4	12	65	53
-3	5	91	95
-3	7	33	38
-3	9	22	35
-2	4	9	25
-2	8	41	39
-2	10	25	6
-1	3	90	91
-1	7	26	37
-1	9	36	31
-1	11	16	25
0	0	21	11
0	4	26	27
0	6	24	24
0	8	52	62
0	10	30	22
0	12	72	74
1	1	11	12
1	-1	82	78
1	3	54	58
1	5	33	29
1	7	60	66
1	9	17	27
1	11	45	42
2	0	19	14
2	2	18	23
2	-2	23	26
2	4	33	35
2	6	34	35
3	1	105	100
3	-1	24	32
3	3	39	45
3	-3	64	64
3	5	75	73
3	7	32	10
3	9	42	43
3	11	21	15
4	0	39	34
4	4	25	24
4	-4	139	144
4	6	37	33
4	8	32	29
5	1	59	69
5	-1	30	19
5	3	3	7
5	-3	52	59
5	5	9	23
6	0	22	5
6	2	31	21
6	-2	32	34
6	-4	62	64
6	6	49	47
6	8	25	28
7	1	27	14
7	-1	80	83
7	3	51	53
7	-5	18	30
7	7	28	12
7	-7	60	59
7	9	33	39
8	0	135	131
8	2	78	77
8	-2	72	68
8	4	38	44
8	-4	66	75
8	6	40	40
8	-6	88	84
8	8	25	17
8	-8	94	98
9	1	51	49

H	L	|FC|	|FC|
9	-1	40	38
9	3	5	28
9	-3	46	46
9	5	43	44
9	-5	28	32
9	7	18	17
9	-7	45	48
9	-3	32	27
10	2	4	2
10	-2	35	21
10	-8	22	29
11	1	52	46
11	-1	31	19
11	3	36	38
11	-3	60	62
11	5	18	8
11	-5	67	75
11	-7	24	13
12	0	86	38
12	2	34	37
12	-2	60	58
12	4	51	51
12	-4	79	77
12	-6	57	70
13	1	50	60
13	-1	47	42
13	-3	24	33
13	-5	74	69

K=11

H	L	|FC|	|FC|
-8	9	90	94
-7	8	24	23
-6	7	44	47
-6	9	15	30
-6	11	74	71
-5	6	53	67
-5	8	18	10
-5	10	29	15
-4	5	62	53
-4	7	83	33
-4	9	59	58
-3	4	128	129
-3	6	71	72
-3	8	46	47
-3	10	47	43
-3	12	25	29
-2	3	60	54
-2	5	7	31
-2	11	44	31
-1	2	35	46
-1	4	42	40
-1	6	13	17
-1	8	18	16
-1	10	19	12
-1	12	36	33
0	1	70	65
0	3	79	90
0	5	25	34
0	7	31	35
0	9	54	45
0	11	86	85
1	0	17	11
1	4	24	20
1	6	17	27
1	10	36	27
2	1	31	27
2	3	13	2
2	5	36	24
2	7	56	57
2	9	37	24
2	11	28	37
3	0	31	32
3	2	58	49
3	-2	18	10
3	4	17	22
3	8	41	47
4	1	19	36
4	-1	51	55
4	3	46	41
4	-3	131	132
4	5	26	34
4	7	14	4
4	9	21	9
4	11	25	16
5	0	19	14
5	2	11	25
5	-2	35	39

H	L	|FO|	|FC|
5	4	12	25
5	-4	14	22
5	6	17	28
5	8	23	20
6	1	41	40
6	-1	19	20
6	3	22	19
6	-3	6	10
6	-5	31	40
6	7	31	28
6	9	17	11
7	0	101	107
7	2	72	69
7	4	51	50
7	-4	32	35
7	6	25	19
7	-6	55	55
8	1	116	113
8	-1	24	33
8	3	55	54
8	-3	35	29
8	5	34	34
8	-5	96	93
8	-7	21	20
9	2	41	36
9	-2	45	55
9	4	25	22
9	-4	27	26
9	6	49	48
9	-6	30	30
9	-8	50	68
10	1	27	22
10	-1	38	47
10	3	17	22
10	-3	77	78
10	-5	48	36
10	-7	41	38
10	-9	51	52
11	0	25	39
11	-2	18	21
11	4	20	19
11	-4	40	44
11	-6	44	39
11	-8	42	45
12	1	42	34
12	-1	72	73
12	3	38	39
12	-3	91	92
12	-5	30	30
12	-7	100	101
13	0	47	33
13	2	26	13
13	-2	36	32
13	-4	35	43

K=12

H	L	|FO|	|FC|
-8	10	30	19
-7	9	22	48
-6	8	111	112
-6	10	98	83
-5	7	52	54
-5	9	27	25
-5	11	39	83
-4	6	34	91
-4	8	21	33
-4	10	129	130
-3	5	221	228
-3	7	55	53
-3	9	62	75
-3	11	17	24
-2	4	35	42
-2	6	121	121
-2	8	60	68
-1	3	255	251
-1	5	93	95
-1	7	37	42
-1	9	119	121
-1	11	21	24
0	0	47	37
0	2	305	301
0	4	121	121
0	6	39	40
0	8	134	190
0	10	29	12
1	1	49	46
1	-1	64	58
1	3	160	155

H	L	|FC|	|FC|
1	5	103	101
1	7	130	128
1	9	9	46
1	11	32	39
2	0	100	104
2	2	125	121
2	-2	213	209
2	4	243	236
2	6	57	51
2	8	82	85
2	10	111	111
3	1	209	205
3	-1	49	46
3	3	35	34
3	-3	109	104
3	5	34	45
3	7	101	102
3	9	15	30
3	11	135	137
4	0	202	196
4	2	105	104
4	-2	11	8
4	4	8	26
4	-4	112	114
4	6	217	220
4	8	54	49
4	10	94	95
5	1	131	124
5	-1	210	203
5	3	87	83
5	-3	100	98
5	5	163	162
5	-5	173	180
5	7	21	17
5	9	31	29
6	0	13	21
6	2	231	227
6	-2	32	33
6	-4	213	211
6	6	121	115
6	-6	17	9
6	8	117	116
7	1	38	40
7	-1	157	153
7	3	148	145
7	-3	61	64
7	5	86	86
7	-5	54	48
7	7	12	24
7	-7	42	52
7	9	136	129
8	0	51	51
8	2	96	87
8	-2	175	178
8	4	106	103
8	-4	66	67
8	6	43	32
8	-6	72	82
8	8	83	89
8	-8	127	120
9	1	31	36
9	-1	51	50
9	3	154	149
9	-3	120	125
9	5	51	52
9	-5	44	38
9	7	108	110
9	-7	37	42
9	-9	35	37
10	0	146	149
10	2	19	17
10	-2	47	53
10	4	94	92
10	-4	47	49
10	6	73	79
10	-6	110	110
10	-8	28	23
11	1	45	50
11	-1	83	68
11	-3	35	46
11	5	37	42
11	-5	65	53
11	-7	88	97
12	0	113	113
12	2	73	72
12	-2	26	23
12	-4	69	76
13	1	83	82

H	L	|FO|	|FC|
13	-3	35	23

K=13

H	L	|FO|	|FC|
-8	9	8	20
-7	8	65	65
-7	10	58	69
-6	7	43	47
-6	9	78	83
-5	6	21	38
-5	8	31	25
-4	5	5	19
-4	7	10	18
-4	9	64	62
-4	11	38	38
-3	4	29	23
-3	6	58	63
-3	8	55	57
-3	10	31	19
-2	3	71	72
-2	5	91	95
-2	7	47	50
-2	9	53	53
-2	11	22	41
-1	2	31	35
-1	4	9	6
-1	6	18	26
-1	8	31	31
-1	10	33	30
0	1	65	61
0	3	51	48
0	5	55	53
0	7	24	41
0	11	35	39
1	0	66	65
1	2	79	88
1	4	67	65
1	6	29	33
1	10	70	60
2	1	59	57
2	-1	66	69
2	3	34	30
2	5	17	18
2	9	56	55
2	11	45	29
3	0	27	23
3	2	17	27
3	-2	55	49
3	4	70	71
3	6	57	69
3	8	12	10
3	10	22	9
4	1	25	17
4	-1	42	43
4	3	75	75
4	-3	22	27
4	7	21	30
4	9	6	16
5	2	6	15
5	-2	21	12
5	4	13	6
5	-4	21	7
5	6	34	38
5	8	41	42
6	1	89	90
6	3	39	33
6	-3	36	40
6	5	29	37
6	-5	79	82
6	9	23	23
7	0	64	59
7	2	52	53
7	-2	40	43
7	4	38	17
7	-4	81	85
7	5	11	8
7	-6	33	20
7	8	22	23
8	1	14	27
8	-1	53	51
8	3	46	43
8	-3	70	73
8	5	24	19
8	-5	27	27
8	7	38	23
9	0	19	23
9	2	42	42
9	-2	50	39

H	L	|FO|	|FC|
9	-4	7	5
9	-4	7	9
9	-6	22	23
9	-8	31	31
10	1	74	69
10	-1	114	110
10	3	10	4
10	-3	6	35
10	-5	50	53
10	-5	98	93
10	-7	79	84
11	0	38	46
11	-2	58	59
11	-4	47	53
11	-4	43	43
11	-6	53	54
12	1	26	28
12	-1	24	23
12	3	19	17
12	-3	33	37
12	-5	48	54
13	-2	50	51

K=14

H	L	|FO|	|FC|
-7	9	38	24
-6	8	115	113
-6	10	46	45
-5	9	15	29
-4	8	22	7
-4	10	54	38
-3	5	64	64
-3	7	22	37
-3	9	75	77
-3	11	41	49
-2	4	21	29
-2	6	77	82
-2	8	56	57
-2	10	28	23
-1	3	9	10
-1	5	71	71
-1	7	31	6
-1	9	25	35
0	2	21	7
0	4	34	31
0	6	56	56
0	8	26	30
0	10	44	43
1	-1	38	41
1	-3	86	85
1	1	58	57
1	3	27	36
1	5	20	32
1	7	9	21
1	9	20	11
2	0	45	42
2	2	38	26
2	-2	42	42
2	4	39	43
2	6	27	21
2	8	29	33
3	-1	23	16
3	1	54	38
3	-3	65	60
3	3	62	58
3	5	35	5
3	7	57	56
4	0	29	29
4	2	20	31
4	-2	25	31
4	4	25	30
4	6	18	24
4	8	24	27
5	-1	40	36
5	1	22	28
5	-3	20	33
5	3	36	36
5	-5	34	35
5	5	27	15
5	-7	34	38
5	7	18	29
5	9	37	41
5	9	89	92
5	-2	51	54
5	2	24	11
5	-4	118	114
5	4	28	36
5	-6	38	43

H	L	|FO|	|FC|
6	8	12	30
6	1	35	26
6	-1	78	73
6	3	58	65
6	-3	55	61
6	5	23	37
6	-5	23	18
6	7	22	20
6	-7	36	42
7	0	48	39
7	-2	56	56
7	2	23	22
7	-4	48	36
7	4	21	25
7	-6	39	38
7	6	7	20
7	-8	45	39
8	1	32	22
8	-1	41	48
8	3	23	21
8	-3	21	20
8	5	18	30
8	-5	25	21
8	7	65	62
9	0	33	18
9	-2	39	19
9	2	50	58
9	-4	60	58

K=15

H	L	|FO|	|FC|
-8	9	35	31
-7	8	11	22
-6	7	96	94
-5	6	92	91
-5	8	58	67
-5	10	112	107
-4	5	26	27
-4	7	87	88
-4	9	20	9
-3	4	53	54
-3	6	142	143
-3	8	42	52
-3	10	17	32
-2	3	176	176
-2	5	133	127
-2	7	205	207
-2	9	79	78
-1	2	71	67
-1	4	137	139
-1	6	87	84
-1	8	79	77
-1	10	24	28
0	1	65	65
0	3	152	148
0	5	43	48
0	7	46	46
1	0	161	152
1	2	226	220
1	4	30	12
1	6	55	51
1	8	59	61
1	10	33	22
2	-1	172	167
2	1	214	209
2	-3	179	182
2	3	158	157
2	-5	111	107
2	5	137	132
3	-2	83	79
3	2	121	118
3	-4	174	174
3	4	104	106
3	-6	124	124
3	6	54	57
3	-8	17	17
4	-1	46	31
4	1	45	50
4	-3	48	54

H	L	|FO|	|FC|
4	7	70	70
5	0	143	138
5	-2	73	71
5	2	62	61
5	-4	54	56
5	4	67	72
5	-6	61	59
5	6	34	42
6	1	235	228
6	-1	33	91
6	3	138	132
6	-3	206	206
6	5	114	126
6	-5	58	58
6	7	190	186
7	0	42	46
7	2	53	60
7	-2	172	171
7	4	124	129
7	-4	72	67
7	6	62	66
7	-6	104	109
7	8	52	33
8	1	21	28
8	-1	75	66
8	3	82	81
8	-3	65	57
8	5	32	24
8	-5	35	38
8	7	30	26
8	-7	53	44
9	0	143	141
9	2	53	56
9	-2	44	46
9	4	21	19
9	-4	67	67
9	6	73	76
9	-6	57	54
9	8	111	102
10	-1	85	87
10	1	46	39
10	-3	83	73
10	3	144	147
10	-5	58	62
10	-7	62	72
11	2	115	111
11	-2	44	39
11	4	90	96
11	-6	43	43
12	1	64	68
12	-1	16	4
12	3	49	26

K=16

H	L	|FO|	|FC|
-7	9	25	8
-6	8	28	30
-5	7	50	61
-5	9	32	36
-4	6	22	19
-4	8	68	63
-4	10	25	28
-3	5	33	38
-3	9	23	28
-2	4	61	67
-2	6	25	32
-2	8	56	61
-2	10	28	48
-1	3	115	116
-1	5	62	61
-1	7	77	77
-1	9	33	22
0	2	9	20
0	4	62	62
0	6	15	18
0	8	38	24
0	10	39	37
1	1	53	56
1	-1	50	57
1	5	23	21
1	7	38	26
1	9	33	40
2	0	66	64
2	2	33	42
2	-2	40	42
2	4	34	36
2	6	18	21
2	8	45	49

H	L	|FO|	|FC|
2	10	16	16
3	1	20	18
3	-1	23	4
3	3	24	23
3	-3	23	9
3	5	34	25
3	7	53	54
3	9	35	35
4	2	26	32
4	4	25	35
4	-4	13	10
4	6	25	9
4	8	28	29
5	1	88	82
5	-1	44	44
5	3	67	68
5	-3	59	61
5	5	61	63
5	-5	26	25
5	7	36	32
5	9	22	29
6	0	29	31
6	2	23	20
6	-2	45	47
6	4	39	44
6	-4	35	30
6	6	57	58
6	-6	62	65
6	8	24	27
7	1	29	34
7	-1	33	24
7	3	26	39
7	5	13	22
7	7	14	28
7	-7	18	14
8	0	37	84
8	-2	17	20
8	4	29	17
8	-4	78	77
8	-6	26	29
8	-8	15	25
9	1	41	41
9	-1	43	37
9	3	39	28
9	-3	78	70
9	5	12	19
9	-5	50	49
9	-7	66	58
10	0	25	24
10	2	59	58
10	-2	67	61
10	4	26	33
10	-4	82	87
10	-6	30	41
11	-1	18	29
11	3	22	24
11	-5	46	26
12	-2	44	49

K=17

H	L	|FO|	|FC|
-6	9	30	38
-5	8	88	93
-5	3	35	22
-4	5	22	14
-4	7	17	30
-4	9	21	4
-3	4	65	56
-3	6	31	38
-3	10	59	55
-2	3	20	5
-2	5	15	18
-2	7	47	54
-2	9	36	46
-1	2	63	58
-1	4	45	41
-1	6	18	18
-1	8	69	62
-1	10	53	51
0	3	56	60
0	5	32	20
0	7	29	35
1	0	86	94
1	2	35	28
1	4	52	50
1	6	39	34
1	8	42	54
1	10	12	33

H	L	|FO|	|FC|
2	1	34	40
2	-1	22	19
2	3	31	29
2	-3	20	16
2	5	32	8
2	-5	21	19
2	7	13	21
2	-7	54	55
2	8	44	40
2	-8	34	36
2	9	25	15
2	-9	50	51
2	10	30	22
2	-10	20	19
2	11	43	33
2	-11	71	69
3	0	67	71
3	-2	20	25
3	2	45	51
3	-4	42	34
3	4	17	23
3	-6	46	49
3	6	30	23
3	-8	68	71
3	8	15	11
3	-10	25	32
3	10	14	13
3	-12	31	29
4	1	25	36
4	-1	22	24
4	3	20	16
4	-3	35	38
4	5	114	110
4	-5	54	46
4	7	52	53
4	-7	22	30
4	9	54	44
4	-9	19	22
4	11	70	53

K=18

H	L	|FO|	|FC|
5	0	18	37
5	-2	7	22
5	2	44	31
5	-4	8	8
5	4	200	233
5	-6	38	47
5	6	81	75
5	-8	51	52
5	8	163	161
5	-10	42	38
5	10	78	74
5	-12	20	16
6	1	45	42
6	-1	60	63
6	3	56	51
6	-3	302	312
6	5	34	36
6	-5	125	127
6	7	181	182
6	-7	20	36
6	9	136	133
6	-9	20	4
6	11	54	53
7	-1	34	32
7	1	70	61
7	-3	24	25
7	3	155	163
7	-5	27	15
7	5	123	127
7	-7	115	108
7	7	28	36
7	-9	32	32
7	9	115	120
7	-11	41	31
8	0	80	78
8	-2	45	39

H	L	|FO|	|FC|
3	7	49	49
3	-7	30	26
4	2	181	178
4	-2	242	241
4	4	165	166
4	-4	84	85
4	6	27	24
4	-6	207	192
4	8	118	112
4	-8	48	55
4	10	97	96
4	-10	57	65
4	12	32	27
5	-1	32	29
5	1	84	80
5	-3	97	96
5	3	44	42
5	-5	99	96
5	5	67	65
5	-7	32	27
5	7	46	33
5	-9	32	29
5	9	84	80
5	-11	97	96
5	11	145	145
6	-2	35	38
6	2	14	24
6	-4	117	116
6	4	78	80
6	-6	53	53
6	6	41	45
6	-8	23	33
6	8	187	181
6	-10	116	108
6	10	10	17
6	-12	19	15
7	-1	122	114
7	1	10	13
7	-3	13	25
7	3	36	33
7	-5	31	26
7	5	41	45
7	-7	20	29
7	7	62	55
7	-9	155	135
7	9	21	18
7	-11	88	91
7	11	71	84

K=19

H	L	|FO|	|FC|
6	7	36	25
6	-7	56	52
6	9	53	56
6	-9	49	53
6	11	32	30
6	-11	57	58
7	0	70	56
7	-2	33	33
7	2	31	22
7	-4	38	35
7	4	33	11
7	-6	31	16
7	6	42	32
7	-8	51	51
7	8	40	41
7	-10	77	77
7	10	46	44
7	-12	23	24
8	-1	42	37
8	1	27	31
8	-3	37	30
8	3	47	44
8	-5	59	55
8	5	27	26
8	-7	58	58
8	7	53	53
8	-9	39	33
8	9	16	20
8	-11	52	57
8	11	42	50
9	-2	33	35
9	2	31	26
9	-4	42	38
9	4	22	22
9	-6	58	61
9	6	44	42
9	-8	59	58
9	8	28	22
9	-10	23	20
9	10	38	42
10	-1	73	76

H	L	|FO|	|FC|
5	-2	51	51
5	4	33	30
5	-4	32	38
5	6	59	46
6	1	24	20
6	-1	21	18
6	3	32	24
6	-3	17	13
6	5	25	21
6	-5	18	12
7	0	34	32
7	-2	55	61
7	2	54	59
7	-4	46	33
7	4	4	12
7	-6	55	61
7	6	59	65
8	-1	16	22
8	1	55	58
8	-3	31	29
8	3	82	71
8	-5	44	43
8	5	43	45
8	-7	83	80
9	1	31	30
9	-2	11	21
9	2	53	49
9	-4	56	59
9	4	41	37
10	-1	30	24
10	-3	22	26

K=20

H	L	|FO|	|FC|
5	7	53	46
5	-7	81	78
5	8	31	29
5	-8	19	19
6	4	26	29
6	-4	12	16
6	6	33	32
6	-6	43	49
6	8	29	32
6	-8	17	17
6	10	45	45
6	-10	44	44
6	12	27	31
7	-5	44	37
7	5	65	59
7	-7	31	16
7	7	58	62
7	-9	29	28
7	9	28	18
7	-11	55	56
7	11	35	40
8	-2	5	24
8	2	23	26
8	-4	29	22
8	4	15	25
8	-6	13	22
8	6	31	36
8	-8	60	63
8	8	47	50
8	-10	37	27
8	10	51	54
8	-12	21	16
9	-1	36	33
9	1	42	38
9	-3	37	30
9	3	12	30
9	-5	25	25
9	5	42	46
9	-7	35	33
9	7	35	33
9	-9	14	22
9	9	29	14
9	-11	52	52
9	11	38	55
10	-2	26	33
10	2	53	56
10	-4	34	35
10	4	32	33
10	-6	33	46
10	6	22	22
10	-8	33	59
10	8	20	18
10	-10	54	36
10	10	105	112

H	L	|FO|	|FC|
8	-6	41	48
9	1	31	29
9	-1	17	19
9	3	45	22

K=21

H	L	|FO|	|FC|
6	7	36	27
6	-7	92	91
6	9	155	152
6	-9	12	11
6	11	40	41
7	-8	8	27
7	8	24	26
7	-10	25	35
7	10	130	131
7	-12	103	95
8	1	98	93
8	-1	109	115
8	3	79	75
8	-3	162	163
8	5	131	121
8	-5	15	23
8	7	175	175
8	-7	55	58
8	9	54	61
8	-9	56	55
8	11	21	24
9	-2	131	134
9	2	72	78
9	-4	85	95
9	4	33	33
9	-6	74	66
9	6	79	69
9	-8	33	32
9	8	41	49
9	-10	141	139
9	10	141	144
9	-12	110	109
10	-1	68	63
10	1	174	168
10	-3	146	147
10	3	38	33
10	-5	59	53
10	5	36	31
10	-7	127	115
10	7	93	92
10	-9	29	13
10	9	39	24
10	-11	27	42
10	11	100	103
11	-2	36	37
11	2	19	21
11	-4	47	35
11	4	111	110
11	-6	89	88
11	6	52	68
11	-8	64	47
11	8	68	68
11	-10	158	155
11	10	106	105
11	-12	17	16
12	-1	21	13
12	1	77	79

K=22

H	L	|FO|	|FC|
6	6	37	37
6	-6	49	27
6	8	68	72
6	-8	20	6
6	10	35	32
6	-10	70	65
6	12	20	12
7	-7	17	28
7	7	21	25
7	-9	23	30
7	9	23	7
7	-11	30	20
7	11	24	25
8	-6	19	14
8	6	42	49
8	-8	56	51
8	8	60	57
8	-10	34	26
8	10	32	29
8	-12	41	22

H	L	|FC|	|FC|
2	5	21	15
3	1	71	73
3	-1	87	79
3	3	53	42
3	-3	62	54
3	5	24	26
4	0	21	21
4	-2	16	31
4	4	24	27
4	-4	12	24
5	1	10	23
5	-1	30	32
5	3	21	24
5	-3	18	16
5	5	15	11
5	-5	32	37
6	0	42	43
6	2	26	30
6	-2	52	56
6	4	31	24
6	-4	74	77
6	6	20	31
7	1	46	51
7	-1	30	35
7	3	70	78
7	-3	51	59
8	0	27	32
8	-2	30	28

K=23

H	L	|FO|	|FC|
-4	5	73	61
-3	4	39	34
-3	6	63	52
-1	2	33	32
-1	4	31	7
-1	6	39	35
0	1	31	29
0	3	32	13
1	2	32	25
1	4	58	57
1	6	57	51
2	1	40	33
2	3	41	45
2	5	33	20
2	7	11	12
3	0	68	79
3	2	48	43
3	-2	48	47
3	4	35	31
4	1	39	46
4	-1	20	25
4	3	17	21
4	-3	29	34
5	2	24	35
5	4	31	14
5	-2	31	34
5	4	31	30
5	-4	21	38

H	L	|FC|	|FC|
6	3	6	21
6	-3	57	52
6	-5	42	37
7	2	51	53
7	-2	64	65

K=24

H	L	|FC|	|FC|
-3	5	92	80
-2	4	84	87
-1	3	65	74
-1	5	69	64
0	0	40	39
0	2	39	41
0	4	21	28
1	1	35	32
1	-1	81	82
1	3	44	42
1	5	101	108
2	0	154	152
2	2	73	80
2	-2	124	126
2	4	148	150
3	1	107	110
3	-1	47	55
3	3	92	99
3	-3	35	42
4	0	33	34
4	2	34	29
4	-2	12	11

H	L	|FO|	|FC|
4	4	21	40
4	-4	19	22
5	1	25	26
5	-1	52	59
5	3	82	88
5	-3	128	132
6	0	53	56
6	2	107	100
6	-2	84	80

K=25

H	L	|FO|	|FC|
-2	3	32	48
-1	2	38	30
-1	4	12	28
0	1	18	18
0	3	27	38
1	0	52	49
1	2	72	68
1	4	33	34
2	1	25	2
2	3	9	25
3	0	26	31
3	2	60	59
3	-2	29	23
3	4	32	35
4	-1	31	32
4	-3	35	31
5	0	26	27
5	-2	75	72

A.6 $(VO)_2P_2O_7$

H	L	|Fo|	|Fc|
	K = 0		
0	2	23	17
0	4	37	30
0	6	48	40
0	8	115	121
0	10	46	42
0	12	363	392
0	14	29	33
0	16	39	39
0	18	27	29
0	20	153	141
0	22	29	24
0	24	72	63
1	0	20	6
1	2	82	82
1	4	16	15
1	6	200	230
1	8	21	22
1	10	240	251
1	12	18	25
1	14	124	136
1	16	12	10
1	18	34	42
1	20	10	17
1	22	120	110
1	24	21	18
2	0	141	157
2	2	19	16
2	4	390	460
2	6	28	33
2	8	108	116
2	10	34	36
2	12	45	55
2	14	30	32
2	16	240	243
2	18	24	23
2	20	52	45
2	22	15	25
2	24	63	61
3	0	14	15
3	2	283	332
3	4	25	32
3	6	326	339
3	8	32	44
3	10	255	276
3	12	26	40
3	14	19	36
3	16	23	38
3	18	43	34
3	20	26	29
3	22	105	106
3	24	21	28
4	0	144	171
4	2	26	27
4	4	175	182
4	6	17	19
4	8	86	96
4	10	18	22
4	12	79	83
4	14	26	22
4	16	160	161
4	18	11	22
4	20	132	132
4	24	20	7
5	0	29	29
5	2	67	64
5	4	15	23
5	6	375	417
5	8	30	33
5	10	58	60
5	12	38	43
5	14	147	150
5	18	121	121
5	20	28	28
5	22	23	30
6	0	320	346
6	2	12	22
6	4	129	133
6	6	28	22
6	8	10	8
6	10	18	6
6	12	160	160
6	14	13	14
6	16	101	91
6	22	14	7
7	0	42	46
7	2	173	183
7	4	15	16
7	6	54	58
7	8	17	17
7	10	256	264
7	12	20	28
7	14	20	21
7	16	32	27
7	18	61	64
8	0	175	178
8	2	27	30
8	4	161	171
8	6	9	15
8	8	62	72
8	10	27	33
8	14	20	23
8	16	111	118
8	18	9	15
8	20	27	22
9	0	18	18
9	2	20	22
9	4	33	35
9	6	171	174
9	8	21	18
9	10	83	72
9	12	17	7
9	14	80	77
9	16	27	21
9	18	63	50
10	0	146	149
10	2	18	16
10	4	12	5
10	6	38	35
10	8	99	102
10	10	24	17
10	12	90	90
10	14	15	30
10	16	63	54
10	18	25	32
11	0	31	42
11	2	49	49
11	6	152	144
11	8	8	5
11	10	73	63
11	12	24	22
11	14	39	22
12	0	19	20
12	4	149	147
12	6	23	26
12	8	58	61
12	10	25	25
12	12	26	32
13	0	26	25
13	2	51	50
13	4	13	26
13	6	34	24
13	8	11	18
13	10	99	93
14	0	164	159
14	2	32	31
	K = 1		
1	1	75	11
1	2	8	16
1	3	73	19
1	4	9	14
1	5	70	10
1	6	7	5
1	7	86	33
1	8	11	12
1	9	19	18
1	10	8	8
1	11	50	29
1	13	14	24
1	15	25	23
1	16	4	4
1	17	22	13
1	18	12	2
1	19	22	28
1	21	8	14
1	23	17	25
1	24	14	5
2	1	41	16
2	2	15	16
2	3	43	24
2	4	14	3
2	5	23	22
2	6	6	9
2	7	6	9
2	8	6	14
2	9	49	21
2	10	9	12
2	11	27	12
2	12	4	8
2	13	20	19
2	14	3	7
2	15	4	11
2	16	5	2
2	17	7	22
2	21	17	28
2	22	16	7
2	24	25	5
3	1	52	25
3	2	21	21
3	3	51	14
3	4	12	24
3	5	45	37
3	6	19	11
3	7	21	12
3	8	19	20
3	9	8	10
3	11	38	29
3	12	18	33
3	13	12	17
3	14	5	8
3	15	13	13
3	22	13	4
3	24	28	6
4	0	16	13
4	1	40	23
4	2	26	32
4	3	50	24
4	4	8	25
4	5	80	41
4	7	40	18
4	8	5	18
4	9	42	22
4	10	16	10
4	11	20	23
4	12	13	9
4	13	23	19
4	14	11	15
4	15	26	12
4	16	12	4
4	17	32	32
4	18	15	9
4	22	17	4
4	23	10	18
5	0	6	12
5	1	42	24
5	2	16	21
5	3	12	29
5	4	7	22
5	5	11	9
5	6	29	15
5	7	14	24
5	8	12	25
5	9	26	28
5	10	14	7
5	11	28	19
5	12	10	12
5	13	4	8
5	14	12	12
5	15	15	22
5	16	6	12
5	18	20	11
5	20	9	10
5	21	12	17
5	22	10	2
5	23	19	11
6	0	28	14
6	1	81	39
6	2	16	32
6	3	34	27
6	4	19	22
6	5	33	20
6	6	23	16
6	7	21	33
6	8	15	15
6	9	38	37
6	10	9	14
6	11	41	22
6	12	20	12
6	13	37	33
6	15	13	19
6	18	23	11
6	21	8	26
6	22	30	6
7	1	5	25
7	2	9	23
7	3	10	21
7	4	26	22
7	5	41	24
7	6	13	15
7	7	36	33
7	8	22	20
7	9	7	21
7	10	25	15
7	11	6	15
7	12	9	14
7	14	21	11
7	15	20	17
7	17	6	13
7	19	24	18
8	0	24	20
8	1	21	31
8	2	24	21
8	3	20	27
8	4	21	10
8	5	42	29
8	6	13	14
8	7	19	23
8	8	20	16
8	9	20	16
8	10	14	13
8	12	10	11
8	14	20	13
8	15	25	17
8	17	31	27
8	18	6	14
8	19	13	20
9	1	30	30
9	2	17	17
9	3	34	27
9	4	18	15
9	5	25	30
9	6	23	16
9	7	6	17
9	8	28	19
9	9	23	24
9	10	2	11
9	11	25	40
9	12	10	13
9	13	8	19

H	L	|FO|	|FC|
9	14	18	10
9	16	13	6
9	18	14	10
9	19	25	11
10	0	19	16
10	1	12	18
10	2	29	17
10	3	22	32
10	4	13	16
10	5	17	25
10	6	16	8
10	7	20	24
10	8	25	12
10	10	21	8
10	11	21	6
10	13	18	23
10	14	27	12
10	15	18	27
10	17	8	9
10	18	17	10
11	1	20	18
11	2	10	10
11	3	24	33
11	5	12	24
11	6	34	14
11	7	30	27
11	8	29	14
11	9	10	20
11	10	14	12
11	12	6	8
11	13	14	25
11	14	23	5
11	15	18	36
11	16	12	7
12	1	8	32
12	2	20	11
12	4	30	15
12	6	24	7
12	7	13	19
12	8	26	6
12	9	17	15
12	11	4	28
12	13	12	2
13	0	23	2
13	2	39	9
13	3	15	14
13	4	26	8
13	7	13	28
13	8	33	7
13	9	7	16
13	10	26	12
14	1	16	15
14	2	13	6
14	3	17	25
14	5	15	19
14	6	45	16

K = 2

H	L	|FO|	|FC|
0	0	440	518
0	1	70	68
0	2	13	14
0	3	94	102
0	4	28	26
0	5	16	17
0	6	17	20
0	7	75	79
0	8	75	84
0	9	65	64
0	10	6	7
0	12	243	232
0	13	68	65
0	14	18	20
0	15	23	26
0	16	35	36
0	17	25	34
0	18	24	19
0	19	44	42
0	20	110	100
0	21	18	15
0	22	20	20
0	23	33	28
0	24	51	42
1	0	5	20
1	1	65	65
1	2	25	36
1	3	95	106

H	L	|FO|	|FC|
1	4	3	8
1	5	14	26
1	6	6	28
1	7	70	80
1	8	13	5
1	9	58	62
1	10	129	131
1	11	19	20
1	12	8	3
1	13	61	61
1	14	89	90
1	15	23	24
1	16	5	3
1	17	30	27
1	18	15	12
1	19	39	40
1	20	12	10
1	21	13	8
1	22	71	63
1	23	31	31
1	24	14	9
2	0	21	35
2	1	50	61
2	2	18	10
2	3	92	103
2	4	176	195
2	5	14	26
2	6	13	8
2	7	69	72
2	8	50	51
2	9	58	59
2	10	16	10
2	11	26	21
2	12	32	27
2	13	56	58
2	14	15	9
2	15	30	29
2	16	152	152
2	17	32	32
2	18	31	17
2	19	40	38
2	20	32	35
2	22	30	18
2	23	35	31
2	24	60	57
3	0	15	2
3	2	42	46
3	3	112	108
3	4	92	90
3	5	6	12
3	6	18	19
3	7	215	197
3	8	70	71
3	9	12	2
3	10	59	62
3	11	126	134
3	12	20	29
3	13	9	11
3	14	47	51
3	15	16	23
3	16	25	25
3	17	15	11
3	18	33	32
3	19	17	23
3	22	40	38
3	23	55	57
3	24	42	34
4	0	31	23
4	1	9	25
4	2	41	53
4	3	20	33
4	4	82	86
4	5	87	91
4	6	5	14
4	7	10	1
4	8	64	61
4	9	79	77
4	10	53	57
4	12	8	1
4	13	26	31
4	14	52	51
4	15	13	19
4	16	24	24
4	17	95	84
4	19	31	31
4	20	29	37
4	23	102	100

H	L	|FO|	|FC|
5	1	47	49
5	2	34	38
5	3	69	72
5	4	12	11
5	6	234	232
5	7	53	57
5	8	12	12
5	9	44	48
5	10	18	15
5	11	12	17
5	12	8	6
5	13	56	53
5	14	116	116
5	15	25	19
5	16	14	15
5	17	25	23
5	19	47	34
5	20	26	23
5	22	20	27
5	23	28	28
6	0	198	186
6	1	49	49
6	3	64	60
6	4	92	89
6	5	18	8
6	6	29	19
6	7	50	50
6	8	19	20
6	9	44	40
6	10	21	8
6	11	7	15
6	12	99	85
6	13	53	53
6	15	27	20
6	17	19	26
6	18	27	16
6	19	28	34
6	20	52	47
6	22	20	5
7	0	17	13
7	1	34	37
7	2	111	119
7	3	57	58
7	4	11	12
7	5	18	15
7	6	63	65
7	7	40	47
7	8	17	13
7	9	45	42
7	10	200	192
7	11	14	14
7	12	22	15
7	13	44	42
7	14	11	4
7	15	22	16
7	16	23	17
7	17	28	22
7	18	75	73
7	20	10	12
8	0	151	138
8	1	18	26
8	3	56	56
8	4	98	102
8	6	12	5
8	7	37	36
8	8	32	36
8	9	38	36
8	10	8	7
8	11	18	16
8	12	66	61
8	13	38	34
8	14	6	12
8	15	28	24
8	16	79	79
8	17	34	29
8	18	4	5
8	19	30	27
8	20	38	23
9	0	19	3
9	1	23	16
9	2	11	25
9	3	45	47
9	4	15	9
9	6	134	129
9	7	43	38
9	8	2	15
9	9	29	35
9	10	57	42

H	L	|FO|	|FC|
9	11	19	21
9	13	30	31
9	14	68	76
9	15	27	20
9	16	3	12
9	17	26	20
9	18	43	46
9	19	40	26
10	0	108	104
10	1	25	29
10	3	33	39
10	4	9	18
10	5	18	12
10	7	40	37
10	8	73	79
10	9	22	24
10	12	64	70
10	13	34	32
10	14	22	27
10	15	16	17
10	16	54	38
10	17	23	18
11	0	12	4
11	1	24	22
11	2	40	42
11	3	39	28
11	5	18	16
11	6	128	114
11	7	37	37
11	9	24	25
11	10	64	60
11	11	5	12
11	13	26	32
11	14	15	21
11	15	17	12
12	0	21	9
12	1	29	26
12	2	22	13
12	3	35	32
12	4	128	123
12	6	12	14
12	7	38	22
12	8	47	60
12	9	24	22
12	10	13	15
12	12	29	30
12	13	28	31
13	1	30	15
13	3	24	32
13	5	12	8
13	6	44	28
13	7	12	19
13	8	14	18
13	9	36	30
13	10	88	82
14	0	149	135
14	1	9	18
14	2	14	13
14	3	21	30
14	4	15	23

K = 3

H	L	|FO|	|FC|
1	0	18	11
1	1	74	32
1	2	3	5
1	3	42	25
1	4	9	11
1	5	109	59
1	6	15	14
1	7	78	56
1	8	10	6
1	9	62	17
1	11	89	54
1	12	16	7
1	13	47	15
1	14	4	12
1	15	60	29
1	16	16	9
1	17	39	16
1	18	9	8
1	19	57	33
1	21	27	6
1	22	14	5
1	23	58	38
1	24	21	6
2	1	33	43
2	2	2	13

H	L	|FO|	|FC|
2	3	61	45
2	4	4	5
2	5	24	20
2	6	6	17
2	7	29	25
2	9	61	41
2	10	8	7
2	11	46	25
2	13	26	9
2	14	10	8
2	15	23	16
2	16	8	7
2	17	7	13
2	18	23	9
2	19	22	16
2	21	32	27
2	22	20	6
2	23	14	12
3	0	15	20
3	1	34	29
3	2	15	3
3	3	45	21
3	4	10	19
3	5	37	29
3	6	22	11
3	7	46	21
3	8	14	10
3	9	41	8
3	10	12	8
3	11	36	15
3	12	16	12
3	13	41	28
3	14	11	7
3	15	49	19
3	16	16	11
3	17	24	16
3	19	51	19
3	20	14	9
3	21	26	5
3	22	11	5
3	23	23	16
4	1	47	23
4	2	12	23
4	3	49	25
4	4	19	11
4	5	42	35
4	6	23	7
4	7	59	39
4	8	11	8
4	9	57	28
4	10	18	20
4	11	44	14
4	12	11	10
4	13	62	32
4	14	10	10
4	15	33	7
4	16	8	7
4	17	34	25
4	18	22	9
4	19	25	17
4	20	16	7
4	21	44	24
4	22	24	6
5	1	16	16
5	2	12	5
5	3	52	46
5	4	9	16
5	5	38	21
5	6	19	6
5	7	34	26
5	8	3	16
5	9	30	28
5	10	18	11
5	11	10	15
5	12	11	13
5	13	5	14
5	14	11	11
5	15	27	27
5	17	30	13
5	18	6	9
5	19	11	10
5	22	12	10
6	0	31	19
6	1	72	57
6	2	8	17
6	3	65	40
6	5	75	36
6	6	16	23

H	L	|FO|	|FC|
6	7	47	6
6	8	13	2
6	9	60	41
6	10	13	22
6	11	66	39
6	12	18	13
6	13	56	36
6	15	42	19
6	17	77	47
6	18	20	11
6	19	35	15
6	20	8	6
6	21	53	29
7	0	14	26
7	2	11	15
7	3	29	24
7	4	21	29
7	5	19	10
7	6	11	12
7	7	19	24
7	8	17	20
7	9	22	14
7	10	5	12
7	11	16	9
7	13	7	7
7	14	21	7
7	16	13	16
7	19	21	7
8	0	4	6
8	1	66	41
8	2	9	11
8	3	25	13
8	4	16	8
8	5	53	36
8	6	11	21
8	7	52	32
8	8	24	15
8	9	28	9
8	10	21	17
8	11	42	15
8	12	4	8
8	13	63	39
8	14	5	10
8	15	23	7
8	17	48	31
8	18	21	9
8	19	30	22
9	1	45	34
9	2	20	12
9	3	37	26
9	4	9	17
9	5	28	27
9	7	38	23
9	8	8	11
9	9	32	18
9	10	12	10
9	11	21	26
9	12	23	17
9	13	32	32
9	14	11	10
9	15	30	20
9	17	25	17
10	0	12	10
10	1	16	13
10	2	25	12
10	3	33	27
10	4	21	17
10	9	38	24
10	11	22	9
10	12	17	11
10	15	22	19
10	17	7	10
11	1	31	11
11	2	17	12
11	3	66	45
11	5	36	24
11	6	16	9
11	7	36	21
11	9	52	29
11	10	8	10
11	11	43	18
11	12	8	11
11	13	25	14
11	14	14	12
11	15	61	39
12	1	27	29

H	L	|FO|	|FC|
12	2	11	12
12	4	32	14
12	6	23	10
12	8	21	16
12	9	18	12
13	1	62	28
13	4	29	14
13	5	36	22
13	6	30	10
13	7	36	37
13	8	15	7
14	1	24	14
14	0	28	8

K = 4

H	L	|FO|	|FC|
0	0	376	344
0	1	68	92
0	2	10	11
0	3	121	142
0	4	21	41
0	5	19	25
0	6	17	27
0	7	99	93
0	8	38	43
0	9	85	94
0	10	27	34
0	11	23	23
0	12	164	147
0	13	92	92
0	14	24	18
0	15	31	35
0	16	28	43
0	17	51	47
0	18	7	20
0	19	63	56
0	20	56	45
0	21	20	10
0	22	5	19
0	23	48	48
1	0	30	9
1	1	81	84
1	2	50	63
1	3	124	133
1	4	9	14
1	5	17	18
1	6	73	99
1	7	102	102
1	8	12	6
1	9	82	87
1	10	122	115
1	11	16	29
1	12	18	8
1	13	90	91
1	14	44	41
1	15	31	36
1	16	14	13
1	17	48	44
1	18	20	13
1	19	67	60
1	21	8	11
1	22	73	61
1	23	53	49
2	0	81	99
2	1	68	73
2	2	9	14
2	3	121	129
2	4	149	151
2	5	23	24
2	6	14	17
2	7	98	105
2	8	32	42
2	9	76	81
2	10	24	19
2	11	35	26
2	12	40	47
2	13	89	87
2	14	21	22
2	15	40	39
2	16	93	87
2	17	44	44
2	19	59	60
2	20	43	39
2	23	56	48
3	0	28	17
3	1	61	62
3	2	97	87
3	3	127	132

H	L	|FO|	|FC|
3	4	18	10
3	5	17	30
3	6	168	148
3	7	91	104
3	8	19	25
3	9	81	82
3	10	90	98
3	11	34	31
3	12	28	24
3	13	75	74
3	14	16	17
3	15	47	36
3	16	22	16
3	17	48	43
3	18	40	39
3	19	59	59
3	20	19	23
3	22	41	37
3	23	55	48
4	0	41	72
4	1	60	63
4	2	23	19
4	3	117	117
4	4	94	100
4	5	18	15
4	6	27	14
4	7	88	91
4	8	26	3
4	9	79	78
4	10	6	9
4	11	27	25
4	12	13	29
4	13	74	76
4	15	34	40
4	16	100	88
4	18	32	11
4	19	60	60
4	20	43	44
4	21	10	6
4	22	22	6
5	0	25	5
5	1	71	63
5	2	28	17
5	3	97	104
5	4	13	11
5	5	12	20
5	6	152	150
5	7	81	84
5	8	14	19
5	9	69	76
5	10	41	51
5	11	18	25
5	12	13	24
5	13	76	76
5	14	47	42
5	15	25	29
5	17	44	38
5	18	47	38
5	19	56	52
5	20	18	13
5	21	4	11
6	0	148	136
6	1	75	78
6	2	6	14
6	3	88	95
6	4	50	53
6	5	24	14
6	6	11	10
6	7	74	69
6	8	21	12
6	9	63	55
6	10	7	9
6	11	15	13
6	12	82	74
6	13	88	81
6	14	4	3
6	15	29	32
6	16	49	42
6	17	37	40
6	20	41	33
7	0	36	21
7	1	52	51
7	2	65	69
7	3	89	83
7	4	14	15
7	5	12	23
7	6	32	8
7	7	69	73

H	L	$\lvert F_O \rvert$	$\lvert F_C \rvert$
7	8	12	10
7	9	54	57
7	10	101	31
7	11	25	24
7	12	10	15
7	15	29	21
7	16	21	13
7	17	43	33
7	18	23	14
7	19	58	53
8	0	94	99
8	1	38	49
8	2	17	7
8	3	88	87
8	4	56	52
8	5	19	20
8	6	10	5
8	7	53	57
8	8	18	18
8	9	59	56
8	10	22	12
8	11	38	17
8	12	55	51
8	13	51	59
8	15	35	37
8	16	41	37
8	17	31	45
8	18	4	9
8	19	47	47
9	1	31	25
9	2	23	15
9	3	80	77
9	4	19	22
9	5	14	28
9	6	53	59
9	7	66	56
9	8	17	15
9	9	61	59
9	10	40	48
9	11	22	33
9	13	54	43
9	14	26	17
9	15	32	32
9	16	23	7
9	17	34	28
10	0	37	40
10	1	33	45
10	2	28	9
10	3	58	64
10	4	29	24
10	5	13	12
10	6	30	13
10	7	59	57
10	8	24	19
10	9	47	37
10	11	17	14
10	12	9	17
10	13	58	53
10	14	14	15
10	15	29	35
10	16	42	41
11	0	16	18
11	1	43	32
11	2	19	16
11	3	51	51
11	5	23	39
11	6	79	57
11	7	63	62
11	8	20	5
11	9	50	45
11	10	31	19
11	13	63	49
12	0	16	3
12	1	49	48
12	2	13	6
12	3	59	55
12	4	54	47
12	5	21	13
12	7	35	35
12	8	21	15
12	9	38	39
12	10	21	12
12	11	5	15
13	1	27	23
13	2	8	14
13	3	50	51
13	5	11	18
13	6	5	13

H	L	$\lvert F_O \rvert$	$\lvert F_C \rvert$
13	7	39	36

K = 5

H	L	$\lvert F_O \rvert$	$\lvert F_C \rvert$
1	0	2	4
1	1	97	64
1	2	13	13
1	3	67	59
1	4	7	1
1	5	120	88
1	6	13	15
1	7	129	91
1	8	9	8
1	9	50	36
1	10	15	9
1	11	98	73
1	12	14	11
1	13	36	24
1	14	10	8
1	15	56	43
1	16	10	3
1	17	57	38
1	18	11	9
1	19	63	44
1	20	20	7
1	21	34	21
1	22	13	6
2	1	31	25
2	2	15	15
2	3	64	50
2	4	6	21
2	5	25	9
2	7	29	32
2	8	7	19
2	9	76	60
2	10	4	8
2	11	30	28
2	12	4	9
2	13	25	12
2	14	17	4
2	15	18	9
2	18	9	7
2	19	28	29
2	21	45	29
3	0	4	2
3	1	69	39
3	2	10	15
3	3	71	47
3	4	7	11
3	5	43	35
3	6	18	27
3	7	45	21
3	8	11	16
3	9	40	27
3	10	13	5
3	11	52	26
3	12	22	11
3	13	33	25
3	15	43	29
3	16	13	3
3	17	20	17
3	19	47	21
3	20	9	9
3	21	23	10
3	22	12	7
4	0	27	39
4	1	63	39
4	2	11	19
4	3	60	54
4	4	15	19
4	5	100	62
4	6	12	9
4	7	72	48
4	8	15	19
4	9	75	54
4	10	3	5
4	11	23	21
4	12	17	26
4	13	49	39
4	15	45	25
4	16	15	4
4	17	54	36
4	19	31	22
4	20	15	13
4	21	44	28
5	1	70	7
5	2	13	32
5	3	41	35

H	L	$\lvert F_O \rvert$	$\lvert F_C \rvert$
5	5	32	31
5	6	8	12
5	7	22	15
5	9	16	5
5	10	13	24
5	11	38	20
5	15	39	28
5	18	15	12
5	19	4	5
6	0	30	31
6	1	135	69
6	3	67	48
6	4	20	31
6	5	75	59
6	6	11	12
6	7	38	71
6	8	12	21
6	9	75	50
6	11	83	60
6	13	77	57
6	15	27	21
6	16	11	19
6	17	52	50
6	19	21	12
6	20	12	5
7	0	23	3
7	1	3	11
7	3	35	23
7	4	4	17
7	5	50	20
7	6	12	25
7	7	41	19
7	9	22	10
7	12	5	11
7	14	22	18
7	15	38	21
7	17	28	13
7	18	17	14
7	19	27	10
8	0	12	28
8	1	46	43
8	2	14	24
8	3	40	23
8	4	11	25
8	5	82	48
8	7	44	34
8	8	3	31
8	9	29	25
8	10	5	12
8	11	18	22
8	13	52	35
8	15	33	19
8	16	12	19
8	17	55	37
9	1	57	38
9	2	19	23
9	3	57	42
9	4	13	12
9	5	35	29
9	6	14	44
9	7	36	16
9	9	38	28
9	11	50	23
9	13	39	32
9	15	42	28
10	1	27	6
10	2	15	20
10	3	30	15
10	5	34	17
10	6	16	5
10	9	42	22
10	13	24	7
10	14	15	12
11	0	27	7
11	1	37	25
11	2	7	27
11	3	63	44
11	5	52	32
11	6	16	19
11	7	53	73
11	9	23	26
11	10	9	32
11	11	34	27
11	12	3	8
12	1	53	29
12	4	13	31
12	5	13	9
12	6	20	6

H	L	$\lvert F_O \rvert$	$\lvert F_C \rvert$
12	7	11	9
12	8	18	22
13	0	12	5
13	1	50	34
13	2	4	22

K = 6

H	L	$\lvert F_O \rvert$	$\lvert F_C \rvert$
0	0	60	61
0	1	63	73
0	2	4	19
0	3	120	128
0	4	18	4
0	5	7	24
0	6	39	31
0	7	39	91
0	8	31	36
0	9	86	84
0	10	21	14
0	11	17	29
0	12	35	37
0	13	87	86
0	15	38	39
0	16	24	16
0	17	57	57
0	18	18	15
0	19	62	63
0	20	29	33
0	21	8	14
1	0	17	23
1	1	55	65
1	2	15	32
1	3	117	116
1	4	6	8
1	5	13	26
1	6	89	74
1	7	89	96
1	8	12	10
1	9	75	81
1	11	27	30
1	12	15	18
1	13	94	86
1	14	25	23
1	15	40	35
1	17	41	43
1	18	38	35
1	19	50	62
1	20	11	10
1	21	8	13
2	1	70	73
2	2	17	10
2	3	105	111
2	4	72	67
2	5	21	22
2	6	6	16
2	7	91	91
2	8	43	41
2	9	58	71
2	10	14	24
2	11	24	23
2	13	92	86
2	15	46	42
2	16	38	39
2	17	51	48
2	18	30	5
2	19	59	61
3	0	30	24
3	1	51	64
3	2	74	64
3	3	102	109
3	4	11	24
3	5	23	24
3	6	33	28
3	7	93	92
3	8	24	16
3	9	74	81
3	10	74	63
3	11	20	33
3	12	20	13
3	13	78	74
3	14	20	24
3	15	37	33
3	17	46	43
3	18	29	25
3	20	23	6
4	0	101	80
4	1	59	65
4	2	3	6

H	L	|FO|	|FC|
4	3	108	114
4	4	24	20
4	5	13	6
4	6	37	16
4	7	77	78
4	8	22	29
4	9	79	74
4	10	6	16
4	11	27	24
4	12	59	49
4	13	79	75
4	14	3	12
4	15	37	39
4	16	25	6
4	17	53	48
4	19	58	50
4	20	23	14
5	0	9	20
5	1	56	53
5	2	23	28
5	3	105	33
5	4	17	21
5	5	17	19
5	6	54	51
5	7	65	74
5	8	20	2
5	9	70	69
5	11	25	29
5	13	76	75
5	14	31	25
5	17	48	37
5	18	29	26
5	19	51	55
6	0	12	22
6	1	69	64
6	3	89	85
6	4	18	11
6	5	22	15
6	6	28	26
6	7	78	68
6	9	61	59
6	10	3	9
6	11	20	13
6	12	13	24
6	15	27	30
6	16	12	15
6	17	39	40
6	18	18	9
7	1	47	47
7	2	29	35
7	3	73	73
7	5	22	20
7	6	22	22
7	7	77	70
7	8	24	10
7	9	62	60
7	10	26	28
7	11	19	19
7	12	12	11
7	13	73	65
7	14	20	15
7	15	10	22
7	16	21	19
7	17	43	35
8	0	38	20
8	1	38	40
8	3	81	76
8	4	51	41
8	5	15	19
8	6	15	16
8	7	61	54
8	8	28	27
8	9	54	49
8	10	5	17
8	11	20	19
8	12	24	20
8	13	57	54
8	15	27	34
8	16	37	35
9	1	34	25
9	2	22	11
9	3	77	71
9	4	25	13
9	6	19	23
9	7	50	54
9	9	53	33
9	11	19	29
9	13	54	49

H	L	|FO|	|FC|
9	14	19	14
10	0	53	49
10	1	31	38
10	2	25	12
10	3	67	57
10	4	34	18
10	5	9	7
10	7	56	51
10	8	73	19
10	9	50	37
10	10	25	18
10	11	21	14
10	12	40	34
11	0	33	20
11	1	38	32
11	2	22	9
11	3	78	44
11	5	8	21
11	7	64	55
11	8	13	5
11	9	45	41
11	10	11	14
12	1	59	42
12	2	17	7
12	3	56	50
12	4	22	14

K = 7

H	L	|FO|	|FC|
1	0	18	4
1	1	43	41
1	2	13	6
1	3	30	41
1	5	73	65
1	6	21	5
1	7	57	57
1	8	20	11
1	9	35	41
1	10	14	9
1	11	58	49
1	12	19	4
1	13	26	32
1	14	8	5
1	15	38	34
1	16	7	4
1	17	41	37
1	19	42	37
1	20	6	9
2	1	36	34
2	2	17	12
2	3	32	28
2	4	21	15
2	5	20	5
2	7	20	23
2	8	10	10
2	9	40	31
2	10	11	8
2	11	35	34
2	12	19	10
2	13	24	5
2	14	7	8
2	16	27	13
2	17	12	4
2	18	18	1
2	19	12	21
3	0	11	10
3	1	26	21
3	2	8	9
3	3	25	30
3	4	6	7
3	5	29	15
3	7	25	14
3	8	12	6
3	9	10	19
3	10	15	2
3	11	25	15
3	13	20	25
3	14	8	12
3	15	27	27
3	16	7	8
3	17	29	14
3	18	12	10
3	19	37	17
4	0	23	22
4	1	36	26
4	2	3	8
4	3	35	29
4	4	3	7

H	L	|FO|	|FC|
4	5	34	27
4	7	39	33
4	8	23	15
4	9	34	33
4	11	37	24
4	12	25	17
4	13	43	27
4	14	23	5
4	15	19	13
4	16	15	1
4	17	24	20
4	18	13	4
5	1	12	15
5	2	21	14
5	3	32	25
5	4	16	17
5	5	30	33
5	7	26	21
5	9	11	14
5	11	19	2
5	13	19	23
5	15	15	19
5	17	24	22
5	18	5	6
6	1	64	67
6	2	13	4
6	3	51	43
6	5	50	48
6	6	21	16
6	7	31	31
6	9	40	41
6	10	17	13
6	11	48	48
6	12	17	12
6	13	43	44
6	15	24	34
6	17	54	49
7	3	22	12
7	4	15	18
7	8	7	3
7	9	20	11
7	11	6	5
7	12	17	11
8	0	19	12
8	1	57	46
8	2	20	11
8	3	13	22
8	5	38	29
8	7	41	29
8	8	8	20
8	9	23	21
8	10	14	17
8	11	35	39
8	13	52	37
8	14	11	2
9	0	17	16
9	1	21	18
9	3	19	32
9	5	21	14
9	7	22	9
9	10	11	8
9	12	4	11
10	0	19	15
10	1	8	9
10	2	5	13
10	3	25	15
10	4	17	17
10	5	7	3
10	9	27	14
11	0	10	24
11	1	21	30
11	3	52	30
11	4	5	10
11	5	39	23

K = 8

H	L	|FO|	|FC|
0	0	37	64
0	1	33	32
0	3	73	69
0	4	12	15
0	5	14	11
0	6	18	15
0	7	51	54
0	8	50	39
0	9	57	44
0	10	9	23
0	11	31	24

H	L	|FO|	|FC|
0	12	65	47
0	13	52	52
0	14	12	3
0	15	41	30
0	16	12	23
0	17	50	38
0	18	29	12
1	0	16	18
1	1	33	39
1	2	21	26
1	3	73	72
1	4	11	10
1	5	20	18
1	6	55	59
1	7	57	58
1	8	17	7
1	9	56	48
1	10	15	34
1	11	17	18
1	13	50	50
1	14	49	34
1	15	29	27
1	16	8	11
1	17	37	28
1	18	23	21
2	0	17	27
2	1	50	44
2	3	65	63
2	4	83	65
2	5	8	17
2	6	9	11
2	7	57	54
2	8	40	34
2	9	35	46
2	12	26	11
2	13	66	55
2	15	27	22
2	16	76	62
2	17	22	30
3	0	32	10
3	1	46	38
3	2	70	43
3	3	63	59
3	4	18	12
3	5	19	13
3	7	50	52
3	9	39	48
3	10	89	70
3	12	18	12
3	13	53	54
3	14	26	15
3	15	8	18
3	16	23	10
3	17	22	30
4	0	88	78
4	1	37	44
4	3	69	65
4	4	22	32
4	5	15	14
4	6	35	19
4	7	44	45
4	8	55	31
4	9	55	52
4	11	8	7
4	12	63	54
4	13	51	49
4	14	3	9
4	15	26	22
4	16	25	17
5	0	20	13
5	1	27	28
5	2	33	21
5	3	58	58
5	4	15	14
5	5	95	66
5	7	32	50
5	8	6	3
5	9	55	48
5	11	26	21
5	12	9	10
5	13	51	46
5	14	55	52
5	15	35	18
5	16	24	18
6	0	50	42
6	1	43	38
6	2	4	9
6	3	54	57

H	L	|FO|	|FC|
3	6	51	57
3	7	40	25
3	8	13	6
3	9	22	34
3	10	132	95
3	11	16	19
4	1	129	113
4	2	20	25
4	3	38	27
4	4	44	50
4	5	24	21
4	6	41	24
4	9	24	17
4	10	7	12
4	11	23	4
5	1	20	11
5	2	24	21
5	3	34	21
5	4	14	12
5	5	19	11
5	6	145	91
5	7	26	27
5	8	30	24
5	9	35	32
6	2	9	6
6	4	61	54
6	6	31	17
6	7	5	18
7	2	25	26
		73	54

K = 11

H	L	|FO|	|FC|
1	1	11	0
1	1	27	20
1	2	16	7
1	3	19	28
1	4	6	6
1	5	18	8
1	6	12	8
1	7	22	17
1	8	31	38
2	1	14	9
2	3	15	21
2	5	27	14
2	7	15	7
3	1	21	24
3	2	30	9
3	3	22	10
3	5	11	19
3	7	8	0
4	2	18	2
4	3	22	21

H	L	|FO|	|FC|
6	11	39	23
7	3	18	10
7	7	28	11
7	10	24	23
8	2	11	11
8	3	22	23
8	4	23	19
8	5	28	17
8	6	5	12
8	7	18	15
8	8	27	12
9	1	9	2

K = 10

H	L	|FO|	|FC|
0	0	196	113
0	1	15	19
0	2	16	4
0	3	41	40
0	4	23	45
0	5	20	3
0	6	31	9
0	7	10	25
0	8	44	37
0	9	23	19
0	10	28	12
1	1	24	6
1	2	24	35
1	3	19	25
1	4	19	8
1	5	19	13
1	6	79	79
1	7	21	25
1	8	24	8
1	9	16	8
2	1	133	81
2	3	13	5
2	5	25	22
2	7	44	18
2	9	22	5
3	2	15	3
3	4	10	10
3	6	54	52
3	8	21	14

H	L	|FO|	|FC|
1	5	39	35
1	6	17	4
1	7	43	36
1	8	7	11
1	9	18	11
1	10	4	3
1	11	19	22
1	13	11	11
1	15	20	12
2	1	5	23
2	2	9	11
2	3	10	5
2	5	3	7
2	6	6	10
2	8	15	8
2	9	20	16
2	11	17	21
2	12	15	9
2	13	17	10
2	14	19	11
2	15	17	4
3	1	14	1
3	2	21	14
3	3	16	10
3	4	16	9
3	5	12	14
3	6	20	9
3	7	5	14
3	8	21	14
3	9	14	10
3	11	12	9
3	12	12	4
3	13	25	8
4	1	17	16
4	3	8	14
4	4	23	14
4	5	24	9
4	6	16	8
4	7	17	20
4	8	12	11
4	9	13	14
4	10	22	11
4	11	13	26
4	12	22	14
4	13	18	14
4	14	15	11
4	15	13	18
5	1	17	4
5	2	16	7

K = 9

H	L	|FO|	|FC|
0	0	20	35
0	1	15	6
0	2	11	8
0	3	52	44
0	4	45	36
0	5	10	13
0	6	28	25
0	7	36	38
0	8	40	26
1	1	57	52
1	2	50	54
1	3	7	13
1	4	26	33
1	5	33	33
1	6	36	32
1	7	8	9
1	8	24	16
1	9	22	11
1	10	8	4
1	11	27	17

A.7 $VAsO_5$

L = 0

H	K	|FO|	|FC|
2	0	39	56
4	0	82	98
6	0	102	94
8	0	13	1
1	1	6	19
-1	1	8	6
3	1	31	38
-3	1	53	44
5	1	8	6
-5	1	18	9
7	1	14	7
-7	1	13	5
9	1	13	15
0	2	81	166
2	2	2	6
-2	2	62	81
4	2	177	160
-4	2	26	27
6	2	66	62
-6	2	124	119
8	2	27	25
-8	2	28	29
1	3	51	41
-1	3	3	7
3	3	18	3
5	3	12	5
-5	3	38	41
7	3	11	11
-7	3	5	5
-9	3	20	13
0	4	53	75
2	4	40	44
-2	4	187	170
4	4	144	121
-4	4	15	16
6	4	26	12
-6	4	76	83
8	4	59	52
-8	4	49	46
1	5	28	24
-1	5	27	31
3	5	13	5
5	5	8	9
-5	5	14	16
-7	5	12	5
0	6	18	9
2	6	96	87
-2	6	64	105
4	6	89	82
-4	6	27	27
6	6	16	6
-6	6	34	29
1	7	12	3
-1	7	12	12
3	7	10	10
-3	7	2	1
5	7	7	10
0	8	19	10
2	8	90	78
-2	8	33	59
4	8	31	21
-4	8	58	61
-1	9	21	22
3	9	23	13
-3	9	11	14

L = 1

H	K	|FO|	|FC|
1	0	9	17
2	0	120	162
3	0	54	49
4	0	87	93
5	0	10	3
6	0	28	24
7	0	4	11
8	0	76	68
-8	1	61	48
-7	1	15	27
-6	1	35	42
-5	1	2	1
-4	1	4	8
-3	1	10	4
-2	1	16	10
-1	1	64	58
0	1	27	24
1	1	7	4
2	1	36	30
3	1	15	12
4	1	13	8
5	1	11	5
6	1	16	11
7	1	10	2
8	1	54	63
-8	2	6	3
-7	2	149	130
-6	2	46	69
-5	2	14	16
-4	2	16	19
-3	2	35	29
-2	2	117	110
-1	2	7	3
0	2	65	60
1	2	13	7
2	2	36	29
3	2	9	6
4	2	81	76
5	2	59	57
6	2	11	9
7	2	21	15
8	2	47	34
-8	3	33	43
-7	3	9	4
-6	3	19	15
-5	3	10	8
-4	3	55	44
-3	3	6	2
-2	3	16	21
-1	3	20	15
0	3	10	10
1	3	13	13
2	3	9	3
3	3	27	29
4	3	5	6
5	3	33	25
6	3	141	112
7	3	45	37
8	3	88	95
-8	4	26	18
-7	4	6	7
-6	4	20	23
-5	4	11	15
-4	4	109	112
-3	4	12	1
-2	4	15	14
-1	4	76	64
0	4	40	45
1	4	11	8
2	4	36	31
3	4	25	24
4	4	4	5
5	4	10	1
6	4	24	37
7	4	3	5
8	4	16	17
-8	5	57	48
-7	5	17	19
-6	5	17	17
-5	5	12	2
-4	5	12	14
-3	5	3	6
-2	5	14	13
-1	5	18	14
0	5	13	19
1	5	12	13
2	5	6	5
3	5	13	11
4	5	6	5
5	5	8	6
6	5	12	11
7	5	116	97
8	5	27	24
-8	6	17	4
-7	6	51	40
-6	6	17	20
-5	6	9	7
-4	6	13	4
-3	6	46	45
-2	6	32	51
-1	6	25	21
0	6	7	5
1	6	87	74
2	6	59	60
3	6	13	13
4	6	12	4
5	6	14	3
6	6	19	19
7	6	17	23
8	6	32	27
-8	7	21	18
-7	7	11	12
-6	7	12	2
-5	7	4	4
-4	7	10	5
-3	7	12	3
-2	7	9	2
-1	7	5	4
0	7	12	4
1	7	14	3
2	7	5	4
3	7	12	4
4	7	13	13
5	7	7	5
6	7	59	60
7	7	14	9
8	7	10	11
-8	8	50	66
-7	8	15	8
-6	8	8	7
-5	8	13	1
-4	8	40	48
-3	8	11	7
-2	8	57	48
-1	8	26	21
0	8	7	12
1	8	12	16
2	8	14	6
3	8	16	17
4	8	17	2
5	8	26	16
6	8	21	11
7	8	6	21

L = 2

H	K	|FO|	|FC|
0	0	171	175
1	0	42	55
2	0	31	39
3	0	9	3
4	0	54	60
5	0	11	2
6	0	80	78
7	0	20	12
8	0	9	11
-1	1	36	45
-1	1	9	16
-2	1	43	37
-2	1	14	18
-3	1	53	55
-3	1	55	54
-4	1	11	11
-4	1	50	51
-5	1	9	1
-5	1	11	17
-6	1	9	2
-6	1	9	3
-7	1	37	32
-7	1	18	17
-8	1	23	23
-8	1	13	16
-9	1	25	19
-9	1	35	27
0	2	145	116
-1	2	10	11
-1	2	56	43
2	2	6	5
-2	2	75	81
3	2	8	10
-3	2	4	5
4	2	108	98
-4	2	16	17
5	2	28	28
-5	2	50	46
6	2	90	84
-6	2	10	8
7	2	34	29
-7	2	25	16
8	2	25	25
-8	2	4	7
-9	2	9	3
0	3	57	38
1	3	60	51
-1	3	12	6
2	3	38	41
-2	3	9	12
3	3	29	27
-3	3	34	40
4	3	8	8
5	3	13	15
-5	3	33	36
6	3	5	8
-6	3	11	5
7	3	40	36
-7	3	5	3
8	3	23	19
-9	3	10	6
0	4	29	25
1	4	76	50
2	4	8	3
-1	4	14	24
-2	4	39	37
3	4	115	106
-3	4	11	2
-4	4	37	38
4	4	105	90
-4	4	13	14
5	4	13	10
-5	4	6	5
6	4	17	13
-6	4	50	55
7	4	11	3
-7	4	18	20
8	4	38	37
-8	4	45	44
6	5	8	3
1	5	64	49
-1	5	25	24
2	5	7	9
-2	5	7	2
3	5	14	6
-3	5	13	15
4	5	17	7
-4	5	7	13
5	5	31	27
-5	5	36	37
6	5	13	13
-6	5	29	28
7	5	26	25
-8	5	16	2
8	5	17	6
-1	6	10	13
-1	6	6	9
2	6	71	62
-2	6	73	60
3	6	21	21
-3	6	13	10
4	6	64	56
-4	6	31	34
5	6	18	13
6	6	17	7
-6	6	12	20
-7	6	7	8
0	7	32	29
1	7	32	25

H	K	|FO|	|FC|
-1	7	31	31
2	7	16	11
-2	7	18	18
3	7	16	8
-3	7	8	0
4	7	15	12
5	7	35	30
-5	7	18	26
6	7	19	13
-6	7	25	23
0	8	7	14
1	8	13	10
2	8	79	63
-2	8	26	42
-3	8	17	22
4	8	23	19
-4	8	52	50
-5	8	11	15
0	9	10	9
1	9	16	7
-1	9	30	29
2	9	11	4
-2	9	13	13

L = 3

H	K	|FO|	|FC|
1	0	20	23
2	0	85	85
3	0	72	69
4	0	44	46
5	0	11	7
6	0	15	13
7	0	19	20
8	0	66	59
0	1	74	76
1	1	41	47
-1	1	79	84
2	1	12	5
-2	1	18	19
3	1	23	24
-3	1	6	8
4	1	25	27
-4	1	20	17
5	1	56	51
-5	1	58	56
6	1	14	16
-6	1	53	50
7	1	12	13
-7	1	39	45
8	1	8	1
-8	1	8	10
9	1	13	18
-9	1	14	4
0	2	38	30
1	2	22	25
-1	2	3	3
2	2	131	117
-2	2	49	56
3	2	25	29
-3	2	33	36
4	2	22	19
-4	2	90	82
5	2	9	2
-5	2	38	37
6	2	11	6
-6	2	45	46
7	2	36	36
-7	2	42	39
8	2	18	15
-8	2	26	29
9	2	61	48
-9	2	25	14
0	3	95	78
1	3	6	1
-1	3	46	35
2	3	57	57
-2	3	32	35
3	3	75	66
-3	3	11	1
4	3	57	55
-4	3	20	22
5	3	6	17
-5	3	28	28
6	3	13	4
-6	3	43	44
7	3	14	10
-7	3	9	4
8	3	64	47

H	K	|FO|	|FC|
-1	4	70	57
1	4	10	2
-1	4	73	70
2	4	12	11
-2	4	14	12
3	4	26	34
-3	4	10	1
4	4	61	64
-4	4	8	6
5	4	33	27
-5	4	74	66
6	4	17	16
-6	4	21	19
7	4	4	2
-7	4	32	27
8	4	29	18
-8	4	13	10
0	5	9	15
-1	5	38	38
1	5	40	37
-2	5	54	47
3	5	54	54
-3	5	34	33
4	5	6	3
-4	5	29	21
5	5	16	1
-5	5	25	23
6	5	21	17
-6	5	44	44
7	5	75	68
-7	5	46	38
8	5	15	3
-8	5	29	25
0	6	3	7
-0	6	19	16
1	6	37	45
-1	6	34	33
2	6	16	18
-2	6	51	47
3	6	40	36
-3	6	16	22
4	6	10	1
-4	6	3	4
5	7	40	36
-5	7	19	16
6	7	40	34
-6	7	31	36
7	7	55	44
-7	7	53	56
8	7	22	21
-8	7	16	11
9	7	11	15
-9	7	12	4
0	8	60	53
1	8	17	14
-1	8	16	10
2	8	25	5
-2	8	21	18
3	8	11	5
-3	8	13	1
4	8	43	39
-4	8	9	2
5	9	31	35
-5	9	14	4
6	9	31	30
-6	9	7	13

L = 4

H	K	|FO|	|FC|
0	0	24	22
1	0	33	44
-1	0	13	16
2	0	5	5
-2	0	16	15
3	0	33	27
-3	0	41	46
4	0	11	7
-4	0	16	8
5	0	10	9
-5	0	82	73
6	0	31	27
-6	0	45	42
7	0	43	40
-7	0	85	84
8	0	164	156
-8	0	22	19
9	0	42	36
-9	0	13	3

H	K	|FO|	|FC|
-5	1	31	30
6	1	15	14
-6	1	10	3
7	1	76	69
-7	1	48	44
8	1	34	28
-8	1	25	25
9	1	32	28
-9	1	50	49
0	2	43	48
-0	2	18	19
1	2	34	33
-1	2	59	61
2	2	12	19
-2	2	4	5
3	2	23	19
-3	2	9	5
4	2	33	32
-4	2	13	19
5	2	22	22
-5	2	38	30
6	2	24	22
-6	2	15	4
7	2	19	15
-7	2	135	28
8	2	168	146
-8	2	52	47
0	3	18	17
-0	3	62	57
1	3	102	90
-1	3	41	35
2	3	31	27
-2	3	38	40
3	3	24	23
-3	3	7	5
4	3	79	72
-4	3	21	11
5	3	21	21
-5	3	23	15
6	3	15	16
-6	3	12	6
7	3	35	34
-7	3	21	24
8	3	24	22
-8	3	24	22
0	4	22	20
-0	4	45	41
1	4	11	7
-1	4	22	20
2	4	14	9
-2	4	8	11
3	4	15	13
-3	4	3	4
4	4	26	23
-4	4	23	13
5	4	28	32
-5	4	39	28
6	4	107	87
-6	4	26	23
7	4	21	24
-7	4	8	4
8	4	9	8
-8	4	34	33
0	5	25	28
-0	5	58	53
1	5	72	73
-1	5	23	28
2	5	20	18
-2	5	53	48
3	5	12	12
-3	5	12	3
4	5	18	7
-4	5	23	17
5	5	21	24
-5	5	29	37
6	5	27	27
-6	5	22	20
7	5	14	17
-7	5	31	34
8	5	15	11
-8	5	14	3
0	6	15	7
-0	6	16	6
1	6	32	32
-1	6	85	58
2	6	54	60
-2	6	16	12

H	K	|FO|	|FC|
-2	7	8	9
3	7	16	7
-3	7	11	0
4	7	23	15
-4	7	10	15
5	7	67	61
-5	7	47	57
6	8	18	15
-6	8	13	12
7	8	10	5
-7	8	34	34
8	8	14	13
-8	8	17	19
9	8	18	22
-9	8	19	14
0	9	26	25
-0	9	21	20
1	9	19	12
-1	9	41	47

L = 5

H	K	|FO|	|FC|
1	5	14	7
-1	5	26	28
2	5	13	11
-2	5	13	13
3	5	11	4
-3	5	9	3
4	5	11	8
-4	5	32	33
5	5	27	30
-5	5	63	72
6	5	114	117
-6	5	9	5
7	5	17	16
-7	5	31	36
8	5	22	22
-8	5	7	7
0	6	82	76
-0	6	87	81
1	6	23	23
-1	6	15	16
2	6	14	14
-2	6	51	63
3	6	9	1
-3	6	13	8
4	6	27	24
-4	6	61	59
5	6	23	23
-5	6	14	14
6	6	18	21
-6	6	8	6
7	6	41	41
-7	6	5	4
8	6	11	15
-8	6	13	13
0	7	9	4
-0	7	13	10
1	7	21	16
-1	7	13	12
2	7	36	24
-2	7	135	112
3	7	9	8
-3	7	34	27
4	7	82	79
-4	7	42	46
5	7	12	12
-5	7	13	2
6	7	82	80
-6	7	39	35
7	7	11	7
-7	7	19	21
8	7	12	6
-8	7	62	63
9	7	8	6
-9	7	15	18
0	8	13	13
-0	8	11	12
1	8	5	7
-1	8	24	31
2	8	12	6
-2	8	13	5
3	8	13	3
-3	8	19	25
4	8	14	14
-4	8	38	39
5	8	15	5

H	K	|FO|	|FC|
7	4	14	15
0	5	16	7
1	5	12	17
-1	5	65	61
2	5	20	21
-2	5	25	27
3	5	73	68
-3	5	71	72
4	5	18	19
-4	5	12	10
5	5	42	33
-5	5	12	2
6	5	19	8
-6	5	27	27
7	5	65	66
-7	5	31	33
0	6	9	9
-1	6	19	17
2	6	9	8
-2	6	7	3
3	6	25	24
-3	6	18	4
4	6	15	20
-4	6	17	18
5	6	8	16
-5	6	11	4
6	7	49	47
-6	7	35	28
7	7	15	14
-7	7	72	56
0	7	88	78
-1	7	9	9
1	7	19	17
-2	7	25	3
2	7	13	17
-3	7	36	27
3	7	17	7
-4	7	14	16
4	7	10	1
-5	7	13	5
5	7	8	10
-6	7	6	2

L = 6

H	K	|FO|	|FC|
0	0	18	17
1	0	5	3
2	0	13	9
3	0	10	2
4	0	12	15
5	0	16	23
6	0	20	24
7	0	4	1
8	0	8	1
1	1	64	70
-1	1	26	26
2	1	62	59
-2	1	22	20
3	1	86	94
-3	1	128	123
4	1	8	9
-4	1	10	2
5	1	11	1
-5	1	33	32
6	1	14	5
-6	1	76	58
7	1	39	38
-7	1	14	13
8	1	14	14
-8	1	21	28
0	2	45	49
-1	2	12	1
1	2	23	27
-2	2	8	6
2	2	7	1
-3	2	20	19
3	2	6	4
-4	2	19	5
4	2	19	16
-5	2	14	13
5	2	13	18
-6	2	6	4
6	2	11	5
-7	2	16	4
7	2	12	7
-8	2	18	1
8	2	3	1
-1	3	125	114

H	K	|FO|	|FC|
-1	3	11	12
2	3	19	14
-2	3	11	7
3	3	50	51
-3	3	90	82
4	3	28	31
-4	3	23	25
5	3	56	57
-5	3	24	18
6	3	10	3
-6	3	75	73
7	3	12	8
-7	3	14	11
0	4	13	19
-1	4	13	13
1	4	24	24
-2	4	8	3
2	4	11	9
-3	4	31	28
3	4	9	9
-4	4	11	4
4	4	18	14
-5	4	11	5
5	4	18	15
-6	4	12	9
6	4	11	1
-7	4	31	28
7	4	10	1
-8	4	13	10
8	4	6	2
-1	5	61	56
2	5	9	4
-2	5	36	36
3	5	19	9
-3	5	12	7
4	5	23	20
-4	5	19	18
5	5	9	4
-5	5	12	4
6	5	8	10
-6	5	11	5
7	5	10	1
-7	5	24	20
8	5	21	3
-8	5	5	3
1	6	32	26
-1	6	33	27
2	6	23	13
-2	6	72	69
3	6	60	63

L = 7

H	K	|FO|	|FC|
-3	0	72	78
4	0	27	31
-4	0	11	12
5	0	3	4
-5	0	28	27
6	0	21	20
-6	0	22	24
7	0	3	11
-7	0	97	105
1	1	7	2
-1	1	44	53
2	1	15	19
-2	1	10	8
3	1	11	16
-3	1	68	75
4	1	54	57
-4	1	5	8
5	1	21	19
-5	1	9	3
6	1	20	22
-6	1	12	7
7	1	43	42
-7	1	13	22
8	1	27	35
-8	1	8	13
1	2	17	20
-1	2	10	2
2	2	15	16

H	K	|FO|	|FC|
-3	2	12	16
4	2	14	3
-4	2	45	45
5	2	14	7
-5	2	24	27
6	2	17	15
-6	2	21	16
7	2	32	36
-7	2	10	3
0	3	27	22
-1	3	13	14
2	3	52	52
-2	3	13	8
3	3	21	20
-3	3	13	2
4	3	31	32
-4	3	44	50
5	3	14	18
-5	3	52	58
6	3	12	9
-6	3	17	0
7	3	19	19
-7	3	10	5
0	4	27	27
-1	4	18	11
2	4	50	50
-2	4	23	17
3	4	25	19
-3	4	35	34
4	4	14	6
-4	4	15	18
5	4	12	8
-5	4	11	1
6	4	25	26
-6	4	9	8
7	4	40	35
-7	4	52	54
8	4	7	0
-8	4	8	8
1	5	14	14
-1	5	28	28
2	5	24	28
-2	5	29	24
3	5	5	17
-3	5	20	26
4	5	6	4
-4	5	14	16
5	5	29	33
-5	5	37	41
6	5	9	10
-6	5	4	5

L = 9

H	K	|FO|	|FC|
-3	2	13	11
4	2	42	47
-4	2	26	29
5	2	27	35
-5	2	18	7
6	2	13	10
-6	2	21	20
7	2	19	35
-7	2	51	60
0	3	7	3
-1	3	5	9
2	3	17	13
-2	3	14	14
3	3	6	5
-3	3	59	68
4	3	32	41
-4	3	13	16
5	3	18	20
-5	3	26	26
6	3	35	35
-6	3	11	20
7	3	28	31
-7	3	14	9
0	4	36	35
-1	4	11	4

H	K	|FO|	|FC|
-5	2	20	18
6	2	18	24
-6	2	9	1
0	3	9	10
1	3	15	9
-1	3	57	63
-2	3	7	18
3	3	27	28
-3	3	11	16
4	3	13	13
-4	3	9	2
5	3	35	35
-5	3	16	23
6	3	14	7
-6	3	10	18
0	4	41	41
1	4	21	29
-1	4	17	9
2	4	30	31
-2	4	12	7
3	4	13	9
-3	4	16	15
4	4	10	8
-4	4	45	41
5	4	14	13
-5	4	16	26
0	5	9	4
1	5	17	3
-1	5	36	46
2	5	18	13
-2	5	20	21
3	5	53	59
-3	5	37	32
0	6	33	34
1	6	14	23
-1	6	20	21
2	6	22	15
-2	6	7	10
3	6	10	2
-3	6	14	4

L = 10

H	K	|FO|	|FC|
0	0	66	73
1	0	13	26
2	0	17	16
3	0	25	27
4	0	34	44
5	0	6	3
0	1	21	31
1	1	42	45
-1	1	17	22
2	1	30	41
-2	1	14	12
3	1	12	0
-3	1	23	11
4	1	39	45
-4	1	18	16
5	1	57	58
-5	1	15	4
0	2	18	31
1	2	13	17
-1	2	14	6
2	2	49	52
-2	2	8	6
3	2	32	33
-3	2	20	30
4	2	30	30
-4	2	14	12
5	2	23	11
-5	2	11	13

L = 11

H	K	|FO|	|FC|
2	3	27	23
-2	3	9	10
3	3	7	20
-3	3	17	29
4	3	7	1
-4	3	27	34
5	3	29	29
0	4	19	22
1	4	4	3
-1	4	28	35
2	4	19	16
-2	4	48	57
3	4	34	37
-3	4	15	8
4	4	41	46
-4	4	16	11
0	5	27	29
1	5	33	36
-1	5	13	20
2	5	20	21
3	5	22	8
-3	5	11	13

L = 12

H	K	|FO|	|FC|
-4	1	12	6
0	2	9	22
1	2	16	27
-1	2	7	4
2	2	59	59
-2	2	23	36
3	2	24	22
-3	2	25	27
4	2	10	14
-4	2	51	58
0	3	14	7
-1	3	15	22
2	3	10	6
-2	3	8	14
3	3	18	13
-3	3	31	10
4	4	38	41
-4	4	20	19
2	4	43	52
-2	4	8	12

L = 12

H	K	|FO|	|FC|
0	0	42	49
1	0	3	6
0	1	13	1
1	1	11	11
2	1	13	12
-2	1	7	0
0	2	40	53
1	2	6	4
-1	2	28	25
2	2	8	3
-2	2	31	47

REFERENCES

1. A. Escardino, C. Solá, and F. Ruiz. An. Quim. 69, 385 (1973).
2. H. G. Bachman, F. R. Ahmed, and W. H. Barnes. Zeit. Krist. 115, 110 (1961).
3. K. Waltersson, B. Forslund, and K-A. Wilhelmi. Acta Cryst. B30, 2644 (1974).
4. K-A. Wilhelmi and K. Waltersson. Acta Chem. Scand. 24, 3409 (1970).
5. K-A. Wilhelmi, K. Waltersson, and L. Kihlborg. Acta Chem. Scand. 25, 2675 (1971).
6. F. Théobald, R. Cabala, and J. Bernard. J. Solid State Chem. 17, 431 (1976).
7. (a) G. Andersson. Acta Chem. Scand. 10, 623 (1956).
   (b) J. M. Longo and P. Kierkegaard. Acta Chem. Scand. 24, 420 (1970).
8. W. R. Robinson. Acta Cryst. B31, 1153 (1975).
9. H. Horiuchi, M. Tokonami, N. Morimoto, and K. Nagasawa. Acta Cryst. B28, 1404 (1972).
10. H. Horiuchi, N. Morimoto, and M. Tokonami. J. Solid State Chem. 17, 407 (1976)
11. B. Jordan and C. Calvo. Can. J. Chem. 51, 2621 (1973).
12. R. Gopal and C. Calvo. J. Solid State Chem. 5, 432 (1972).
13. F. Marumo, M. Isobe, and S. Iwai. Acta Cryst. B30, 1628 (1974).
14. R. Gopal and C. Calvo. Can. J. Chem. 51, 1004 (1973).
15. P. G. Dickens and P. J. Wiseman. International Review of Sciences 10. Series 2. Butterworth Press. p. 211 (1975).
16. (a) I. D. Brown and R. D. Shannon. Acta Cryst. A29, 266 (1973).
   (b) I. D. Brown. Acta Cryst. B33, 1305 (1977).
17. C. Calvo. unpublished results.
18. G. Grymonprez, L. Fiermans and J. Vennik. Acta Cryst. A33, 834 (1977).

19. J. Galy, J. Darriet, and P. Hagenmuller. Rev. Chim. Minerale 8, 509 (1971).

20. S. Andersson. Acta Chem. Scand. 19, 1371 (1965).

21. J. Galy, M. Pouchard, A. Casalot, and P. Hagenmuller. Bull. Soc. Fr. Min. 90, 544 (1967).

22. A. D. Wadsley. Acta Cryst. 8, 695 (1955).

23. A. D. Wadsley. Acta Cryst. 10, 261 (1957).

24. K. H. Jost. Acta Cryst. 14, 844 (1961).

25. B. E. Robertson and C. Calvo. J. Solid State Chem. 1, 120 (1970).

26. H. M. Ondik. Acta Cryst. 18, 226 (1965).

27. H. M. Ondik. Acta Cryst. 17, 1139 (1964).

28. H. C. J. de Decker and C. H. MacGillavry. Rec. Trav. Chim. 60, 153 (1941).

29. H. C. J. de Decker. Rec. Trav. Chim. 60, 413 (1941).

30. C. H. MacGillavry, H. C. J. de Decker, and L. M. Nyland. Nature 164, 448 (1949).

31. K. Dornberger-Schiff, F. Liebau, and E. Thilo. Acta Cryst. 8, 752 (1955).

32. E. Thilo. Rev. Chim. Min. 5, 179 (1968).

33. C. Calvo and K. Neelakantan. Can. J. Chem. 48, 890 (1970).

34. K-H. Jost, H. Worzala, and E. Thilo. Acta Cryst. 21, 808 (1966).

35. M. Jansen. presented at the European Crystallographic Meeting, Oxford, Aug.197

36. K. L. Idler, C. Calvo, and H. N. Ng. accepted for publication in J. Solid State Chem.

37. K-H. Jost, H. Worzala, and E. Thilo. Z. Anorg. Allgem. Chem. 325, 98 (1963).

38. B. Nádor. Acta Chim. Hung. 40, 1 (1964).

39. G. Ladwig. Z. Anorg. Allg. Chem. 338, 266 (1965).

40. E. Bordes and P. Courtine. accepted for publication in J. Catal.

41. E. Bordes, P. Courtine, and G. Pannetier. Ann. Chim. 8, 105 (1973).

42. B. D. Jordan and C. Calvo. Acta Cryst. B32, 2899 (1976).

43. G. Ladwig. Z. Chem. 8, 307 (1968).

44. A. V. Lavrov, L. S. Guzeeva, and P. M. Fedorov. Izv. Akad. Nauk SSSR, Neorgan. Mat. 10, 2180 (1974).

45. B. C. Tofield, G. R. Crane, G. A. Pasteur, and R. C. Sherwood. J. C. S. Dalton, 1806 (1975).

46. C. E. Rice, W. R. Robinson, and B. C. Tofield. Inorg. Chem. 15, 345 (1976).

47. N. Middlemiss and C. Calvo. Acta Cryst. B32, 2896 (1976).

48. G. Ladwig and E. Thilo. Z. Chem. 4, 350 (1964).

49. E. Bordes and P. Courtine. private communication

50. A. Winkler and E. Thilo. Z. Anorg. Allg. Chem. 339, 71 (1965).

51. J. S. Anderson and B. G. Hyde. J. Phys. Chem. Solids. 28, 1393 (1967).

52. S. Horiuchi, M. Saeki, Y. Matsui, and F. Nagata. Acta Cryst. A31, 660 (1975).

53. L. Fiermans and J. Vennik. Surface Science 9, 187 (1968)
and Surface Science 18, 317 (1969).

54. R. J. D. Tilley and B. G. Hyde. J. Phys. Chem. Solids. 31, 1613 (1970).

55. W. M. H. Sachtler. Cat. Rev. 4, 27 (1970).

56. K. Tamara, S. Teranishi, S. Yoshida, and N. Tamura. Proc. 3rd Int. Congr. Cat. 1, 282 (1965).

57. D. J. Cole, C. F. Cullis, and D. J. Hucknall. J.C.S. London Far.I. 2185 (1972).

58. M. Ai. Bull. Chem. Soc. Japan. 43, 3490 (1970).

59. H. Seeboth, B. Kubias, H. Wolf, and B. Lücke. Chem. Techn. 28, 730 (1976).

60. H. Seeboth, G. Ladwig, B. Kubias, G. Wolf, B. Lücke. Ukr. Khim. Zh. 93, 842 (1977).

61. M. Nakamura, K. Kawai, and Y. Fujiwara. J. Catal 34, 345 (1974).

62. M. Ai and S. Suzuki. Bull. Chem. Soc. Japan. 47, 3074 (1974).

63. W. H. Zachariasen. Theory of X-Ray Diffraction in Crystals, Dover Press, New York, 1967.

64. J. M. Cowley. Diffraction Physics, North-Holland Publishing Co., New York, 1975.

65. R. W. James. The Optical Principles of the Diffraction of X-Rays, North-Holland Publishing Co., Amsterdam, 1062.

66. B. E. Warren. X-Ray Diffraction, Addison-Wesley Publishing Co., Reading, Mass., 1969.

67. D. T. Cromer and J. B. Mann. Acta Cryst. B24, 321 (1968).

68. D. T. Cromer and J. T. Waber. Acta Cryst. 18, 104 (1965).

69. H. Jagodzinski and K. Haefner. Z. Krist. 125, 188 (1967).

70. J. Kakinoki and Y. Komura. J. Phys. Soc. Japan 9, 169 (1954) and J. Phys. Soc. Japan 9, 177 (1954).

71. J. M. Cowley. Acta Cryst. A32, 83 (1976).

72. W. H. Zachariasen. Acta Cryst 16, 1139 (1963).

73. A. C. Larson. Acta Cryst 23, 664 (1967).

74. International Tables for X-Ray Crystallography. Vol. II, Kynoch Press, Birmingham, 1963.

75. C. Scheringer. Acta Cryst. 19, 504 (1965).

76. D. W. J. Cruickshank and D. E. Dilling. Computing Methods and the Phase Problem in X-Ray Crystal Analysis, Pergamon Press, 1961.

77. B. C. Tofield, G. R. Crane, P. M. Bridenbaugh, and R. C. Sherwood. Nature 253, 722 (1975).

78. International Tables for X-Ray Crystallography. Vol. I, Kynoch Press, Birmingham, 1963.

79. J. M. Longo and R. J. Arnott. J. Solid State Chem. 1, 394 (1970).

80. Y. Takeuchi and W. Joswig. Mineral. J. 5, 98 (1967).

81. E. Tillmanns, W. Gevert, and W. H. Baur. J. Solid State Chem. 7, 69 (1973).

82. F. Liebau and K-F. Hesse. Z. Krist. 133, 213 (1971).

83. G. Bissert and F. Liebau. Acta Cryst. B26, 233 (1970).

84. H. Völlenkle, A. Wittmann, and H. Nowotny. Monatsh. Chem. 94, 956 (1963).

85. C-H. Huang, O. Knop, and D. A. Othen. Can. J. Chem. 53, 79 (1975).

86. L-O. Hagman and P. Kierkegaard. Acta Chem. Scand. 23, 327 (1968).

87. G. R. Levi and G. Peyronel. Z. Krist. 92, 190 (1935).

88. R. Hubin and P. Tarte. Spectrochim. Acta. 23A, 1815 (1967).

89. G. N. Ramachandran and R. Srinivasan. Fourier Methods in Crystallography, Wiley-Interscience, New York, 1970.

90. H. van der Meer. Acta Cryst. B32, 2423 (1976).

91. P. Remy and A. Bouille. Bull. Soc. Chim. Fr. 6, 2213 (1972).

92. P. Remy and A. Bouille. C. R. Acad. Sci. Paris, 258, 927 (1964).

93. F. d'Yvoire. Bull. Soc. Chim. Fr. 1224 (1962).

94. W. H. Baur. Trans. Am. Crystallogr. Assoc. 6, 129 (1970).

95. R. M. Douglass and E. Staritzky. Anal. Chem. 28, 984 (1957).

96. F. Liebau and H. P. Williams. Angew. Chem. 3, 315 (1964).

97. N. Middlemiss, F. Hawthorne, and C. Calvo. Can. J. Chem. 55, 1673 (1977).

98. H. N. Ng and C. Calvo. Can. J. Chem. 51, 2613 (1973).

99. J. M. Cowley. Acta Cryst. A32, 88 (1976).

100. S. Iijima. J. Appl. Phys. 42, 5891 (1971).

101. S. Iijima and J. G. Allpress. Acta Cryst. A30, 22 & 29 (1974).

102. A. J. Skarnulis, S. Iijima, and J. M. Cowley. Acta Cryst. A32, 799 (1976).